



Molecular Detection of *virB9* Gene of *Ehrlichia canis* in Dogs of Northern Kerala

C.Angeline Felicia Bora¹, Anju Varghese^{1*}, A.Nandini¹, Lanchalung Malangmei¹, Preena P.², C. K. Deepa¹, B.M.Amrutha¹, S.K. Prashant¹, R.K.Pradeep¹, M.Nimisha¹, K.G.Ajith Kumar¹, Lijo John² and Reghu Ravindran¹

¹Department of Veterinary Parasitology, College of Veterinary and Animal Sciences, Pookode, Wayanad, Kerala, India.

²Veterinary Surgeon, District Veterinary Centre (DVC), Kannur, Kerala, India

Received: 30 June 2019

Revised: 02 Aug 2019

Accepted: 04 Sep 2019

*Address for Correspondence

Anju Varghese

Assistant Professor,

Department of Veterinary Parasitology,

College of Veterinary and Animal Sciences,

Pookode, Lakkidi, Wayanad,

Kerala, India.

Email: dranjuvarghese@gmail.com



This is an Open Access Journal / article distributed under the terms of the **Creative Commons Attribution License** (CC BY-NC-ND 3.0) which permits unrestricted use, distribution, and reproduction in any medium, provided the original work is properly cited. All rights reserved.

ABSTRACT

A study was conducted to detect *Ehrlichia canis* infection in dogs from northern Kerala based on molecular technique like Polymerase chain reaction (PCR). A total of 113 peripheral blood smears and whole blood samples were collected from dogs presented to Teaching Veterinary Clinical Complex, Pookode and District Veterinary Centre (Kozhikode, Kannur). Out of 113 Giemsa stained blood smears screened, none of the samples were positive for *E. canis* by microscopical examination. But out of 113 blood samples, only one sample was positive for *E. canis* by PCR with *virB9* gene of *E. canis*. The BLAST (Basic Local Alignment Search Tool) analysis revealed 99 per cent identity with the published sequences of *E. canis* from Chennai and Uttar Pradesh. Phylogenetic analysis showed genetic similarity of Kerala isolate with the isolates from different parts of India (Uttar Pradesh and Chennai) and isolates from foreign countries like New Mexico, Venezuela, Hawaii, California, USA and Arizona.

Key words: *Ehrlichia canis*, Dogs, *virB9* gene, PCR, Kerala.



**Angeline Felicia Bora et al.**

INTRODUCTION

In India, the climatic conditions (hot and humid) are favourable for the growth of arthropods. The change in climate has resulted in emergence and re-emergence of various tick borne pathogens (Rani *et al.*, 2010). Babesiosis, Hepatozoonosis and Ehrlichiosis are the main arthropod borne diseases in India (Jadhav *et al.*, 2011). *E. canis* is a gram negative, obligate intracellular bacteria belong to the Order Rickettsiales, Family Anaplasmataceae and genus *Ehrlichia* (Mylonakis *et al.*, 2017). Canine monocytic ehrlichiosis caused by *Ehrlichia canis* is a tick borne rickettsial disease which infects monocytes, lymphocytes and macrophages. Transmission is mainly by the tick vector *Rhipicephalus sanguineus*. During acute or subclinical phase, immunocompetent dogs eliminates the infection (Breitschwerdt, *et al.*, 1998; Codner *et al.*, 1986; Harrus *et al.*, 1998) and some will develop to chronic phase characterized by peripheral pancytopenia, bone marrow aplasia, high mortality due to septicemia or severe bleeding (Mylonakis *et al.*, 2004). Clinical signs range from mild to life threatening disease (Waner *et al.*, 2013). The typical clinical signs include fever, lethargy, splenomegaly, lymphadenopathy, bleeding tendency and ocular abnormalities (Sainz *et al.*, 2015; Shipov *et al.*, 2008; Mylonakis *et al.*, 2011). The common biochemical abnormalities comprise hyperproteinemia, hyperglobulinemia, hypoalbuminemia and mild elevation of alkaline phosphatase and alanin aminotransferase activity (Waner *et al.*, 1997; Frank *et al.*, 1999; Shipov *et al.*, 2008; Harrus *et al.*, 1996; Mylonakis *et al.*, 2010). Owing to its fatality, it is necessary that the disease must be diagnosed at the earliest, with considerable amount of sensitivity to ensure successful treatment (Lakshmanan *et al.*, 2007). Indirect fluorescent antibody is considered as the gold standard for diagnosis of canine Ehrlichiosis, but many tests are being considered as outdated and necessary validation is in the process to replace them with nucleic acid based detection methods (Parikh *et al.*, 2008).

The diagnosis of canine Ehrlichiosis is based on haematological, biochemical and serological tests. Microscopic evaluation of stained blood smears is not sensitive as organisms are not readily demonstrable in blood smears. Serological tests fail to distinguish current infection from previous or unestablished infections. Serological cross-reactivity considerably alters its specificity (Lakshmanan *et al.*, 2007). Nucleic acid based detection or screening methods are nowadays considered for the diagnosis. Some of the diagnostic molecules targeted for *E. canis* include, 16S rRNA gene (Yabsley *et al.*, 2008), *virB9* gene (Kledmanee *et al.*, 2009) and *gp200* gene (Maekawa *et al.*, 2018). *VirB9* is one of the outer membrane proteins of the Type IV secretion system and considered as an ideal target as is highly antigenic and expressed in both mammalian and tick host (Felek *et al.*, 2003). The present study was designed to evaluate the nucleic acid based test targeting *virB9* gene and compared the microscopic examination for the diagnosis of *E. canis*.

MATERIALS AND METHODS

Study area

The study area comprised different regions of Northern Kerala (Kannur - latitude 11.87° and longitude 75.37°, Wayanad - latitude 11.68° and longitude 76.13° and Kozhikode- latitude 11.25° and longitude 75.78°) (Fig 1).

Collection and processing of samples

A total of 113 peripheral blood smears and whole blood sample of the dogs suspected for ehrlichiosis was collected from Teaching Veterinary Clinical Complex, Pookode and District Veterinary Centres (Kozhikode, Kannur). The peripheral blood smears were stained with Giemsa stain for microscopic examination. The whole blood was collected with an anticoagulant and the genomic DNA was isolated using DNeasy® blood and tissue kit (Qiagen, Germany) according to the manufacturer's protocol. The genomic DNA was used as a template in the PCR using species specific primer (Table 1) for the detection of *virB9* gene (Kledmanee *et al.*, 2009). The PCR reaction was standardized for a

17608



**Angeline Felicia Bora et al.**

25µL reaction which consisted of 2.5µL of 10X buffer, 2.5µL (0.2mM) dNTP mix, 1 IU *Taq* DNA Polymerase, 10 pmol each of forward and reverse primer, 2µL (20 ng) of template DNA and the volume was made up using autoclaved millipore water. The PCR reaction was standardized at the following cycling conditions: initial denaturation at 94°C for 2 mins, 35 cycles of denaturation at 94°C for 30 sec, annealing at 60°C for 30 sec, extension of 72°C for 1 min and final extension at 72°C for 10 min. Samples were analyzed by electrophoresis using 2 per cent agarose in 10mg ethidium bromide and visualized by Gel documentation System (UVITECH, Cambridge). The positive samples were purified using Nucleospin® Gel and PCR Clean-up kit (Macherey-Nagel, Germany) and sequencing was done at AgriGenome Lab Private Limited, Kochi, Kerala by Sanger dideoxy sequencing method. The sequences were analysed by EditSeq (DNASTar) and homology between sequences was conferred based on NCBI-BLAST.

RESULTS

In the present investigation, out of 113 peripheral blood smears examined, none of the samples were positive for morula stage of *Ehrlichia canis*. Positive control was collected from TVCC, Veterinary College Gunnavaram, Andhra Pradesh. Out of 113 blood samples processed by PCR, only one sample showed amplification of ~380 bp fragment specific for *E. canis* (Fig: 2). The NCBI-BLAST (National Centre for Biotechnology Information- Basic Local Alignment Search Tool) analysis revealed 99 per cent identity with the published sequences of *E. canis* from Chennai and U. P. The evolutionary history of *E. canis* isolate based on *virB9* gene was inferred by using Neighbor-joining method based on Tamura-3 (T92) model. The evolutionary history of *E. canis* isolate based on *vir B9* gene was inferred by using Neighbor-joining method based on Tamura-3 (T92) model. The analysis using 10 nucleotide sequences and the phylogenetic tree based on *virB9* gene of *E. canis* indicated that *E. canis* field isolates of Kerala in the present study formed a single clade clustered along with the other Indian isolates from Chennai and Uttar Pradesh and sequences from countries like New Mexico, Venezuela, Hawaii, California, USA and Arizona. The *Toxoplasma gondii* was used as outgroup (Fig.3)

DISCUSSION

In the present study, 0.88 per cent prevalence of *E.canis* could be detected by PCR targeting *virB9* gene from northern zone of Kerala. The BLAST (Basic Local Alignment Search Tool) revealed 99 per cent identity with *E. canis* of previously published sequences from Chennai and Uttar Pradesh. Kledmanee *et al.* (2009) used multiplex PCR for detection of *E. canis*, *H. cani* and *Babesia* spp. in Thailand. They targeted the *virB9* gene of *E. canis* by PCR and five dogs were found positive. Nazari *et al.* (2013) detected 2 per cent prevalence of *E. canis* infection in Malaysia targeting 16S rRNA gene. Based on *virB9* gene of *E. canis*, Kukreti *et al.* (2018) reported prevalence of 8.8 per cent of *E. canis* from north and western parts of India with 98 per cent similarity with the isolates from Mexico, Venezuela, Hawaii and California.

From South India, Azhahianambi *et al.* (2018) reported a prevalence of 16.4 per cent of *E. canis* infection among dogs of Chennai by targeting *virB9* gene by multiplex PCR. Similarly, Lakshmanan *et al.* (2007) reported a prevalence of 50 per cent of dogs in Chennai were infected with *E. canis* infection by PCR. Rajagopal *et al.* (2009) detected *E. canis* infection in dogs of Chennai by serological test (Indirect Fluorescent Antibody Test) and polymerase chain reaction (PCR). This is the first attempt in Kerala to study the *E. canis* infection in dogs by targeting *virB9* gene. In the present investigation, the phylogenetic tree was constructed based on the *virB9* gene of *E. canis*. The field isolates of Kerala formed a clade along with Indian (Uttar Pradesh and Chennai isolates) and foreign countries (Mexico, USA, Venezuela, Hawaii and California). This study indicated that the isolates of *E. canis* present in Southern and Northern parts of India has an ancestral evolutionary relationship with the North and South American isolates. This is the first attempt to study the phylogenetic relationship among the *E. canis* isolates of Kerala. This study supported the previous findings by Kukreti *et al.*, 2018.





REFERENCES

1. Azhahianambi P, Jyothimol G, Baranidharan GR, Aravind M, Latha BR, Raman M (2018) Evaluation of multiplex PCR assay for detection of *Babesia* spp, *Ehrlichia canis* and *Trypanosoma evansi* in dogs. *Acta tropica* 188: 58-67
2. Breitschwerdt EB, Hegarty BC, Hancock SI (1998) Sequential Evaluation of Dogs Naturally Infected with *Ehrlichia canis*, *Ehrlichia chaffeensis*, *Ehrlichia equi*, *Ehrlichia ewingii*, or *Bartonella vinsonii*. *J Clin Microbiol* 36: 2645-2651
3. Codner EC, Farris-Smith LL (1986) Characterization of the subclinical phase of Ehrlichiosis in dogs. *J Am Vet Med Ass* 189: 47-50
4. Felek S, Huang H, Rikihisa Y (2003) Sequence and expression analysis of virB9 of the type IV secretion system of *Ehrlichia canis* strains in ticks, dogs, and cultured cells. *Infection and Immun* 71: 6063-6067
5. Frank JR, Breitschwerdt EB (1999) A retrospective study of Ehrlichiosis in 62 dogs from North Carolina and Virginia. *J Vet Internal Med* 13: 194-201
6. Harrus S, Waner T, Aizenberg I, Bark H. (1998) Therapeutic effect of doxycycline in experimental subclinical canine monocytic ehrlichiosis: evaluation of a 6-week course. *J Clin Microbiol* 36: 2140-2142
7. Harrus S, Waner T, Avidar Y, Bogin E, Peh HC, Bark H (1996) Serum protein alterations in canine ehrlichiosis. *Vet Parasitol* 66: 241-249
8. Jadhav RK, Kumari RR, Jameel A, Kumar P (2011) Emergence of Arthropod Transmitted infections in Kennel Dogs. *Vet World* 4: 522-528
9. Kledmanee K, Suwanpakdee S, Krajangwong S, Chatsiriwech J, Suksai P, Suwannachat P, Sariya L, Buddhirongawatr R, Charoonrut, P, Chaichoun K, Pathom N (2009) Development of multiplex polymerase chain reaction for detection of *Ehrlichia canis*, *Babesia* spp and *Hepatozoon canis* in canine blood Southeast Asian J Trop Med Public Hlth. 40: 35-39
10. Kukreti K, Pandey L, Das M, Rastogi A, Dubey R, Sharma P (2018) Prevalence of Canine Monocytic Ehrlichiosis in Canine Population Across India. *Archives of Razi Inst* 73: 87-93
11. Lakshmanan B, John L, Gomathinayagam S, Dhinakarraj G (2007) Molecular detection of *Ehrlichia canis* from blood of naturally infected dogs in India. *Veterinarski arhiv* 77: 307
12. Maekawa N, Konnai S, Balbin MM, Mingala CN, Gicana KR, Bernardo FA, Murata S, Ohashi K (2018) Molecular detection and phylogenetic analysis of *Ehrlichia canis* in a Philippine dog. *Ticks and tick-borne Dis* 9: 266-269
13. Mylonakis ME, Theodorou KN (2017) Canine monocytic Ehrlichiosis: An update on diagnosis and treatment. *Acta Veterinaria* 67: 299-317
14. Mylonakis ME, Ceron JJ, Leontides L, Siarkou VI, Martinez S, Tvarijonaviciute A, Koutinas AF, Harrus S (2011) Serum acute phase proteins as clinical phase indicators and outcome predictors in naturally occurring canine monocytic Ehrlichiosis. *J Vet Internal Med* 25: 811-817
15. Mylonakis ME, Koutinas AF, Breitschwerdt EB, Hegarty BC, Billinis CD, Leontides LS, Kontos, VS (2004) chronic canine Ehrlichiosis (*Ehrlichia canis*): a retrospective study of 19 natural cases. *J Am Anim Hospital Ass* 40: 174-184
16. Mylonakis ME, Kritsepi-Konstantinou M, Dumler JS, Diniz PPVP, Day MJ, Siarkou VI, Breitschwerdt EB, Psychas V, Petanides T, Koutinas (2010) Severe hepatitis associated with acute *Ehrlichia canis* infection in a dog. *J Vet Internal Med* 24: 633-638
17. Nazari M, Lim SY, Watanabe M, Sharma RS, Cheng NA, Watanabe M. 2013. Molecular detection of *Ehrlichia canis* in dogs in Malaysia. *PLoS neglected Trop Dis*. 7: 1982
18. Parikh R, Mathai A, Parikh S, Sekhar GC, Thomas R. 2008. Understanding and using sensitivity, specificity and predictive values. *Indian J Ophthalmol* 56:45
19. Rajagopal A, Basith SA, Gomathinayagam S, Dhinakarraj G (2009) Evaluation of PCR and IFAT in the Diagnosis of Canine Ehrlichiosis *J Appl Anim Res* 35: 189-191
20. Rani PAMA, Irwin PJ, Gatne M, Coleman GT, Traub RJ (2010) Canine vector-borne diseases in India: a review of the literature and identification of existing knowledge gaps. *Parasite vectors* 3: 28





Angeline Felicia Bora et al.

21. Sainz A, Roura X, Miro G, Estrada-Pena A, Kohn B, Harrus S, Solano-Gallego, L (2015) Guideline for Vet practitioners on canine Ehrlichiosis and Anaplasmosis in Europe. Parasites vectors 8: 75
22. Shipov A, Klement E, Reuveni-Tager L, Waner T, Harrus S (2008) Prognostic indicators for canine monocytic Ehrlichiosis Vet Parasitol 153: 131-138
23. Waner T, Harrus S (2013) Canine monocytic Ehrlichiosis-from pathology to clinical manifestations Isr J Vet Med 68: 12-18
24. Waner T, Harrus S, Bark H, Bogin E, Avidar Y, Keysary A (1997) Characterization of the subclinical phase of canine Ehrlichiosis in experimentally infected beagle dogs Vet Parasitol 69: 307-317
25. Yabsley MJ, McKibben J, Macpherson CN, Cattani PF, Cherry NA, Hegarty BC, Breitschwerdt EB, O'Connor T, Chandrashekar R, Paterson T, Perea ML (2008) Prevalence of *Ehrlichia canis*, *Anaplasma platys*, *Babesia canis vogeli*, *Hepatozoon canis*, *Bartonella vinsonii berkhoffii* and *Rickettsia* spp. in dogs from Grenada Vet Parasitol 151: 279-285

Table1. Primer sequence for virB9 gene of Ehrlichia canis

Species	Sequence name	Amplicon size
<i>Ehrlichia canis</i> (Kledmanee et al., 2009)	<p>E. canis Ehr 1401 protein gene forward: CCA TAA GCA TAG CTG ATA ACC CTG TTA CAA (30 bp)</p> <p>E. canis Ehr1780R protein gene reverse: TGG ATA ATA AAA CCG TAC TAT GTA TGC TAG (30bp)</p>	380bp



Fig. 1. Place of sample collection





Angeline Felicia Bora et al.

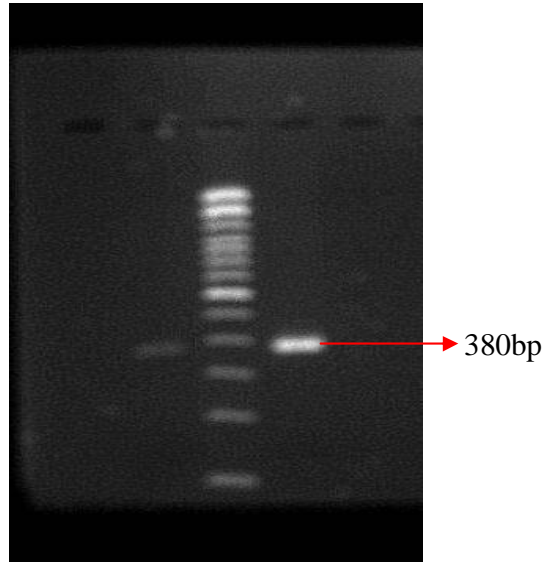


Fig.2. Lane 1: Sample; Lane P: Positive control N: Non template control
PCR amplification of *virB9* gene of *Ehrlichia canis*

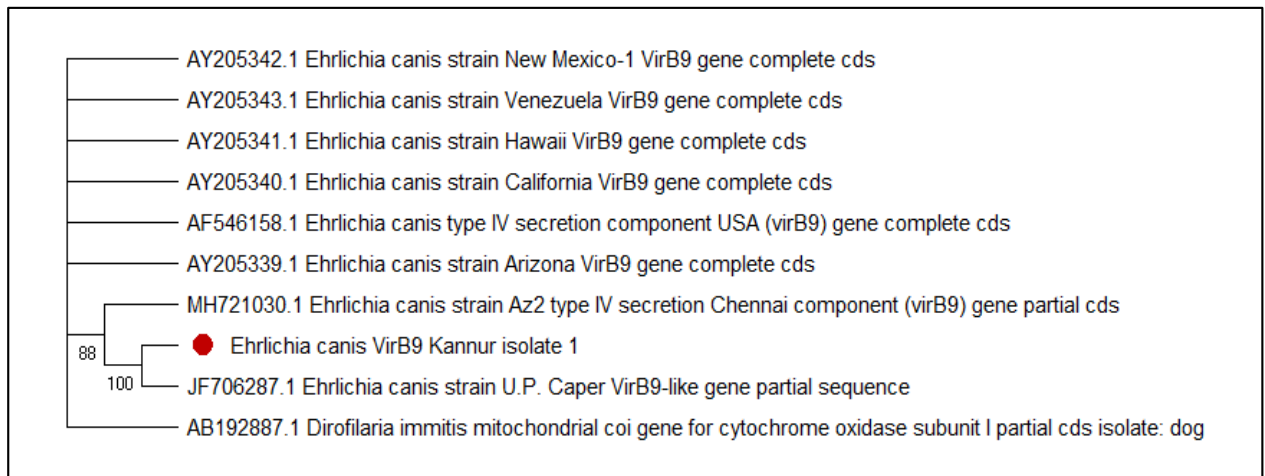


Fig.3. Phylogenetic analysis based on *virB9* gene of *Ehrlichia canis*





Characterization of Salt Tolerance in Rice Landraces (*Oryza sativa* L.) at Seedling Stage

Md.Monjurul Huda¹, Md. Nuruzzaman¹, M.Asaduzzaman Prodhan², Aleya Ferdausi¹ and Md.Amir Hossain^{1*}

¹Department of Genetics & Plant Breeding, Bangladesh Agricultural University, Mymensingh - 2202, Bangladesh

²School of Biological Sciences, The University of Western Australia, 35 Stirling Highway, Crawley, Perth, WA 6009, Australia.

Received: 20 June 2019

Revised: 24 July 2019

Accepted: 26 Aug 2019

*Address for Correspondence

Md.Amir Hossain

Department of Genetics & Plant Breeding,
Bangladesh Agricultural University,
Mymensingh - 2202, Bangladesh
Email: amirgpb@gmail.com



This is an Open Access Journal / article distributed under the terms of the **Creative Commons Attribution License** (CC BY-NC-ND 3.0) which permits unrestricted use, distribution, and reproduction in any medium, provided the original work is properly cited. All rights reserved.

ABSTRACT

Soil salinity is the greatest challenge for crop production worldwide. Rice production, in particular, is critically encountered with this stress as rice is the most salt sensitive cereal. Developing salt tolerant rice variety might mitigate this challenge. Characterization and genetic diversity analysis of the existing rice landraces in relation to the salt-tolerance could provide novel traits for breeding salt tolerant genotypes. Here, we aimed to evaluate whether there was any genetic diversity among thirty common rice landraces in Bangladesh in terms of salt tolerance. We screened the landraces using molecular markers to identify the salt tolerant genotypes. Our results showed that Boilam, Nonabokri, Gunshi, and Motabamonkhir showed greater salt tolerance at different levels of salt stress (6 dSm^{-1} and 10 dS m^{-1}) in hydroponics culture. Our microsatellite markers assay revealed that there was *Saltol* loci in twenty-four genotypes except Jamaibabu, Chinikanai, Changai, Ghigoj, BRR1 dhan 23 and BRR1 dhan 55. *Saltol* confers salinity tolerance in plants. Collectively considering all of the above results the existence of high genetic diversity for salt tolerance among the studied rice genotypes was prevailed, thus lay a breeding foundation for developing salt tolerant rice varieties.

Key words: Genetic variability, Salt stress, hydroponic culture and molecular marker.





Monjurul Huda et al.

INTRODUCTION

Rice (*Oryza sativa* L.) is one of the most important cereals in the world. It is staple food for about 50% of the total population worldwide. It is the third-highest produced crops, after sugarcane and maize, across the globe (1). Among the rice producing countries, Bangladesh is fourth in terms of total rice production. Bangladesh produces about 34,500 thousand metric ton rice annually from approximately 11,790 thousand hectare of land (2). An increased rice production was reported through the 'Green Revolution' in 1970s, but afterwards the production rate dropped and remained steady (3). Many factors are attributed to this decline. However, reduction of arable lands due to the extension of industrialization on arable lands is one of the major players. Agricultural production is also threatened by many environmental obstacles such as drought, flood and salinity (4). Among these, soil salinity has become more alarming. Because of the saline area around the globe is gradually increasing due to increasing use of ground water for irrigation, resulted gradual increasing of the sea level (5). Salinity is considered as the second most widespread soil problem in rice growing areas of the world after drought (6). Rice plants are very sensitive to salinity at seedling stage (7). However, salinity at reproductive stage causes delayed flowering and reduction in the number of effective tillers, grains per panicle, grain weight and ultimately grain yield (4, 8). These circumstances have been a bottleneck for rice production in saline areas. Salt tolerant rice varieties can potentially relieve this problem. Screening of the existing rice landraces might guided a genetic target for breeding salt-tolerant rice varieties (9). Progress has been made in molecular marker analysis allowing for identification of genes conferring salt tolerance (10). For an example, microsatellite markers are available for pre-breeding screening of rice germplasm for the presence for *Saltol*, an important Quantitative Trait Locus (QTL) linked to salt tolerance (11, 12, 13). Such markers have already been deployed in several breeding strategies, for example, genetic mapping under saline condition (9, 14, 15, 16). The present study was conducted to evaluate the performance of rice landraces in salt stress including *Saltol* specific SSR markers based molecular characterization and the result was evaluated with the morphological performance and along with the genetic diversity studies of the genotypes.

MATERIALS AND METHODS

Plant materials

A total of thirty rice genotypes (twenty four landraces and six high yielding varieties) were used in this experiment. The seeds of these materials are collected from Bangladesh Rice Research Institute (BRRI) (Table 1).

Screening of salt tolerance genotypes under hydroponic culture

The hydroponic experiment was conducted in a growth chamber of 10×11 square feet concreted room with controlled light and temperature facilities. Sterilized and dried seeds were placed in petridishes containing moist filter paper and kept in dark for 3 to 4 days for sprouting. The four to five days old seedlings were transferred to hydroponic medium (Peters professionals Product Use Guide, Water Soluble Fertilizers) by wrapping with sponge. Two salt treatments (6dSm^{-1} and 10dSm^{-1}) were used by adding 2g and 4.25g NaCl to the normal nutrient solution (1.3dSm^{-1}) to observe the performances of rice seedlings at different salinity levels. Seedlings were treated to salt treatments for seven days and then they were transferred to the normal nutrient solution. The International Rice Research Institute (IRRI) documented modified SES (Standard Evaluation Score) was used to estimate the visual symptoms of salt toxicity (Supp. Table 1). The scoring was used to discriminate the genotypes into tolerant, moderately tolerant, and susceptible varieties. The scoring was performed after 14 to 16 days after salt treatment.



**Monjurul Huda et al.****Data collection and analysis**

Data were collected on different shoot (percent of live leaves, main axis diameter, number of primary axis, primary axis diameter, primary axis length and shoot dry weight) and root (root length, total number of roots and root dry weight) parameters after 18 days of hydroponic culture by successive destructive harvest. The experiment was designed by two-factor Randomized Complete Block Design (RCBD) with three replicates. Analysis of variance (ANOVA) was performed using the plant breeding statistical program (Utzzal, MSTATc and PLABSTAT, Version 2N, 2007).

Microsatellite marker based screening of rice genotypes for salinity tolerance

Leaf samples were collected from 15 days old vigorous seedlings of thirty rice genotypes grown on hydroponic media to extract genomic DNA. Leaves samples were sterilized processed and stored following the same protocol used by Nuruzzaman (9). DNA was extracted using Cetyl Trimethyl Ammonium Bromide (CTAB) mini-prep method. The simplified mini scale procedure for DNA isolation in PCR analysis developed at IRRI was used (9, 17). Isolated genomic DNA was evaluated using 1% agarose gel electrophoresis (9). Three pairs of primers (Salt-1, RM1287 and RM7075) were tested in one randomly chosen individual from 30 rice genotypes to evaluate their suitability for amplifying DNA sequences, which could be accurately scored. Primers were selected based on band resolution intensity, presence of smearing, consistency within individuals and potential for population discrimination. The details of the primers used are given in Table 2.

RESULTS**Screening of rice genotypes for salt tolerance at seedlings stage**

Various stress symptoms were recorded under different levels of salinity (control, EC-6 dSm⁻¹ and EC-10 dSm⁻¹) such as yellowing of leaves, drying of leaves, leaf curling, reduced growth rate and seedling drying (Figure 1) in thirty rice genotypes after seven days of salinization. Seedlings that were not exposed to salinity showed normal growth and salt tolerant genotypes (according to SES, Table 4) showed relatively better growth and lower symptoms than susceptible genotypes (according to SES, Table 3) (Figure 1). Nonabokri and Motabamonkhir were highly tolerant (without any stress symptoms), eight genotypes were tolerant (minimum level of stress symptoms), fifteen genotypes were moderately tolerant (high level of stress symptoms but survived) and remaining five of them were found susceptible at lower salt treatment (6 dSm⁻¹) (Table 3). On the contrary, at higher salt concentration (10 dSm⁻¹) most of the genotypes (fifteen out of thirty) were susceptible. Some of which were moderately tolerant at lower salt concentration. Eleven genotypes were moderately tolerant and only four genotypes were tolerant at high salinity (Table 3).

Mean performance of the genotypes

Significant variation was observed among the thirty genotypes for various morphological traits for different level of salinity. The survival rate varies from 1.11 to 100% among the studied genotypes. The genotype Nonabokri had the highest percentage of live leaves (87.04%), number of roots (5.40), root dry weight (0.366 mg) as these traits are desired for high salt tolerance. Similarly the genotype Kutipathai showed the maximum diameter of main axis (24.24 μm) and primary axis (3.19 μm). Both the highest number of root hairs (41.31) and longest root hair (17.49 μm) in main axis was found in Pokkali. The maximum fresh (13.73 mg) and dry (18.79 mg) weight of root and number of primary axis (8.71) were found in Gunshih while these traits were lowest in Jamaibabu. Lower Standard Evaluation Score (SES) is expected for salt tolerant genotypes. The average range of the SES among the genotypes was 4.81 to



**Monjurul Huda et al.**

1.72 and the standard deviation was ± 0.68 . Among the genotypes, the highest estimation of SES was found in Thikeirum (4.81) and the lowest was in Nonabokri (1.72).

Mean effects of the treatments on different morphological traits

The control treatment showed better performance compare to others for all of the studied growth parameters except the main axis diameter. Where the maximum percentage of live leaves (65.49%), survival rate (82.13%), total number of roots (4.55), root length (9.18 cm) were observed for control followed by treatments EC-6 dSm⁻¹ and EC-10 dSm⁻¹ respectively. In case of number of primary axis (7.20), length of primary axis (38.61 μm), diameter of primary axis (2.076 μm), number of root hairs (38.84), length of root hairs (15.45 μm), root fresh and dry weight (8.71 & 0.241 mg), shoot fresh and dry weight (2.29 & 0.24 mg) were also high in control treatment followed by treatments EC-6 dSm⁻¹ and EC-10 dSm⁻¹ respectively. SES was highest in EC-10 dSm⁻¹ treatment (3.908) followed by EC-6 dSm⁻¹ (3.235) and control (2.233) treatment.

Mean combined effects of genotypes and treatments on different morphological traits

The combinations of genotypes and control treatment showed the maximum percentage of live leaves, survival rate, shoot dry weight, number of roots, length of roots, number of primary axis, length of primary axis, diameter of primary axis, number and length of root hairs on main axis, fresh and dry weight of root and shoot whereas these traits scored lowest in the combination of genotypes and higher salt concentration (EC-10 dSm⁻¹). However, the main axis diameter was an exception. It was highest in case of combinations of genotype and EC-10 dSm⁻¹ treatment and lowest in combination of Chinikanai and control treatment. It is expected that salt tolerant genotypes will have lower SES score. The average range of the SES score among the combinations was 1 to 5. The lowest value was in combination of Nonabokhri and control treatment (1) while the highest value was in combination of BRR1 dhan 23 and EC-10 dSm⁻¹ (5).

Nature and magnitude of diversity

Depending upon the range of diversity, 30 genotypes were grouped into five clusters (Table 5). The distribution pattern revealed maximum number of genotypes (10 genotypes) in cluster II whilst cluster IV included minimum number of genotypes (3 genotypes). Cluster I, III and V included 6, 4 and 7 genotypes, respectively. The inter-cluster distances in all the cases were greater than the intra-cluster distances suggesting wider diversity among the genotypes of the distant groups (Table 6). Maximum intra-cluster degree of diversity was observed in cluster II (95.19) and minimum in cluster I (49.37). The maximum inter-cluster distance (139.55) was from cluster II and IV and the minimum between cluster I and V (59.20). Mean performance of different clusters for different morphological traits studied are shown in supplementary table 4.

Presence of salt tolerant QTL in thirty rice genotypes using microsatellite markers

Three sets of microsatellite markers i.e. SalT-1, RM1287 and RM7075 were used to identify the presence of salt tolerant QTL, which confers salt tolerance in rice. These primers produced a 155 base pair long Polymerase Chain Reaction (PCR) amplicon and detected the presence of *Salto* QTL in some rice genotypes. However, in some rice genotypes the primers did not produce such an amplicon suggesting the absence of *Salto* QTL in these genotypes. The RM7075 produced the PCR amplicon in maximum rice genotypes under this study. Banding pattern of these three primers are presented in supplementary table 3 and Figure 2.1, 2.2 and 2.3.



**Monjurul Huda et al.**

DISCUSSION

Screening of rice genotypes for salt tolerance at seedlings stage

Various stress symptoms such as yellowing of leaves, drying of leaves, leaf curling, reduced rate of growth and finally seedling drying were recorded within 10-14 days after salt stress (control, EC-6 dSm⁻¹ and EC-10 dSm⁻¹). These salinity-stress symptoms have also been reported by several scientists (14, 15, 18, 19). While the seedlings which were not subjected to salinization (controlled treatment) showed normal growth and the salt tolerant lines also showed relatively better growth and lower symptoms than susceptible genotypes after salinization. The genotypes were sorted according to modified standard evaluation score (SES) (1-5 scale) developed by the International Rice Research Institute (IRRI) (20). At lower salt concentration, Nonabokri and Motabamonkhir were highly tolerant (without any injury), eight genotypes were tolerant (minimum level of injury), fifteen genotypes were moderately tolerant (injured but survived) and remaining five of them was found susceptible. But when the salt concentration was higher, then the tolerance level became lower. At higher salt concentration, most of the genotypes (fifteen out of thirty) were found susceptible, some of them were moderately tolerant at lower salt concentration but at higher salt stress they could not survive. Eleven genotypes were moderately tolerant and only four genotypes were tolerant at higher salt concentration. It indicates that the tolerance level decreases by the increase of salinity. Similar observation was reported by Zeng and Shanon (21). The four tolerant (Boilam, Nonabokri, Gunshi, Motabamonkhir) genotypes at higher salt concentration can be used for further breeding program to incorporate the salinity tolerance in the elite rice varieties.

Evaluation of mean performance of thirty rice genotypes under different salt concentration

All the genotypes revealed considerable amount of differences in their mean performance with respect to all the traits studied. This had also been exemplified by highly significant mean sum of squares for these characters, which indicated that, the lines under study were genetically diverse. Mean performance of plant materials helps to determine the diversity of the rice genotypes. Multivariate statistical analysis regarding the combined effects of genotypes and treatments on different morphological traits provides important information about the tolerance level of the genotypes. Percentage of live leaves and the survival rate of the plants are very important to estimate their tolerance level. High percentage of live leaves and survival rate under saline condition indicate high tolerance level (22). Genotypes having high root length, root number, root fresh and dry weight, and shoot fresh and dry weight under saline conditions indicate that the particular genotypes grow well under salinity stresses (23).

Nature and magnitude of diversity

Depending upon the range of diversity, 30 rice genotypes were grouped into five clusters (Table 5). The inter-cluster distances in all the cases were greater than the intra-cluster distances revealing a wider diversity among the genotypes of the distant groups (Table 6). Zia-UI-Qamar (24) and Islam (25) described the similar results regarding inter and intra-cluster distances. The range of intra-cluster values showed generally heterogeneous nature of the genotypes within the clusters. The intra-cluster degree of diversity was maximum in cluster II (95.19) and minimum in cluster I (49.37), indicating that the genotypes in cluster II were more heterogeneous than those in cluster I and they were comparatively more closely related. Zia-UI-Qamar (24) and Jagadev (26) also found divergence among various clusters and they concluded that the traits contributing maximum towards the divergence should be given greater emphasis for deciding the type of cluster for the purpose of further selection and the choice of parents for hybridization. In the present study, relatively high genetic distance existed between cluster I and V, Therefore, parents from those clusters having medium magnitude of divergence also have a potential for trait improvement. There are reports that selection of parents for hybridization should be from two clusters having wider inter-cluster distance to get maximum variability in the segregating generations and subsequent selection of ideotypes (27, 28).





Monjurul Huda et al.

Detection of salt tolerant QTL using microsatellite markers

The three microsatellite markers produced clear bands in some genotypes, which revealed the presence of *Saltol* QTL. Among the thirty rice genotypes, Salt-1 and RM1287 identified 23 genotypes having *Saltol* QTL and RM7075 identified 24 genotypes having *Saltol* QTL. That does not reveal that all of these genotypes are successfully tolerant to salinity stress. Most of them are 'moderately tolerant' to 'tolerant in lower salt concentration' but they are susceptible while salt concentration is higher in the soil (Table 3). The phenotypic study showed four genotypes as tolerant and eleven genotypes as moderately tolerant at higher salt concentration. These 15 genotypes also showed bands for three microsatellite markers (Salt-1, RM1287 and RM7075), which revealed that these 15 genotypes would be considered as the tolerant genotypes in response to salinity. However, further research is needed for the confirmation of their tolerance level. On the other hand, the absence of *Saltol* QTL in Jamaibabu, Chinikanai, Changai, Ghigoj, BRRI dhan 23 and BRRI dhan 55 was confirmed by all three pair of primers. Therefore, these genotypes could be considered as susceptible rice varieties in response to salinity stress.

CONCLUSION

The present study assessed the genetic variation in 30 rice landraces in Bangladesh and revealed the morphological traits that are highly related to salt tolerance. Our results detected the presence of high genetic diversity in several morphological traits under the saline conditions. These traits are considered as a major yield contributing factors in rice. Our results also showed the relationship between different important morphological traits in response to different salinity levels based on the SES scores, which would help to identify the yield contributing traits as well as salt tolerance level of different rice genotypes under moderate to high saline conditions. While our findings narrow down the search for salt-tolerant rice genotypes, a further confirmation of the presence of salt tolerant QTL (*Saltol* QTL) in Boilam, Nonabokri, Gunshi, Motabamonkhir, Chapsali, Jamainadu, Horkuch, Chiknul, Gopalbhog, Hogla, BRRI dhan-40, Changai, BRRI dhan54, Pokkali and Birpala would be a rational next step forward towards developing salt-tolerant high yielding rice varieties.

ACKNOWLEDGEMENT

The authors would like to thank the department of Genetics and Plant Breeding, Bangladesh Agricultural University for the support to conduct the experiment.

REFERENCES

1. FAOSTAT 2015. World's crop production. Food and agriculture organization.
2. USDA 2015. Bangladesh: Grain and Feed Annual-2015. GAIN Report. USDA Foreign Agricultural Service. (<http://www.usda.gov/wps/portal/usda/usdahom>).
3. Maclean JL, Dawe DC, Hardy B, Hettel GP, Almance R. International Rice Research Institute, Bouake (Cote d'ivoire); West Africa Rice Development Association, Cali (Colombia); International Centre for Tropical Agriculture, Rome, Italy. 2002; 253.
4. Gregorio GB, Senadhira D, Mendoza RD, Manigbas NL, Roxas JP, Guerta CQ. Progress in breeding for salinity tolerance and other abiotic associated stresses in rice. *Journal of Field Crops Research*. 2002; 76: 91-101.
5. Mori I, Koh T. Salt tolerance of rice callus clones. *Rice Genetics Newsletter*. 1987; 4: 112-113.
6. Gregorio GB. Tagging salinity tolerance genes in rice using amplified fragment length polymorphism (AFLP). PhD. thesis, University of the Philippines, Los Baños, 1987, pp. 118.
7. Akber M, Yabuno T. Breeding for saline resistant varieties of rice: Comparative performance of rice varieties to salinity during early development stage. *Journal of Breeding*. 1974; 25: 176-181.



**Monjurul Huda et al.**

8. Khatun S, Rizzo CA, Flowers TJ. Genotypic variations in the effect of salinity on fertility in rice. *Journal of Plant and Soil*. 1995; 123:239-250.
9. Nuruzzaman M, Hassan L, Begum SN, Huda MM. Molecular characterization and genetic diversity of nerica mutant rice lines using SSR marker. *International Journal of Experimental Agriculture*. 2017; 7: 9-21.
10. Flowers TJ. Improving crops salt tolerance. *Journal of Experimental Botany*. 2004; 55:307-319.
11. Singh RK, Gregorio GB, Jain RK. QTL mapping for salinity tolerance in rice. *Journal of Physiology and Molecular Biology*. 2007; 13: 87-99.
12. Gregorio GB, Aliyu R, Adamu AK, Muazu S, Alonge SO. Tagging and Validation of SSR markers to Salinity Tolerance QTLs in Rice. *International Conference on Biology, Environment and Chemistry*. 2011; 1: 328-332.
13. Aliyu R, Adamu AK, Muazu S, Alonge SO. Tagging and Validation of SSR markers to Salinity Tolerance QTLs in Rice, Department of Biological Sciences, Ahmadu Bello University, Zaria, Nigeria. 2012; 5: 333-336.
14. Islam MM. Mapping salinity tolerance genes in rice at reproductive stage, PhD dissertation, University of the Philippines Los Baños, College, Laguna, Philippines. 2004; 1-149.
15. Niones JM. Fine mapping of the salinity tolerance gene on chromosome 1 of rice using near-isogenic lines, MSc. Dissertation, University of the Philippines Los Baños College, Laguna, Philippines. 2004; 76-78.
16. Haque T, Akhtar J, Nawaz S, Ahmad R. Morpho-physiological response of rice (*Oryza sativa* L.) varieties to salinity stress. *Pakistan Journal of Botany*. 2009; 41: 2943-2956.
17. Murray MG, Thompson WF. Rapid isolation of high molecular weight plant DNA. *Journal of Nuclear Research*. 1980; 8:4321-4326.
18. Bhuiyan MR. Efficiency in evaluating salt tolerance in rice using phenotypic and marker assisted selection, M.Sc. dissertation, Department of Genetics and Plant Breeding, Bangladesh Agricultural University, Mymensingh, Bangladesh. 2005:96.
19. Bonilla P, Dvorak J, Mackill D, Deal K, Gregorio G. RLFP and SSLP mapping of salinity tolerance genes in chromosome 1 of rice using recombinant inbred lines. *Philippine Journal of Agricultural Science*. 2002; 85: 68-76.
20. International Rice Research Institute 2006. Breeding for salt tolerance in rice. International Rice Research Institute. (<http://www.knowledgebank.irri.org/ricebreedingcourse.html>).
21. Zeng L, Shanon MC. Salinity effects on seedlings growth and yield components of rice. *Journal of Crop Science*. 2000; 40: 996-1003.
22. Shereen A, Mumtaz S, Raza S, Khan MA, Solang S. Salinity effects on seedling growth and yield components of different inbred rice lines. *Pakistan Journal of Botany*. 2005; 37:131-139.
23. Rahmanzadeh S, Kazemitabar K, Yazdifar S, Jafroudi AT. Evaluation of rice cultivars response to salinity stress through greenhouse experiment and tissue culture technique. *Asian journal of Plant Science*. 2008; 7: 207-212.
24. Zia-ul-Qamar, Akhtar J, Ashraf M, Akram M, Hameed A. A multivariate analysis of rice genetic resources. *Pakistan Journal of Botany*. 2012; 44: 1335-1340.
25. Islam MR, Bhuiyan MAR, Salam MA, Akter K. Genetic diversity in rained low land rice. *SAARC Journal of Agriculture*. 2003;1: 45-50.
26. Jagadev PN, Shamal KM, Lenka L. Genetic divergence in rapeseed. *Journal of Breeding*. 1991; 51: 465-466.
27. Rahman M, Acharya B, Sukla SN, Pande K. Genetic divergence in low land rice genotypes. *Oryza*. 1997; 34: 209-212.
28. Bose LK, Pradhan SK. Genetic divergence in deep water genotypes. *Journal of Central European Agriculture*. 2005; 6: 635-640.





Monjurul Huda et al.

Table 1. List of rice genotypes with their types and source of collection

Types	Genotypes	Source
Local Varieties	Chapsali, Thikeirum, Jamainadu, Dorkumor, Jataibalam, Kutipathai, Horkuch, Chiknul, Boilam, Jamaibabu, Gopalbhog, Ghigoj, Akundi, Nonabokri, Hogla, Chinikanai, HonumanJata, Ashfal, Changai, Gunshi, Motabamonkhir, Pokkali, Birpala, Bashfulbalam	BRRRI
HYVs	BRRRI dhan 61, BRRRI dhan 41, BRRRI dhan 23, BRRRI dhan 40, BRRRI dhan 54, BRRRI dhan 55	BRRRI

BRRRI = Bangladesh Rice Research Institute

Table 2. Details of the microsatellite markers (SSRs) used for the screening of rice genotypes for salinity tolerance

Primer Name	Repeat motif	Sequence (5' - 3')	Expected PCR ProductSize	Annealing Temperature (°C)
SalT-1	(GT) ¹⁰	F: GATGGTATTCATCGGCTACG R: AGTCCAAGAATGTCGTTTCG	159	55
RM1287	(GA) ¹⁷	F: GTGAAGAAAGCATGGTAAATG R: CTCAGCTTGCTTGTGGTTAG	162	55
RM7075	(GA) ¹⁶	F:GCGTTGCAGCGGAATTTGTAGG R: CCCTGCTTCTCTCGTGCAGTCG	155	55

F= Forward sequence; R= Reverse sequence

Table 3. Evaluation of thirty rice genotypes at seedling stage under different saline conditions based on Standard Evaluation Score (SES)

Salinity level	Tolerance level (SES scores)	Genotypes
EC-6 dSm ⁻¹	Highly tolerant (2.3 to 2.4)	Nonabokri, Motabamonkhir
	Tolerant (3.4 to 4.7)	Chapsali, Jamainadu, Boilam, Akundi, Hogla, Gunshi, Pokkali, Bashfulbalam
	Moderately tolerant (4.8 to 6.4)	Dorkumor, BRRRI dhan 61, Jataibalam, Kutipathai, Horkuch, Chiknul, Gopalbhog, Chinikanai, BRRRI dhan 40, HonumanJata, Ashfal, Changai, BRRRI dhan 54, Birpala, BRRRI dhan-55
	Susceptible (7.0 to 8.5)	Thikeirum, Jamaibabu, Ghigoj, BRRRI dhan 41, BRRRI dhan 23
EC-10 dSm ⁻¹	Tolerant (4.0 to 4.5)	Boilam, Nonabokri, Gunshi, Motabamonkhir
	Moderately tolerant (5.4 to 6.8)	Chapsali, Jamainadu, Horkuch, Chiknul, Gopalbhog, Hogla, BRRRI dhan 40, Changai, BRRRI dhan 54, Pokkali, Birpala
	Susceptible (6.9 to 8.6)	Thikeirum, BRRRI dhan 61, Dorkumor, Jataibalam, Kutipathai, BRRRI dhan 41, Jamaibabu, Ghigoj, Akundi, Chinikanai, HonumanJata, Ashfal, BRRRI dhan-55, Bashfulbalam
	Highly susceptible (9.0)	BRRRI dhan 23





Monjurul Huda et al.

Table 4. Mean effects of the treatments of different morphological traits related to Standard Evaluation Score (SES)

Treatment	Traits							
	LL	SR	TRT	RL	MAD	NPA	PAL	PAD
Control	65.49 a	82.13 a	4.559 a	9.181 a	20.22 b	7.202 a	38.61 a	2.076 a
EC-6	38.87 b	64.36 b	3.630 b	8.337 b	20.14 b	6.421 b	35.83 b	1.977 b
EC-10	21.54 c	37.65 c	2.719 c	7.666 c	20.73 a	5.891 c	34.05 c	2.068 a
LSD _{0.05}	1.13	1.63	0.133	0.238	0.304	0.165	1.03	0.062
Level of sign.	**	**	**	**	**	**	**	**
CV%	9.17	9.04	12.45	9.67	5.10	8.64	9.71	10.26
	nRHMA	LRHMA	RFW	RDW	SFW	SDW	SES	
Control	38.84 a	15.45 a	8.712 a	0.2411 a	11.74 a	2.229 a	2.233 c	
EC-6	29.38 b	8.693 b	7.007 b	0.1813 b	9.128 b	1.835 b	3.235 b	
EC-10	20.60 c	4.707 c	5.928 c	0.1276 c	6.587 c	1.420 c	3.908 a	
LSD _{0.05}	0.385	0.360	0.253	0.009	0.344	0.037	0.114	
Level of sign.	**	**	**	**	**	**	**	
CV%	4.44	12.77	11.92	14.13	12.83	6.99	12.42	

** indicates significant at 0.01 probability level.

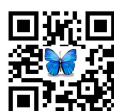
Notes: LL- Live leaves (%), SR- Survival Rate (%), TRT- Total number of Roots, RL- Root length, MAD- Main Axis Diameter, NPA- Number of primary axis, PAL- Primary axis length, PAD- Primary axis diameter, nRHMA- Number of Root hairs on the main axis, LRHMA- length of root hair on the main axis, RFW- Root fresh weight, RDW- Root dry weight, SFW- Shoot fresh weight, SDW- Shoot dry weight, SES- Standard Evaluation Score

Table 5. Number, percent and name of genotypes in different clusters

Cluster number	Number of genotypes	Percent (%)	Name of genotypes
I	6	20.00	V ₁ , V ₃ , V ₉ , V ₁₁ , V ₁₃ and V ₂₁
II	10	33.33	V ₂ , V ₄ , V ₅ , V ₆ , V ₇ , V ₈ , V ₁₀ , V ₁₂ , V ₁₄ and V ₁₅
III	4	13.33	V ₁₆ , V ₁₈ , V ₁₉ and V ₂₀
IV	3	10.00	V ₁₇ , V ₂₄ and V ₂₆
V	7	23.33	V ₂₂ , V ₂₃ , V ₂₅ , V ₂₇ , V ₂₈ , V ₂₉ and V ₃₀

Table 6. Intra and inter cluster distance in 30 rice genotypes

Cluster	I	II	III	IV	V
I	2437.67 (49.37)	5950.72 (77.14)	4160.04 (64.50)	13416.73 (115.83)	3504.38 (59.20)
II		9060.45 (95.19)	7827.12 (88.47)	19474.57 (139.55)	5804.62 (76.19)
III			2819.81 (53.10)	7241.29 (85.10)	5050.08 (71.06)
IV				5014.47 (70.81)	16423.08 (128.15)
V					3287.12 (57.33)





Monjurul Huda et al.

Supplementary Table 1. Modified Standard Evaluation Score (SES) for visual salt injury (score scale 1 to 9) (IRRI, 2010)

Score	Observation	Tolerance level
1	Normal growth, no leaf symptoms	Highly tolerant
3	Nearly normal growth, but leaf tips of few leaves whitish and rolled	Tolerant
5	Growth severely retarded , most leaves rolled; only a few are elongating	Moderately tolerant
7	Complete cessations of growth, most leaves dry; some plants dying	Susceptible
9	Almost all plants dead or dying	Highly susceptible

Supplementary Table 2. Mean performance of 30 rice genotypes on different morphological traits related to Standard Evaluation Score (SES)

Variety	LL	SR	TRT	RL	MAD
Chapsali	43.67hij	63.33gh	3.867efgh	10.33c	22.53cd
Thikeirum	3.808t	1.110p	3.311 ijk	4.367 k	23.05bc
Jamainadu	38.85klm	71.11ef	3.544hij	9.322d	22.01cdef
Dorkumor	22.10r	34.72o	3.233 jk	7.078gh	20.83ghi
BRR1 dhan 61	28.15pq	55.56jk	2.867 kl	5.400 j	20.31hij
Jataibalam	35.11mn	52.22kl	3.833fgh	7.267g	20.08 hijk
Kutipathai	28.27pq	40.00 no	3.267jk	7.756fg	24.24a
Horkuch	32.46 no	47.54lm	3.667hij	6.944gh	21.94def
Chiknul	40.19jkl	71.11ef	3.633hij	10.40c	23.57 ab
BRR1 dhan 41	25.41qr	42.96mn	3.200jk	8.700de	23.72 ab
Boilam	61.14cd	87.41bc	3.700hij	7.678fg	22.16cde
Jamaibabu	29.50op	35.56o	2.311m	7.000gh	21.42efg
Gopalbhog	48.46g	74.69 de	2.544lm	10.49c	20.97fgh
Ghigoj	27.93pq	43.33mn	2.922kl	7.289g	21.64defg
BRR1 dhan 23	16.67s	36.30o	2.667lm	8.844de	21.79defg
Akundi	54.29e	71.11ef	4.911b	6.289hi	18.75lmnop
Nonabokri	87.04a	100.0a	5.400a	8.844de	18.08 nop
Hogla	63.52c	77.78d	4.500bcd	8.900de	17.94op
Chinikanai	44.34hi	54.44jk	4.278cdef	5.800 ij	17.79p
BRR1 dhan 40	42.85hij	58.89hij	3.600hij	7.811fg	18.45mnop
HonumanJata	41.71ijk	62.22ghi	2.500lm	11.13bc	19.79 ijkl
Ashfal	37.77lm	56.67ijk	3.233jk	7.389g	19.19klmn
Changai	46.70gh	65.56fg	3.222jk	5.067jk	19.42jklm
Gunshi	59.49d	86.11c	4.711bc	11.34b	18.75 lmnop
BRR1 dhan 54	29.61op	58.12hij	4.333cde	8.289 ef	18.31 mnop
Motabamonkhir	72.63b	92.22b	3.922efgh	12.74a	17.71p
Pokkali	60.06 cd	87.78bc	3.767ghi	8.800de	18.97lmno
Birpala	49.27fg	78.40d	3.700hij	10.49 c	19.34jklm
BRR1 dhan 55	35.54mn	62.96gh	4.244cdef	7.733 fg	19.20klmn
Bashfulbalam	52.51ef	72.22e	4.189defg	12.33a	18.97klmno
LSD _{0.05}	3.58	5.16	0.421	0.754	0.962



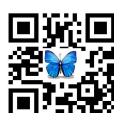


Monjurul Huda et al.

Mean	41.97	61.38	3.64	8.39	20.36
Standard Error	3.16	3.83	0.134	0.383	0.354
Standard Deviation	17.31	20.97	0.73	2.10	1.94
Minimum	3.81	1.11	2.31	4.37	17.71
Maximum	87.04	100.00	5.40	12.74	24.24
Level of sign.	**	**	**	**	**
CV%	9.17	9.04	12.45	9.67	5.10

Supplementary table 2. Mean performance of 30 rice genotypes on different morphological traits related to Standard Evaluation Score (SES) (Cont'd)

Variety	NPA	PAL	PAD	nRHMA	LRHMA
Chapsali	6.572ghi	25.05 kl	2.379de	27.48j	5.337p
Thikeirum	5.267op	23.94kl	2.289def	34.96 ef	8.006klm
Jamainadu	6.211hijk	22.68lm	2.222 ef	29.09i	6.449nop
Dorkumor	6.000 ijkl	24.90kl	2.297def	25.66k	12.01cde
BRRI dhan 61	5.867jklmn	30.68j	2.251def	30.93h	6.671no
Jataibalam	6.111ijk	39.35defg	2.096fg	36.99bc	10.90efg
Kutipathai	6.567ghi	27.35k	3.197a	21.34m	13.49b
Horkuch	7.300def	32.16ij	2.889b	21.42m	10.00ghi
Chiknul	7.911bc	35.79ghi	2.259def	30.76h	8.153klm
BRRI dhan 41	6.533ghi	19.94m	2.666c	25.13k	10.67fgh
Boilam	6.778fgh	35.35hi	1.837hi	35.78cde	9.189ijk
Jamaibabu	6.067ijk	41.20cde	1.763hij	36.39bcd	12.67bc
Gopalbhog	7.022defg	35.05hi	2.133fg	34.43ef	11.04efg
Ghigoj	5.633 klmno	40.32def	2.282def	34.80ef	8.893ijkl
BRRI dhan 23	5.211op	30.98j	2.473cd	27.74j	6.671no
Akundi	5.378 mnop	38.17efgh	2.089fg	23.20l	7.708lmn
Nonabokri	8.267ab	37.28fgh	1.777hij	27.04j	8.747ijkl
Hogla	5.000p	36.02gh	1.718hijk	19.36n	6.002op
Chinikanai	5.467lmnop	35.50hi	1.926gh	20.80m	7.114mno
BRRI dhan 40	7.356de	35.87gh	1.600jk	18.84n	5.857 op
HonumanJata	6.778efgh	38.61efgh	1.688ijk	27.24j	8.226klm
Ashfal	5.889jklm	40.46def	1.676ijk	29.18i	9.561hij
Changai	7.400 cd	48.62a	1.777hij	35.60def	12.3bcd
Gunshi	8.711a	44.54bc	1.600jk	34.39f	11.56cdef
BRRI dhan 54	8.056b	47.06ab	1.527kl	29.20i	12.38bcd
Motabamonkhir	5.267nop	47.21ab	1.376l	23.18l	8.746ijkl
Pokkali	5.422lmnop	42.91cd	2.103fg	41.31a	17.49a
Birpala	6.556ghi	40.32def	1.926gh	36.49bcd	11.27defg
BRRI dhan 55	6.467ghij	40.69def	1.704hijk	32.27g	12.82bc
Bashfulbalam	8.078b	46.84ab	1.689ijk	37.22 b	8.523jkl
LSD _{0.05}	0.523	3.27	0.195	1.22	1.14
Mean	6.50	36.16	2.04	29.61	9.62
Standard Error	0.186	1.42	0.076	1.13	0.505





Monjurul Huda et al.

Standard Deviation	1.02	7.75	0.417	6.16	2.77
Minimum	5.00	19.94	1.38	18.84	5.34
Maximum	8.71	48.62	3.20	41.31	17.49
Level of sign.	**	**	**	**	**
CV%	8.64	9.71	10.26	4.44	12.77

Supplementary Table 2. Mean performance of 30 rice genotypes on different morphological traits related to Standard Evaluation Score (SES)(Cont'd)

Variety	RFW	RDW	SFW	SDW	SES
Chapsali	7.903gh	0.1511klm	7.457gh	1.658g	2.889hijk
Thikeirum	5.037mn	0.0722q	4.288m	0.8233mn	4.810a
Jamainadu	7.770ghi	0.1700ijk	9.539de	1.807f	3.193efghi
Dorkumor	6.473kl	0.0900pq	5.121klm	1.103 k	4.023b
BRR1 dhan 61	3.603o	0.1000opq	4.570lm	0.9767l	3.426def
Jataibalam	4.454n	0.1267lmno	6.918hi	1.397hi	3.322efg
Kutipathai	5.043mn	0.08778pq	6.629hij	1.103k	3.800bcd
Horkuch	6.450kl	0.2056 gh	5.601jkl	0.9233lm	3.554cde
Chiknul	6.586jkl	0.1578jklm	8.102fg	1.291 ij	3.078fghij
BRR1 dhan 41	4.758n	0.1433 klmn	5.680jkl	0.8967lmn	3.811bcd
Boilam	8.001fgh	0.09000pq	6.776hij	1.427h	2.447lm
Jamaibabu	5.716lm	0.1000opq	3.981m	0.7867n	3.933bc
Gopalbhog	8.043fgh	0.1033opq	8.143fg	1.410hi	2.867ijk
Ghigoj	7.491hij	0.1600jkl	8.512efg	1.494h	3.812bcd
BRR1 dhan 23	3.604o	0.1122 nop	4.882klm	0.9433 lm	3.981b
Akundi	6.872ijk	0.2467f	13.79c	2.777c	2.711jkl
Nonabokri	11.20 b	0.3667a	17.47b	3.310b	1.722n
Hogla	7.229hijk	0.2267fg	12.92c	2.853c	2.411lm
Chinikanai	4.707n	0.1256mno	5.900ijk	1.180jk	3.044fghijk
BRR1 dhan 40	6.742jk	0.1867hij	8.722ef	2.060e	3.044fghijk
HonumanJata	6.464 kl	0.1678ijk	9.452de	2.068e	3.211efghi
Ashfal	8.433 efg	0.2233fg	12.98c	3.370b	3.067fghijk
Changai	7.186 hijk	0.1278lmno	9.201def	1.850f	2.978ghijk
Gunshi	13.73a	0.3289bc	18.79a	3.617a	2.329lm
BRR1 dhan 54	8.862def	0.1978ghi	9.960d	2.249d	3.454def
Motabamonkhir	10.02c	0.3156cd	17.72ab	3.391b	1.889n
Pokkali	8.968de	0.2767 e	12.62c	2.339d	2.289m
Birpala	8.547defg	0.2922de	9.955d	1.859f	2.648 klm
BRR1 dhan 55	7.161hijk	0.1956ghi	8.667efg	1.653g	3.314efgh
Bashfulbalam	9.413cd	0.3522ab	10.22d	2.222 d	2.700jkl
LSD _{0.05}	0.800	0.029	1.09	0.118	0.361
Mean	7.22	0.183	9.15	1.83	3.13
Standard Error	0.405	0.015	0.731	0.154	0.124
Standard Deviation	2.22	0.085	4.00	0.84	0.68
Minimum	3.60	0.072	3.98	0.79	1.72





Monjurul Huda et al.

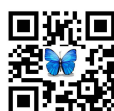
Maximum	13.73	0.367	18.79	3.62	4.81
Level of sign.	**	**	**	**	**
CV%	11.92	14.13	12.83	6.99	12.42

** indicates significant at 0.01 probability level.

Notes: LL- Live leaves (%), SR- Survival Rate (%), TRT- Total number of Roots, RL- Root length, MAD- Main Axis Diameter, NPA- Number of primary axis, PAL- Primary axis length, PAD- Primary axis diameter, nRHMA- Number of Root hairs on the main axis, LRHMA- length of root hair on the main axis, RFW- Root fresh weight, RDW- Root dry weight, SFW-Shoot fresh weight, SDW- Shoot dry weight,SES-Standard Evaluation Score

Supplementary Table 3. Mean combined effects of genotypes and treatments of different morphological traits related to Standard Evaluation Score (SES)

Genotypes	Treatment	LL	SR	TRT	RL	MAD	NPA	PAL	PAD	nRHMA	LRHMA	RFW	RDW	SFW	SDW	SES
Chapsali	Control	67.59	86.67	4.50	10.90	22.90	7.46	23.35	2.53	33.83	9.34	8.67	0.22	8.66	2.03	1.96
	EC-6	47.75	73.33	3.93	9.80	21.56	6.20	27.57	2.04	28.47	4.89	6.87	0.14	7.69	1.61	2.86
	EC-10	15.66	30.00	3.16	10.30	23.12	6.05	24.24	2.55	20.13	1.77	8.17	0.09	6.02	1.33	3.83
Thikeirum	Control	11.42	0.00	4.33	4.66	22.68	4.86	22.24	2.22	40.27	13.13	5.68	0.10	5.71	0.99	4.73
	EC-6	0.000	3.33	2.66	4.30	22.01	5.60	20.68	2.13	34.60	7.78	4.77	0.07	4.55	0.95	4.86
	EC-10	0.000	0.00	2.93	4.13	24.46	5.33	28.91	2.51	30.00	3.11	4.66	0.04	2.60	0.53	4.83
Jamainadu	Control	43.86	66.67	4.36	9.80	23.79	6.63	20.68	2.44	36.33	11.34	8.20	0.20	12.42	1.89	3.13
	EC-6	47.68	80.00	3.90	9.30	21.12	5.80	26.68	2.09	30.53	5.33	9.04	0.17	10.53	2.56	2.86
	EC-10	25.00	66.67	2.36	8.86	21.12	6.20	20.68	2.13	20.40	2.67	6.07	0.13	5.66	0.97	3.58
Dorkumor	Control	32.47	46.67	3.93	7.53	21.35	6.70	20.23	2.17	38.33	19.79	7.12	0.11	6.61	1.53	3.66
	EC-6	29.08	54.17	3.00	7.10	20.46	5.30	32.68	2.35	23.33	11.56	6.54	0.10	4.89	1.02	3.67
	EC-10	4.760	3.33	2.76	6.60	20.68	6.00	21.79	2.35	15.30	4.67	5.76	0.06	3.86	0.76	4.73
BRRIdhan 61	Control	55.56	100.0	3.26	5.66	20.46	6.50	35.13	2.28	40.47	10.67	4.96	0.19	6.85	1.15	2.33
	EC-6	28.89	66.67	2.80	4.43	20.46	5.70	29.35	2.13	31.60	7.11	3.18	0.07	4.23	0.90	3.33
	EC-10	0.000	0.00	2.53	6.10	20.01	5.40	27.57	2.33	20.73	2.22	2.67	0.04	2.62	0.88	4.61
Jataibalam	Control	53.63	66.67	4.50	7.26	20.45	6.10	41.35	2.13	43.53	15.12	5.23	0.16	7.44	1.47	2.73
	EC-6	34.78	63.33	3.66	7.03	19.79	5.60	40.91	2.13	36.40	12.01	4.91	0.12	6.44	1.42	3.20
	EC-10	16.93	26.67	3.33	7.50	20.01	6.63	35.80	2.02	31.03	5.56	3.21	0.10	6.86	1.30	4.03
Kutipathai	Control	39.75	56.67	3.86	8.33	24.46	8.06	27.57	3.25	35.53	21.12	4.88	0.14	7.07	1.29	3.50
	EC-6	34.77	50.00	3.60	7.10	22.68	5.80	21.79	3.13	19.20	12.23	4.93	0.07	7.16	1.19	3.50
	EC-10	10.28	13.33	2.33	7.83	25.57	5.83	32.68	3.20	9.300	7.11	5.31	0.04	5.64	0.83	4.40
Horkuch	Control	51.49	57.14	4.66	7.66	21.57	7.63	33.79	2.80	33.27	14.67	9.51	0.28	6.87	1.22	3.22
	EC-6	30.33	52.14	3.83	6.56	22.90	7.60	28.90	3.06	20.73	10.89	5.30	0.19	5.72	0.91	3.55
	EC-10	15.54	33.33	2.50	6.60	21.34	6.66	33.80	2.80	10.27	4.44	4.54	0.13	4.20	0.64	3.89
Chiknul	Control	60.40	86.67	4.66	11.5	23.79	7.60	39.57	2.22	44.47	12.90	6.33	0.19	9.45	1.44	2.40
	EC-6	31.60	70.00	3.66	10.33	24.01	7.60	34.24	2.19	27.67	7.33	5.53	0.14	8.17	1.28	3.30
	EC-10	28.57	56.67	2.56	9.33	22.90	8.53	33.57	2.35	20.13	4.22	7.88	0.13	6.68	1.15	3.53
BRRIdhan 41	Control	46.28	82.22	4.33	9.46	24.23	6.46	19.34	2.44	35.00	19.12	5.01	0.19	6.61	1.01	2.83
	EC-6	23.47	40.00	2.86	8.56	23.12	6.46	16.90	2.71	22.07	7.56	4.50	0.12	5.61	0.93	4.06
	EC-10	6.480	6.670	2.40	8.06	23.79	6.66	23.57	2.84	18.33	5.33	4.76	0.11	4.81	0.75	4.53





Monjurul Huda et al.

Supplementary Table 3: Mean effects of the interaction of genotypes and treatments of different morphological traits related to Standard Evaluation Score (SES) (Cont'd)

Genotypes	Treatment	LL	SR	TRT	RL	MAD	NPA	PAL	PAD	nRHMA	LRHMA	RFW	RDW	SFW	SDW	SES
Boilam	Control	80.87	96.67	4.50	8.46	21.12	6.33	31.57	1.95	41.13	16.01	10.67	0.11	8.14	1.79	1.66
	EC-6	49.72	83.33	3.60	7.16	22.01	6.86	38.02	1.77	36.53	7.55	6.87	0.10	6.88	1.41	3.26
	EC-10	52.82	82.22	3.00	7.40	23.34	7.13	36.46	1.78	29.67	4.00	6.46	0.06	5.30	1.08	2.40
Jamaibabu	Control	57.03	76.67	2.60	8.00	22.01	6.40	36.68	1.73	41.77	20.23	5.76	0.16	4.77	1.00	2.60
	EC-6	17.98	16.67	2.33	5.26	21.56	5.60	48.02	1.69	34.87	9.11	4.45	0.08	4.08	0.73	4.56
	EC-10	13.49	13.33	2.00	7.73	20.68	6.20	38.91	1.86	32.53	8.67	6.92	0.06	3.09	0.63	4.63
Gopalbhog	Control	73.37	92.96	3.36	9.50	20.90	7.66	40.46	2.35	42.33	15.12	6.36	0.12	8.56	1.47	1.90
	EC-6	38.73	77.78	2.60	11.13	21.12	6.73	32.24	1.91	32.27	10.23	8.93	0.10	8.63	1.48	3.16
	EC-10	33.29	53.33	1.66	10.83	20.90	6.66	32.46	2.13	28.70	7.78	8.83	0.09	7.23	1.28	3.53
Ghigoj	Control	53.57	83.33	3.56	8.46	21.12	6.00	41.80	2.31	41.87	14.90	8.23	0.18	10.68	2.23	2.46
	EC-6	17.89	26.67	3.26	6.70	22.68	6.00	35.57	2.22	32.67	7.78	6.76	0.16	9.58	1.31	4.37
	EC-10	12.31	20.00	1.93	6.70	21.12	4.90	43.58	2.31	29.87	4.00	7.47	0.14	5.27	0.94	4.60
BRRIdhan 23	Control	38.89	72.22	3.86	10.23	21.79	5.83	34.69	2.66	35.33	10.23	5.30	0.14	7.16	1.31	2.61
	EC-6	11.11	36.67	3.13	9.50	21.79	5.20	29.57	2.26	27.47	5.78	2.78	0.12	4.72	1.08	4.33
	EC-10	0.00	0.00	1.00	6.76	21.79	4.60	28.68	2.48	20.43	4.00	2.72	0.07	2.75	0.44	5.00
Akundi	Control	92.22	100.0	6.30	7.06	18.90	6.20	42.47	2.17	34.60	11.56	9.41	0.32	18.54	3.16	1.23
	EC-6	55.10	83.33	5.03	6.76	17.57	6.33	37.13	1.78	22.67	6.67	6.20	0.28	14.15	3.26	2.66
	EC-10	15.56	30.00	3.40	5.03	19.79	3.60	34.91	2.31	12.33	4.89	5.00	0.13	8.66	1.91	4.23
Nonabokri	Control	100.0	100.0	6.13	10.63	17.57	10.30	39.80	1.80	35.80	13.34	12.36	0.41	19.50	3.59	1.00
	EC-6	100.0	100.0	5.63	8.53	17.34	8.30	38.46	1.66	34.07	8.89	10.87	0.39	18.44	3.39	1.66
	EC-10	61.11	100.0	4.43	7.36	19.34	6.20	33.57	1.86	11.27	4.00	10.37	0.30	14.46	2.95	2.50
Hogla	Control	89.30	86.67	6.13	9.16	17.57	5.80	35.57	1.95	29.53	9.56	8.86	0.34	19.75	4.07	1.53
	EC-6	63.36	86.67	4.70	9.06	18.45	5.10	37.58	1.55	18.47	4.89	8.17	0.20	11.52	2.75	2.50
	EC-10	37.92	60.00	2.66	8.46	17.79	4.10	34.91	1.64	10.07	3.55	4.65	0.14	7.50	1.74	3.20
Chinikanai	Control	93.33	100.0	6.10	7.50	16.68	6.30	38.24	2.08	38.20	13.56	6.35	0.19	9.13	1.71	1.20
	EC-6	30.91	50.00	4.13	4.50	16.90	5.80	34.24	1.73	16.47	5.78	4.91	0.11	5.00	1.08	3.53
	EC-10	8.771	13.33	2.60	5.40	19.79	4.30	34.02	1.95	7.733	2.00	2.84	0.07	3.56	0.75	4.40
BRRIdhan 40	Control	82.49	96.67	4.66	9.16	18.01	8.40	40.02	1.73	27.13	10.23	8.92	0.27	12.53	2.58	1.63
	EC-6	20.83	40.00	3.60	6.80	18.01	7.43	30.68	1.46	18.13	4.67	6.26	0.17	7.47	1.91	3.73
	EC-10	25.22	40.00	2.53	7.46	19.34	6.23	36.91	1.60	11.27	2.67	5.04	0.12	6.16	1.69	3.76
Honuman]ata	Control	73.89	96.67	3.00	12.90	20.46	6.93	42.02	1.73	35.33	14.67	9.24	0.22	12.51	2.66	1.86
	EC-6	35.98	70.00	2.16	11.60	19.79	6.80	38.24	1.60	30.27	6.89	5.97	0.17	9.98	1.92	3.26
	EC-10	15.26	20.00	2.33	8.90	19.12	6.60	35.58	1.73	16.13	3.11	4.18	0.11	5.86	1.61	4.50

Supplementary Table 3. Mean effects of the interaction of genotypes and treatments of different morphological traits related to Standard Evaluation Score (SES)(Cont'd)

Genotypes	Treatment	LL	SR	TRT	RL	MAD	NPA	PAL	PAD	nRHMA	LRHMA	RFW	RDW	SFW	SDW	SES
Ashfal	Control	62.22	83.33	3.60	8.66	18.45	6.700	41.80	1.64	40.13	17.36	9.96	0.26	18.35	3.680	2.133
	EC-6	34.72	60.00	3.03	8.60	19.34	6.133	41.35	1.82	30.33	7.783	10.28	0.26	12.07	2.620	3.100
	EC-10	16.35	26.67	3.06	4.90	19.79	4.833	38.24	1.55	17.07	3.337	5.05	0.14	8.523	3.810	3.967
Changai	Control	71.66	90.00	3.83	5.60	18.01	8.200	52.25	2.08	47.33	18.68	8.76	0.17	10.59	2.180	2.067
	EC-6	47.48	66.67	3.33	5.10	19.56	7.500	51.58	1.73	33.73	11.12	8.22	0.11	9.893	2.050	3.000
	EC-10	20.95	40.00	2.50	4.50	20.68	6.500	42.02	1.51	25.73	7.340	4.57	0.09	7.120	1.320	3.867
Gunshi	Control	68.39	87.96	5.33	11.7	18.68	10.20	46.02	1.55	46.53	21.12	15.67	0.37	21.43	3.970	2.163
	EC-6	58.34	92.59	4.93	12.77	18.46	8.667	44.69	1.73	36.53	8.670	14.68	0.34	20.26	3.847	2.200
	EC-10	51.74	77.78	3.86	9.56	19.12	7.267	42.91	1.51	20.10	4.893	10.84	0.27	14.68	3.033	2.623
BRRIdhan 54	Control	38.25	61.48	5.26	9.00	18.45	9.067	50.25	1.60	36.20	20.45	9.93	0.25	11.80	2.490	3.113
	EC-6	25.35	60.00	4.26	7.56	18.68	8.033	46.02	1.55	30.47	10.90	8.98	0.21	10.68	2.470	3.433
	EC-10	25.24	52.88	3.46	8.30	17.79	7.067	44.91	1.42	20.93	5.780	7.66	0.12	7.400	1.787	3.817
Motabam-onkhir	Control	93.34	96.67	4.56	14.67	17.36	6.000	52.92	1.33	30.07	15.34	12.47	0.38	21.99	4.033	1.200
	EC-6	77.51	96.67	4.10	13.67	17.36	5.400	48.91	1.37	22.07	6.893	11.60	0.34	18.29	3.597	1.700
	EC-10	47.05	83.33	3.10	9.90	18.01	4.400	39.80	1.42	17.40	4.003	5.99	0.21	12.89	2.543	2.767
Pokkali	Control	91.11	100.0	5.50	9.06	18.90	5.800	48.25	2.00	46.80	23.12	13.63	0.37	17.94	3.293	1.267
	EC-6	57.78	100.0	3.50	8.66	18.68	5.267	42.02	2.26	41.93	16.68	7.81	0.27	10.18	1.973	2.267
	EC-10	31.28	63.33	2.30	8.66	19.34	5.200	38.46	2.04	35.20	12.67	5.46	0.19	9.747	1.750	3.333





Monjurul Huda et al.

Birpala	Control	85.55	100.0	4.73	11.80	19.34	7.800	50.25	1.73	45.27	16.01	11.47	0.42	13.61	2.540	1.433
	EC-6	40.13	75.20	3.76	10.47	18.90	6.067	39.13	1.86	35.87	11.34	7.31	0.25	9.233	1.787	2.943
	EC-10	22.13	60.00	2.60	9.20	19.79	5.800	31.57	2.17	28.33	6.447	6.86	0.20	7.020	1.250	3.567
BRRI dhan 55	Control	69.45	100.0	5.73	7.86	17.37	8.000	50.92	1.69	39.73	20.90	9.15	0.25	11.96	1.930	1.917
	EC-6	26.85	72.22	4.16	8.26	19.34	6.000	34.90	1.64	31.80	14.01	6.09	0.18	8.581	1.590	3.443
	EC-10	10.32	16.67	2.83	7.06	20.68	5.400	36.24	1.78	25.27	3.560	6.23	0.15	5.460	1.440	4.583
Bashfulba -lam	Control	87.30	93.33	5.53	13.10	17.79	10.10	59.14	1.60	49.13	13.79	13.19	0.46	15.57	3.157	1.467
	EC-6	47.96	83.33	3.66	13.43	18.45	7.733	46.69	1.64	40.07	8.447	7.43	0.36	9.163	2.020	2.667
	EC-10	22.28	40.00	3.36	10.47	20.68	6.400	34.68	1.82	22.47	3.337	7.61	0.23	5.917	1.490	3.967
LSD _{0.05}		6.20	8.94	0.72	1.31	1.67	0.905	5.65	0.33	2.23		1.38	0.05	1.89	0.205	0.626
Level of sign.		**	**	**	**	**	**	**	**	**	**	**	**	**	**	**
CV ₀		9.17	9.04	12.45	9.67	5.10	8.64	9.71	10.26	4.44	12.77	11.92	14.13	12.83	6.99	12.42

** indicates significant at 0.01 probability level Notes: LL- Live leaves (%), SR- Survival Rate (%), TRT- Total number of Roots, RL- Root length, MAD- Main Axis Diameter, NPA- Number of primary axis, PAL- Primary axis length, PAD- Primary axis diameter, nRHMA- Number of Root hairs on the main axis, LRHMA- length of root hair on the main axis, RFW- Root fresh weight, RDW- Root dry weight, SFW-Shoot fresh weight, SDW- Shoot dry weight, SES-Standard Evaluation Score

Supplementary table 4: Cluster mean for thirteen traits of 30 rice genotypes

Characters	Cluster I	Cluster II	Cluster III	Cluster IV	Cluster V
LL	45.669	24.940	51.251	73.053	44.494
SR	71.643	38.925	65.553	92.777	68.811
TRT	3.298	3.128	4.322	4.678	3.813
RL	9.893	7.065	7.200	10.977	8.586
MAD	21.839	21.900	18.233	18.182	19.058
NPA	6.879	6.056	5.800	7.415	6.838
PAL	32.090	31.083	36.389	43.009	43.843
PAD	2.086	2.420	1.833	1.585	1.772
nRHMA	30.796	29.537	20.550	28.204	34.467
LRHMA	8.066	9.998	6.670	9.685	12.060
RFW	7.461	5.263	6.388	11.651	8.367
RDW	0.140	0.120	0.197	0.337	0.238
SFW	8.245	5.618	10.333	17.993	10.515
SDW	1.610	1.045	2.218	3.439	2.220
SES	2.948	3.847	2.803	1.980	2.921

Notes: LL- Live leaves (%), SR- Survival Rate (%), TRT- Total number of Roots, RL- Root length, MAD- Main Axis Diameter, NPA- Number of primary axis, PAL- Primary axis length, PAD- Primary axis diameter, nRHMA- Number of Root hairs on the main axis, LRHMA- length of root hair on the main axis, RFW- Root fresh weight, RDW- Root dry weight, SFW-Shoot fresh weight, SDW- Shoot dry weight, SES-Standard Evaluation Score

Supplementary Table 5. Banding pattern and level of tolerance of thirty rice genotypes against salinity stress using Salt-1, RM1287 and RM7075 markers.

Primers	Banding pattern / tolerance level	Genotypes
Salt-1	Band present (P) / Tolerant (T)	Thikeirum, Jamainadu, Dorkumor, Jataibalam, Kutipathai, Horkuch, Chiknul, Boilam, Gopalbhog, Akundi, Nonabokri, Hogla, HonumanJata, Ashfal, Gunshi, Motabamonkhir,





Monjurul Huda et al.

SalT-1		Pokkali, Birpala, Bashfulbalam, BRRi dhan 61, BRRi dhan 41, BRRi dhan 40, BRRi dhan 54
	Band absent (A) / Susceptible (S)	Chapsali, BRRi dhan 23, Jamaibabu, Chinikanai, Changai, Ghigoj, BRRIdhan 55
RM1287	Band present (P) / Tolerant (T)	Thikeirum, Jamainadu, Dorkumor, Jataibalam, Kutipathai, Horkuch, Chiknul, Boilam, Gopalbhog, Akundi, Nonabokri, Hogla, HonumanJata, Ashfal, Gunshi, Motabamonkhir, Pokkali, Birpala, Bashfulbalam, BRRi dhan 61, BRRi dhan 41, BRRi dhan 40, BRRi dhan 54
RM1287	Band absent (A) / Susceptible (S)	Chapsali, BRRi dhan 23, Jamaibabu, Chinikanai, Changai, Ghigoj, BRRIdhan 55
RM7075	Band present (P) / Tolerant (T)	Thikeirum, Jamainadu, Dorkumor, Jataibalam, Kutipathai, Horkuch, Chiknul, Boilam, Gopalbhog, Akundi, Nonabokri, Hogla, HonumanJata, Ashfal, Gunshi, Motabamonkhir, Pokkali, Birpala, Bashfulbalam, Chapsali , BRRi dhan 61, BRRi dhan 41, BRRi dhan 40, BRRi dhan 54
RM7075	Band absent (A) / Susceptible (S)	BRRi dhan 23, Jamaibabu, Chinikanai, Changai, Ghigoj, BRRIdhan 55

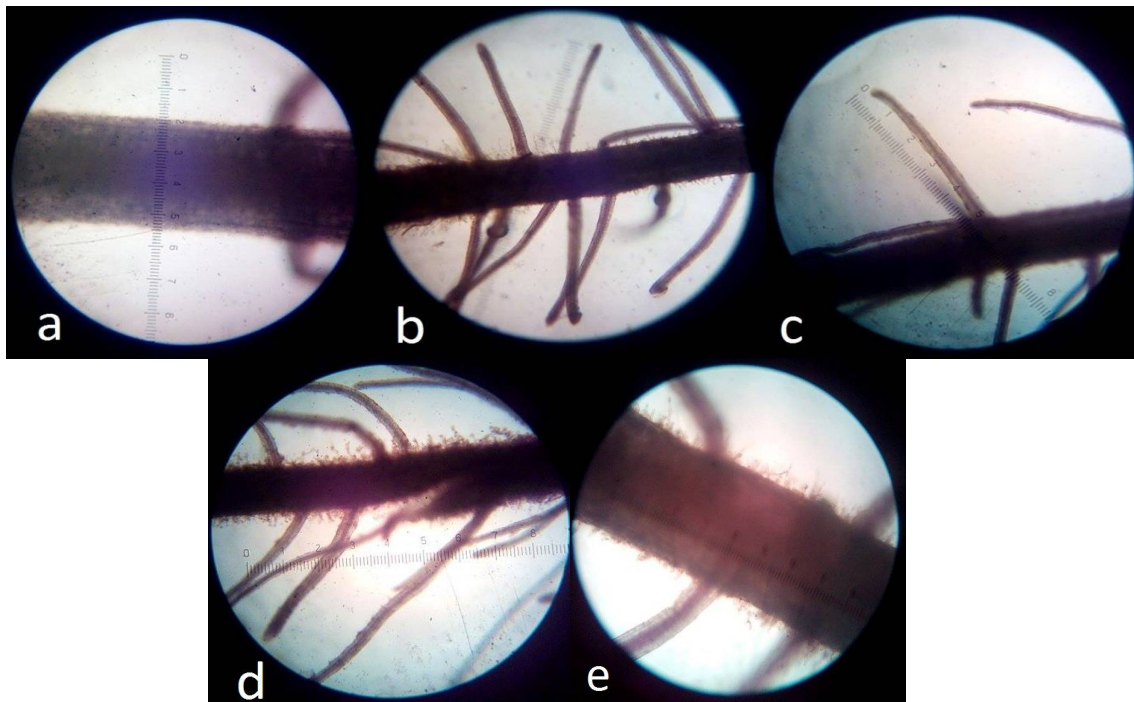


Figure 1. Measurements of root traits under microscope. a) main axis diameter t; b) number of primary axis; c) length of the primary axis; d) diameter of the primary axis; e) traits of root hair in primary axis.





Monjurul Huda et al.

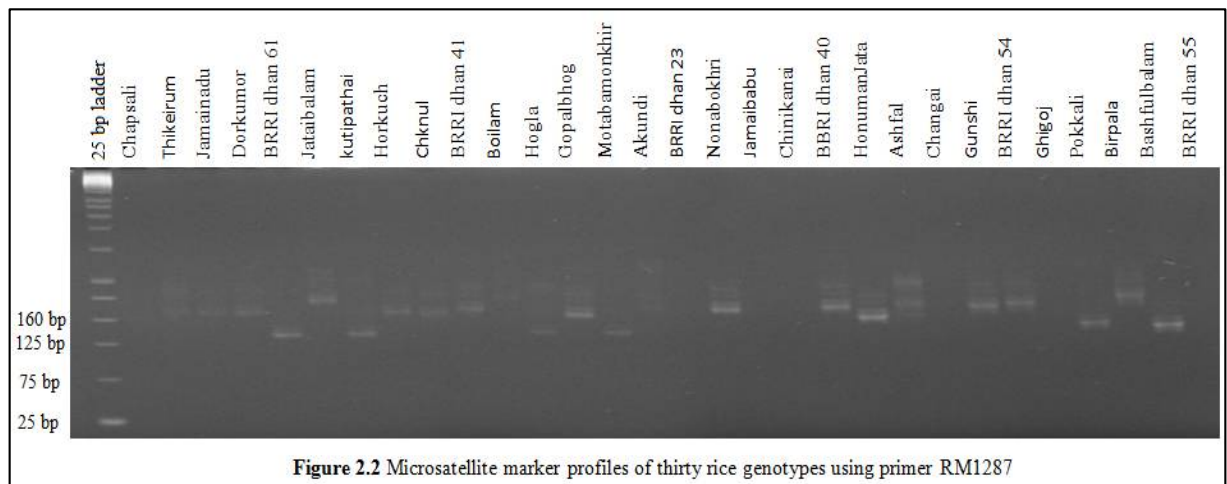
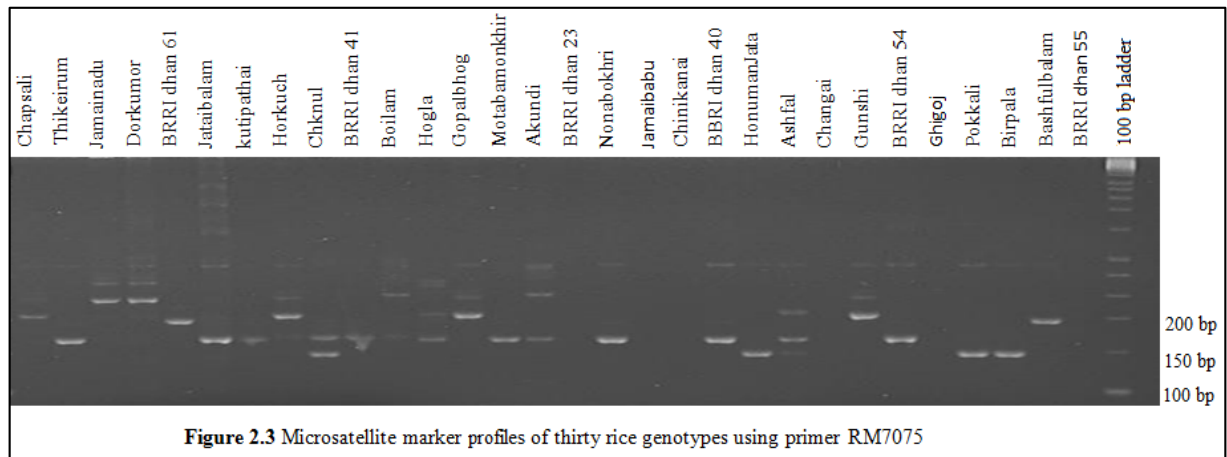
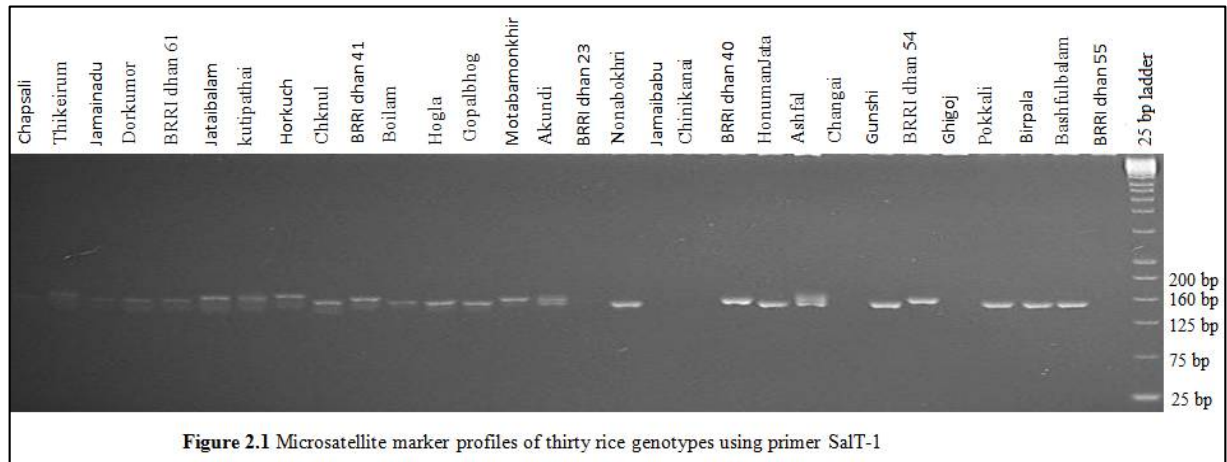


Figure 2. Banding pattern and level of tolerance of thirty rice genotypes against salinity stress using Salt-1, RM1287 and RM7075 markers





Screening for Detection of *Borrelia burgdorferi* Infection in Dogs Showing Neurological Signs in Wayanad Region, Kerala

Vidyarani.H. B, Prasanna K.S*, Anoopraj R, Ajith Jacob George, Bipin K.C, Naik Madhura Prashant and Nikhil S.R

Department of Veterinary Pathology and Department of Veterinary Epidemiology and Preventive Medicine, College of Veterinary and Animal Sciences, Pookode, Kerala Veterinary and animal Sciences University, Pookode, Wayanad, Kerala – 673576, India.

Received: 03 July 2019

Revised: 07 Aug 2019

Accepted: 09 Sep 2019

*Address for Correspondence

Prasanna K.S

Assistant Professor

Department of Veterinary Pathology

College of Veterinary and Animal Sciences,

Pookode, Wayanad, Kerala – 673576, India

Email: prasanna@kvasu.ac.in



This is an Open Access Journal / article distributed under the terms of the **Creative Commons Attribution License** (CC BY-NC-ND 3.0) which permits unrestricted use, distribution, and reproduction in any medium, provided the original work is properly cited. All rights reserved.

ABSTRACT

Neurological disorders in dogs with brain affections have multiple aetiology and often confused as rabies. In the present research work, rabies negative brain samples were screened for the presence of *Borrelia burgdorferi*, to know the involvement of neuroborreliosis in dogs showing neurological signs in Wayanad region. Out of the 84 dog carcasses presented to the Department of Veterinary Pathology, College of Veterinary and Animal Sciences, Pookode during January 2018 to June 2019, 36 brain samples were found negative for rabies (42.9 per cent) by using direct Fluorescent Antibody test (dFAT). In these 36 rabies negative dogs, we did evaluation of gross and histopathological lesions in brain tissue along with rapid immunochromatographic test for detection of antibodies against the *B. burgdorferi* in blood samples. Molecular test was carried out for *B. burgdorferi* detection by nested PCR targeting *16SrRNA* gene in both brain and blood samples. All 36 dog samples were found negative for the presence of *B. burgdorferi*.

Keywords: *Borrelia burgdorferi*, dog, neurological dysfunction, rapid immunochromatographic test, nested PCR.





INTRODUCTION

There are many infectious agents capable of causing nervous dysfunctions in dogs out of which some have zoonotic potential. Rabies is one of the most fatal zoonotic diseases that can cause death and that has no effective treatment so far. Therefore, whenever the pet animals show nervous symptoms culminating in death, the owners confuse the condition for rabies. The studies conducted at Department of Veterinary Pathology, Pookode have revealed that out of the 198 suspected cases in dogs with nervous signs, 110 dogs (55.55 per cent) were diagnosed as rabies by direct fluorescent antibody technique (dFAT) during the past three years (January 2015 to December 2017). The causes for the remaining 88 dogs (44.44 per cent) of cases could be other infectious or non-infectious agents. In a study conducted by Shyam (2018), out of 41 dogs presented with neurological signs, 15 dogs (36.6 per cent) were diagnosed as rabies and two dogs (4.87 per cent) were diagnosed as canine distemper using RT-PCR (Reverse Transcription-Polymerase chain reaction) (1). The causes of nervous dysfunction in the remaining 24 dogs (58.53 per cent) could not be identified.

There are many reports of nervous signs caused by *Borrelia burgdorferi* in dogs, which is referred to as neuroborreliosis. Previously, it was thought that arthritis is the sole condition occurring in canine borreliosis. Later, Azuma *et al.*, (1993) for the first time reported neuroborreliosis in two dogs showing neurological disorder (2). Neurological signs in canine borreliosis include ataxia, hyper-reflexia, persistent tonic convulsions, hyperesthesia with vocalization, opisthotonus, disorientation, episodes of myoclonia of forelimbs, varying mental status from hysteria to stupor and depression (3).

Borrelia burgdorferi is a motile, Gram negative bacteria having periplasmic flagella with bundle of seven to eleven flagella which belongs to the Genus *Borrelia*, Family Spirochaetaceae and Order Spirochaetales (4). *Borrelia burgdorferi* is mainly transmitted to the vertebrate host by the bite of *Ixodes* species ticks (5). Lyme disease (Borreliosis) was reported in 2013 from Wayanad district of Kerala in six women with the history of tick bite having close proximity with the deer population in nearby forest area (6), which was transmitted by deer tick, *Ixodes scapularis*. Wayanad district in Kerala being very close to the forest area, probability of occurrence of borreliosis is more in dogs. There are many reports regarding the involvement of *B. burgdorferi* in inducing neurological signs in dogs. So far, no studies have been carried out to detect these specific agents in brain of dogs died of nervous disorders in India. Hence, this research work was carried out for the detection of *Borrelia burgdorferi* in dogs showing neurological dysfunction in Wayanad district by rapid immunochromatographic test and molecular methods.

MATERIALS AND METHODS

A total of 84 brain samples from dogs were tested for rabies by Direct Fluorescent Antibody test (dFAT) was conducted using Fluorescein iso thiocyanate (FITC) conjugated nucleocapsid monoclonal antibody (Merck, Germany) on impression smears from cerebrum, cerebellum, hippocampus and brain stem as per the standard protocol for FAT (7) with slight modifications, and observed under fluorescent microscope (Zeiss, Progres C5). Tissue samples were collected from 36 dogs that were died after showing nervous symptoms and confirmed negative for rabies virus. The neurological signs reported to have shown by these dogs included ataxia, seizures, convulsions, staggering, depression, stupor and hysteria. Samples collected included cerebrum, cerebellum and meninges and heart blood from rabies negative dogs. The brain samples (cerebrum, cerebellum and meninges) were examined for both gross and histopathological lesions.

The blood samples collected were screened for the presence of *Borrelia burgdorferi* using qualitative rapid immunochromatographic test kits (quickVET canine lyme antibody rapid test kit, Ubio Biotechnology Systems Pvt Ltd, Kerala, India). The quickVET canine lyme antibody rapid test kit works on chromatographic immunoassay. Whole blood from all dogs were collected and tested immediately by adding two drops into the sample well. Once



**Vidyarani et al.**

the sample was fully absorbed, two drops of assay diluent as per the manufacturer's guidelines were added into the well. Results were interpreted within five to ten minutes. Brain samples were collected and stored in 10 per cent formalin. After proper fixation, the tissues were washed overnight, dehydrated through ascending grades of alcohol and cleared in xylene before being embedded in paraffin blocks for sectioning. Four to five-micron thick sections were taken and mounted on clean glass slides and kept for drying in incubator for 30 min at 37° C. These thin sections were stained by routine Haematoxylin and Eosin (H&E) stain (8) and were examined after mounting with DPX.

For nested PCR, brain and blood samples were collected and stored at -20°C till DNA extraction. Total DNA was extracted from brain and blood samples using conventional phenol-chloroform method. The PCR for *Borrelia burgdorferi* detection was carried out as described by Lee *et al.* (2010)[9]. The outer set primers are LD1 - 5'ATGCACACTTGGTGTAACTA 3' and LD2 - 5'GACTTATCACCGGCAGTCTTA 3' for amplifying 351 base pair sequence and inner set primers TEC1 -5'CTGGGAGTATGCTCGCAAGA 3' and LD2 - 5'GACTTATCACCGGCAGTCTTA 3'for amplifying 293 base pair sequence. The 25 µL reaction mix consisted of 12.5 µL of 2X Emerald Amp GT PCR Master mix containing *Taq* polymerase (TaKaRa), 1 µL each of 10 pmol forward and reverse primers, 5 µL of DNA and the rest NFW. The cycling conditions for amplification of *Borrelia burgdorferi* were 30 cycles at 85°C for 30 seconds (initial denaturation), 50° C for 30 sec (denaturation), 65° C for 1 min (annealing) followed by 85° C for 10 min (polymerization) and 65° C for 10 min (final extension) for both primary and nested PCR. For the nested PCR, the product of the first PCR was taken as template. The 25 µL reaction mix consisted of 12.5 µL of 2X Master mix, 1 µL each of 10 pmol inner forward and reverse primers, 3 µL of PCR product and the rest NFW. After, each run, visualization of the PCR products was carried out.

RESULTS AND DISCUSSION

Out of the 84 dog carcasses presented to the Department of Veterinary Pathology, Pookode during January 2018 to June 2019, with neurological signs, 36 brain samples (42.9 per cent) were found negative for rabies using dFAT. These 36 rabies negative dogs were included in the present study. The clinical signs showed by these dogs included ataxia, seizures, convulsions, staggering, depression, stupor and hysteria. These signs were similar to those observed by Azuma *et al.* (1993) and Schánilec *et al.* (2010) in dogs affected with neuroborreliosis (2)(3). There are reports on occurrence of *Borrelia burgdorferi* infection in women from Wayanad, Kerala (6). So, the involvement of *B. burgdorferi* in nervous disorders in dogs has to be investigated.

The gross lesions observed in the brain of these dogs included mainly congested blood vessels of meninges and cerebrum, cerebral haemorrhages, thickening of meninges and oedema of brain. In three of the cases there was no specific gross lesion. The lesions noticed during histopathological examination were classified predominantly as vascular (86 per cent) and cellular (41.66 per cent) changes. The prominent vascular changes were congestion, haemorrhage and vasculitis (90.3 per cent), perivascular cuffing and mononuclear cells infiltration (22.6 per cent). The prominent neuronal changes were chromatolysis, shrinkage of neurons, perineuronal vacuolations, degeneration of neurons and neuronophagia. The common glial changes observed were satellitosis, peri glial vacuolations and gliosis. Chang *et al.* (2000) recorded perivascular cuffing with mononuclear cells infiltration and local gliosis in the meninges in a dog infected with *Borrelia burgdorferi* (10).

Rapid ICT was performed using lateral flow kits for the blood samples collected from the 36 dog carcasses. Gomes-Solecki *et al.* (2001) compared rapid immunochromatographic test (ICT) with commercial ELISA method in screening the antibodies against the *Borrelia burgdorferi*. They observed that the rapid assay is more specific and equally sensitive than commercial whole cell ELISA (11). All the blood samples examined were negative for the presence of *Borrelia burgdorferi* antibodies which showed only the visible control line without formation of test line. So far, *B. burgdorferi* infection is not reported and not prevalent in dogs in Kerala and this might be a reason for not detecting



**Vidyarani et al.**

antibodies against it. Nested PCR was conducted for the detection of *Borrelia burgdorferi* targeting the 16SrRNA gene. Lee *et al.* (2010) optimized nested PCR technique for detection of *Borrelia burgdorferi* organisms targeting 16SrRNA gene. They found that the nested PCR technique is 100 to 1000 times more sensitive compared to that of non-nested PCR technique (9). Of the 36 blood and brain samples tested, the amplicons of 351 bp for first cycle and 293 bp for second cycle of PCR were not observed. This suggested that all the examined samples are negative for presence of DNA of *Borrelia burgdorferi*. In the present study, all dog carcasses received were reared as pets and kept at home. They might not have any contact with deer ticks (*Ixodes ricinus*). The effective tick control practices considerably reduced the chances of tick infestation and transmitting diseases like Lyme disease caused by *Borrelia burgdorferi*.

This might be the reason that none of the samples were positive for the same. Though the clinical signs, gross and histopathological lesions are in correlation with previously reported cases of neuroborreliosis, all 36 blood samples found negative for rapid immunochromatographic test. All 36 brain and blood samples found negative for nested PCR performed. It is recommended to have further investigations in more samples and also the possibility of finding out other infectious as well as non-infectious agents capable of producing brain lesions and nervous dysfunctions in dogs.

ACKNOWLEDGEMENTS

The authors are thankful to all staffs of Department of Veterinary Pathology who have cooperated for the collection of samples and also for providing technical support to complete the research work.

REFERENCES

1. Shyam S. Molecular detection and histopathological studies of common viral diseases affecting nervous system of dogs and cats. M.V.Sc thesis, Kerala Veterinary and Animal Sciences University, Pookode; 2018.
2. Azuma Y, Kawamura K, Isogai H, Isogai E. Neurologic abnormalities in two dogs suspected Lyme disease. *Microbiol. Immunol* 1993;37: 325-329.
3. Schánilec P, Kybicová K, Agudelo CF, Tremi F. Clinical and Diagnostic Features in Three Dogs Naturally Infected with *Borrelia* spp. *Acta Veterinaria Brno* 2010;79: 319-327.
4. Paster BJ, Dewhirst FE. Phylogenetic foundation of spirochetes. *J Mol Microbiol Biotechnol* 2000;2: 341-344.
5. Stanek G, Reiter M. The expanding Lyme *Borrelia* complex—clinical significance of genomic species. *Clin Microbiol Infect Off Publ Eur Soc Clin Microbiol Infect Dis* 2011;17: 487-493.
6. Sukumaran A, Pradeepkumar AS. One Health approach: A platform for intervention in emerging public health challenges of Kerala state. *Int J One Health* 2015;1: 14-25.
7. Dean DJ. The fluorescent antibody tests. *Laboratory techniques in rabies*. World Health Organization, Geneva; 1996. p. 88-93.
8. Suvarna KS, Layton C, Bancroft JD. *Bancroft's theory and practice of histological techniques*. 7th ed. Philadelphia: Churchill Livingstone Elsevier; 2012. p. 654
9. Lee SH, Vigliotti VS, Vigliotti JS, Jones W, Pappu, S. Increased sensitivity and specificity of *Borrelia burgdorferi* 16S ribosomal DNA detection. *Am J Clin Pathol* 2010; 133: 569-576.
10. Chang YF, Novosel, V, Chang CF, Summers BA, Ma DP, Chiang YW, Acree WM, Chu HJ, Shin S, Lein DH. Experimental induction of chronic borreliosis in adult dogs exposed to *Borrelia burgdorferi*-infected ticks and treated with dexamethasone. *Am J Vet Res* 2001; 62:1104-1112.
11. Gomes-Solecki MJ, Wormser GP, Persing DH, Berger BW, Glass JD, Yang X, Dattwyler RJ. A first-tier rapid assay for the serodiagnosis of *Borrelia burgdorferi* infection. *Arch Intern Med* 2001; 161:2015-2020.





Histo-Morphometric Study and Immunohistochemical Evaluation of Alpha Smooth Muscle Actin (α -SMA) in Preterm Human Placenta

Marwah A.K.Hameedi^{1*}, Huda Rashid Kareem² and Muayad S.Abood¹

¹High Institute of Infertility Diagnosis and Assisted Reproductive Technologies, Al-Nahrain University, Iraq.

²College of Medicine, Al-Nahrain University, Baghdad City, Iraq

Received: 22 June 2019

Revised: 25 July 2019

Accepted: 28 Aug 2019

*Address for Correspondence

Marwah A.K.Hameedi

High Institute of Infertility Diagnosis and Assisted Reproductive Technologies,
Al-Nahrain University, Iraq.

Email: Bakr91@gmail.com



This is an Open Access Journal / article distributed under the terms of the **Creative Commons Attribution License** (CC BY-NC-ND 3.0) which permits unrestricted use, distribution, and reproduction in any medium, provided the original work is properly cited. All rights reserved.

ABSTRACT

Preterm labour can cause neonatal morbidity and mortality, placental dysfunction during pregnancy could uncover vascular pathway, as failure of transformation of spiral arteries in relation to preterm delivery. Most of previous work focused on maternal vascular pathologies in relation to preterm delivery, little is known on fetal vascular study in relation to preterm labor. This study performed a detailed macroscopic examination, histo-morphometric analysis of vascular smooth muscle layer in placental vessels, and immune-histochemical study of α -SMA in preterm compared to term placentas in central and peripheral regions of the chorionic plate and chorionic placental villi. A significant reduction was evident in placental weight, central thickness, and the widest diameter in preterm placentas, with a borderline increase in smooth muscle layer thickness in the blood vessels of the central chorionic plate, and significant reduction in peripheral chorionic plate in preterm placentas. Immunohistochemical evaluation of α SMA showed significant variation in the expression of α -SMA in peripheral region of chorionic plate and central region of placental villi, in addition significant differences in myofibroblasts distribution was recorded in preterm fetoplacental vasculature compared to the term one, these differences were limited to the chorionic villi region. Our results indicate a significant role of contractile profile of foetal placental vasculature for foetal placental vasculopathy as part of placental pathogenesis that induces preterm labour.

Keywords: Preterm placenta, Histo-morphometric, α SMA.





Marwah A.K.Hameedi et al.

INTRODUCTION

Placental vasculature including large vessels radiated from the chorionic plate to small capillaries in the villi that provide the basic vascular system of the placenta (Jamseet al ;2012), the physiological changes that occur during pregnancy necessitate continuous changes in weight, shape and placental structure to ensure proper placental function (Avaglian, 2015), and changes in placental villi throughout gestation is reflecting a continuous development in the branching of villous tree (Fox, 1997). Changes in placental vascular structure appear at various stages during pregnancy; start by formation of lacunar system during early pregnancy to formation of tertiary villi at later stages (Avsagian, 2015). Many regulatory factors act on placental angiogenesis to insure adequate placental vascular function and development (Jim & karumanchi, 2017).

Alpha smooth muscle actin (α -SMA) is a component of microfilament of cytoskeleton of contraction cells including smooth muscle cell, and myofibroblast of villous stroma (Matsomora, 2011) of placental stem, anchoring, and intermediate villi, differentiation of myofibroblast, and smooth muscle cells, in perivascular region is of great importance for maturation of stem villi, that affect the intensity of fetoplacental blood flow, their contraction and relaxation regulate the volume of intervillous space, that involved in control of placental hemodynamics (Huszar & Bailey, 1979). Changes in α -SMA gene its expression in vascular smooth muscle cell by hormones, cell proliferation and pathological condition was reported by (Li Luo et al ;2018). Vascular pathways to preterm labor have considered clinical signs and symptoms as in preeclampsia, gestational hypertension, intrauterine growth restriction and overt bleeding (Rozance et al; 2016). Evaluation of placental vascular findings offer another avenue for uncovering vascular pathways, most of previous work focused on decidua vasculopathy (Morgan & Parks, 2018). Failure of transformation of spiral arteries in relation to preterm delivery (Kim et al; 2003). Abnormal placentation, uterine-placental ischaemia and hemorrhage (Kameret et al; 2006). So most of attention is focused on maternal vascular pathologies in relation to preterm delivery, little is known on influence of fetal vascular study in relation to preterm labor. This study aimed to elucidate fetal vascular changes in terms of contractile profile as a placental factor for preterm labour.

MATERIALS AND METHODS

A random sample of 40 normal human placentae were included in the study that delivered by either normal vaginal delivery and caesarian sections: twenty of them at term and other twenty at preterm of gestational age, maternal age ranged from 16 - 38 years old. Exclude placenta from mother with history of: polyhydramnios, multiple pregnancy (twins), abnormal placentation, cervical weakness, uterine fibroid, smokers, drug abuse, preeclampsia, diabetes, hypertension. Macroscopic measurements of the fresh placental samples from each group were studied for certain measurements, these include: shape, widest diameter, central thickness, and weight of placenta. Samples of placental tissue from the preterm and term placentae were selected from central and peripheral regions of the chorionic plate and chorionic villi, paraffin blocks were prepared and sectioned at 5 μ m for histological and immunohistochemical study (Bancroft and Layton, 2013). Sections were stained for Hematoxyline and eosin (H&E) according to (Srivana & Bancroft, 2012). Histomorphometric analysis of tunica media thickness in relation to vascular wall thickness done on placental vasculature by (Image J version 1.52a) as in (Fig.1) in preterm and term placenta. Immunohistochemical evaluation of alpha smooth muscle (α -SMA) using mouse monoclonal antibody to alpha smooth muscle actin (orb317295) and detection kit (biorbyt, orb90443), that provided by biorbyt. (www.biorbyt.com). Aperio scope image analysis software positive pixel count (V12.4) Using positive pixel count algorithms to analyze digital slides that used to assess the total positivity of α -SMA in blood vessels wall and in myofibroblast that stained positive for α -SMA. Statistical analysis performed by Microsoft Excel (2010) program, values were presented as Mean \pm SD, the relationships between variables were assessed using unpaired t-test, Chi-square Fisher Exact Test was used for placental shape evaluation. P value \leq 0.05 was considered as statistically significant.



**Marwah A.K.Hameedi et al.**

RESULTS

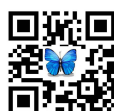
Macroscopic measurements of human placenta revealed a significant difference in placental weight, widest diameter, and central thickness that showed a significant reduction in preterm compared to term placentas at $p \leq 0.05$ (Table 1). Placental shape revealed a nonsignificant variation between preterm and term placentas; but the commonest form is circular in preterm group (Table 2). Morphometric measurements of the vessels wall tunica media thickness in relation to vascular wall thickness showed a borderline increment in the blood vessels of the central chorionic plate with (p-value : 0.161) (figure 2), and a significant reduction in blood vessels of peripheral chorionic plate with (p-value: 0.026) in preterm placentae compared to the term ones (figure 3). On the other hand, non-significant changes were detected in the other placental regions (Table 3) (figure 4-5).

Alpha smooth muscle actin was expressed as brown color at the smooth muscle layer of tunica media of muscular arteries of chorionic plate and placental villi. (α -SMA) showed significant reduction in immunohistochemical expression in peripheral region of chorionic plate and central region of placental villi with p values 0.001, 0.019 respectively (Table 4) (figure 6-7). A non significant changes in α -SMA Immunohistochemical expression was seen in central region of chorionic plate and peripheral region of placental villi (table 4). Myofibroblast at the vascular core stained positive for α -SMA, a significant differences in myofibroblasts distribution was evident in preterm fetoplacental vasculature compared to the term placentas. These differences were limited to the chorionic villi region, and surprisingly they were different between the central (p value= 0.022) and the peripheral regions in (p value = 0.019) respectively (Table 5), (figure 8-9).

DISCUSSION

Preterm labour is an important cause of neonatal morbidity and mortality (Manuck et al., 2016). Recent studies provided evidences that placental dysfunction during pregnancy is a major risk factor for preterm birth and foetal maldevelopment (Hodyl et al., 2017; Redline, 2015). Studying the gross features of placenta is important in evaluating pregnancy associated abnormalities (Jaiman, 2015; Nakayama, 2017; Kaplan, 2019). In this concept, these features were examined in preterm and term placentas. The significant differences in placental weight, thickness, and widest diameter, between preterm and term placentas, which showed lower measurements in preterm placentas, can be related to the differences in the gestational ages of placentas. On the other hand, the changes in gross features of preterm placentas might reflect potential placental and/ or foetal problems (Burton, 2016; Salvati et al., 2019). Placental shape did not exhibit any specific characteristics that were distinctive to preterm placentas at the expense of term ones.

The co-occurrence of the significant changes in the gross features with the significant changes in fetoplacental vasculature of preterm placentas; could provide a strong evidence of that evaluating gross placental features can predict placental dysfunction. In agreement with these findings, increasing evidence showed that gross placental features are linked to placental functional capacity (Burton, 2016). Higher uterine and umbilical arteries pulsatility indices were found to be associated with lower placental weight and area (Salavati et al., 2016). Placental dysfunction is a leading cause of birth abnormalities including preterm labour (Morgan, 2016; Lean et al., 2017). Defective placental vasculature causes malperfusion that interferes with the normal placental function in providing adequate amounts of oxygen and nutrients to the foetus in order to maintain normal foetal development (Silver, 2018). Placental malperfusion can be related to impaired maternal and/or foetal vasculature (Khong et al., 2016). Examining the histology of foetal placental vasculature in the chorionic plate and the chorionic villi in both central and peripheral regions of preterm and term placentas revealed differences in their vascular morphology that is related mainly to the size of the vessels and the thickness of smooth muscle layer. No previous studies have examined the morphometric characteristics of muscular layer in fetoplacental vasculature of preterm and term placentas. However, many studies have investigated other vascular morphometric characteristics like vascular diameter, length,



**Marwah A.K.Hameedi et al.**

tortuosity, and luminal perimeter (Junaid et al., 2017; Lu et al., 2017). Interestingly, these changes were remarkable in the vessels of chorionic plate region, but not in the vessels of the chorionic villi. Morphometric measurements showed a borderline increment in smooth muscle layer thickness in relation to the whole vessel thickness ratio in the blood vessels of the central chorionic plate, and a significant reduction in this ratio in the blood vessels of peripheral chorionic plate in preterm placentas compared to the term ones. On the other hand, there were no significant changes in the vascular smooth muscle layer thickness in the chorionic villi between preterm and term placentas, both centrally and peripherally. Collectively, these differences in smooth muscle layer thickness in the different regions of preterm foetal placenta are more likely indicating a defective vasculogenesis rather than a defective angiogenesis throughout placental vascular development. This is because of the fact that vasculogenesis process of placental vascular development occur earlier in pregnancy, till late first trimester, and mainly in the region of chorionic plate, whereas the process of angiogenesis starts later and takes place mainly in the chorionic villi region of the placenta (Aplin et al., 2015).

A recent study on vascular generation in preterm, term, and post term placentas conducted by Hashim et al., 2016 showed no significant differences in the diameter of chorionic terminal villi blood vessels, but there was a significant reduction in the length and number of terminal villi in preterm placenta compared to the term ones. Another recent study by Lu et al., 2017 who studied the morphological features of stem villi blood vessels in preterm and term placentas showed no significant differences in the thickness of blood vessels in stem villi of preterm and term placentas. In 2014, Junaid and colleagues reported a defective microvasculature profile with severe hypovascularity in the peripheral region of the chorionic plate (Junaid et al., 2014). Again, these data support our assumption of significant defective vasculature in the peripheral region of chorionic plate in preterm placentas. Collectively, these findings come in accordance with our observations of chorionic villi vascular morphometric characteristics in preterm and term placentas.

Proper blood perfusion in fetoplacental vasculature is entirely dependent on vascular tone that is controlled by the muscular components of the vascular wall, and therefore moderate blood pressure and blood flow within the placenta (Shi et al., 2015). As the placenta lacks nervous innervation, the contractile activity of smooth muscle fibers in placental vessels are regulated by factors like mechanical actions, oxygenation levels, autocrinesignaling, and circulating molecules in foetal circulation (Wareing et al., 2013; Jones et al., 2015). The significant down-regulation of the contractile marker α -SMA in blood vessels' smooth muscle cells of the peripheral chorionic plate and in the central chorionic villi region of preterm placentas compared to term ones indicates impairment of their contractile function. These data mean that the muscular layers of the blood vessels in these regions are not able to maintain proper contractile function that secure proper blood perfusion in the fetoplacental vasculature. This contractility defect might be part of the pathogenesis that involved in preterm labour.

Defective vascular contractility profile in different parts of placental vasculature of eventful pregnancies has been observed by other researchers. Roffino et al., 2012 examined the contractility of smooth muscle cells in the umbilical arteries of early, late preterm, and term births. They concluded that smooth muscle cells of umbilical arteries acquire full differentiation just late in pregnancy and that's why smooth muscle cells of umbilical arteries do not show full differentiation and contractility in preterm births. Lu et al., 2017 have studied the contractile profile of stem villi blood vessels of placentas from eventful pregnancies associated with intrauterine growth retardation. They found that the smooth muscle cells of those blood vessels profoundly down-regulates ACTA gene expression, that codes for α -SMA, in addition to the expression of α -SMA itself. Interestingly, the expression level of α -SMA is not only a marker for smooth muscle contractility; its expression level in the smooth muscle cells can indicate the differentiation state of these cells as well (Rzucidlo et al., 2007). Smooth muscle cells are, to a certain extent, plastic cells that have the ability to change their phenotype in response to vascular injury and external stimuli. The fully differentiated contractile smooth muscle cells can revert back to the dedifferentiate state, the synthetic or proliferative phenotype, where the cells acquire migratory and proliferative characteristics (Shi et al., 2015; Orlandi, 2015). One of the molecular features of those dedifferentiated smooth muscle cells is low expression levels of α -SMA protein (Lu et al.,





Marwah A.K.Hameedi et al.

2017). We assume that the significant decrement of α -SMA in smooth muscle cells of the blood vessels in the peripheral region of the chorionic plate and the central region of the chorionic villi indicates dedifferentiation of these cells, and this dedifferentiation state can be part of the pathology in fetalplacental vasculature that induce preterm labour. Correlating our significant morphometric findings to α -SMA immunohistochemistry findings in the smooth muscle cells of chorionic blood vessels in the peripheral region of the chorionic plate strongly indicate that the pathological process involves dedifferentiation of the smooth muscle cells, reflected by low α -SMA level of expression, and migration of the dedifferentiated smooth muscle cell to the intima, reflected by thinner muscular layer. Our results point out that the defective vasculature of the peripheral chorionic plate vessels is a critical factor involved in placental pathology and aetiology of preterm labour.

The significant differences of myofibroblasts distribution were limited to the chorionic villi region, and surprisingly they were different between the central and the peripheral regions. To the best of our knowledge, no other works have investigated myofibroblasts distribution in fetoplacental vasculature of abnormal pregnancy placentas. However, the results that we had in this study are unexpected and reflect a possible hidden role of myofibroblasts in placental pathology of preterm labour that needs further investigation. Ma et al., 2015 studied the number of myofibroblasts in fetal membranes of early and late onsets pre-eclampsia patients and they observed that the number of myofibroblasts was decreased significantly in early onset pre-eclampsia patients' foetal membranes, whereas their number increased significantly in late onset ones. The authors relate this change in the number of myofibroblasts in the two conditions to the duration of exposure to hypoxia that affects the proliferation and the apoptosis of myofibroblasts.

The central part of the chorionic villi region of preterm placenta showed significant decrement in the number of myofibroblasts in its blood vessels compared to the term one. Collectively, this observation with the significant decrement of α -SMA in the smooth muscle cells of the same blood vessels indicates significant defective vascular contractile machinery in the central chorionic villi region of the placenta. Surprisingly, the number of myofibroblasts was significantly higher in the blood vessels of the peripheral region of chorionic villi of preterm placenta compared to the term ones. This might indicate that vessels in this region are increasing the number of myofibroblasts reactively to improve its contractility profile aiming at maintaining proper vascular function. These changes might be related to the significantly impaired vascular contractility observed in the peripheral chorionic plate vasculature. The changes we observed in the contractile elements of the fetoplacental vasculature of preterm placentas do not show clearly whether they have causative role in the pathogenesis of preterm labour or they are consequences of, or perhaps occur in parallel with, other factors. However, further investigations are needed to understand the reasons behind these regional changes in fetoplacental vasculature of preterm labour.

REFERENCES

1. Aplin, J.D., Whittaker, H., Lim, Y.T.J., Swietlik, S., Charnock, J. and Jones, C.J., 2015. Hemangioblastic foci in human first trimester placenta: distribution and gestational profile. *Placenta*, 36(10), pp.1069-1077.
2. Avagliano L, Terraneo L, Virgili E, Martinelli C, Doi P. Autophagy in Normal and Abnormal Early Human Pregnancies. *Reprod Sci*. 2015; 22: 838-844.
3. Bancroft JD, Layton C (2013) The hematoxylin and eosin . In: Suvarna SK, Layton C, Bancroft JD, Bancroft 's Theory and Practice of Histological Techniques, 7th ed., Churchill Livingstone, Elsevier Ltd., Philadelphia. pp. 174 – 178.
4. Burton, G.J., Fowden, A.L. and Thornburg, K.L., 2016. Placental origins of chronic disease. *Physiological reviews*, 96(4), pp.1509-1565.
5. Fox, H. (1997): Aging of the placenta. *Archives of Disease in Childhood*. 77: 165–170



**Marwah A.K.Hameedi et al.**

6. Hashim, Z.H., Kareem, Kamoona H.R. and Jaafar, H.A., 2016. The Evaluation of Placental Vascular Generation and Placental Apoptosis in Preterm and Post-date Placentae in Relation to Apgar Score at Birth. *Medical Journal of Babylon*, 13(1), pp.79-84.
7. Hodyl, N.A., Aboustate, N., Bianco-Miotto, T., Roberts, C.T., Clifton, V.L. and Stark, M.J., 2017. Child neurodevelopmental outcomes following preterm and term birth: What can the placenta tell us?. *Placenta*, 57, pp.79-86.
8. Huszar G, Bailey P., 1979 : Isolation and characterization of myosin in the human term placenta. *Am J Obstet Gynecol*;135:707e12
9. Jaiman, S., 2015. Gross examination of the placenta and its importance in evaluating an unexplained intrauterine fetal demise. *Journal of Fetal Medicine*, 2(3), pp.113-120.
10. James J, Carter A, Chamley L. 2012. Human placentation from nidation to 5 weeks of gestation. Part II: tools to model the crucial first days. *Placenta* 33, 335–342. (10.1016/j.placenta.2012.01.019) [PubMed] [CrossRef]
11. Jim B, Karumanchi SA. Preeclampsia: Pathogenesis, Prevention, and Long-Term Complications. *Semin Nephrol*. 2017 Jul;37(4):386-397.
12. Jones, S., Bischof, H., Lang, I., Desoye, G., Greenwood, S.L., Johnstone, E.D., Wareing, M., Sibley, C.P. and Brownbill, P., 2015. Dysregulated flow-mediated vasodilatation in the human placenta in fetal growth restriction. *The Journal of physiology*, 593(14), pp.3077-3092.
13. Junaid, T.O., Bradley, R.S., Lewis, R.M., Aplin, J.D. and Johnstone, E.D., 2017. Whole organ vascular casting and microCT examination of the human placental vascular tree reveals novel alterations associated with pregnancy disease. *Scientific reports*, 7(1), p.4144.
14. Junaid, T.O., Brownbill, P., Chalmers, N., Johnstone, E.D. and Aplin, J.D., 2014. Fetoplacental vascular alterations associated with fetal growth restriction. *Placenta*, 35(10), pp.808-815.
15. Kaplan, C., 2019. Gross Examination. In *Pathology of the Placenta* (pp. 41-46). Springer, Cham.
16. Khong, T.Y., Mooney, E.E., Ariel, I., Balmus, N.C., Boyd, T.K., Brundler, M.A., Derricott, H., Evans, M.J., Faye-Petersen, O.M., Gillan, J.E. and Heazell, A.E., 2016. Sampling and definitions of placental lesions: Amsterdam placental workshop group consensus statement. *Archives of pathology & laboratory medicine*, 140(7), pp.698-713.
17. Kim YM, Bujold E, Chaiworapongsa T, et al. Failure of physiologic transformation of the spiral arteries in patients with preterm labor and intact membranes. *Am J Obstet Gynecol*. 2003;189(4):1063–1069.[PubMed]
18. Kramer MS, Chen MF, Roy I, et al. Intra- and interobserver agreement and statistical clustering of placental histopathologic features relevant to preterm birth. *Am J Obstet Gynecol*. 2006;195(6):1674–1679.[PubMed]
19. Lean, S.C., Heazell, A.E., Dilworth, M.R., Mills, T.A. and Jones, R.L., 2017. Placental dysfunction underlies increased risk of fetal growth restriction and stillbirth in advanced maternal age women. *Scientific reports*, 7(1), p.9677.
20. Li Luo, WuhongZheng, GuiliLian, Huaning Chen, Ling Li, ChangshengXu, and LiangdiXie .,2018 : Combination treatment of adipose-derived stem cells and adiponectin attenuates pulmonary arterial hypertension in rats by inhibiting pulmonary arterial smooth muscle cell proliferation and regulating the AMPK/BMP/Smad pathway *Int J Mol Med* 41:51-60 .(PubMed: 29115380)
21. Lu, L., Kingdom, J., Burton, G.J. and Cindrova-Davies, T., 2017. Placental stem villus arterial remodeling associated with reduced hydrogen sulfide synthesis contributes to human fetal growth restriction. *The American journal of pathology*, 187(4), pp.908-920.
22. Ma, X., Yang, F., Yang, S., Rasul, A., Li, T., Liu, L., Kong, M., Guo, D. and Ma, T., 2015. Number and distribution of myofibroblasts and α -smooth muscle actin expression levels in fetal membranes with and without gestational complications. *Molecular medicine reports*, 12(2), pp.2784-2792.
23. Manuck, T.A., Rice, M.M., Bailit, J.L., Grobman, W.A., Reddy, U.M., Wapner, R.J., Thorp, J.M., Caritis, S.N., Prasad, M., Tita, A.T. and Saade, G.R., 2016. Preterm neonatal morbidity and mortality by gestational age: a contemporary cohort. *American journal of obstetrics and gynecology*, 215(1), pp.103-e1.
24. Morgan, T. K., & Parks, W. T. (2018). Pregnancy-Induced Uterine Vascular Remodelling and the Pathophysiology of Decidual Vasculopathy. *Pathology of the Placenta*, 221–231.





Marwah A.K.Hameedi et al.

25. Morgan, T.K., 2016. Role of the placenta in preterm birth: a review. American journal of perinatology, 33(03), pp.258-266.
26. Nakayama, M., 2017. Significance of pathological examination of the placenta, with a focus on intrauterine infection and fetal growth restriction. Journal of Obstetrics and Gynaecology Research, 43(10), pp.1522-1535.
27. Orlandi, A., 2015. The contribution of resident vascular stem cells to arterial pathology. International journal of stem cells, 8(1), p.9.
28. Redline, R.W., 2015. Classification of placental lesions. American journal of obstetrics and gynecology, 213(4), pp.S21-S28.
29. Roffino, S., Lamy, E., Foucault-Bertaud, A., Risso, F., Reboul, R., Tellier, E., Chareyre, C., Dignat-George, F., Simeoni, U. and Charpiot, P., 2012. Premature birth is associated with not fully differentiated contractile smooth muscle cells in human umbilical artery. Placenta, 33(6), pp.511-517.
30. Rozance PJ, Brown LD, Thorn SR, Anderson MS, Hay WW., Jr . Avery's Neonatology: Pathophysiology and Management of the Newborn 7th ed. Wolters Kluwer; 2016. Intrauterine Growth Restriction and Small-For-Gestational-Age Infant. [Google Scholar]
31. Rzucidlo, E.M., Martin, K.A. and Powell, R.J., 2007. Regulation of vascular smooth muscle cell differentiation. Journal of vascular surgery, 45(6), pp.A25-A32.
32. Salavati, N., Smies, M., Ganzevoort, W., Charles, A.K., Erwich, J.J., Plösch, T. and Gordijn, S.J., 2018. The Possible Role of Placental Morphometry in the Detection of Fetal Growth Restriction. Frontiers in physiology, 9.
33. Salavati, N., Sovio, U., Mayo, R.P., Charnock-Jones, D.S. and Smith, G.C.S., 2016. The relationship between human placental morphometry and ultrasonic measurements of utero-placental blood flow and fetal growth. Placenta, 38, pp.41-48.
34. Shi, N. and Chen, S.Y., 2016. Smooth muscle cell differentiation: model systems, regulatory mechanisms, and vascular diseases. Journal of cellular physiology, 231(4), pp.777-787.
35. Silver, R.M., 2018. Examining the link between placental pathology, growth restriction, and stillbirth. Best Practice & Research Clinical Obstetrics & Gynaecology, 49, pp.89-102.
36. Wareing, M., 2014. Oxygen sensitivity, potassium channels, and regulation of placental vascular tone. Microcirculation, 21(1), pp.58-66.
37. www.biorbyt.com

Table 1. Macroscopic Measurements of placenta, in preterm and term human placentae

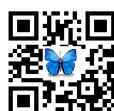
Age groups	Widest diameter (cm)	Central thickness (cm)	Weight (Kg)
Preterm	16.95± 0.94	1.96 ± 0.163	0.88 ± 0.07
Term	18.1 ± 3.41	2.3 ± 0.126	1.38 ± 0.106
P-value	*0.000	*0.04	*0.004

*Significant p-value ≤0.05

Table 2.Type of placental Shape in preterm and term groups.

Shape of placenta	Term(n=20)		Preterm(n=20)		Total		Chi-square Fisher Exact Test
	NO	%	NO	%	NO	%	
Oval	8	(40)	6	(30)	14	(35)	P= 0.7411
Circular	12	(60)	14	(70)	26	(65)	
total	20	(100)	20	(100)	40	(100)	

*Significant p-value ≤0.05





Marwah A.K.Hameedi et al.

Table 3. Histo-morphometric analysis of tunica media thickness in preterm and term placenta in central and peripheral regions, with their level of significance by un -paired t test.

Chorionic plate			Placental villi	
Term	Central	Peripheral	Central	Peripheral
Means±S.D.	0.465±0.0439	0.529±0.079	0.491±0.047	0.521±0.055
Preterm	Central	Peripheral	Central	Peripheral
Means±S.D.	0.610±0.230	0.427±0.053	0.502±0.052	0.523± 0.058
p-value	0.161	0.026*	0.690	0.952

*Significant p-value ≤0.05

Table 4.The mean positivity of α-SMA immunohistochemical reactivity in preterm and term placenta in central and peripheral regions, with their level of significance by un paired t test.

Chorionic plate			Placental villi	
Term	Central	Peripheral	Central	Peripheral
Means ±S.D.	0.68 ± 0.11	0.69 ± 0.11	0.67 ± 0.07	0.57 ± 0.15
Preterm	Central	Peripheral	Central	Peripheral
Means ±S.D.	0.68 ± 0.10	0.62 ± 0.09	0.63 ± 0.10	0.56 ± 0.09
p-value	0.78	0.001*	0.019*	0.751

*Significant p-value ≤0.05

Table5 :Myofibroblasts distribution in preterm and term placenta in central and peripheral regions, with their level of significance by un- paired t test

Chorionic plate			Placental villi	
Term	Central	Peripheral	Central	Peripheral
Means±S.D.	27.64±11.30	15.92± 5.928	19.071± 7.363	8± 4.590
Preterm	Central	Peripheral	Central	Peripheral
Means±S.D.	20.07±10.92	16.071± 5.210	12.21± 7.617	14± 7.755
p-value	0.083	0.946	0.022*	0.019*

*Significant p-value ≤0.0

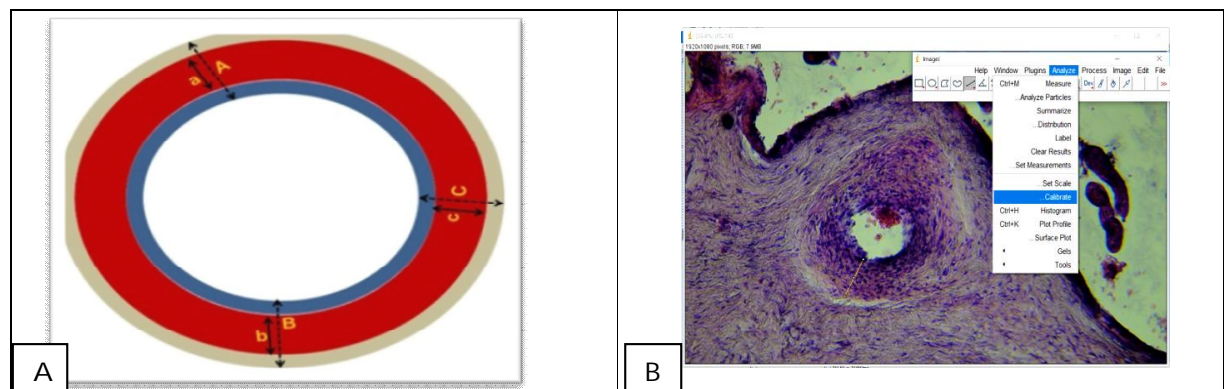
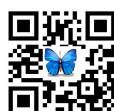


Figure 1. A. Measuring method of tunica media thickness in relation to whole wall thickness of blood vessels. B. Snap shot of screen of Image J version 1.52a





Marwah A.K.Hameedi et al.

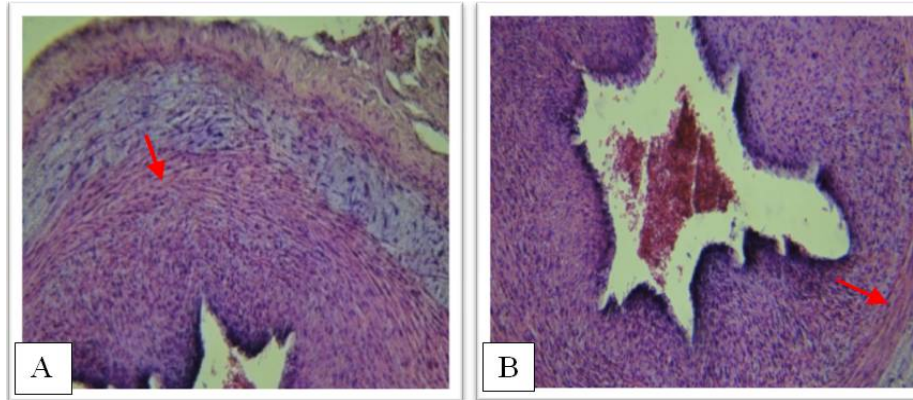


Figure 2. Sections in chorionic plate at central region in (A) preterm placenta (B) term placenta showed variation in vascular wall structure mainly tunica media (red arrows). H&E, X10

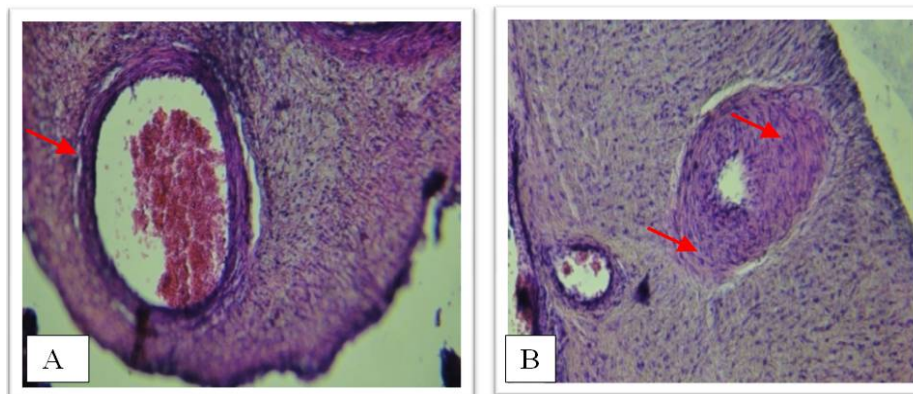


Figure 3. Sections in chorionic plate at peripheral region in (A) preterm placenta (B) term placenta showed variation in vascular wall structure mainly tunica media (red arrows). H&E, X10

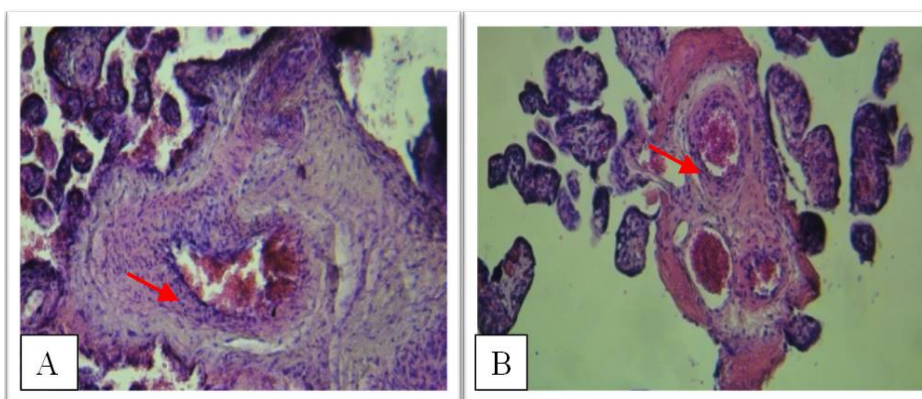
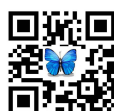


Figure 4. Sections in placental villi at central region in (A) preterm placenta (B) term placenta showed variation in vascular wall structure mainly tunica media (red arrows). H&E, X10





Marwah A.K.Hameedi et al.

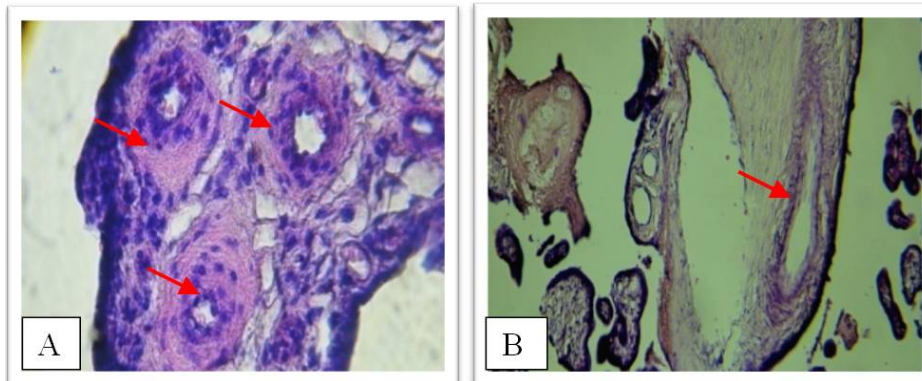


Figure 5. Sections in placental villi at peripheral region in (A) preterm placenta (B) term placenta showed variation in vascular wall structure mainly tunica media (red arrows). H&E, X10

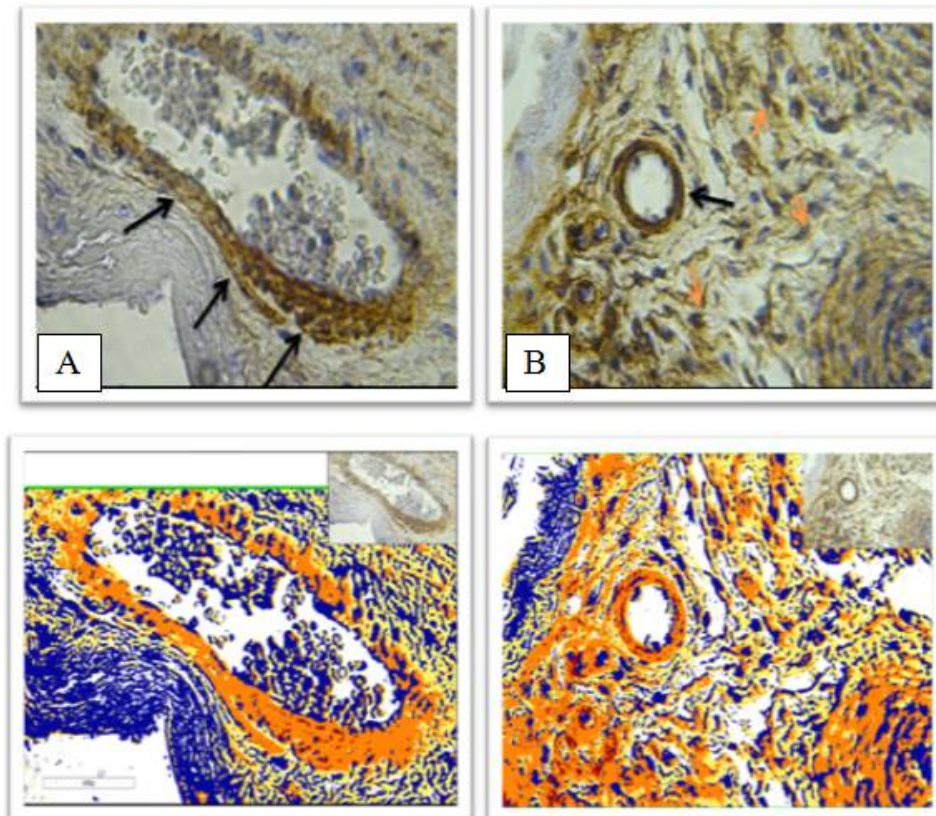
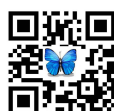


Figure 6. Sections in chorionic plate at peripheral region in (A) preterm placenta (B) term placenta showed variation in α -SMA immunohistochemical expression in tunica media smooth muscles (black arrows) and myofibroblasts (orange arrows) with their markup image of aperiO, X10.



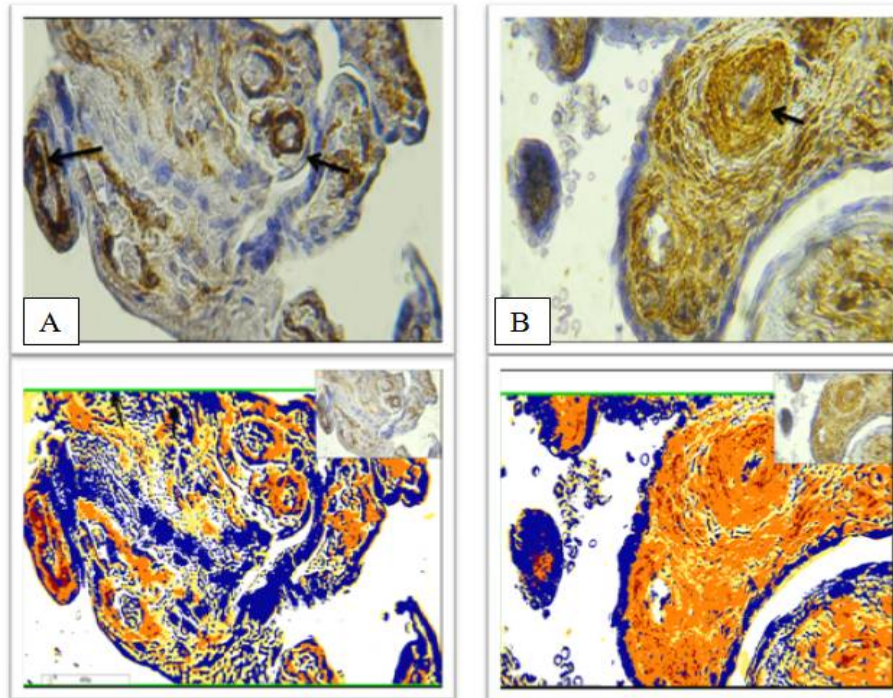


Figure 7. Sections in placental villi at central region in (A) preterm placenta (B) term placenta showed variation in α -SMA immunohistochemical expression in tunica media smooth muscles (black arrows) with their mark up image of aperio, X10.

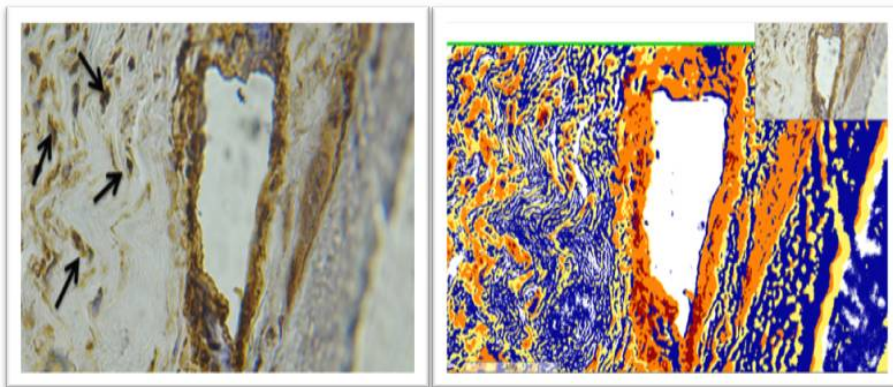


Figure 8. Preterm placental central region of placental villi showed little distribution of myofibroblast in villous core (black arrows) with Mark up image by aprioscop image analyses,10X





Marwah A.K.Hameedi et al.

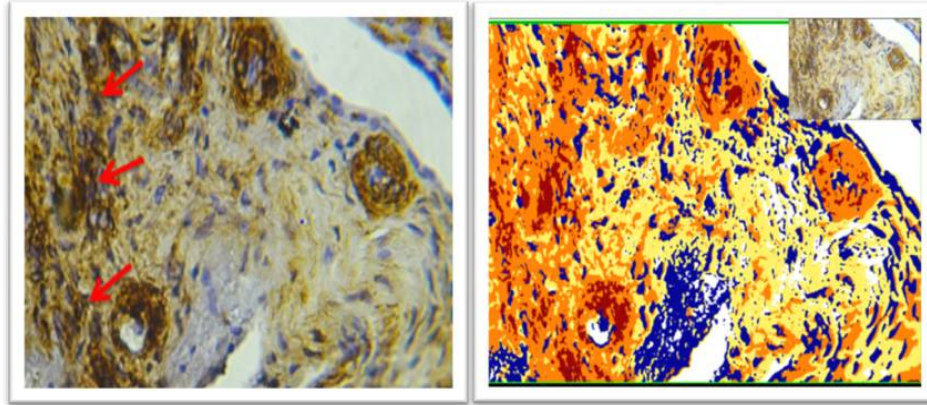


Figure 9. Term placental peripheral region of placental villi showed dense population of myofibroblast in villous core (red arrows) Immunohistochemistry for α -SMA., with mark up image by a microscope image analyses, 10X.





RESEARCH ARTICLE

Investigation and Identification of Pathogenic Bacterial Pollution in Some Local Trocars of Ramadi City, Iraq

Al SafaSaed Al Kubaisi* and Sufyan Mohammed Shartooh

Biology Department, College of Science, University of Anbar, Iraq.

Received: 02 July 2019

Revised: 04 Aug 2019

Accepted: 06 Sep 2019

*Address for Correspondence

Al SafaSaed Al Kubaisi

Biology Department,

College of Science,

University of Anbar, Iraq.

Email: alsafa.saed@gmail.com



This is an Open Access Journal / article distributed under the terms of the **Creative Commons Attribution License** (CC BY-NC-ND 3.0) which permits unrestricted use, distribution, and reproduction in any medium, provided the original work is properly cited. All rights reserved.

ABSTRACT

Water is a vital natural resource required by living organisms, it provides a strategic dimension for all different life types, and guarantees ongoing sustainability. The work objective was to determine the level of pathogenic pollution in some local trocars of Ramadi City, and to find a relationship between the ecological and pathogenic bacterial isolates. Materials and methods comprised some physical, chemical and bacteriological parameters includes (temperature, pH, BOD, TSS, TDS, turbidity, and EC, additionally the enumeration of Coliforms, Faecal Coliforms and Streptococci), as well as the isolation of some pathogenic bacterial species using the proper biochemical tests and VITEK 2 compact system for the confirmation of pathogens results. Also, the bacterial finger printing was accomplished by ERIC-PCR technique and dendrogram analyzing program-(samples for *Klebsiella* spp. were collected form trocars water and from patient's wounds, burns and sputum in Ramadi General Hospital) - where six water samples were collected from polluted sites of local trocars in the Ramadi City for six months, during the period from November 2018 to April 2019. Results showed that the under study locations were polluted with the studied environmental characteristics during the study period. However, the results of temperature, turbidity, pH, EC, TDS, TSS and BOD, reached for high mean values and where 19.5°C, 109.66 NTU, 7.81, 2962.1µs/cm, 2785.1 ppm, 1434.7 ppm and 51.66 ml/l respectively. Whilst for bacteriological tests including the Coliforms, Faecal Coliforms, Streptococci, and Faecal Streptococci reached for the highest mean values which were 653.5, 201.8, 508.5, and 359.7 cell/100ml respectively. Regarding the finger printing of *Klebsiella* spp. isolated from different environments, dendrogram statistical analysis find a similarity ratio of 66% using ERIC-PCR technique. In conclusion the extracted results revealed that the under study trocars were very contaminated with different pathogens related to the residual patients in Ramadi General Hospital which were affected by the pollution of such waters.



**Al SafaSaed Al Kubaisi and Sufyan Mohammed ShartooH**

Thus, the study findings may help to elevate the environmental awareness among people living in such environments.

Keywords: bacterial pollution, trocars, Ramadi City, dendrogram, Coliforms.

INTRODUCTION

Environment remain the silent victim of all conflicts worldwide, Who causes significant injury to it , alongside with the communities depending on natural resources . Most ground water is contaminated with municipal sewage, which is the primary cause of microbial pollution, particularly close big population centers (shartooH, 2017). The Iraqi Rivers, including the trocars, seem to be polluted with pathogenic organisms, especially in summer. Most bacterial isolates are human origin as a consequence of the release of untreated wastewater straight into waterways and sediments that exceed permissible environments. However, the absence of adequate therapy of wastewater can accelerate the transmission of waterborne diseases and other contaminants to vegetable crops irrigated by such wastewater (Do costa *et al* ,2001). Environment is considered to be the geographical set-up group of a region that involves both biotic and abiotic components of all habitats, i.e. aquatic, terrestrial. Water is one of the most significant factors that can play a vital part in any change in the setting by influencing the neighboring flora and fauna and its contamination can cause excellent damage to human beings. The quality of river water is significantly affected by industrial, agricultural and plenty of human activities affecting its physical-chemical features and microbial qualities (Singh *et al* , 2015)Two bacterial groups, coliforms and fecal streptococci, were used as indicators of possible contamination of sewage (Doron,2011) because they are commonly found in human and animal feces and are generally not harmful themselves and indicate the possible presence of enteric pathogenic bacteria, viruses and protozoans (Lesley,2008). Their presence in streams indicates the existence of pathogenic microorganisms, making E. Coli an indicator of fecal pollution for decades (Singh *et al* , 2015).

Detailed understanding of microbial pollution in river water is essential for watershed management activities in order to preserve secure waters for recreational and economic purposes. The levels of heterotrophic bacteria are frequently associated with organic contamination .that changes with the climate. Many nations in the globe, particularly those in arid and semi-arid regions according to the climate classification, suffering from the occurrence of salinity of agricultural soils owing to droughts, decreasing rainfall cycles and mismanagement of water resources, resort to discovering water corridors that penetrate agricultural areas, salinity concentrations through soil scrubbing processes The development and spread of aquatic organisms is affected by several variables, including biotic variables such as the connection of microbes, their connection with crops and animals found in water, and non-biotic factors, including a mixture of physical and chemical variables that have important effect on the amount, species and activity of aquatic organisms (ShartooH *et al* ,2012). In Iraq, drinking water has become the primary source of coliform, fecal coliform bacteria incidence a normal cohabitation in the human intestines Contamination of drinking water from human or animal outlets. Furthermore, this bacteria is contaminated and is a contagious cause of intestinal inflammation and infection Vagina and uterus in females accountable for severe diarrhea in babies and E. coli nursing strain Death of many kids under the age of five Due to diarrhea, particularly in developing nations (turky, 2013). Bacterial pathogens levels decline downstream a river as a consequence of river assimilation but may continue and move long distances presenting a public health danger to downstream populations dependent on the river as a primary source of water (Abraham, 2010)





Al SafaSaed Al Kubaisi and Sufyan Mohammed Shartooh

MATERIALS AND METHODS

Study area

The study area included six local trocars in the city of Ramadi as it show in figure (1). Water samples were collected each month from each of the six sites during the period from November 2018 to April 2019. The sampling stations were selected precisely because they pass through the most areas of the city of Ramadi population density added to the large quantities of water passing by these trocars, which flow directly in the Euphrates River without treatment, adding to the diseases spread among the inhabitants near these trocar. The sites coordinates were determined by using Geographic Position System (GPS) as it is seen in Table (1).

Collection of samples

The samples were collected from the surface layer at a depth of 10-15 cm using 250 ml sterile bottles prepared for this purpose. It were taken to the laboratory to carry out the required bacteriological analysis. The time period between taking the sample and conducting the analysis was very short, so that it did not exceed three hours to see the accuracy of the results. Also, water samples were brought from the same site for different chemical and physical analysis. The samples were placed in (cool box) and samples were brought to the laboratory for the required bacteriological analyzes. The following information is recorded with each model (sample number, place of collection, history, climate condition). A number of physical and chemical tests have been carried out in the Ramadi water project, including pH by PH - Meter. The conductivity was measured by the conductivity - meter ,BOD, Total Suspended Solids (TSS) Measured using 0.45 μ filter paper ceramic evaporating dish and drying oven at 103-105EC temperature by evaluating the difference between blank and charged item weights to extract outcomes. Other variables were also measured such as; TS, Turbidity by Turbidity meter (HI98703).

In order to calculate the total count of coliform, fecal coliform the most probable number (MPN) method was used by using the multi-pipe method by preparing two concentrations of macConky broth media. 15 tubes were prepared for each sample, so that 5 tubes, each containing 10 ml of media concentration, 10 ml of the sample, 10 other tubes containing 10 ml of single concentration and 5 of them added 1 ml Streptococci and fecal streptococci have used the same method used to measure coliform bacteria but using azidedexteros broth media. The probability table, which estimates the most likely number of bacteria in 100 ml of sample water, has been used In addition, the samples were isolated and diagnosed using tests including Indol test, Simmon citrate test, VP test, Methyl red test and Urea test. Gram stain, catales test and finally oxidase test, where *E coli*, *klepsiellapenumoniae*, *staphylococcus aureus*, entero -bacter were obtained, Some samples were also diagnosed by VITEK-2 compact system equipped by Bio Merieux Company Of the bacterial species diagnosed with VITKE -2 are *Pantoeaspp*, *kiuyveracryocrescens*, *Escherichia coli*, *pseudomonas alcaligenes* .and other hand. The polymerase chain reaction (PCR) was used in order to amplify different parts of specific gens (relative gens),using ERIC-PCR experiments which is done by comparing different species of *Klebsiella spp* separated from various environments depending on (finger printing technique).Thistechnique includes preparation, selection and amplification of primers in addition to agarose gel electrophoresis, the results of this technique is analyzed statistically using dendrogram. And then to determine the moral differences of the measured characteristics using statistical analysis of the SAS program.

RESULTS AND DISCUSSION

o diagnose bacterial isolates using VITEK _2 compact system to confirm the biochemical test results. After the purification of bacterial isolates it was diagnosed by VITEK _2 compact system, Thus ,it has been obtained the species following : *Kluyvera cryocrescens*, *Escherichia coli* , *Pantoea spp* , *Pseudomonas alcaligenes* , *Klebsiella pneumonia*.



**Al SafaSaed Al Kubaisi and Sufyan Mohammed Shartooh****Physical and chemical properties**

Several physical and chemical environmental parameters were studied in order to determine their effects on water of local trocars with its correlation. These parameters include: Temperature, pH, Electrical conductivity, Turbidity, Total dissolved solids, Total suspended solid, total solid and BOD. The highest temperature were recorded as expected during the summer and spring months, while the lowest temperatures were recorded during the months of winter, the highest temperature value was 21C in Alzira'a location during November, while the lowest temperature value was 14 C in both sjaria and swifia location during January, Spatial and temporal variations were not observed in temperature mean values between the studied locations, the temperature mean values ranged from 17.46 ± 0.55 C in Altash location to 18.15 ± 0.9 C in Alzira'a location, Statistical analysis shows a significant differences ($P \leq 0.05$) between temperature mean values during the study months, the highest temperature mean value was 19.5 ± 0.34 C in November and the lowest temperature mean value was 14.66 ± 0.3 C in January.

Water temperature affects the solubility of gases and salts in the water and thus plays an important role in rotting Determination of many physical and chemical properties of water and different neighborhoods in the extent of tolerance to heat, some can withstand high temperatures and some live in a narrow range of temperature (Al hadithi, 1986). and about PH There was no specific variations in general for pH values during the study period. the highest value of pH was 8.2 in Altash location during February, while the lowest value was 7.4 in sjaria location during November. Regarding the location under study, spatial and temporal variations were observed in pH mean values, the highest mean value was recorded in Alzira'a location ($pH = 7.02 \pm 0.04$) and the lowest mean pH value was 7.4 ± 0.0 in Alta'amim location. However, statistical analysis show no significant differences ($p \leq 0.05$) between pH mean value during the study months, the mean values ranged from 7.55 ± 0.06 during November, to 7.81 during march, The pH of most real water varies from 4 to 9 and soluble gasses Such as carbon dioxide and hydrogen sulfide and ammonia significantly reduce pH values The results of the present study were consistent with the results of the previous studies on the shallow basins of Iraq's surface water due to the abundance of bicarbonate and carbonate ions (Shartooh, 2002). While the highest turbidity was recorded 803 NTU in sawifia during November while the lowest value was 4 NTU in Altash during December, regarding the locations under study, spatial and temporal variations were observed in turbidity mean values the highest mean value was recorded in al swifia location ($turb = 185.167 \pm 124.838$) and the lowest mean turbidity value was 26.200 ± 8.670 in Altash location. However, statistical analysis show significant differences ($p \leq 0.5$) between turbidity mean values during the study months, the mean value ranged from 217.6 ± 123.064 during November, to 27.883 ± 17.033 during December, because of the increased flow, high turbidity contributes to a reduction in the amount of sunlight accessible, a reduction in algae and macrophyte production (Sabri *et al.*, 2001). Therefore, we find that the values of turbidity were lower than it was during the month of April, due to the rain that raged during this month.

The results are in agreement with previous studies of (Al-Fatlawy, 2007; Zaidan *et al.*, 2009; Gangwar, 2012). Whilst electrical conductivity shows the highest electrical conductivity was $4405 \mu\text{s/cm}$ in Al-Tash during December, and the lowest electrical conductivity was $1092 \mu\text{s/cm}$ in Al-Tash during April. Pertains the under study trocars, spatial and temporal variations were observed in the mean values of the electrical conductivity Thus, the mean values were ranged from $2916.50 \pm 359.358 \mu\text{s/cm}$ in Al-Ta'amim trocar to $1685.33 \pm 148.482 \mu\text{s/cm}$ in Al-Mala'ab trocar. Nevertheless, statistical analysis shows a significant differences ($p \leq 0.05$) between the electrical conductivity mean values during study period, the highest mean value was $2962.166 \pm 444.87 \mu\text{s/cm}$ during December and the lowest mean value was $2075.66 \pm 258.17 \mu\text{s/cm}$ during April, The types of salts (ions) that cause conductivity are usually sodium, calcium magnesium, potassium chlorides, carbonates and sulfates (El Shakouret *et al.*, 2012), Natural water has low conductivity but will increase when there is pollution due to the effect of sewage water and household wastewater, which increases the EC. Through correlation coefficient, there was a strong correlation between electrical conductivity and total dissolved solid matter (TDS). but regarding total dissolved solid (TDS), the highest TDS mean value was 6234 mg/l in AL tash location during November, while the lowest TDS mean value was 1190 mg/l in AL-Swifia during November. The TDS mean values ranged from $3124.48 \pm 584.37 \text{ mg/l}$ in AL-Ta'amim location





Al SafaSaed Al Kubaisi and Sufyan Mohammed Shartooh

to 1597.47 ± 153.05 mg/l in Al-swifia location. However, statistical analysis shows no significant differences ($p \leq 0.5$) between TDS mean values during the study months, the highest TDS mean value was 2785.166 ± 724.51 mg/l in November, and the lowest TDS mean value was 1431.783 ± 124.89 mg/l in April. The quality of water input and evaporation processes are concentrated in the TDS. However, due to the rainy months during in the study period, while the lowest values were obtained during the month of April and March, The quantity of TDS varies on water supplies, so water has greater levels of TDS when it moves through sediments rich in minerals or soluble salts, even when water gets agricultural or residential drainage (Barker, 2008). And about Total suspended solids (TSS), there was no specific variations in general for TSS values during the study locations the highest value of TSS was 2096 mg/l in Al-Zira'a location during November, while the lowest value was 11.7 mg/l in AL-ta'amim during February.

Regarding locations under study, spatial and temporal variation were observed in TSS mean value, the highest mean value was recorded in AL-Zira'a location ($TSS = 735.67 \pm 274.64$) and the lowest mean value was 251.83 ± 129.699 in Swifia location. However, statistical analysis show significant differences ($p \leq 0.05$) between TSS mean values during study months, the mean values ranged from 1434.66 ± 223.980 mg/l during November, to 163.2 ± 74.002 mg/l during April. Suspended solids can occur from urban runoff and agricultural property erosion, industrial waste, bank erosion, development of algae, or wastewater discharges. (Zaidan *et al*, 2009). It is noted from the results that the highest values were in November the reason is due to the small amount found in the trocars, On the contrary, during the month of April, the lowest value recorded as a result of the amount of heavy rains that collided this 129.699 month, this result agreed with prior research by (Ibrahim, 2016). Regarding to Total solid (TS) there was specific variations in general for TS values during the study period. the highest value of TS was 21543 mg/l in AL-Ta'amim during November, while the lowest value was 399.5 mg/l in AL-Swifia location during February, Regarding locations under study, spatial and temporal variations were observed in TS mean values, the highest mean value was recorded in AL-Ta'amim location ($TS = 6678.78 \pm 3034.62$ mg/l) and the lowest mean TS value was 1683.95 ± 304.34 mg/l in AL-Swifia location. Never the less, statistical analysis shows a significant differences ($p \leq 0.5$) between TS mean values during the study months, the mean values ranged from 7083.833 ± 2965.482 during November to 1597.9 ± 190.500 during April.

While BOD5 the highest BOD was 57 mg/l in AL-Swifia trocar during November, and the lowest BOD was 2 mg/l in AL-Sjaria, AL-Zira'a trocars during April. Pertains study trocars, spatial and temporal variations were not observed in the mean values of the BOD, thus, the mean values were ranged from 16.83 ± 5.86 mg/l in AL-Tash trocar to 33.67 ± 7.13 mg/l in AL-Swifia trocar. Nevertheless statistical analysis shows a significant differences ($p \leq 0.5$) between the BOD mean values during the study period, the highest mean value was 51.66 ± 3.062 mg/l during November and the lowest mean value was 5 ± 1.21 mg/l during April The decline in the month of April is due to the high rainfall, high water levels, low temperature and increased algae growth, which increased the concentration of oxygen. BOD is described as the quantity of oxygen absorbed by micro-organisms to oxidize organic matter contained in the water, BOD value dependent on the communities that place their garbage in the trocars water add to the residues and remains of animals that are transferred immediately or indirectly and cause pollution of this water and also the reason for the elevated BOD numbers is the elevated rise in the amount of bacteria and this outcome is compatible with (Sabri *et al*, 2001), (Shartooh, 2002). The findings show an important connection The highest values were recorded In al swifia during November may be attributed to increased flows of sewage water and waste Industrial products containing organics into trocars and whose analysis requires consumption Large amounts of dissolved oxygen.

Bacterial Pollution

Total coliform bacteria (TC) and Fecal Coliform (FC), the presence of coliform bacteria in water is a general indicator of pollution and can be of nature or stool (kalaf, 1987). However, that the highest count of coliform bacteria was 1600 cell/100ml in Swifia trocar during December, and the lowest count was 2 cell / 100 ml in Almala'ab trocar during January. However, spatial and temporal variations were not observed in the mean values of values of the coliform bacteria most propable number as it seen in (table 3.9), thus the mean were ranged from 36.83 ± 22.8 cells / 100 ml in





Al SafaSaed Al Kubaisi and Sufyan Mohammed Shartooh

Almala'ab trocar to 427.170 ± 238.89 cells / 100 ml in swifia trocar. Whilest , statistical analysis shows a significant differences ($p \leq 0.05$) between the coliform count mean values during study period , the highest mean values was 653.5 ± 208.3 cells / 100 ml during December and the lowest mean value was 14 ± 5.17 cells / 100 ml during January. Is detected fecal coliform to investigate other pathogenic bacteria such as cholera and typhoid, where fecal coliform bacteria are present in these intestines because their preparation is more frequent and longer in water. Detection is easier and is a sign of the presence of bacterial pathogens in the water It should be observed that it is not necessary to have a human intestine. It is also found in the intestines of warm-blooded animals (Edberg *et al*,2000).

The highest fecal coliform bacteria was 2400 cell\100mlin Alzira'a trocar during March, and the lowest count was 11 cell / 100 ml in Ata'amim trocar during April .Pertains study trocars, spatial and temporal variations were not observed in the mean values of the fecal coliform, thus, the mean values were ranged from 291.830 ± 165.308 mg\l in AL-Swifia trocar to 27.670 ± 18.561 mg\l in AL-mala'ab trocar. However, statistical analysis shows a significant differences ($p \leq 0.05$) between the fecal coliform count mean values during study period , the highest mean values was 201.833 ± 179.671 cells / 100 ml during December and the lowest mean value was 9.33 ± 3.62 cells / 100 ml during January , due to the internal water capacity On self-purification, and the susceptibility of bacteria to remain in such water even though intestinal bacteria can stay alive in the water for a limited period of time , But they are increasing in large quantities within polluted water without losing their ability to be infected .The rise in total coliform bacteria at this time of year It was also recorded by others (Al-Shuwani, 2001) for studying the lower Zab water as well as by (Sabri *et al*,2001).

Finally streptococci bacteria and Fecal streptococci (FS), the highest streptococci bacteria count was 1100 in Swifia during December, and the lowest streptococci bacteria count was 2 cell\100ml in Al-Tash and Almala'ab during January, Pertains study trocars, spatial and temporal variations were observed in the mean values of the streptococci bacteria count, thus, the mean values were ranged from $832.50b \pm 408.655$ in Alzira'a trocar to $117.17a \pm 42.659$ in Ata'amim trocar. However, statistical analysis shows a significant differences ($p \leq 0.05$) between the streptococci bacteria count mean values during study period, the highest mean values was $508.5a \pm 382.196$ cells / 100 ml during March and the lowest mean value was $29.666a \pm 9.902$ cells / 100 ml during April. Andabout Fecal streptococci, The highest count Fecal streptococci of bacteria was 1100 cell\100ml in Almala'ab trocar during December, and the lowest count was 4 cell / 100 ml in Ata'amim trocar during January. . Pertains study trocars , spatial and temporal variations were observed in the mean values of values of the Fecal streptococci bacteria ,,thus the mean were ranged from $81.830a \pm 35.596$ cells / 100 ml in Altash trocar to $484.000b \pm 179.651$ cells / 100 ml in Almala'ab trocar. Nevertheless, statistical analysis shows a significant differences ($p \leq 0.05$) between the fecal streptococci mean values during study period, the highest mean values was. $359.666b \pm 55.832$ cells / 100 ml dMarch and the lowest mean value was $16.666a \pm 5.731$ cells / 100 ml during April.

As a result of the increase in human and animal activity in addition to waste water in this site. Where the results proved that high rainfall played a major role in reducing the rate of streptococci bacteria during April to $29.666a \pm 9.902$ cell\100ml while the highest rate was during March. While the highest number of fecal streptococci bacteria was found in Almala'ab trocar, this is attributed to the presence of human and animal activity in that location. In the AL-tash site, the number of bacteria was very few compared with the other sites. This is because the location of trocar is far from the residential neighborhoods, thus reducing the waste that reaches the trocar. faecal streptococci, used as markers of water pollution. Depending on fig(2) we can divide the isolated bacteria's to three different genetic patterns with 66% similarity ratio according to its relativistic degree with each other in spite of the isolation source variation depending on the statistical analysis results of (Dendrogram). These bacteria's have been isolated from the environmental samples taken from local trocars water and from the patients those who lies in Al Ramadi general hospital. First Group (G1) includes K2,K6 bacterial isolates with 86% similarity ratio while the second group (G2) included the bacterial isolates (K1,K7) with 52% similarity ratio, as regards to third group (G3) contained (K8,K9) with 53% similarity ratio. In the other hand the isolated bacteria's (K3,K4,K10) showed departed genetic relations with interference with other groups, However.(K5) did not included in any group A rapprochement





Al SafaSaed Al Kubaisi and Sufyan Mohammed Shartooh

is shown between the environmental isolates and the isolates taken from the patients like (K1,K2,K6 and K7). Where a 100% similarity ratio is founded between (K6, K7) and (K9, K8). And the environmental isolates (K1,K2). These results showed that the trocars's isolates is similar to the isolates taken from the patients as a confirmation to that the patient diseases being transmitted to them through consumption of these trocars water because they are living beside these local trocars. These results came similar to the study results of (Aldulaimy, 2015) who found that there is a 52% genetic similarity between the *Klebsiella* isolates gained from sewage water of Al Ramadi hospital and the bacterial isolates taken from the patient's lies in the same hospital. Table (2) Number of *Klebsiella spp.* isolated from clinical specimens and different environmental samples (patients lies in Ramadi General Hospital and the water of the trocars).

Genetic proximity of bacterial isolates

Genetic fingerprinting was determined to amplify different parts of the proximal genes for ten bacterial isolates of *Klebsiella* genus from different environment as shown in table (2). ERIC-PCR method is used to identify the different genetic variations of elected bacterial isolates and detecting the real sources of isolates which causes bacterial infections, through using Polymerized chain Reaction specified primer and primary Specialist. In order to diagnose proximal genes, the reaction was carried out at a size of 50 microliters. After carrying the output on the agarose gel at a concentration of 2 %, 5 V / cm For an hour and a half, the beams produced from the reaction showed that there were many genes in the bacterial isolates. The isolates differed in their containment of the genes as in the Figure (3). Is analyzed using statistical group analyzer program (Dendrogram), three different groups of bacterial isolates were detected (G1,G2,G3)

REFERENCES

1. APHA, AWWA and WFF.(2005).Standard Methods for the Examination of Water and waste water, 21 the d.,edited by Eaton, A.D.;L.S Clesceri ;E .W .Rice, and A .E. Greenberg.
2. Abraham, W;R.(2010), Megacities as source for pathogenic bacteria in rivers and their fate downstream. Intl. J. Microbiol; 10(1155): 13.
3. Aldulaymi, N, M, H. (2015). The use of some bacteria as vital indicators of pollutants in the wastewater of Ramadi General Hospital. PhD thesis, College of Science - Anbar University.
4. AL Shwani, T, M . (2001) , Environmental study and microprocessing of the lower Zab River from Elton Bridge to Hawija / Nationalization Governorate. Master Thesis College of Education Girls University of Tikrit.
5. Al hadithi, H; T . (1986) . Aquatic Microbiology. National Library for Printing and Publishing, University of Mosul.
6. Al Fatlawy, Y.F.(2007).Study the drinking water quality of some Baghdad drinking water treatment stations (Doctoral dissertation Ph. D. College of Science ,Baghdad University).
7. Barker, H.J.(2008). Physio-chemical characteristics and metal bioaccumulation infour major river systems that transect the Kruger National Park (Doctoraldissertation, University of Johannesburg).
8. Doron, T; A. (2011), Unacceptable level of sewage bacteria in river creek, Hudson – Catskill newspaper, 1-3 .
9. -DO Costa, A;C;A. and Duta, F;P.(2001), Bioaccumulation of copper, zinc, cadmium and lead by *Bacillus sp.*, *Bacillus cereus*, *Bacillus sphaericus* and *Bacillus subtilis*. 32: 1-5.
10. Edberg, S.C. Rice, E.W. Karlin, R.J. & Allen, M.J. (2000). *E. Coli*: the best biological drinking water indicator for public health protection. *Journal of applied microbiology*, 88, 106-116.
11. El Shakour, E. H. A., & Mostafa, A. (2012). Water quality assessment of river Nile at Rosetta branch: impact of drains discharge. Middle-East Journal of Scientific Research, 12(4), 413-423.
12. Gangwar,R.K.,Khare ,P .,Singh ,J.,& Singh ,A.P.(2012).Assessment Of physic –chemical properties of water: River Ramganga at Bareilly ,UP. Journal of Chemical and Pharmaceutical Research 4(9) ,4231-4234.




Al SafaSaed Al Kubaisi and Sufyan Mohammed ShartooH

13. Ibrahim, Shariff bin Che, (2016) Experiment 2,3,4: Total solid (ts), total suspended solid (TSS), volatile suspended solid(VSS), Iraq. Journal of Water Resource and Protection, 3(11), 812-823.
14. Lesley C:L. (2008), Extent of *E.coli* contamination of Cagayan De Oro River & factor causing contamination Liceo J. of higher Edu. Res. CHED accredited Res. J. 1-20.
15. ShartooH, S.M.(2017). Environmental and Microbial Investigation on the Dredged Sediment of Soil of Diyala River in Iraq. Journal of environmental Science and technology, ISSN 1994-7887 , v (10) : 147-156 .
16. Singh, s. Raj , A. (2006) . Seasonal Bacteriological Analysis of Gola River Water Contaminated with Pulp Paper Mill Waste in Uttaranchal, India . Volume 118, Issue 1–3, pp 393–406 .
17. ShartooH, S.M. and Al-Hiyaly , s ; a ; k.(2012), Study of Seasonal variations of Main Outfall Drain and Four Northern Trocars in Iraq, Ministry of Science and Technology – Directorate of Hazardous Waste Treatment & Destruction, University of Technology - Environmental Research Center , Baghdad – Iraq.
18. ShartooH ,S.M.(2002), BACTERIAL POLLUTION IN AL-HABANIA AND AL-THARTHAR RESERVOIRS, to the College of Science-University of Baghdad in Partial fulfillment of the requirement for the Master's degree of Science in Biology.
19. Sabri, A.W. Rasheed, K. Thijar, L.A.(2001). Limnological studies in reservoirs impoundment and ponds of central Iraqi: zooplankton central of environmental studies of department of industrial technique , Iraqi atomic energy commission .
20. Turkey, A, M. (2013) , Study of the different types of *E coli* isolated from the waters of the Euphrates River in the city of Ramadi , ISSN1991- 8941 , Anbar University Journal of Pure Sciences – Volume(7) .NO.1 .
21. Zaidan, T., Rahman, I., and Saad, W. (2009). An environmental study of chemical and physical pollutants in Euphrates river water in Ramadi and Fallujah. Journal of university of Anbar for Pure science, 3(3), 107-117 .

Table 1. Coordinates of Study Sites

Sites	Latitude (N°)	Longitude (E°)
S.1	33,4254	43,3236
S.2	33,425129	43,308361
S.3	33,409030	43,400303
S.4	33.420638	43,261736
S.5	33,418949	43,259850
S.6	33,421876	43,261178

Table 2.Number of *Klebsiella* spp. Isolated from clinical specimens and different environmental samples

Samples type	No of samples	<i>Klebsiella</i> spp no.	percentage
Urine	40	8	20%
Wounds and burns	55	9	16.36%
Sputum	19	3	15.78%
Water trocars	10	5	50%
Total	124	25	20.16%





Al SafaSaed Al Kubaisi and Sufyan Mohammed Shartooh

Table 3. Standard error (se) with significant differences according to Duncan test Mean value and ±

Standard error (se) with significant differences according to Duncan test Mean value and ±								
Months	Tem		Turb		PH		EC	
November	19.500d	±0.342	217.6c	±123.064	7.55a	±0.067	2145.500	±273.641
December	16.666b	±0.211	27.883a	±17.033	7.7a	±0.089	2962.166a	±444.871
January	14.666a	±0.333	32.466a	±12.081	7.6667a	±0.095	2269.666a	±356.334
February	18.450c	±0.243	109.666ab	±25.765	7.8a	±0.106	2263.1166a	±236.598
March	18.7666c	±0.161	93.666ab	±23.288	7.816a	±0.087	2439.1a	±350.753
April	18.6166c	±0.170	74.5ab	±21.250	7.7166a	±0.117	2075.666a	±256.171

Months	TDS		TSS		TS		BOD	
November	2785.166a	±724.517	1434.666c	±223.980	7083.833ab	±2965.482	51.666b	±3.062
December	2775a	±620.563	728.666b	±186.778	3615ab	±728.217	44b	±3.022
January	2693.833333	±306.630	249a	±67.897	3463.333ab	±668.208	17a	±7.090
February	2560.5a	±661.279	261.45a	±106.053	2471.933a	±709.563	12a	±5.183
March	1701.833a	±234.258	315.083a	±70.035	2066.9a	±251.722	10.17	±3.049
April	1431.783a	±124.891	163.2a	±74.002	1597.9a	±190.500	5a	±1.211

Different letters indicate of significant differences at (p≤0.05).

Table 4. Standard error (se) with significant differences according to Duncan test Mean value and ±

Standard error (se) with significant differences according to Duncan test Mean value and ±				
Months	Coliform cell\100ml		fecal coliform cell/100ml	
November	653.5b	±208.314	250a	±75.740
December	292.666ab	±261.490	201.833a	±179.671
January	14a	±5.170	9.333a	±3.621
February	103.666a	±46.961	81.333a	±37.933
March	148.333a	±56.414	100.666a	±37.447
April	46.666a	±23.011	25.33	±11.497

Different letters indicate of significant differences at (p≤0.05).

Table 5. Standard error (se) with significant differences according to Duncan test Mean value and ±

Standard error (se) with significant differences according to Duncan test Mean value and ±				
Months	streptococci cell/100m		faecal streptococci cell/100ml	
November	237a	±175.140	111ab	±73.278
December	483.666a	±263.632	314.333ab	±177.004
January	417.166a	±248.984	232.833ab	±141.667
February	482a	±235.259	232ab	±77.607
March	508.5a	±382.196	359.666b	±55.832
April	29.666a	±9.902	16.666a	±5.731

Different letters indicate of significant differences at (p≤0.05).





Al SafaSaed Al Kubaisi and Sufyan Mohammed Shartooch

Table 6. Mean value and ± Standard error (se) with significant differences according to Duncan test

Mean value and± Standard error (se) with significant differences according to Duncan test								
Locations	Temp.		Turb		Ph		EC	
Almal'ab	17.583a	±0.770	50.917a	±22.557	7.70bc	±0.077	1685.33a	±148.482
Swifih	17.733a	±0.807	185.167b	±124.838	7.60b	±0.063	1824.00ab	±168.951
Alta'amim	18.117a	±0.536	26.483a	±5.976	7.40a	±0.000	2916.50c	±359.358
Altash	17.467a	±0.558	26.200a	±8.670	7.85cd	±0.099	2340.88abc	±519.719
Alzira'a	18.150a	±0.907	150.250a	±22.237	7.92d	±0.040	2618.33bc	±176.027
Sjaria	17.617a	±0.917	116.767a	±27.401	7.78bcd	±0.083	2770.17c	±93.392
Locations	TDS		TSS		TS		BOD	
Almal'ab	1601.67a	±162.733	504.42a	±220.745	2104.58a	±352.141	29.17a	±6.096
Swifih	1597.47a	±153.050	251.83a	±129.699	1683.95a	±304.347	33.67a	±7.135
Alta'amim	3124.48a	±584.374	690.57a	±317.896	6678.78b	±3034.620	20.67a	±9.618
Altash	3024.83a	±951.562	423.75a	±209.267	4017.75ab	±1219.725	16.83a	±5.868
Alzira'a	2201.67a	±325.311	735.67a	±274.643	2754.00ab	±180.131	19.50a	±10.481
Sjaria	2398.00a	±164.617	545.83a	±178.529	3059.83ab	±268.463	20.00a	±10.951

Different letters indicate of significant differences at (p≤0.05).

Table 7. Mean value and± Standard error (se) with significant differences according to Duncan test

Mean value and± Standard error (se) with significant differences according to Duncan test			
Locations	Coliform cell/100ml		Faecal coliform cell/100ml
Almal'ab	36.830a	±22.873	27.670a ±18.561
Swifih	427.170a	±238.898	291.830a ±165.308
Alta'amim	167.170a	±75.615	101.830a ±43.551
Altash	206.500a	±178.839	94.170a ±73.395
Alzira'a	215.500a	±177.062	59.500a ±36.334
Sjaria	205.670a	±178.903	93.500a ±73.363

Different letters indicate of significant differences at (p≤0.05).

Table 8. Mean value and± Standard error (se) with significant differences according to Duncan test

Mean value and± Standard error (se) with significant differences according to Duncan test			
location	Streptococci cell\100m		faecal streptococci cell/100ml
Almal'ab	750.50ab	±314.892	484.000b ±179.651
Swifih	198.50ab	±108.070	188.170ab ±85.472
Alta'amim	117.17a	±42.659	110.330a ±49.050
Altash	84.33a	±44.655	81.830a ±35.596
Alzira'a	832.50b	±408.655	278.670ab ±118.829
Sjaria	175.00ab	±61.527	123.500a ±45.180

Different letters indicate of significant differences at (p≤0.05).





Al SafaSaed Al Kubaisi and Sufyan Mohammed ShartooH

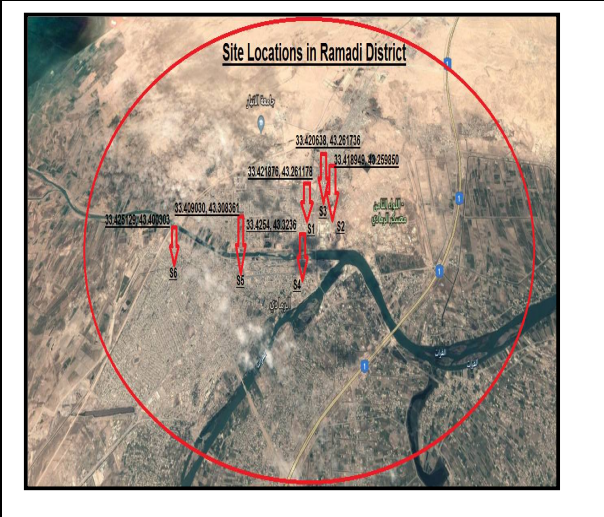


Figure1. Shown the six local trocars in the city of Ramadi.

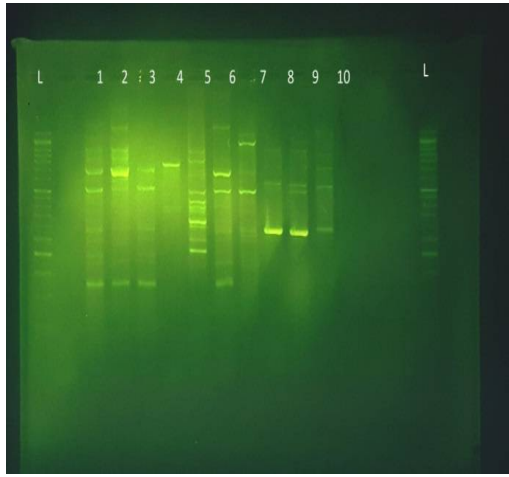


Figure 2. Statistical analysis of three groups by using (Dendrogram) with 66% similarity ratio.

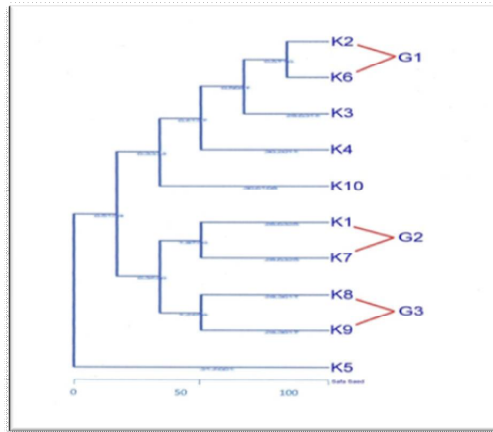


Figure 3. Statistical analysis of three groups by using (Dendrogram) with 66% similarity ratio.





Anti Barnacle Paint Additive – OHUCAX

Deepak Bhattacharya

Honorary Head, Oddisi Research Laboratory, Sri Radha Krishna, Kedar Gouri Road, Bhubaneswar – 751002, India

Received: 14 July 2019

Revised: 17 Aug 2019

Accepted: 19 Sep 2019

*Address for Correspondence

Deepak Bhattacharya

Honorary Head,

Oddisi Research Laboratory,

Sri Radha Krishna, Kedar Gouri Road,

Bhubaneswar – 751002, India.

Email: oddisilab1@dataone.in



This is an Open Access Journal / article distributed under the terms of the **Creative Commons Attribution License** (CC BY-NC-ND 3.0) which permits unrestricted use, distribution, and reproduction in any medium, provided the original work is properly cited. All rights reserved.

ABSTRACT

Organic material (*Colocasia* leaf extract) as starting source ending with inorganic similar (Calcium oxalate). Leafs are shredded, dried, suspended - extracted in commercial thinner. Admixed into commercial grade thinner (toluene) and applied. Termed OHUCAX (Oddisi Hull Coat Additive Experiment). Anti-Fouling; Anti-Barnacle and Friction reducing effects are indicated.

Keywords: Anti-fouling; Anti-Barnacle; Ship-hull Coat; Paint Additive; Friction Reducer; Marine Paint; OHUCAX.

INTRODUCTION

Barnacles are well known so also the associated problems R1; the efforts to overcome R2, 3; the economic & strategic aspects R4 and environment issues R5. In this communication we report the culmination of a 2 decade long effort. It is known as OHUCAX (Oddisi Hull Coat Additive Experiment). It pertains to experiments vis-à-vis anti barnacle and anti-fouling paint additive which also includes historical and cultural heritage as cue and or inspirations. The objective is to develop a eco-friendly; non toxic; effective additive that can be ready mixed into ordinary commercial grade synthetic paint before being sprayed on to ships/vessels hulls and on the bodies of the metal piers that are adversely affected. It does not add any additional weight and whereas, collinearly reduce the co-efficient of the friction (drag) and enables fuel economy cum gain of speed. This is a NGO based not for profit research initiative. OHUCAX shall be for societal benefits, Students and Employment Generators. No patent will be applied for as patent will disable the economically weak from adopting OHUCAX, and further innovations.



**Deepak Bhattacharya**

MATERIALS AND METHODS

Colocasia leaves are in abundance in water sufficient regions\patches of the tropo-equatorial belts. It is not consumed by anthropomorphs nor by the theriopomorphs. Hence is a good source for industrial use. Cut from base (no stalk), shred, grind to paste (add water as necessary as per grinding equipment's standard). Air dry or sun dry. This is base material. Suspend such dried leaf powder in commercial grade thinner (80% toluene) for >12hrs. Saturated, v/v. The leaf contents effluxes into the thinner media. An green solution is got as the supernatant. This is the OHUCAX. It is potent. It can be further concentrated by evaporation methods. The slurry may be discarded. The 'thinner' is the extract medium cum vehicle. Admix such OHUCAX into any commercial grade enamel pain at a ratio raging between 1 : 6 to 1:16. Brush and or spray paint is the method of application. Air dry the coloured surface. The painted surface is ready for anti-barnacle; anti-fouling and anti drag test/use.

EXPERIMENTS

The coated plates were immersed in a large cement tank full with sweet water got from irrigation canals. This (Fig-1) is aquatic water and not marine. However, loaded with aquatic life, and refurbished almost daily via top-ups. Location south Bhubaneswar (20.27°N 85.84°E). Soil conditions being as alike riparian coastal (loam-clay & low energy deposits). The panels shown in Fig- 1 were slung and dunk 3½ feet deep and retained undisturbed for 4 weeks – after which they were wheeled out and photographed in-situ. In Fig – 1, the longer panel was part coated with paint that had the additive as admixed to bring out the contrast if any as 'crisp boundary phenomena CBP' (between admixed and non admixed synthetic paints). Our images brings out the CBP aspect prominently. The neighborhood domain affects not. Significant to context, indeed. The small panel was entirely bereft of OHUCAX. It attracted full onslaught of fouling. This means, there was adequate fouling load with effective property in the same tank so as to colonise the adjacent un-coated platform (small plate) and not the OHUCAX admixed painted area. Thus there was no local area inhibition or thwart factor. On studying the un-coated borders (see small plate – finger beneath) synthetic paint (clearly also) attract more of fouling than plain Al faces.

Fig – 2 contains 2 small Al panels that were identically brush painted with the very same synthetic paint admixed with the same OHUCAX additive (made in that very same batch) at 2 variable potencies vide pick, pour & stir method. Post open room air drying, both the panels were dunk 3½ feet deep, still, in the same tank for identical period under near identical agro-met conditions (non rainy season). Every step identical in both the experiments (which were run repeatedly over years. The panel to the viewer's left had a greater concentration of OHUCAX additive (pond side hand made; hand applied). The panels clearly indicate OHUCAX thwarts fouling. The painted surfaces also shows less friction i.e., rollagon property (additional information; data not adduced). Repeatability is got. The range of the functions of the ingredients posit as objective acquiring (inviting further work). Author stands by to assist the boating community to self make such OHUCAX (as part of family welfare).

Fig- 3a is dated to 1997-99. Three aluminum panels numbered 1-3 from viewer's right. Panel No. 1 had an OHUCAX additive: synthetic paint ratio of 1:12 (Ohucax: Synthetic enamel). Panel No. 2 had a additive ratio of 1 : 8. Panel No. 3 was sans OHUCAX. The panels were submerged in sea water of 20ppt NaCl contained a green coloured plastic bucket. Immersed, covered, undisturbed for 14months at a stretch Fig-3b. RESULT : Post lifting Panel No. 3 shows more detachment effect than the rest (indicates variable ion permeability aspect). The variability between Panel No. 1 & 2 partly may also be due to inconsistencies of hand/manual mixing. Fig.3c is that of galvanized sheet of 2mm thickness. It shows 3 segments. To viewer's left is OHUCAX admixed paint. The mid segment is uncoated (bare metal surface). To the viewer's right is only synthetic enamel paint. Following paint application a week later on datum 01-02-2001 identical quantity of lab grade NaCl crystals was placed and the plate were left in open humid condition indoor. On 01-04-2001 an inspection was made. Photograph was taken on 01-06-2001. RESULT: OHUCAX admixed paint withstands long period saline (20% v/v) insult better and 99% pure salt insult best (series Fig-3). Fig 3c



**Deepak Bhattacharya**

is preserved in our archive. After 2 decades of storing it shows extensive degradation of the entire of the virgin enamel paint portion, even periphery (viewer's right). And whereas the OHUCAX admixed painted region presents remarkable anti-rust property (mss., submission datum). Further, as compared to salt insult OHUCAX admixed paint mildly thwarted spread and penetration of the alkaline insult – NaOH flakes (data not shown). Fig-4 presents the experiments done with pure research grade NaCl & NaOH. Aluminum panels were coated with and without OHUCAX. NaCl & NaOH crystals were placed. Left for 24hrs at room temperature, in open. OHUCAX admixing apparently imparts to the paint film a non-reactive property; thwarts/slow down cross membrane ion transfer. Degradation is least. This could be another reason as to why Cyprids (barnacle larva) and any marine/aquatic suspension feeders cum do not co-house on the coated plates in the short period (for sure). We have derived our cue from the water droplet phenomena on colocasia leaf (Fig-5) and inspiration from related own and other's studies [R6]. Amidst all green & translucent water a cyan tinge is noteworthy to our context.

RESULTS

Slightly longer drying time (than commercial paints). Reduces significantly fouling & barnacle adhesion. Non-toxic. Economic. Eco-friendly. Organic material (Colocasia leaf extract) as starting source ending with inorganic similar (Calcium oxalate). (Scholars) can research further and work out variants. OHUCAX enables human resource (employment) and ennobles Resource persons (doctoral & post doctoral).

Observations

It is well known that synthetic enamel (alkyd based) contain clays, calcium carbonate, mica, silica, lime, barites, talc, etc., as fillers and pigments (apart metal/mineral candidates). Each of these be choice candidates for formation of bio films R7. Commencing with Charles Darwin's R8 observation, Cyprids (barnacle larva) are known to co-house on any of these and on any combinations thereof including biogenic and bio-active surfaces R9. The question is what makes OHUCAX fail formation of a bio film and specially fouling (by the Cyprids or mollusks) in ordinary economic commercial grade synthetic enamel paints (that too white emulsion)? For anti-barnacle objectives, oxides, biocides, copper\ss plating, high gloss alkyds instant drying and toughening with ultra catalysts; Teflon; hard and/or bio active paints, etc, have been used. And, various other means and methods (mechanical included) have also been tried to distract the Cyprids. However, the sessile cyprids continue to colonize the hulls R10. Sea going vessels have grown very large with in-sea stay-put being very long. Barnacle colonizing is proving to be deleterious apart making global maritime\naval activity hugely expensive. The inter-tidal coasts have mostly brown water (least light transmission), have a greater variety of cyprid spp., and higher load per colonization event. Light transmission in sub marine envira is dependant also on in-sea hydrological phenomena of up-welling and down welling. The down welling regions being more transparent due to less degenerated and degraded brown matter. Such regions also have less plankton. Bio film growth is plankton dependant. Plankton growth is red-light (infra red) dependant and blooms least in blue-green (cyan) radiance. The average oceanic transmission of cyan colour band is of 450-650nm at a frequency range of 500-650THz R11, Where as, most of oceanic sailing routes have 300-400nm radiance R12 i.e., planktonic. The cyprids need to settle down as they be suspension feeders. A green tinged white surface offers well lit up property. This is due to the abundant IR for the sessile and yet in our plates (OHUCAX regions Fig-1 & 2) they have refused to colonise selectively the OHUCAX regions. Specially the bio-film formation failure is worth noting (Fig-2). Studies R13 shows synergistic roles of lipids and proteins in making the glue that enables co-housing on sub-marine, benthic surfaces.

DISCUSSION

Colocasia is an abundant source R14. It is most easily accessible by the economically weak segments of the sub populations in any nation. Hence we have preferred to re-focus on it. Its leaf contains Vitamin-A and Calcium oxalate. Extraction in toluene at room temp., conserves Vit-A (retinol) well. Thus yield is good. Barnacle\Mollusk





Deepak Bhattacharya

larvae are virgin as alike Vero cells. Vit-A is toxic to larva (to all Vero cells) is well known. Colocasia leaf also contains Calcium Oxalate that too in raphides form i.e., needle-shaped crystals R15. These are of nano scale. And whereas the larva is of macro scale and its settling gear are of micro scale. These (nano needles) can deliver physical pricks to the soft membranes of the larva and also inoculate retinol and or any toxin that may have accumulated or attached \ spiked with. Due boundary phenomena of the non compressible fluid settling at any site (herein on the OHUCAX coated surface) involves violent action/force by the mariner (as compared to its body wt and mass it applies a very large force) which facilitates pricks resulting in pain-edema-immobility-immunological disregulation. The architecture of the settling/landing side of any larva or any suspension feeder's and for that matter in particular the Cypris's architecture is least designed against any pricks. With OHUCAX physical cum chemical lancing happens (dual prong antagonism). Not any catabolism. Nano raphides repel. Nano raphides / Ohucax do not add any drag.

Our Ref-13 (which is considered as the latest in the art) indicates an initial secretion of lipid followed by phosphoprotein. It is a unique preferred mechanics. Lipids have ketons which makes them versatile in reactions. As described therein, the whole process of settlement and co-housing is a case of anabolic cascade. Isotopes & toxins induce catabolism. Catabolic conditions are well sensed by the cyprids. It leads to avoidance (well known). In the case of OHUCAX vrs benthic / marine larva our considered view point is that OHUCAX triggers a catabolic cascade. Catabolism - 1: Ca oxalate present in OHUCAX fails the hydrophobic lipid phase (peroxidation), difficulty in hardening of the cement (glue). The cyprid can sense such failure well. Settlement\co-housing gets thwarted. Catabolism - 2: Due Ca oxalate and subsequent lipid excretion by the cyprid superoxide, anion and hydroxyl radicals may as well be generated in excess, causing cellular injury. It is a loop process. Any one first = same result. Co-housing gets thwarted. Interaction between Ca oxalate and lipid is eminent leading to formation of superoxide anion and hydroxyl radicals well in excess. It causes cellular injury. And whereas sea water conserves Ca oxalate. On one level (in sea) oxalate crystal conservation (even addition) and on the other hand Lipid peroxidation failure. It is a poly phasic loop process. Any one first = same result. Co-housing gets thwarted. Furthermore, due such in-sea addition of Ca Oxalate bio film formation also becomes less marked on OHUCAX coated surface on one hand and on the other co-efficient of the friction remains low (less drag). Catabolism - 3: Assuming (successful) initial settlement directly on neat hull or on a bio-film due swarming by a large mass of Cyprids there is a likelihood of Glycolic acid group generation; hydroxyl radicals and transition metal ions (viz., copper) accumulation = permanent glue failure. The transition metal in the Snail\Barnacle is hemocynin (for they all be blue blooded). Accumulation leads to granulation (alike embolism). This makes the outer adhesive rimmed plaque leaky. Settlement gets thwarted. Barnacles and cyprid the micro organisms in particular synthesize and secrete siderophores (organic cyclic peptides). This increases transition metal (metalloprotein) e.g., hemocynin (it is O₂ & Electron & Proteins of wide Dalton spectrum potentiated) the pro cement material leads to the super glue/metallo-cement. It is a biochem cascade that synthesizes (macro-cyclic) metalloligands which is electron uptake dependant (absence of electrons = inefficient metalloligand synthesis). Macrocylic metalloligands are helical and act as co-ordination polymers R16.

They are large in mass; length; charge potential; versatility packed in minimum space = preferred architecture. In the case of the Cyprid, hemocynin (a large metalloprotein) acts as the ligand for the super glue phenomena. Lipids/oils (keton loaded) are metabolites stored by the sessile mariner for it helps in buoyancy. Oils ejected facilitates better stability on landing. There is thus a poly path rapid electron transfer (between the larval exudates and the platform). Interestingly, hemocynine is marked by less/inefficient co-operative binding of O₂. Inefficient binding leads to offloading of O₂ which is very necessary in the quick cementing of a non brittle, non elastic plaque alias the "super cement". Citrate modified quick fix hard cements are gaining in use R17. An citrate pump facilitates extravasation of oil/lipids for down drive and also in maintaining the viscosity of the metalloligands (cement). The admixed end product may be akin to be citrate platelets\nodules because optimum efficient hydration in the presence of saturated O₂ (in benthic\dynamic submarine conditions), large metalloligands, water & versatile lipid/s, efficient poly-phase electron exchange, least therm build up, nil ettringite formation = successful gluing i.e., permanent settlement. It is an alternating combination of exocytosis process and endothermic reactions. The citrate cysts are one time release members only for settlement else they would adversely interact with the blue blood



**Deepak Bhattacharya**

(supporting info). Catabolism – 4: Ca Oxalate impedes electron transfer (remains almost intact). Initial prospecting by the Cyprid is fobbed – thereby the micro organism senses as not suitable platform. Citrates are anti-oxalate. In sub-marine conditions citrate is absent = Auto degradation or dissolution of Oxalate does not happen. Only citrates scour oxalates. When more & more citrate plaques\ cysts are released by the Barnacle there is surface degradation in a delayed action mechanism and the outer plaque leaks = Co-housing becomes ineffective post initial success. This is Catabolism-4. Accordingly, Table-1 gives a derivative quick fix glue\cement.

Safety & Declaration

The ingredient of OHUCAX are non toxic – cottage industry making possible. Hence employment enabling. No inhalation acute problems. No grants. No agreements. Free. Open for seamless exploitation.

Heritage Aspects

In 1942 (II WW period) British war ships, and vessels of maritime logistics used to be serviced at Calcutta in great numbers. An Indian private Mr. Tara Lal had taken a sub-part contract for cleansing, repainting, leakage plugging. He was rich & illiterate. He used an army of labourers 24 x 7. Mr Lal's work force in order to cheat & do anti-British activity used to scrub all sorts of live weeds (leaf & stalk) onto the boat hulls, specially water hyacinths. Author's father (Mr Harapasanna Bhattacharya) being literate was relied upon by Mr. Lal to translate private & confidential written communications. Mr. Harapasanna had detected such activity. Such family story has been in the back of our mind all along. This apart, Odisha (ancient Kalinga to Chola) had a rich maritime history R18, related sciences R19 and historical connections R20 with the S E Asian archipelago. The raw leaf gives a strong itch to the exposed skin (due raphides). Reptiles (numerous spp.) do not approach the leaf although the stalk (of a sweeter variety) is used as a culinary item in Bengal. We examined a number of low-land coastal weeds, interviewed present times traditional boat-makers and examined recorded documents. Found non. Such usage may have arisen also due to intangible-unrecorded heritage. Nevertheless, colocasia leaf is conspicuous by absence as an ingredient in boat hull paints or for any objectives. Nevertheless, we got our cue from such family story.

CONCLUSION

Anti-Fouling; Anti-Barnacle and Friction reducing effects are indicated. It fends (lances) and also fails adhesion via penta cascades. Possibly therefore the whole spectrum of submarine parasite are not noted on OHUCAX admixed coats. Starting material can be organic and as well inorganic. Either routes easy, economic & effective. In sea life needs to be evaluated in vessels of large draught. This communication is nascent, opens scope for diffused studies about the candidates of OHUCAX, jointly or severally. Afro Asian societies may benefit by translating the process to the common man at boat building and repair centers. No patent(s) is sought. Open for exploitation.

ACKNOWLEDGEMENTS

Two decade long period haul. Work stands on many a broad shoulders. Specially boat owners/boatmen. Hence this work is dedicated to the boat owners/boatmen, with heartfelt regards. Author is to thank Dr, Biswajit of CIFA (very specially for in field his physical participation); Prof. S. Ayyapan, Ex DG cum Secretary DARE, Govt of India cum Chancellor NE Agril Uni., for unlimited help; Dr. B B Rath, Dy Sec US Naval Material Rch Lab (personal meeting). Got also delayed partly to the machinations by Pradeep B and entourage in conspiracy & calumny against me. OHUCAX sample & submissions given to NMRL; Navy; Nilimaa nanotech; others from time to time. Save & except the ordinary, the poor & the hapless non found merit.

DECLARATION

No conflict of interest, No funds or grants, Sole author.





Deepak Bhattacharya

REFERENCES

1. Wahl, M. 2010. Biofouling, Ed by S. Du'rr, & J C Thomason, Full Book (Wiley-Blackwell, 2010).
2. Kamino, K. 2013. Mini-Review: Barnacle Adhesives and Adhesion. *Biofouling*, Vol. 29, pp.735–749.
3. Lunn, Iver (1974). *Antifouling: a brief introduction to the origins and development of the marine antifouling industry*. Thame, UK: BCA Publications. ISBN 0950129917
4. Schultz, M. P., Bendick, J. A., Holm, E. R. & Hertel, 2011. W. M. Economic Impact Of Biofouling On A Naval Surface Ship. *Biofouling*, Vol.27, pp.87–98.
5. Callow, J. A. & Callow, M. E. 2011. Trends In The Development Of Environmentally Friendly Fouling-Resistant Marine Coatings. *Nature Communication*. 2, 244.
6. <https://www.sciencefriday.com/educational-resources/hydrophobicity-will-the-drop-stop-or-roll/> Downloaded & used with thanks.
7. Hall-Stoodley L, Costerton JW, Stoodley P, Feb 2004. Bacterial Biofilms: From The Natural Environment To Infectious Diseases. *Nature Reviews Microbiology*. 2 (2): 95 108. Doi:10.1038/nrmicro821. PMID 15040259.
8. Darwin, C. A Monograph on the Sub-class Cirripedia, with Figures of all the Species Vol. I (Ray Society, 1852).
9. Buhmann M, Kroth PG, Schleheck D, 2012. Photoautotrophic-Heterotrophic Biofilm Communities: A Laboratory Incubator Designed For Growing Axenic Diatoms And Bacteria In Defined Mixed-Species Biofilms. *Environ Microbiol Rep*. 4 (1): 133–40. doi:10.1111/j.1758-2229.2011.00315.x. PMID 23757240.
10. Walker, G. 1971. A Study Of The Cement Apparatus Of The Cypris Larva Of The Barnacle Balanus Balanoides. *Marine Biology*, Vol.9, pp.205–212.
11. Jerlov, N. G., 1976, *Marine Optics*, Elsevier Oceanography Series, 14, New York.
12. Moser, P. M., 1992, Spectral Transmission of Light Through Sea Water, *Technical Memorandum*, Naval Air Development Center, Warminster, PA 18974, Pacific-Sierra Research Corporation.
13. Gohad, N. V. et al. 2014. Synergistic Roles For Lipids And Proteins In The Permanent Adhesive Of Barnacle Larvae. *Nat. Communication*. 5:4414 doi: 10.1038/ncomms 5414.
14. Ramanatha, R.V.; Matthews, P.J.; Eyzaguirre, P.B.; Hunter, D., eds. 2010. The Global Diversity Of Taro: Ethnobotany And Conservation. Rome: *Bioversity International*. pp. 9–10. ISBN 978-92-9043-867-0.
15. Bradbury, J. Howard; Nixon, Roger W. 1998. The Acridity Of Raphides From The Edible Aroids. *Journal of the Science of Food and Agriculture*. 76 (4): 608–616. doi:10.1002/(SICI)1097-0010(199804)76:4<608::AID-JSFA996>3.0.CO;2-2.
16. Zhang, S.Z., Yuan, B., Lan, Y.L. et al. 2017. *Russ J Coord Chem* 43: 700. <https://doi.org/10.1134/S1070328417100116>
17. Gareth Wynn-Jones, et.al., 2014. Injectable citrate-modified Portland cement for use in vertebroplasty, *J Biomed Mater Res (Part B Appl Biomater)*, Vol. 102(8): pp. 1799–1808. doi: 10.1002/jbm.b.33160
18. Bhattacharya & P.C. Naik, 2008. Lay Out, Hydrology & Spacio Temporal Aspects Of A Possible Ancient Inland River Dock : India, *Utkal Historical Research Journal, Utkal Uni.*, Vol. XXI, pp. 61-72.
19. Bhattacharya Deepak, 2015. Compass & Vernier Type Models in Indo Archaeology : Engineering Heritage, *Journal Of The Institution Of Engineers, India, Ser. A (July–September 2015)* 96(3):215–221. Springer. DOI 10.1007/s40030-015-0119-x.
20. Bhattacharya Deepak, 2017. European Frigate Fort - Potagada? Naval Heritage of India: A Hypothesis, *Journal of Odishan History*, Vol. XXIX, Dec. 2016, pp192-207.
21. Krailassuwan, S. 2018. History of Thai Maritime Trade. *Maritime Technology and Research*, 1(1), pp 9-14. <https://doi.org/10.33175/mtr.2019.147777>

Table 1. A derivative idea about a quick fix cement /glue

Conditions	Components	Approx range in % v/v
Room Pressure : 2000 hPa	Protein (hydrophilic)	2 - 4
Moisture : 50%	Long chain phosphoLipid	05.-1
Ambient Temperature : 15-200C	Mettaloligand	05.-1
	Saturated Mineralized, Polarized - H2O	0.5-1
	Citrate	0.1-05





Deepak Bhattacharya



Fig. 1. Long plate not coated with commercial grade synthetic enamel paint. Small plate coated with OHUCAX additive. Margins of small plate left bare.



Fig.2. Both plates coated with the same commercial synthetic pain as in Fig-1 admixed with OHUCAX at variable potencies



Fig. 3a

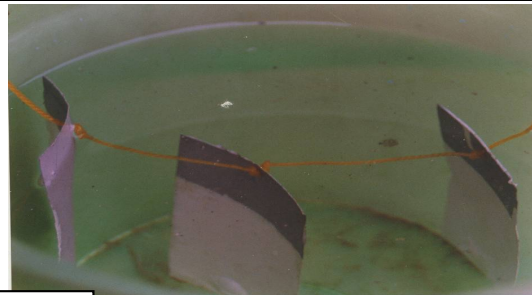


Fig. 3b

Fig. 3c



Fig. 3a to 3b. Long duration test in-lab undisturbed dunk in sea water. Fig-3c : Salt test, ambient room, decadal.

Fig. 4a





Deepak Bhattacharya



Fig. 4b

Fig . 4 a. Salt & Alkali test. White lumps NaCl. Black boils NaOH, photo post 24hrs. Viewer's left synthetic enamel paint as in Fig-1-to-3. Viewer's right has OHUCAX admixed paint. Fig. 4b. The NaOH boils were wiped after 24hrs. OHUCAX additive (viewer's right) thwarts NaOH insult much better



Fig .5. Downloaded from: <https://www.sciencefriday.com/educational-resources/hydrophobicity-will-the-drop-stop-or-roll/> with Thanks (6). It is our mother nature inspired cue





Controlling Early Blight Disease on Tomato Fruits using *moringa oleifera* Extraction as Alternative Option *invitro*

Khalaf M. Alhussaen

Department of Biology, College of Haqel, University of Tabuk, Saudi Arabia

Received: 13 July 2019

Revised: 15 Aug 2019

Accepted: 19 Sep 2019

*Address for Correspondence

Khalaf M. Alhussaen

Department of Biology,

College of Haqel,

University of Tabuk,

Saudi Arabia.

Email: khalaf60@yahoo.com



This is an Open Access Journal / article distributed under the terms of the **Creative Commons Attribution License** (CC BY-NC-ND 3.0) which permits unrestricted use, distribution, and reproduction in any medium, provided the original work is properly cited. All rights reserved.

ABSTRACT

Alternaria solani is an important pathogen and the causal agent of early blight on potato and tomato causing economical losses. *Alternaria solani* was isolated from diseased tomato fruits collected from the local market in Tabuk area, city of Haqel – Saudi Arabia and the species was identified as *Alternaria solani* using morphological and molecular methods. *Moringa oleifera* extract is known for its antibacterial and antifungal activity and is used to treat several plant pathogens. The fungicidal activity of *Moringa oleifera* extract with different concentrations in controlling the growth of the isolated *Alternaria solani* was determined *invitro*. The control activity was highly dependent on *Moringa oleifera* extract concentration. For instance, undiluted *Moringa oleifera* extract (100%) showed the highest control activity with no growth as compared to the biotic control without the extract whereas diluted *Moringa oleifera* extracts 25 and 10% reduced the fungal growth to 85 and 46%, respectively. The results of this study show that *Moringa oleifera* extract could successfully control *Alternaria solani* on tomato fruits and is considered as an environmentally friendly product.

Keywords: *Alternaria solani*, *Moringa oleifera*, early blight, antifungal activity.

INTRODUCTION

The species of *Alternaria solani* (Ellis & G. Martin) Sorauer is an important pathogen to the agriculture industries. This pathogen causing an early blight disease on tomato and potato plants. This disease is widely exposed and important causing economic yield losses throughout the world. Literatures reports that the yield losses due to early blight vary within large limits from 5- 78% (1, 2, 3). Early blight disease affect tomato and potato plants on lower, old and mature leaves, which become chlorotic and abscise prematurely spots. By time the spots become lager until they are one-half



**Khalaf M. Alhussaen**

inch in diameter. Spots have concentric rings or ridges that form a target-like pattern and are often surrounded by a yellow halo. Moreover, these symptoms affect stem and fruits as well (4). According to Simmons (5) *Alternaria solani* classified as belong to the phylum Ascomycota, class othideomycetes, order Pleosporales, and to family Pleosporaceae. *Alternaria solani* belong to larg, long-beaked, and noncatenated spores group of the genus *Alternaria* according to morphological characters and phylogenetic analyses (6). The mycelium consisted of septate, branched, light brown hyphae, which turned darker with age. The conidiophores were short, 50 to 90 μm and dark coloured. Conidia were 120-296 x 12-20 μm in size, beaked, muriform dark coloured and borne singly. However, in culture conidia are formed in short chains. Other study reported that the conidia contained 5-10 transverse septa and 1-5 longitudinal septa (7).

Pathogens were isolated from different areas were have a variation between their populations. This variation in the populations of plant pathogens are directly affects disease management, especially when the method related to the development of resistant cultivars and fungicide usage. *Alternaria solani* were found to be a highly variable pathogen in deferent parts of the word (8, 9). Recently, different molecular techniques were used to identify plant pathogens. Sequencing of the Internal Transcribed Spacer (ITS1) were used to identify *Alternaria solani* by comparing with isolates in the Genbank (10). Plant disease were controlled mainly by pesticides method and were also used to control early blight disease. However, using pesticides as a main method to control plant diseases have different side effects on plant and human. Alternative methods have been used to control plant diseases in aiming to reduce the effects of pesticides. Different natural products have used to control plant pathogens as an alternative of pesticides and fungicides (11, 12, 13, 14). Garlic extract have been used successfully in controlling *Pythium ultimum in vitro* isolated from tomato seedlings and were considered as an environmentally friendly product (15). Rongai (16) used pomegranate peel aqueous extract (pae) to control fusarium wilt of tomato caused by *Fusarium oxysporum*, f. sp. *Lycopersici* and found reduction of the *Fusarium* population in soil and the increase in number of healthy plants.

Moringa oleifera is the most widely cultivated species of a monogeneric family, the *Moringa oleifera* extract that is native to the sub-Himalayan tracts of India, Pakistan, Bangladesh and Afghanistan. *Moringa oleifera* were used wildly as medicine in different parts of the world, dfferent parts used such as the stem bark, root, bark, fruit, flowers, leaves, seeds, and gum (17). *Moringa oleifera* were described in other study and found their nutritional and medicinal properties (18). They reported also that *Moringa oleifera* leaves have vitamins and essential minerals such as vitamin A, vitamin B, vitamin C, calcium, iron, potassium, essential amino acids, and high protein content.

Moringa oleifera found to have antifungal activities and were used to control several species of fungi (19; 20; 21). Jabeen (22) pointed that *Moringa oleifera* extracts were used successfully on bacterial species *Botugetis cinerea* and fungi species *Fusarium oxysporum* and *Mycosphaerella arachidicola*. Other study examine the antimicrobial activity of the essential oil of *Moringa oleifera* against *Pseudomonas aeruginosa*, *Bacillus cereus*, *Escherichia coli*, *Staphylococcus aureus* and different fungal isolates *Penicillium digitatum*, *Penicillium aurantiogriseum*, *Penicillium citrinum*, *Penicillium expansum* and *Aspergillus niger* and were found all microorganisms tested sensitive to the essential oil (23). Moreover, extracts of other parts of *Moringa oleifera* have been examined and found successfully effect bacterial growth of *Streptococcus mutans* and *Staphylococcus aureus* (24). The present study was designed to examine the effect of *Moringa oleifera* extract as an antifungal for early blight disease on tomato fruits caused by *Alternaria solani*.

MATERIALS AND METHODS

Isolate Recovery

Alternaria solani were isolated from diseased tomato fruits collected from the local market in Tabuk area, city of Haqel – Saudi Arabia, and identified using morphological and physiological characters. Small bits measuring about 5 mm



**Khalaf M. Alhussien**

were placed on potato dextrose agar (PDA), and incubated under 12h light and 12h dark at 25±1°C according to (5,25). Pure culture of the fungus was obtained by hyphal tip isolation method.

Morphological Characterization

The morphological characters of representative isolates of the four *Alternaria solani* isolates including conidia size (length and width), length of beak and hyphal width and number of septa in conidia were measured under power objective 40X using light microscope. The *Alternaria solani* cultures were 7 days old grown on PDA.

Molecular Methods

DNA was extract from the mycelium of the isolated *Alternaria solani* and the Internal Transcribed Spacer (ITS1) region of the ribosomal nuclear DNA (rDNA) was amplified using PCR according to Paul (2000). Sequencing of ITS1 was carried out at a commercial facility (Macrogen Inc., Seoul, South Korea) using the stander methods. Sequence analysis was carried out using BLAST search (<http://blast.ncbi.nlm.nih.gov>) while the phylogram of the isolate and its relative was created using ClustalW (<http://www.ebi.ac.uk>).

Moringa oleifera extraction and *Alternaria solani* treatment

The effect of moringa oleifera extract against mycelial growth of *Alternaria solani* was examined in August 2018. Moringa was extracted using the method mentioned by Chumarka (26). Four concentrations (10, 25, 50 and 100%) of moringa extract were applied and sterile distilled water was used as control. Three plates were used for each treatment. Inoculation was carried on by dispersing 1 mL of the moringa extract from each treatment on the surface of each plate. Then, plates were inoculated with 5 mm disc that was cut from the margin of an actively growing *Alternaria solani* culture (5 days old) on PDA media incubated under 12h light and 12h dark at 25±1°C. Treated plates were then incubated at 12h light and 12h dark at 25±1°C. Mycelial growth was assessed daily (visual observation) and the final assessment was recorded after 7 days of incubation using colony counter on Petri dish, by which the total area of the mycelial growth on each plate was measured.

Data analysis

All treatments were arranged in Completely Randomized Design (CRD) with 3 replicates for each treatment. Average growth area of each treatment was assessed using colony counter on Petri dish. General Linear Model (GLM) ANOVA was used to find differences ($p \leq 0.05$) between treatment means (SPSS VER 25).

RESULTS**Morphological Characterization**

The morphology characterization of the isolate of *Alternaria solani* recovery from diseased tomato fruits obtained from the local market of Haqle - Saudi Arabia. Indicated the conidiophores were formed singly or in groups, or flexuous brown to olivaceous brown. The conidia were solitary straight or slightly flexuous or muriform or ellipsoidal tapering to beak, pale and sometimes branched. The conidia were 35-75 µm in length and 10-20 µm in width. There were 2-7 transverse septa and 1-4 longitudinal septa. The mycelial width was 0.8-1.5 µm.



**Khalaf M. Alhussaen****Sequence of ITS region of rDNA**

The sequences of *Alternaria solani* isolates obtained in this study matched *Alternaria solani* (DQ084021) from GenBank (**Error! Reference source not found.**). The sequence of isolate *Alternaria solani* was 786 bp in length and was 100% identical to the corresponding sequence from *Alternaria solani* (DQ084021).

Effect of Moringa extract on the growth of *Alternaria solani*

Moringa extract was found to be effective to control *Alternaria solani* isolated from tomato fruits obtained from the local market of Haqle - Saudi Arabia under *in vitro* conditions (Table 2). One hundred percent moringa extract showed the highest growth inhibition activity. At this level, the fungus has no growth compared with the control (56.72 cm²) (Table 2). Moreover, diluted moringa extract (50%) reduced the fungal growth to 96% (2.21 cm²) compared with the control. The diluted moringa extract (25%) reduced the fungal growth to 85% (8.54 cm²) compared with the control. The last diluted moringa extract (10%) reduced the growth to 46% (26.84 cm²) compared with the control.

DISCUSSION

Alternaria solani isolated from diseased tomato fruits and identified using morphological and physiological characteristics according to the key of Simmons (5), in addition to molecular methods based on ITS1 sequence analysis. The susceptibility of these plant pathogens to *Moringa oleifera* extract were examined in this study. Researchers and farmers need to know the correct identification of plant pathogens to find effective disease management methods because incorrect identification could lead to ineffective control strategies and money losses. Fungi usually identify by using the traditional methods through morphological characteristics but this is sometime difficult when some species have the same characteristics and this will make identification difficult (4). Recently, molecular methods have been used to have a correct identification of plant pathogens and to understand the variation between the population by using several DNA methods (27,10). The sequences of the Internal Transcribed Spacer (ITS1) region of the ribosomal DNA (rDNA) for *Alternaria solani* isolates were obtained for identification to species level. *Alternaria solani* isolate was found to be 100% identical to *Alternaria solani* (DQ084021) in the Gene-Bank database (Table 1). Sequences of ITS were used to confirm the identification by morphological and physical characterization. *Moringa oleifera* extract were found to be effective in the present study when used to control *Alternaria solani* *in vitro* and reduced the mycelia growth. *Moringa oleifera* extract as low as 10% showed a great potential for reducing mycelial growth area to 30.32 cm² of *Alternaria solani* compared with the control (Table 1). These results demonstrate that *Moringa oleifera* extract even of low concentrations could be used to control early blight disease caused by *Alternaria solani*.

Moreover, other *Moringa oleifera* extracts concentrations used in the present study show reduction to complete inhibition of growth of the mycelia. These results agreed with the results from Abu Sayeed ⁽²⁸⁾ who study the effect of *Moringa oleifera* extract and it showed a broad-spectrum antibacterial activity and antifungal activity such as *Pseudomonas aeruginosa*, *Colletotrichum* Sp., *Staphylococcus aureus*, *Bacillus subtilis*, *Vibrio cholera*, *Bacillus cereus*, *Salmonella typhi*, *Shigella dysenteriae*, *Alternaria* SP, *Colletotrichum* SP, *Curvularia* sp and *Fusarium* SP. Other study who explore *In vitro* antifungal activity of *Moringa oleifera* leaves against *Aspergillus fumigatus*, *Aspergillus niger* and *Candida albicans* at four different concentrations (50-300 mg/ml) by agar well diffusion method. The maximum zone of inhibition was recorded in the case of methanolic leaves extract (16 mm) against *Aspergillus niger* at a concentration of 300 mg/ml, which was at par to the standard antibiotic. Methanolic extract showed the highest MIC value (70 mg/ml) against *Aspergillus niger* (29). Furthermore, Tesfy (30) found that the *moringa* extract were effective on controlling *gloeosporioides* and *Alternaria alternata*.





Khalaf M. Alhussaen

REFERENCES

1. Datar, V.V. and C.D. Mayee, (1985) Chemical management of early blight of tomato. *J. Maharashtra Agric. Univ.*, 3: 278-280.
2. Waals JE, Korsten L, Slippers B. (2004) Genetic diversity among *Alternaria solani* isolates from potatoes in South Africa. *Plant Diseases*. 88:959-964. 6.
3. Pasche JS and Piche LM, Gudmestad NC. (2005) Effect of the F129L mutation in *Alternaria solani* on fungicides affecting mitochondrial respiration. *Plant Diseases*. 89:269-278.
4. Agrios GN (2005) 'Plant pathology.' (Academic Press: San Diego, USA)
5. Simmons E. (2007) *Alternaria: An Identification Manual*. Utrecht, Netherlands: CBS Fungal Biodiversity Centre.
6. Simmons, E. (2000) *Alternaria* themes and variations (244-286) species on Solanaceae. *Mycotaxon* 75:1-115.
7. Singh SN (1987). Response of chilli cultivars to *Alternaria alternata* and losses under field conditions. *Farm Sci. J.*, 2(1): 96-97.
8. Castro MEA, Zambolim L Chanes GM, Cruz CD, Matsuoka K (2000) Pathogenic variability of *Alternaria solani*, the causal agent of tomato early blight. *Summa-Phytopathologica* 26(1):24-28.
9. Pryor, B. M., and Michailides, T. J. (2002) Morphological, pathogenic, and molecular characterization of *Alternaria* isolates associated with *Alternaria* late blight of pistachio. *Phytopathology* 92:406-416.
10. Alhussaen, K (2019) Variation in the population of *Alternaria solani* by using sequencing of ITS1 isolated from tomato plants from Jordan valley. *Journal of Biological Sciences*, 19: 46-50.
11. Nithyameenakshi, S., Jeyaramraja P.R. and Manian S. (2006) Investigations on phytotoxicity of two new fungicides, azoxystrobin and difenoconazole. *Am. J. Plant Physiol.*, 1: 89-98.
12. Saravanan, P., Ramya V., Sridhar H., Balamurugan V. and Umamaheswari S. (2010) Antibacterial activity of *Allium sativum* L. on pathogenic bacterial strains. *Global Veterinaria*, 4: 519-522.
13. Hussein E, Kanan G, Al-Batayneh K, Alhussaen K, Al Khateeb W, Qar J, Jacob J, Muhaidat R, and Hegazy M (2012) Evaluation of Food Preservatives, Low Toxicity Chemicals, Liquid Fractions of Plant Extracts and Their Combinations as Alternative Options for Controlling Citrus Post-Harvest Green and Blue Moulds 'In vitro'. *Research Journal of Medicinal plant*. 6, (8), pp. 551-573.
14. Ashtiani A., Arzanlou M., Nasehi A., Kadir J., Vadamalai G. and Azadmard-Damirchi S. (2018) Plant tonic, a plant-derived bioactive natural product, exhibits antifungal activity against rice blast disease. *Industrial Crops & Products*. 112, p: 105-112.
15. Alhussaen K, Hussein E, Al-Batayneh K, Al-Khatib M, Al Khateeb W, Jacob J, Shatnawi M, Khashroum A and Hegazy M (2011) Identification and Controlling *Pythium* sp. Infecting Tomato Seedlings Cultivated in Jordan Valley using Garlic Extract. *Asian Journal of Plant Pathology*, 5: 84-92.
16. Rongai D., Pulcini P., Pesce B. and Milano F. (2017) Antifungal activity of pomegranate peel extract against fusarium wilt of tomato. *European Journal of Plant Pathology*. 147, 1, p: 229-238.
17. Compaore W., Nikiena P., Bassole H., Savadogo A. and Mouecoucou J. (2011) Chemical Composition and Antioxidative Properties of Seeds of *Moringa oleifera* and Pulps of *Parkia biglobosa* and *Adansonia digitata* Commonly used in Food Fortification in Burkina Faso. *Current Research Journal of Biological Sciences*: 3. P: 64-72.
18. Anjorin TS, Ikokoh P, Okolo S (2010) Mineral composition of *Moringa oleifera* leaves, pods and seeds from two regions in Abuja, Nigeria. *Int. J. Agric. Biol.* 12:431-434.
19. Nickon, F., Saud, Z.A., Rehman, M.H. and Haque, M.E. (2003): In vitro antimicrobial activity of the compound isolated from chloroform extract of *M. oleifera* Lam. *Pakistan Journal of Biological Sciences* 22:1888 – 1890.
20. Chuang P., Lee C., Chou J., Murugan M., Shieh B. and Chen H. (2007) Anti-fungal activity of crude extracts and essential oil of *Moringa oleifera* Lam. *Bioresource Technology*. 98: 1. P: 232-236.
21. Moodley J., Krishna S., Pillay K., Sershen and Govender P. (2018) Green synthesis of silver nanoparticles from *Moringa oleifera* leaf extracts and its antimicrobial potential. *Advances in Natural Sciences: Nanoscience and Nanotechnology*. 9. 015008.





Khalaf M. Alhussaen

22. Jabeen, R., Shahid, M., Jamil, A., & Ashraf, M. (2008). Microscopic evaluation of the antimicrobial activity of seed extracts of *Moringa oleifera*. *Pakistan Journal Botany*, 40, 1349–1358.
23. Marrufo T., Nazzaro F., Mancini E., Fratianni F., Coppola R., Martino L., Agostinho A. and Feo V. (2013) Chemical Composition and Biological Activity of the Essential Oil from Leaves of *Moringa oleifera* Lam. *Cultivated in Mozambique. Molecules* 18(9), 10989-11000.
24. Elgamily H, Moussa A, Elboraey A, EL-Sayed H, Al-Moghazy M, Abdalla A. (2016) Microbiological Assessment of *Moringa oleifera* Extracts and Its Incorporation in Novel Dental Remedies against Some Oral Pathogens. *Open Access Macedonian journal of Medical Sciences*. 4(4): 585-590.
25. Naik M. K., Prasady Y., Bhat K., and Devika Rani (2010) Morphological, Physiological, Pathogenic and molecular variability among isolates of *Alternaria solani* from tomato. *Indian Phytopathology* 63 (2) 168-173.
26. Chumarka, P., P. Khunawat, Y. Sanvarinda, S. Phornchirasilp, N. orales, L. Phivthong-ngam, P. Ratanachamngong, S.Srisawat, K. Pongrapeeporn, (2008). The in vitro and ex vivo antioxidant properties, hypolipidaemic and antiatherosclerotic activities of water extract of *Moringa oleifera* Lam. Leaves. *Journal of Ethnopharmacology*, 1-8.
27. Drenth, A., Wagels G., Smith B., Sendall B., O'Dwyer C., Irvine G. and Irwin J. (2006) Development of a DNA-based method for detection and identification of *Phytophthora* species. *Aust. Plant Pathol.*, 35: 147-159.
28. Abu Sayeed M, Hossain M, Chowdhury M and Haque M (2012) in vitro Antimicrobial Activity of Methanolic Extract of *Moringa oleifera* Lam. Fruits. *Journal of Pharmacognosy and Phytochemistry*, 1: 4. P: 94.
29. Maqsood, M., Qureshi, R., Arshad, M., Ahmed, MS. and Ikram, M. (2017) Preliminary Phytochemical Screening, Antifungal and Cytotoxic Activities of Leaves Extract of *Moringa oleifera* Lam. from Satrange, Pakistan. *Pakistan Journal of Botany*, 49 (1): 353-359.
30. Tesfy S., Magwaza I., Mbili N. and Mditshwa A. (2017) Carboxyl methylcellulose (CMC) containing *moringa* plant extracts as new postharvest organic edible coating for Avocado (*Persea americana* Mill.) fruit. *Scientia Horticulturae* 226, pp: 201-207.

Table 1. Sequence length (bp) of ITS region of rDNA for isolate of *Alternaria solani* from diseased tomato fruits obtained from the local market of Haqle - Saudi Arabia and comparison with sequences in GenBank.

Sequence length (bp)	Match from GenBank (Location)	GenBank accession number	Identities (%)	Gaps
786	<i>Alternaria solani</i> 2005 (USA)	DQ084021	100	0

Table 2. Mean growth area (cm²) and the percentage of growth inhibition area of *Alternaria solani* due to treatment with different moringa extract concentrations

Morin extract conc.	Mean growth (cm ²)	Inhibition percentage (%)
Full concentration 100%	00.00 ^a	100
50%	02.21 ^b	96
25%	8.54 ^c	85
10%	30.32 ^d	46
Control	56.72 ^e	0.00





RESEARCH ARTICLE

Hepatocyte Growth Factor (HGF) Regulatory Effects on Satellite Cell Activity after Skeletal Muscle Injury in Rats

Haitham Mohammad Abood* and May Fadhil Al- Habib

College of Medicine, Al-Nahrain University, Baghdad City, Iraq

Received: 13 July 2019

Revised: 15 Aug 2019

Accepted: 19 Sep 2019

*Address for Correspondence

Haitham Mohammad Abood

College of Medicine,

Al-Nahrain University,

Baghdad City, Iraq.

Email: bakir91@gmail.com



This is an Open Access Journal / article distributed under the terms of the **Creative Commons Attribution License** (CC BY-NC-ND 3.0) which permits unrestricted use, distribution, and reproduction in any medium, provided the original work is properly cited. All rights reserved.

ABSTRACT

Skeletal muscle is the largest component in the humane bodies that comprise about 40% of total body mass, the main function of skeletal muscle is drive locomotion, skeletal muscle susceptible to the damage these damages can be repaired through muscle regeneration mediated by muscle stem cells. Satellite cells represent a major group of muscle stem cells. Initially identified by Mauro in 1961, satellite cells are located between the sarcolemma and the basal lamina of myofibers. Hepatocyte growth factor (HGF) is the growth factor that activates quiescent satellite cells in skeletal muscle HGF is a mesenchyme-derived heparin-binding glycoprotein that regulates cell proliferation, cell survival, cell motility, and morphogenesis. In this study extensor digitorumlongus muscle as model for skeletal muscle regeneration using Hepatocyte growth factor (HGF) antibody. In this study, 50 rats apparently normal male selected randomly and divided into five groups. 10 rats serves as control, 10 samples 3rd day after injury, 10 samples at the end of first week after injury, 10 samples at the end of the second week after injury & 10 samples at the fourth week after injury The animals treated during injury of Extensor digitorumlongus (EDL) the muscles tissue were prepared and examined histologically using H&E and immunohistochemically using Hepatocyte growth factor (HGF) antibodies. The Aperio image scope software was used to analyzed immunohistochemical reactivity. Early myoblast appearance and new myotubes formation occurred at the beginning of the 1st week. By the end of the 4th week post operatively the muscle reached histological maturation and muscle fascicles were arranged. This study occluded that (HGF) have an important role in muscle regeneration.

Keywords: skeletal muscle regeneration, Hepatocyte growth factor, quiescent cell (satellite cell).





Haitham Mohammad Abood and May Fadhil Al- Habib

INTRODUCTION

Skeletal muscle considers as the largest component in the human bodies which comprised about 40% from the total body mass, skeletal muscle main function isto drive locomotion. Muscle fibers consist from myofibrils, the myofibrils are composed from actin and myosin filaments interact between actin and myosin from actinomyosin cross bridge, that generating muscle contraction, organization of actin and myosin filaments to form sarcomeres, the sarcomeres considers as the functional units of muscle contraction, the sarcomeres are responsible for the striation appearance of the skeletal muscle and it is form the basic machinery necessary for muscle contraction (Birbrair *et al.*, 2013). The skeletal muscle satellite cell was first described and named based on its anatomical location residebetween the myofibers plasma and basement membranes. The satellite cells inducible ablation in adult muscle resulting in impaired myofibers regeneration. The satellite cell has an important role in muscle repair that has been reaffirmed (Yablonka-Reuveni, 2011).

Satellite cells in the juvenile growth phase, when muscles enlarge, satellite cells have proliferative function and add nuclei for growing myofibers in most adult muscles, satellite cells are stay in quiescent until their activating by muscle injury. Satellite cell minimal activation is result from subtle injuries while maximal activation of satellite cells result from major trauma that can recruit greater numbers of satellite cells and promote prolonged proliferation prior to differentiation. As small injuries of myofibers can occur routinely during daily activity a mechanism for repair is very important for muscle maintenance throughout the life (Ciciliot, & Schiaffino, 2010). Skeletal muscle has an excellent ability to regenerate. The satellite cells (muscle precursor cell) that lie beneath the basement membrane are activated in response to injury. Activation of muscle satellite cells (myoblast) proliferation and differentiation to myotube, mature to form myofibers (Huijbregtset *al.*, 2001).

Hepatocyte growth factor (HGF) is a multifunctional protein which contains mitogenic, morphogenic, motogenic, and angiogenic activities by interacting with its cellular receptor, this interaction subsequently turns on a variety of signaling pathways depending on cell types. HGF has been shown to play important roles in the regeneration process of various tissues by stimulating the proliferation and migration of respective progenitor cells.(Watanabe *et al.*, 2005). HGF has been implicated in both skeletal muscle development and its regeneration after injury (Sissonet *al.*,2009). C-met is the only known receptor for HGF. When HGF is expressed, the c-met protein becomes phosphorylated to be activated (Wooshiket *al.*, 2018). Satellite cells represent a major group of muscle stem cells. Initially identified by Mauro in 1961 (Xin Fu *et al.*,2015). Satellite cells are located between the sarcolemma and the basal lamina of myofibers. These cells usually remain quiescent with a large nuclear to-cytoplasmic ratio and a low number of mitochondria (Yin *et al.*, 2013).

In response to exercise and injury, quiescent satellite cells are activated to enter the cell cycle, proliferate, and eventually exit at G1, fusing to form terminally differentiated multinucleated myofibers. Satellite cells are the major contributor to the remarkable regenerative capabilities of skeletal muscle. Satellite cells were initially discovered by Alex Mauro more than 50 years ago using electron microscopy, as mono nucleated cells located at the periphery of muscle fibers (Xin Fu *et al.*, 2015). Muscle injury leads to the release or activation of preexisting factors, stimulating proliferation of quiescent satellite cells. HGF, a ligand factor that elicits mitogenic, motogenic, and morphogenic activities during development and tissue regeneration (Zarnegar R *et al.*, 1995). Activation of satellite cell they enter the cell cycle, divide, differentiate and fuse with muscle fibers to repair damaged regions after injuries (Yamada *et al.*,2008). HGF has emerged as an important candidate molecule in muscle regeneration recently (Alameddine *et al.*,1994). The c-met receptor is present on quiescent satellite cells in normal muscle tissue (Tatsumi *et al.*, 1998). The interaction between HGF and c-met is required for migration of myogenic progenitors into the limb buds during embryogenesis (Dietrich *etal.*, 1999). Upon muscle injury, HGF activates muscle stem cells that reside in muscle fiber, rendering them to make a myogenic commitment (Sheehan *et al.*, 2000). Exogenously adding of recombinant HGF





Haitham Mohammad Abood and May Fadhil Al- Habib

protein was reported to increase myoblast proliferation while inhibiting differentiation, resulting in delayed regeneration of damaged muscle (Miller *et al.*, 2000).

Objectives of the study

For asses the role of HGF in regulating different phases of muscle regeneration by comparing the quantitative differences in the level of HGF in different stages. To assess the correlation between satellite cell & HGF level during different stages of regeneration.

MATERIALS AND METHODS

Animals housing & feeding

The animals aged 3-6 months, with 300 ± 50 body weights. The cages were kept at 25 ± 2 C °(room temperature) in a clean and well ventilated room. They were fed with standard pellet diet.

Induction of muscle injury

The injury was done under general anesthesia, each animal was anesthetized with mix of ketamine (87 mg /kg) and xylazine (13mg/ kg). The surgical operation were approved by surgical department in Veterinary Collage of Baghdad University ,the site of operation was shaved, cleaned and sterilized by using 70% ethyl alcohol and povidone. The skin incised and separated the subcutaneous fascia and deep fascia were dissected, tibialis muscle was identified and reflected extensor digitorumlongus muscle was recognized where it lie under the lateral, extensor hallucislongus muscle. The extensor digitorumlongus muscle was incised transversely to deprive it from blood supply and then immediately returned to its position after suturing. The incised muscle was sutured using horizontal mattress suture pattern with an absorbable suture material, CHROGUT 3-0. The subcutaneous tissues were closed by continuous suture pattern while the skin was closed by simple interrupted suture pattern using non absorbable suture material. Local antibiotic cover of oxy tetracycline with gentian violet spray (oxy plus spray) used after complete operation and, then extensor digitorumlongus muscle taken after 3,7,14&30 days post operatively.

Sampling & grouping

In this study, 50 apparently normal male rats, will be selected and divided into two groups.

Group (1):10 rats serve as control (no muscle injury induced).

Group (2): 40 rats serves as experimental group Extensor digitorumlongus (EDL) will be selected as a model for muscle injury induction.

A- 10 muscle samples taken after 3rd day of injury.

B- 10 muscle samples taken at the end of first week after injury.

C- 10 muscle samples taken at the end of the second week after injury.

D- 10 muscle samples taken at the end of the fourth week after injury.

The animals treated after collection of Extensor digitorumlongus (EDL) according to National institute of Health guidelines for care of Laboratory Animals.





Haitham Mohammad Abood and May Fadhil Al- Habib

Immunohistochemical (IHC) Procedure of Hepatocyte growth factor (HGF)

Serial thin sections of (5 μ m) thickness were done for each paraffin-embedded tissue block. Sticking of each section on charged slides was done. Paraffin section was deparaffinized in the oven at 65°C for 1 hours. Deparaffinization and rehydration were done by serial dipping the slides in glass staining jars containing the followings: Xylene for 10 min Twice, Ethanol 99 % for 4 min Twice, Ethanol 95% for 2 min, Ethanol 70% for 2 min, Distilled water for 1 min.

Restrict or define a suitable area (by pap pen) from the slide which was tested by IHC. Enough drops of hydrogen peroxide block were added to cover the section (incubated at 25°C for 10 minutes) Slides then washed in Phosphate buffer saline (PBS) for 5 minutes. Protein block was applied and incubated at 25°C for 10 minutes to block nonspecific background staining. Slides then washed in Phosphate buffer saline (PBS) for 5 minutes. Primary AB was added to the slides and incubated according to manufacturer's protocol (70 μ l of 1/500 primary AB diluted /AB diluent and incubated overnight in the humidified chamber). Slides were washed with phosphate buffer 3 times. Secondary AB (complement) was added (1/500 complement diluted in phosphate buffer) and incubated at 25°C for 10 min. Washing was done with phosphate buffer (2 times). HRP was applied on the tissue (enough drops) and slides were incubated at 25°C/15 min. Slides were washed with phosphate buffer saline (4 times). Tissue sections were treated with diluted liquid DAB for 1-10 minutes at room temperature (70 μ l of 30 μ l(1 drop) DAP chromogen to 1.5 ml (50 drops) of DAP substrate, mix by swirling and apply to tissue. Slides were washed with phosphate buffer saline (4 times). Counter staining was done with Myers' Hematoxylin for 2min. Washing with tap water was then followed. Section was mounted with super mount and coverslip added and examined under a light microscope (Wang *et al.*, 2016).

RESULTS

HGF antibody was used to demonstrate the presence of hepatocyte growth factor in skeletal muscle fibers and to quantify the differences of activity and the role of it during skeletal muscle regeneration hepatocyte growth factor (HGF) is said to activate quiescent satellite cell after skeletal muscle injury (HGF) is a ligand for c-met receptor tyrosine kinase in the sarcolemma. Hepatocyte growth factor distribution in both experimental groups and control group showed multiple type of expression, the hepatocyte growth factor distribution was expressed in the endomysium and was faint in perimysium and surrounding, corresponded to the basement membrane of muscle fibers, while the sarcoplasm and endomysium showed a no reactive stain ability towards HGF antibody apart from blood vessels and its surrounding (figure 1). The expression of HGF antibody was seen mainly in the extracellular matrix surrounding, in new muscle fibers and endomysium the staining reactivity was not observed inside their nuclei, the nuclei component stained with counter stain -Harris Hematoxylin and seen in (figure 2).

In regenerated muscles the 4 groups with injured muscle were investigated by using HGF antibody (Abcam, UK), 3rd post-operative day, 1stpost- operative week, 2nd post-operative week and 4th post-operative week respectively and as it was mention above the process of regeneration and degeneration is dynamic one. Changes seen in 3rd post-operative day were striking, multiple profile was seen in the 3rd Post-operative day group, at the time when degeneration process was going on where infiltration of inflammatory cell was observed at the site of injury and even in between intact peripheral muscle fiber, neutrophils are the first cells to arrive at the site of injury, followed by macrophages, lymphocyte, poly morphocells&other (HGF) expression at peak line in this group in order to activation quiescent satellite cells which still found between the basal membrane and sarcolemma until the third day after injury, the reactivity of (HGF) was seen in the sarcoplasm and endomysium (figure 3& 4). In 1st post- operative week heavy mononuclear inflammatory cells were seen infiltrating the area, with heavy vascularity at the site of injury and the reactivity of (HGF) in the sarcoplasm and endomysium. important for SC activation and proliferation by activating quiescent SCs which still found between the basal membrane and sarcolemma until the third day after injury, Subsequently, they are slowly replaced by cells with large nuclei, nucleoli, and cytoplasmatic processes filled with ribonucleo protein granules, these myoblasts display an initial exponential growth phase and after the seventh



**Haitham Mohammad Abood and May Fadhil Al- Habib**

day they start to form myotubes with centrally placed nuclei and peripheral myofibrils so the (HGF) reactivity start gradually get down after proliferation of satellite cells (figure 5). In 2nd post- operative week the presence of mononuclear inflammatory cells were still infiltrating the area , with heavy vascularity on one hand , on the other hand newly formed muscle fibers were easily identified with different ranges of maturity , new muscle fibers, type 2C fiber and myotubes all present at the same site (figure 6).

The other striking feature, recorded in the 2nd week group, was the appearance of HGF reactivity inside the sarcoplasm of newly formed muscle fibers (figure 6, 7, & 8). Peripheral myofibers that survived from injury remains intact forming a zone surrounding the injured area were the muscle sarcoplasm devoid of HGF reaction and the newly formed muscle show clear sarcoplasmic reactivity (figure 9&10). Regenerative process was completed at the end of 4th weeks of post-operative process , the entire muscle showed a well-organized regenerative muscle fibers arranged in bundles with all histological features of maturity .The HGF reaction was limited to a thin stain reaction as like as the control group in the sarcoplasm, endomysium and faint in perimysium (figure 11). The overall appearance the regenerated skeletal muscle was similar to the normal non injured muscle apart from the present of larger area of connective tissue in regenerated muscle more than in control group, the reactivity of HGF the sarcoplasm and endomysium was intense (figure 12).

DISCUSSION

Hepatocyte growth factor is now widely recognized as one of the most important growth factors involved in regeneration HGF appears to increase the myoblast population by means of mitogenic activities, possibly resulting in an optimal myoblast density whereupon fusion can commence, HGF can also act directly on satellite cells, as suggested by its receptor c-met expression in quiescent and activated satellite cells Furthermore, in a study done by (cornelison&Wold, 1997) suggests that HGF activity in myoblasts and newly formed myotubes is mediated through paracrine/autocrine mechanisms (Cornelison&Wold, 1997). Hepatocyte growth factor (HGF) is a multifunctional protein which contains mitogenic, morphogenic, motogenic, and angiogenic activities by interacting with its cellular receptor, c-met (Nakamura & Mizuno, 2010). This interaction subsequently turns on a variety of signaling pathways depending on cell types. HGF has been shown to play important roles in the regeneration process of various tissues by stimulating the proliferation and migration of respective progenitor cells (Watanabe *et al.*, 2005). recent studies have shown that HGF activated by urokinase plasminogen activator (uPA) promotes muscle regeneration (Sisson *et al.*, 2009), receptor, c-met, is responsible for the transition of quiescent muscle stem cells into GAlert, a cellular state in which they have an increased ability to participate in tissue repair (Rodgers *et al.*, 2014)

HGF is secreted by a variety of cell types in cases of muscle injury, macrophages are known to be the primary source of HGF during muscle regeneration (Sisson *et al.*, 2009). The underlying mechanism by which macrophages produce HGF has not yet been understood, one possibility is that HGF may be secreted when these cells are exposed to apoptotic neutrophils. It was previously reported that when macrophages encounter apoptotic cells, HGF is produced (Park *et al.*, 2011). Muscle regeneration is a dynamic process due to activation of multiple factors including satellite cell, growth factors specially Hepatocyte growth factor (HGF) , fibroblast, fibronectin and laminin in the initial proliferative phase called the regeneration Components of muscle regeneration both structurally and functionally are under the effects of these factors plus other environment factors (Negroniet *al.*, 2006). Hepatocyte growth factor (HGF) was first discovered as a potent mitogen for hepatocytes and later found to also contain mitogenic, morphogenic, angiogenic, anti-apoptotic, and anti-fibrotic activities (Mizuno *et al.*, 2006). It is well known that interaction of HGF with its cellular receptor, c-met, turns on a variety of signaling pathways, depending on the cell types. In skeletal muscle, HGF is known to be secreted by activated muscle stem cells (also known as satellite cells) in vivo (Tatumiet *al.*, 1998).as well as in vitro (Sheehan *et al.*, 2000). Upon muscle injury, HGF activates muscle stem cells that reside in muscle fiber, leading to regeneration of damaged muscle (Miller *et al.*, 2000). Exogenously added recombinant HGF protein has been shown to ameliorate pathological conditions in mouse models for hypoxia-



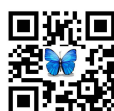
**Haitham Mohammad Abood and May Fadhil Al- Habib**

induced muscle atrophy (Haurerslevet *et al.*, 2014), polymyositis and dermatomyositis (Sugiura *et al.*, 2014). It has been reported that HGF can promote the survival of motor neurons in vitro (Wong *et al.*, 1997). and that HGF over expression might attenuate the death of motor neurons and axon degeneration in ALS mice (Sun *et al.*, 2002). The present study showed the role of Hepatocyte growth factor during skeletal muscle regeneration by using HGF antibody (Abcam, UK) (ab216623) the regenerative process was thoroughly investigated after experimental injury to extensor digitorum longus muscle and showed different profile of reactivity in different post traumatic time. Early myogenic cell differentiation and formation of new muscle fibers and early myotube formation showed an intense reactivity for HGF.

The statistical data of quantitative study of the Hepatocyte growth factor during the process of degeneration and regeneration showed rather difference manner of expression of this marker between the 4 studied groups. Control, and 4th post-operative group showed less intense reactivity towards Hepatocyte growth factor while a heavy intense reactivity was detected and was significantly difference in the 3rd day group. Statistical analysis showed HGF reactivity in skeletal muscle Mean Aperio score for HGF after three days of injury in experimental animal was 0.244 ± 0.095 (range 0.107-0.567) which was higher than that of control animals (mean 0.167 ± 0.046 , range 0.101-0.321) with a highly significant difference after one week of injury, experimental animals still have higher mean HGF Aperio score than control animals (0.231 ± 0.092 versus 0.167 ± 0.046) with a highly significant difference although the mean HGF Aperio score decreased slightly after two weeks of injury in experimental, it did not change much. It was 0.226 ± 0.057 in experimental animals compared to 0.167 ± 0.046 in control animals with a significant difference Mean Aperio score for HGF after four of injury in experimental animal was almost similar for that in control animals (0.176 ± 0.076 versus 0.167 ± 0.046) without a significant difference.

The sticking feature of presence of HGF in sarcoplasm of newly formed muscle and surrounding connective tissue elements including their blood vessels was behind the significant high reactivity seen in the 3rd day group, 1st week group & 2nd week group. HGF sarcoplasmic and endomysium distribution during process of myogenesis can be explained on the fact that (HGF) is activates quiescent satellite cell after skeletal muscle injury and this can be proved by the presence of reactivity in the sarcoplasm after muscle injury so sarcolemma of newly formed myoblasts (young regenerated myofibers) so the reaction is diffused. The overall appearance of regenerated muscle was similar to the normal muscle except that the regenerated muscle showed more areas of fibrous connective tissue. Previous studies agree with results in this study on possible influences of HGF on the development of turkey skeletal muscle, they conducted several cell culture studies with turkey satellite cells. Six clones, previously shown to differ in their rates of proliferation, were used to investigate differences in responsiveness to HGF. The six clones were derived from one muscle from one animal (McFarland *et al.*, 1995). On study done by (Yun *et al.*, 1997).

They cultured satellite cell after 19 day of total growth, and one Late clone, which reached confluence after 29 day, they used in this study. IGF, FGF, PDGF, and insulin they found that the early clone was more responsive to the mitogenic (proliferation) stimuli of IGF, FGF, PDGF, and insulin effect on the early clone more than the Late clone the early clone was also more responsive to the inhibitory effects of transforming growth factor- β (TGF- β) on proliferation and differentiation than the Late clone. In the study turkey satellite cells, it was shown that HGF is a very potent mitogen for turkey satellite cells, on cultured colony they found that maximal stimulation at a level of 1 ng/mL. It appears that HGF has a more pronounced effect on the proliferation of the Late clone 29 day than on the early clone 19 day. It is proposed that the Late clone may have a longer lag phase than the Early clone. (Allen *et al.* 1995). other study demonstrated that the stimulating effect of HGF on proliferation of rat satellite cells appeared to be due to the earlier entry of cells into the cell cycle, the lag phase was shortened. In studies with primary chicken satellite cells, HGF was the only mitogen that stimulated entrance of these cells into the S phase of the cell cycle (Gal-Levi *et al.*, 1998). In study done by (Zeng *et al.*, 2002) it found that when HGF administered for the first 24h or continuously for 96 h maximal proliferation rates occurred when HGF was given continuously. When administered for only the first 24 h, HGF exerted no significant effect on proliferation of the early cultured turkey satellite cells 19day clone but stimulate proliferation of the Late turkey satellite cells clone 29day. These findings suggest that HGF



**Haitham Mohammad Abood and May Fadhil Al- Habib**

does have a classical mitogenic effect on turkey satellite cells, apart from activating quiescent satellite cells. After activating quiescent satellite cells, HGF may continue its activity by stimulating the activated satellite cells to proliferate. The potential of HGF as a cell activator, mitogen, and motogen (stimulates cell movement) has important implications. Following muscle injury, HGF may serve to activate quiescent satellite cells, guide their migration to the injured site, and promote their proliferation. However, as noted by (Miller *et al.*, 2000), regeneration does not depend solely on myoblast numbers demonstrated that exogenous HGF could actually slow regeneration *in vivo*, presumably by inhibiting differentiation (Lee *et al.*, 1999).

During chick and mouse embryonic development, HGF not only stimulates the proliferation of embryonic myoblasts but also guides their migration and development of limbs (Myokai *et al.*, 1995). However HGF also increased proliferation of turkey embryonic myoblasts suggesting that HGF may also play an important role in turkey embryonic skeletal muscle development (Leshemet *et al.*, 2000). HGF probably plays a crucial role during the early stages of muscle myocytes and macrophages throughout the early and middle stages of muscle regeneration. Both IGF-I and IGF-II can stimulate myoblast proliferation and differentiation and improve muscle repair, and IGF-II may be expressed weakly in intact muscle and regulate enlargement. These findings indicate that these three cytokines have pleiotropic effects in regenerating skeletal muscle.

In study done by (Wooshik Choi¹, *et al.*, 2019) it found that after muscle injury, the level of the HGF protein in the injured side was gradually increased, reaching a peak at approximately 1.1 ng mg of total cellular protein at day 4, and then steadily decreased before returning to the sham level at day 12. A similar magnitude of HGF Exogenous supply of the HGF protein to the affected region through i.m. injection of a highly efficient plasmid expression vector promoted the transition of macrophage to the M2 phenotype and facilitated muscle regeneration (Wooshik Choi¹, *et al.*, 2019) the expression level of HGF peaked at 3–4 days post injury, and this is the time when neutrophils induce an early immune response and became apoptotic and cleared by macrophages (Nguyen *et al.*, 2011). Infiltration of immune cells after Muscle injury, stretching, overuse, and degenerative muscle diseases induce the infiltration of large amounts of immune cells, initiated by early neutrophil invasion and followed by macrophage infiltration (Toumi *et al.*, 2006). Inhibition of inflammation by non-steroidal anti-inflammatory drugs in humans reduces the number of activated satellite cells, thus slowing down muscle regeneration (Ziltener *et al.*, 2010). However inhibition of c-met signaling by using an inhibitor specific to the c-met receptor after sciatic nerve transection could worsen muscle mass and cross-sectional area during neurogenic muscle atrophy, suggesting that HGF works as part of the compensatory system. Exogenous supply of the HGF protein by using a plasmid DNA expression vector to the affected region by i.m. injection of a highly efficient plasmid expression vector improved muscle atrophy by all measurements, including muscle weight, cross-sectional area, and the expression levels of miR-206, HDAC4, and atrogenes. This study done by (WooshikChoi¹, *et al.* 2018)

in spite of many growth factor muscle extract, their activities could not account for the ability to modulate the proliferative activity for all of the mitogenic activity in the extract. Bischoff's of satellite cells, factors such as fibroblast growth factors work with this muscle extract indicated that (FGFs), insulin-like growth factors (IGFs), platelet-derived growth factor BB (PDGF-BB), transforming growth factor and epidermal Skeletal muscle satellite cells are normally found in a growth factor (EGF) do not stimulate quiescent cells to enter quiescent state in adult muscle, but when minor damage the cell cycle in *in vitro* assays for activation or injury occur, signals are generated within the muscle (Johnson & Allen, 1995).

Quantitative assessment of Hepatocyte growth factor expression

Statistical analysis (SAS) was used to assess the difference in the expression of the quantitation of HGF reactivity; this was assessed using Apireo positive count Algorithm software. The degree of positivity measured by this program ranged and expressed as follow:



**Haitham Mohammad Abood and May Fadhil Al- Habib**

- Brown color represents strong positive reaction for HGF.
- Orange color represents positive reaction for HGF.
- Yellow color represents weak positive reaction for HGF.
- Blue color represents negative reaction for HGF.
- Statistical analysis of the positive reaction for HGF receptor antibodies in injured skeletal muscle was performed using Aprio Algorithm soft wear for the 4 groups of this study table (1).

Statistical analysis**The mean of percentage of positive reactivity Hepatocyte growth factor Antibodies**

Mean Aperio Score, After 3 days of Injury, Mean Aperio score for HGF after three days of injury in experimental animal was 0.244 ± 0.095 (range 0.107-0.567) which was higher than that of control animals (mean 0.167 ± 0.046 , range 0.101-0.321) with a highly significant difference (table 2, figure 13).

After One Week

After one week of injury, experimental animals still have higher mean HGF Aperio score than control animals (0.231 ± 0.092 versus 0.167 ± 0.046) with a highly significant difference (Table 3, figure 14).

After Two Weeks

Although the mean HGF Aperio score decreased slightly after two weeks of injury in experimental, it did not change much. It was 0.226 ± 0.057 in experimental animals compared to 0.167 ± 0.046 in control animals with a significant difference (Table 4, figure 15).

After Four Weeks

Mean Aperio score for HGF after four of injury in experimental animal was almost similar for that in control animals (0.176 ± 0.076 versus 0.167 ± 0.046) without a significant difference (table 5, figure 16).

Overall Comparison

The overall comparison in HGF Aperio score is shown in figure (17) and (table 6). Beside the significant differences in this score between control animals and experimental animals after 3 days, one week and two weeks of injury, the mean HGF Aperio score after 4 weeks of injury was significantly lower than that recorded after days one week and two weeks of injury. Otherwise there were no significant differences in this score that recorded after three days, one week and two weeks.

Time Trends of HGF Aperio score in Experimental Animals

Figure (18) shows the time trends of HGF Aperio score in experimental animals. From day 3 after injury until two weeks, there was a very slight decline in Aperio score with no significant from the baseline value. However, after four weeks of injury there was a sharp decline with a significant difference.





Haitham Mohammad Abood and May Fadhil Al- Habib

REFERENCES

1. Alameddine H. S., Louboutin J. P., Dehaupas M., Sebille A., Fardeau.(1994). Functional recovery induced by satellite cell grafts in irreversibly injured muscles. *CellTransplant.* 3: 3-14, 1994.
2. Allen DL, Monke SR, Talmadge RJ, Roy RR, Edgerton VR. (1995). Plasticity of myonuclear number in hypertrophied and atrophied mammalian skeletal muscle fibers. *J ApplPhysiol* 78(5):1969–1976
3. Birbrair, A., Zhang, T., Wang, Z. M., Messi, M. L., Enikolopov, G. N., Mintz, A &Delbono, O. (2013). Role of pericytes in skeletal muscle regeneration and fat accumulation. *Stem cells and development*, 22(16): 2298-2314.
4. Ciciliot, S &Schiaffino, S. (2010). Regeneration of mammalian skeletal muscle: basic mechanisms and clinical implications. *Current pharmaceutical design*, 16(8): 906-914.
5. Cornelison DD, Wold BJ. (1997). Single-cell analysis of regulatory gene expression in quiescent and activated mouse skeletal muscle satellite cells. *DevBiol* 191:270–283
6. Dietrich, S, Abou-Rebyeh, F, Brohmann, H, Bladt, F, Sonnenberg-Riethmacher, E,Yamaai, T. (1999). The role of SF/HGF and c-Met in the development of skeletal muscle. *Development* **126**: 1621-1629.
7. Gal-Levi R., Y. Leshem, S. Aoki, T. Nakamura, and O. Halevy. (1998). Hepatocyte growth factor plays a dual role in regulating skeletal muscle satellite cell proliferation and differentiation. *Biochem. Biophys. Acta* 1402:39–51
8. Hauerlev, S., Vissing, J., and Krag, T.O. (2014). Muscle atrophy reversed by growth factor activation of satellite cells in a mouse muscle atrophy model. *PLoS ONE* 9, e100594.
9. Huijbregts, J., White, J. D & Grounds, M. D. (2001). The absence of MyoD in regenerating skeletal muscle affects the expression pattern of basement membrane, interstitial matrix and integrin molecules that is consistent with delayed myotube formation. *Actahistochemica*, 103(4): 379-396.
10. Johnson, S. E., & Allen, R. E. (1993). Proliferating cell nuclea antigen (PCNA) is expressed in activated rat skeletal muscle satellite cells. *J. Cell. Physiol.* 154, 39–43.
11. Lee K, Wong C, Webb S, Tang K, Leung A, Kwok P, Cai D, & Chan K. (1999).Hepatocyte growth factor stimulates chemotactic response in mouse embryonic limb myogenic cells in vitro. *J. Exp.Zool.* 283:170–180.
12. Leshem, Y., D. B. Spicer, R. Gal-Levi, and O. Halevy. (2000). Hepatocyte growth factor (HGF) inhibits skeletal muscle cell differentiation: a role for the bHLH protein Twist and the cdk inhibitor p27. *J. Cell. Physiol.* 184:101–109.
13. McFarland, D. C., K. K. Gilkerson, J. E. Pesall, J. S. Walker, and Y. Yun. (1995). Heterogeneity in growth characteristics of satellite cell populations. *Cytobios* 82:21–27.
14. Miller, KJ, Thaloor, D, Matteson, S, and Pavlath, GK (2000). Hepatocyte growth factor affects satellite cell activation and differentiation in regenerating skeletal muscle.*AmericanJournal of Physiology-Cell Physiology* **278**: C174-C181
15. Myokai, F., N. Washio, Y. Asahara, T. Yamaai, N. Tanda, T. Ishikawa, S. Aoki, H. Kurihara, Y. Murayama, T. Saito, K. Matsumoto, T. Nakumara, S. Noji, and T. Nohno. (1995). Expression of the hepatocyte growth factor gene during chick limb development. *Dev. Dyn.* 202:80–90.
16. Mizuno, S., Matsumoto, K., and Nakamura, T. (2001). Hepatocyte growth factor suppresses interstitial fibrosis in a mouse model of obstructive nephropathy. *Kidney Int.*59, 1304–1314.
17. Negroni, E., Butler-Browne, G. S &Mouly, V. (2006). Myogenic stem cells: regeneration and cell therapy in human skeletal muscle. *PathologieBiologie*, 54(2): 100-108.
18. Nguyen, M.-H., Cheng, M., and Koh, T. J. (2011). Impaired muscle regeneration in ob/ob and db/db mice. *Sci. World J.* 11, 1525–1535. doi: 10.1100/ tsw.2011.137
19. Park, H. J., Choi, Y. H., Cho, Y. J., Henson, P. M., and Kang, J. L. (2011). RhoA-mediated signaling up-regulates hepatocyte growth factor gene and protein expression in response to apoptotic cells. *J. Leukoc. Biol.* 89, 399–411. doi: 10.1189/jlb.0710414
20. Rodgers, J. T., King, K. Y., Brett, J. O., Cromie, M. J., Charville, G. W., Maguire, K. K., et al. (2014). mTORC1 controls the adaptive transition of quiescent stem cells from G0 to G(Alert). *Nature*, 510, 393–396.
21. Sheehan, SM, Tatsumi, R, Temm-Grove, CJ, and Allen, RE (2000). HGF is an autocrine growth factor for skeletal muscle satellite cells in vitro. *Muscle & nerve* 23: 239-245.





Haitham Mohammad Abood and May Fadhil Al- Habib

22. Sisson, TH, Nguyen, M-H, Yu, B, Novak, ML, Simon, RH, and Koh, TJ. (2009). Urokinase-type plasminogen activator increases hepatocyte growth factor activity required for skeletal muscle regeneration. *Blood* **114**: 5052-5061.
23. Sugiura, T., Kawaguchi, Y., Soejima, M., Katsumata, Y., Gono, T., Baba, S., Kawamoto, M., Murakawa, Y., Yamanaka, H., and Hara, M. (2010). Increased HGF and c-Met in muscle tissues of polymyositis and dermatomyositis patients: beneficial roles of HGF in muscle regeneration. *Clin. Immunol.* **136**, 387–399.
24. Tatsumi, R., Anderson, J.E., Nevoret, C.J., Halevy, O., and Allen, R.E. (1998). HGF/SFis present in normal adult skeletal muscle and is capable of activating satellite cells. *Dev. Biol.* **194**, 114–128.
25. Toumi H, F'Guyer S, Best TM. (2006). The role of neutrophils in injury and repair following muscle stretch. *J Anat* **208**(4):459–470
26. Watanabe, M, Ebina, M, Orson, FM, Nakamura, A, Kubota, K, Koinuma, D. (2005). Hepatocyte growth factor gene transfer to alveolar septa for effective suppression of lung fibrosis. *Molecular therapy* **12**: 58-67.
27. Wong ML, Wong JL, Vapniarsky N, Griffiths LG. In vivo xenogeneic scaffold fate is determined by residual antigenicity and extracellular matrix preservation. *Biomaterials*. 2016;92:1-12.
28. Wong, Glass, Arriaga, Yancopoulos, Lindsay, & Conn. (1997). Hepatocyte growth factor promotes motor neuron survival and synergizes with ciliary neurotrophic factor. *J. Biol. Chem.* **272**, 5187–5191.
29. Wooshik Choi¹, Jaeman Lee¹, Junghun Lee², Sang Hwan Lee¹ & Sunyoung Kim. (2019). Hepatocyte Growth Factor Regulates Macrophage Transition to the M2 Phenotype and Promotes Murine Skeletal Muscle Regeneration. Department of Biological Sciences, College of Natural Sciences, Seoul National University, Seoul, South Korea, 2 R&D Center for Innovative Medicines, ViroMed Co., Ltd, Seoul, South Korea doi: 10.3389/fphys.2019.00914
30. Wooshik Choi,¹Junghun Lee,² Jaeman Lee,¹ KyeongRyang Ko,^{1,2} and Sunyoung Kim. (2018). Hepatocyte Growth Factor Regulates the miR-206- HDAC4 Cascade to Control Neurogenic Muscle Atrophy following Surgical Denervation in Mice ¹School of Biological Sciences, Seoul National University, Seoul 08826, Korea; ²ViroMed Co., Ltd., Bldg. 203, Seoul National University, Seoul 08826, Korea doi.org/10.1016/j.omtn. 06.013.
31. Xin Fu •Huating Wang • Ping Hu. (2015). Stem cell activation in skeletal muscle regeneration *Cellular and Molecular Life Sciences* **123**. (2015) **72**:1663–1677 DOI 10.1007/s00018-014-1819-5
32. Yamada, Sankoda, Tatsumi, Mizunoya, Ikeuchi, Sunagawa, Allen. (2008). Matrix metalloproteinase-2 mediates stretch-induced activation of skeletal muscle satellite cells in a nitric oxide-dependent manner, *Int. J. Biochem. Cell Biol.* **40** 2183–2191.
33. Yin H, Price F, Rudnicki MA. (2013). Satellite cells and the muscle stem cell niche. *Physiol Rev* **93**(1):23–67
34. Yun, McFarland, Pesall, Gilkerson, Vander Wal, & Ferrin. (1997). Variation in response to growth factor stimuli in satellite cell populations. *Comp. Biochem. Physiol.* **117A**:463–470.
35. Zarnekar R, Michalopoulos GK. (1995). The many faces of hepatocyte growth factor: from hepatopoiesis to hematopoiesis. *J Cell Biol* **129**(5):1177–1180
36. Zeng, Pesall, Gilkerson & McFarland¹. (2002). The Effect of Hepatocyte Growth Factor on Turkey Satellite Cell Proliferation and Differentiation Department of Animal and Range Sciences, South Dakota State University, Brookings, South Dakota Poultry Science 57007-0392.

Table 1. Show statistical analysis total positivity reaction

groups	control	3 rd day group	1 st week group	2 nd week group	4 th week group
Total positivity	0.167	0.244	0.231	0.226	0.176
p-value	P <0.001				

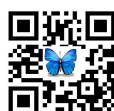
The control group records a value of 0.167±0.008 pixel / (micron)² while the experimental groups recorded the following

The 3rd day group = 0.244 ±0.016 pixel / (micron)²

The 1st post-operative week group = 0.231± 0.016 pixel / (micron)²

2nd post-operative week 0.226±0.009 pixel / (micron)²

4th post-operative week 0.176±0.013 pixel / (micron)².





Haitham Mohammad Abood and May Fadhil Al- Habib

Table 2. Descriptive statistics for HGF Aperiop score in experimental animals after three days of injury and control animals

Groups	Mean	Std. error	Min.	Max.	P-value
Three days	0.244	0.016	0.107	0.567	<0.001
Controls	0.167	0.008	0.101	0.321	

Table 3. Descriptive statistics for HGF Aperiop score in experimental animals after one week of injury and control animals

Groups	Mean	Std. error	Min.	Max.	P-value
One week	0.231	0.016	0.106	0.416	0.005
Controls	0.167	0.008	0.101	0.321	

Table 4. Descriptive statistics for HGF Aperiop score in experimental animals after one week of injury and control animals

Groups	Mean	Std. error	Min.	Max.	P-value
Two weeks	0.226	0.009	0.128	0.387	0.013
Controls	0.167	0.008	0.101	0.321	

Table 5. Descriptive statistics for HGF Aperiop score in experimental animals after one week of injury and control animals

Groups	Mean	Std. error	Min.	Max.	P-value
Four weeks	0.176	0.013	0.102	0.388	0.99
Controls	0.167	0.008	0.101	0.321	

Table 6. Multiple comparisons control group and experimental group at different times after injury

Comparison	P- value
Controls/ three days	<0.001
Control/ one week	0.005
Control/ two weeks	0.013
Control/ four weeks	0.99
Three days/ one week	0.949
Three days/ two weeks	0.849
Three days/ four weeks	0.002
One week/ two weeks	0.999
One week/ four weeks	0.023
Two weeks/ four weeks	0.05





Haitham Mohammad Abood and May Fadhil Al- Habib

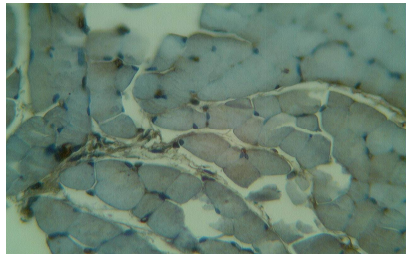


Figure 1. Cross sections in control group showing: HGF reactivity at the endomysium & faint distribution of HGF reactivity at the perimysium (HGF Ab, control group, X20).

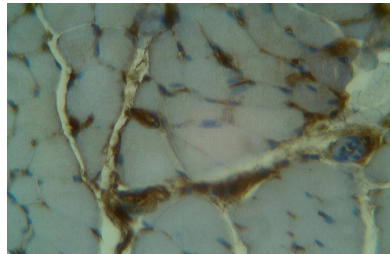


Figure 2. Cross sections in control group showing: intense reactivity around the blood vessels and endomysium the reactivity of HGF was not observed in nuclei (HGF Ab, control group, X20).

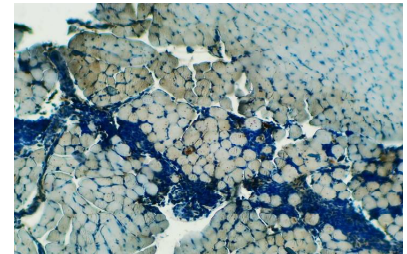


Figure 3. Cross sections in the skeletal muscle showing: the presence of inflammatory cells infiltrating in the area of site of injury in 3rd post-operative day intense HGF reactivity around new muscle formation. (HGF Ab, at 3rd post-operative day group, X10)

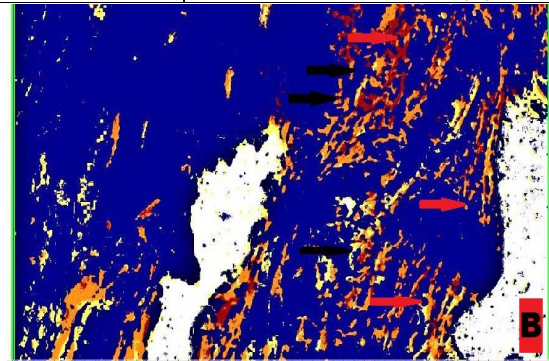
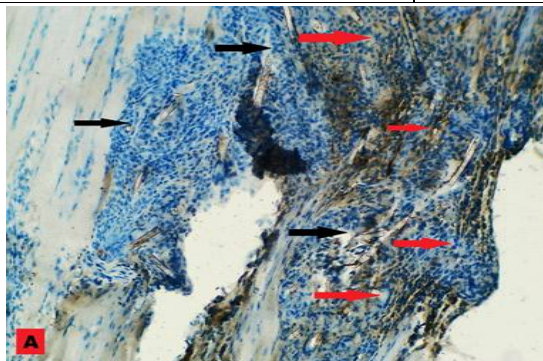


Figure 4. Longitudinal sections in the skeletal muscle showing **A**: Heavy mononuclear cells infiltration (black row) at the site of the injury and congestion in all blood vessels (red row) 1st post-operative week **B**: the same image using Aprio showing positive (yellow –brown) and negative blue reaction. (HGF Ab, at 1st post-operative week group, X10)

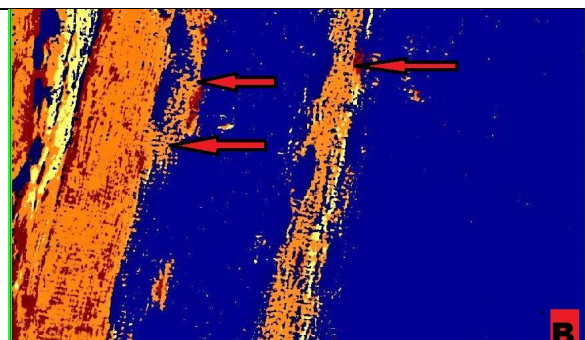
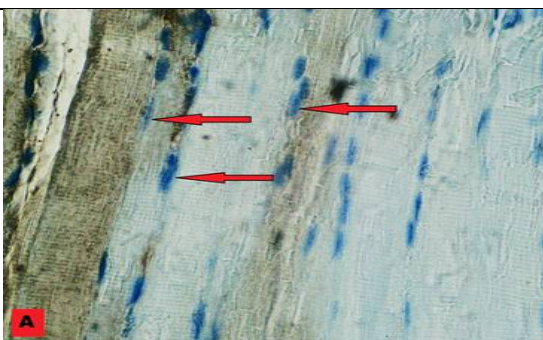


Figure 5. Longitudinal sections in the skeletal muscle showing **A**: regenerating skeletal muscle fibers that histologically characterized by the presence of prominent (activated) stellate cells (red row) rows of internal myoblast nuclei, and basophilic cytoplasm. **B**: the same image using Aprio showing positive (yellow –brown) and negative blue reaction (HGF Ab, at 1st post-operative week group, X40)





Haitham Mohammad Abood and May Fadhil Al- Habib

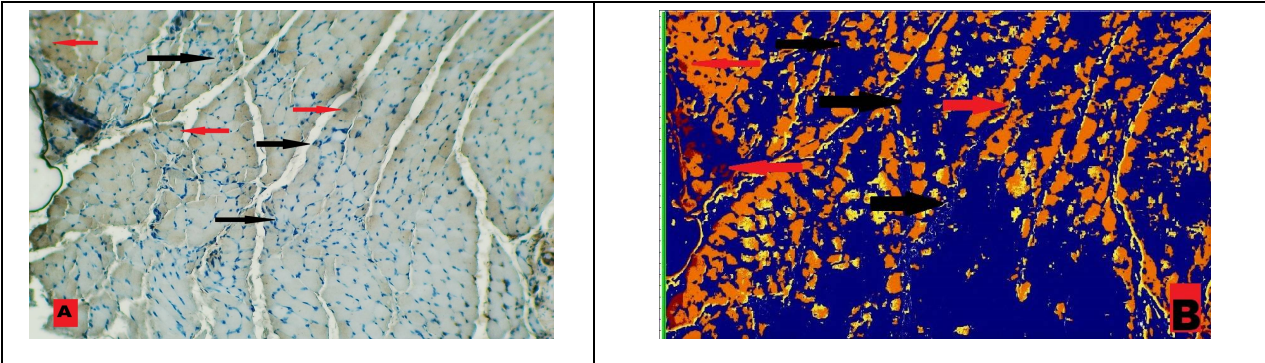


Figure 6. Cross sections in the skeletal muscle showing **A:** In 2nd post- operative week the presence of mononuclear inflammatory cells (black row) were still infiltrating the area, with heavy vascularity on one hand, on the other hand newly formed muscle fibers identified (red row) with a heavy constituent of connective tissue element and blood vessels **B:** the same image using Aprio showing positive (yellow –brown) and negative blue reaction. (HGF Ab, at 2nd post-operative week group, X10)

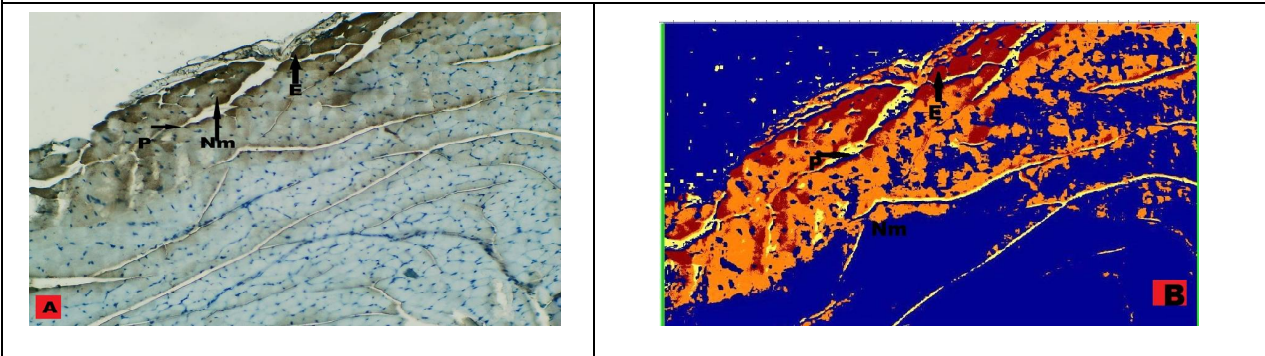


Figure 7. Cross sections in the skeletal muscle showing **A:** showing the intense reactivity at the sarcoplasm of newly formed muscle (NM) together with the perimysium (P) **B:** the same image using Aprio showing positive (yellow – brown) and negative blue reaction. (HGF Ab, at 2nd post-operative week group, X10)

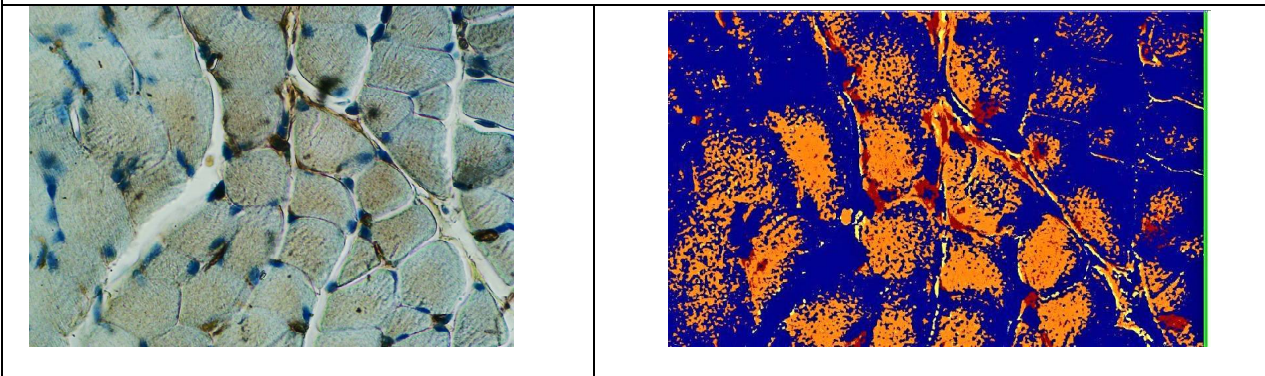


Figure 8. **A:** section in the skeletal muscle showing newly formed muscle with intense reactivity & extracellular matrix **B:** the same image using Aperioreactivity showing positive (yellow-brown) and negative blue reaction (HGF Ab, at 2nd post-operative week group,x40).



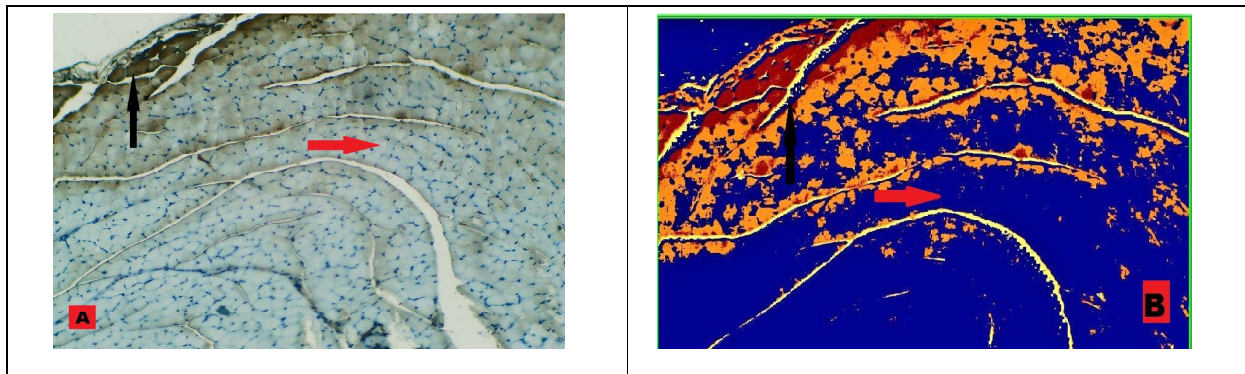


Figure 9. Cross sections in the skeletal muscle showing **A:** Cross sections in the skeletal muscle regeneration showing focus(black row) of regeneration at the site of injury surrounded by mature muscle fibers (red row) sarcoplasmic reactivity in new muscle **B:** the same image using Aprio showing positive (yellow –brown) and negative blue reaction. (HGF Ab, at 2nd post-operative week group, X10).

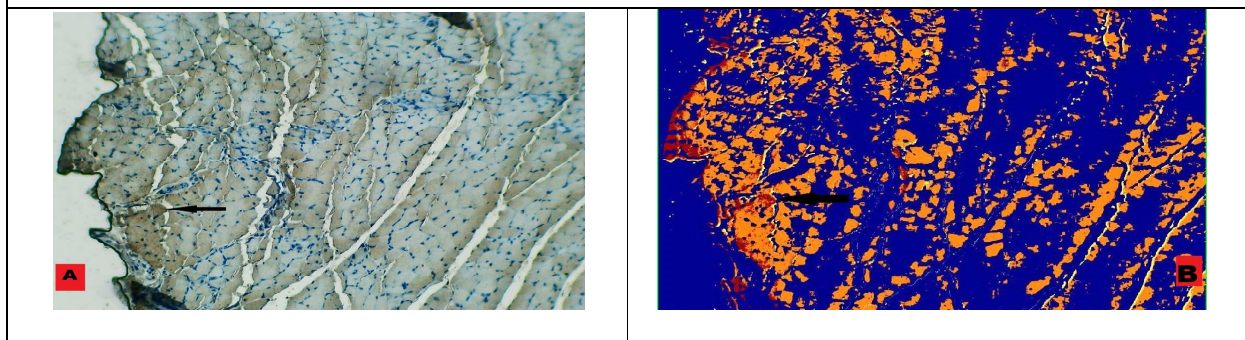


Figure 10. Cross sections in the skeletal muscle showing **A:** Cross sections in the skeletal muscle regeneration showing focus (black row) of regeneration at the site of injury surrounded by mature muscle fibers, notice sarcoplasmic reactivity in new muscle **B:** the same image using Aprio showing positive (yellow –brown) and negative blue reaction. (HGF Ab, at 2nd post-operative week group, X10)

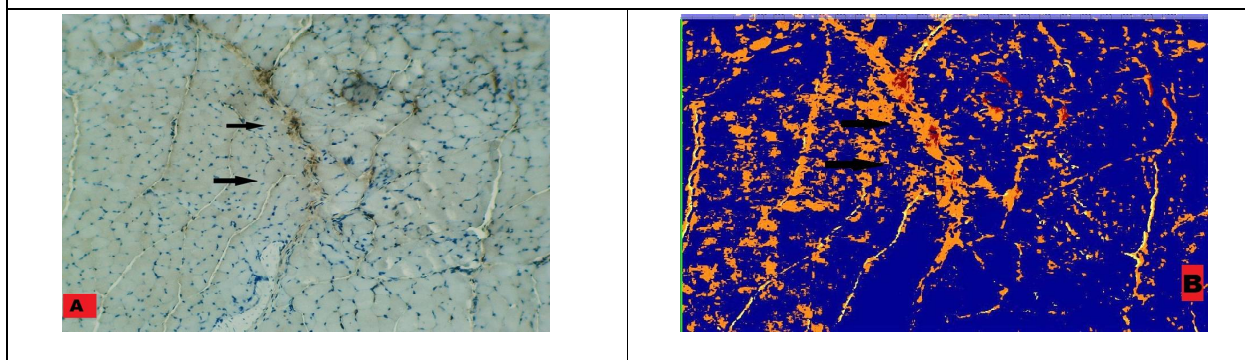


Figure 11. Cross sections in the skeletal muscle showing **A:** Cross sections in the skeletal muscle Regenerative process was completed at the end of 4th weeks of post-operative process, the entire muscle showed a well-organized regenerative muscle fibers arranged in bundles with all histological features of maturity .The HGF reaction was limited to a thin stain reaction in between mature fibers **B:** the same image using Aprio showing positive (yellow – brown) and negative blue reaction. (HGF Ab, at 4th post-operative week group, X10)





Haitham Mohammad Abood and May Fadhil Al- Habib

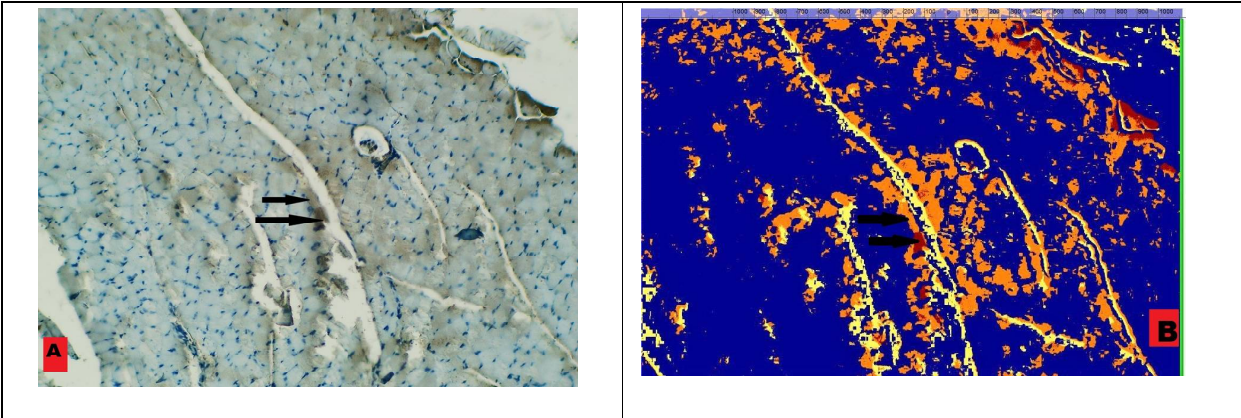


Figure 12. Cross sections in the skeletal muscle showing **A**: Cross sections in the skeletal muscle showing mature muscle fiber with no sarcoplasm reactivity or faint , the reaction was confined in the sarcoplasm, endomysium and faint in perimysium (black row) as similar as control group **B**: the same image using Aperio showing positive (yellow –brown) and negative blue reaction. (HGF Ab, at 4th post-operative week group, X10).

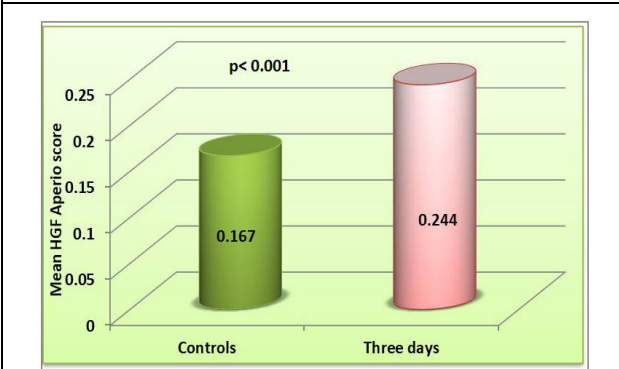


Figure 13. Mean HGF Aperio score in experimental animals after three days of injury and control animals

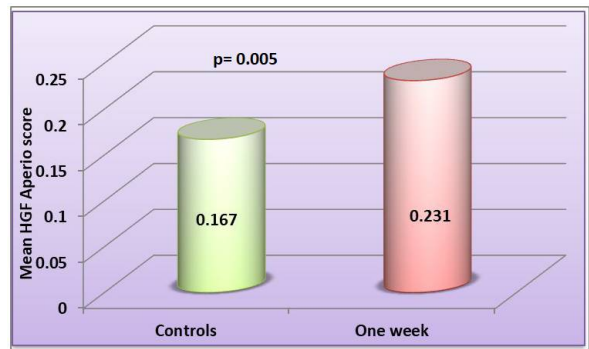


Figure 14. Mean HGF Aperio score in experimental animals after one week of injury and control animals

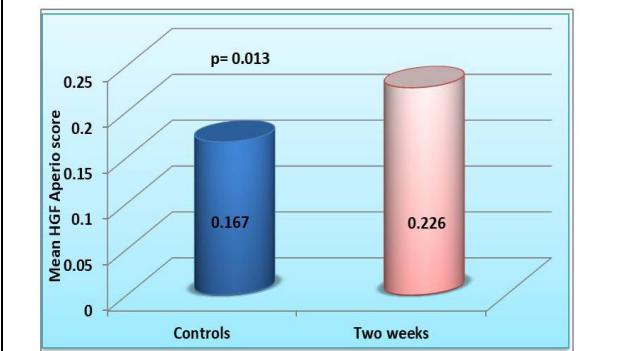


Figure 15. Mean HGF Aperio score in experimental animals after two weeks of injury and control animals

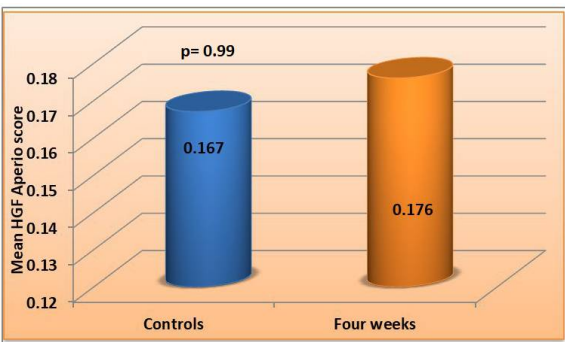


Figure 16. Mean HGF Aperio score in experimental animals after four weeks of injury and control animals





Haitham Mohammad Abood and May Fadhil AI- Habib

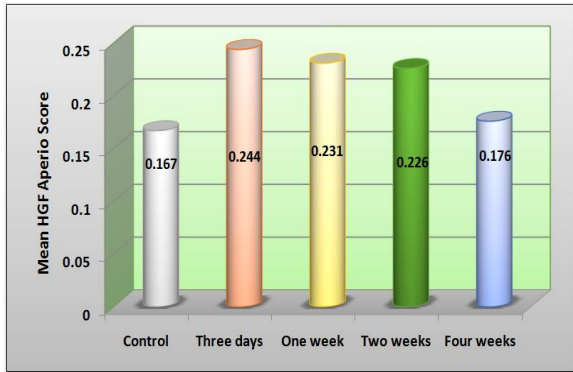


Figure 17. Mean HGF Aperi score in different groups

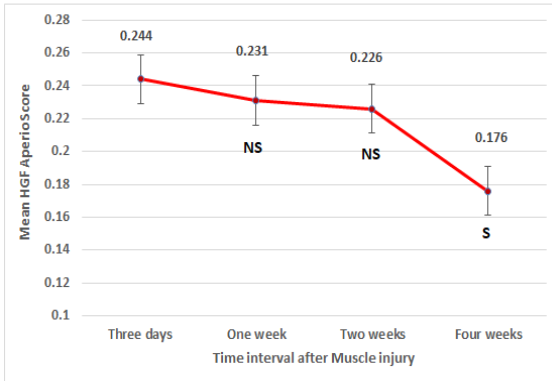


Figure 18. Time trends of HGF Aperi score in experimental animals





Social Dimension and Adoption Behavior of Sugarcane Production and Protection Technologies among Sugarcane Farmers in Coastal District of Cuddalore in Tamil Nadu, India

Karpagam.C*, Udayakumar.N and Mooventhan.P

Central Institute for Cotton Research, Regional Station, Coimbatore – 641 003, Tamil Nadu, India

Received: 17 July 2019

Revised: 20 Aug 2019

Accepted: 23 Sep 2019

*Address for Correspondence

Karpagam.C

Central Institute for Cotton Research,
Regional Station,
Coimbatore – 641 003,
Tamil Nadu, India.
Email: karpsicar@gmail.com



This is an Open Access Journal / article distributed under the terms of the **Creative Commons Attribution License** (CC BY-NC-ND 3.0) which permits unrestricted use, distribution, and reproduction in any medium, provided the original work is properly cited. All rights reserved.

ABSTRACT

Existing sugarcane yield in Tamil Nadu is 101 t/ha, but it is lower than the potential yield of 203.7 t/ha, which in turn resulted in yield gap of 50.42%. The fact is that all the farmers are not getting the potential yield, but by following the recommended production-cum-protection technologies, farmers can get more yield. Keeping the importance in mind; the present study is aiming to study the social dimension and adoption behavior of sugarcane farmers in Cuddalore district. From the Cuddalore district 60 respondents were selected for the study. A semi structured interview schedule was prepared with six independent and one dependent variable. Results revealed that fifty-five per cent of sugarcane farmers were found to be in between 35 -50 age group, whereas thirty per cent of sugarcane farmers were in above 50 years category. Adoption pattern analysis revealed that the production technologies such as earthing-up (95.00%), basal dose of 'p' fertilizer, de-trashing, stubble shaving (91.67%) were fully adopted by more than 90 per cent of the respondents in study area. Regarding protection technologies, Trichogramma for INB (93.33%), integrated weed management (85.00%), use of health planting material (83.33%) were fully adopted by more than 80 per cent of the respondents in the study area.

Keywords: Socio-economic condition, Adoption, Production technologies and Protection technologies.

INTRODUCTION

Area under sugarcane in Tamil Nadu varied widely from 2.3 lakh hectares to 3.9 lakh hectares over the years in the new millennium (2000-01 to 2011-12), the productivity has almost been stabilized at around 105 tones/ ha during the



**Karpagam *et al.***

same period (Ramasubramanian and Karpagam, 2014, Karpagam *et al.*, 2016 and Karpagam *et al.*, 2019). The average cane yield in Tamil Nadu is 101 t/ha, which is lower than the potential yield of 203.7 t/ha resulting in yield gap of 50.42% (Karpagam *et al.*, 2019). Thus, wide gap exists between the actual yield against the potential yield. Bridging the yield gap should be the prime objective of the research efforts. By following the recommended production-cum-protection technologies, farmers can bridge the yield gap (Karpagam *et al.*, 2011). It is evident that sugarcane crop command greater importance for attaining a better position in the world market, which in turn contribute to our national income. At the same time, there is a need to concentrate on certain specific sustainable cultivation practices which are eco-friendly and cost effective. In this juncture, exploring the social dimension and adoption behavior of sugarcane farmers in cane cultivation will pave the way towards sustainable sugarcane cultivation. At present there are hardly few studies on such issues. Hence, a study has been initiated with the objectives to study the social dimension of cane farmers and to study the adoption behaviour for cane production and protection technologies by the cane farmers in E.I.D. Parry sugar mill area, Cuddalore district which is one of the costal districts in Tamil Nadu.

MATERIALS AND METHODS

The present study is aiming to study the socio-economic and adoption behaviour of sugarcane farmers. Based on the predominance in sugarcane cultivation, Cuddalore district was selected for the study. From the Cuddalore district four blocks were selected. From each block, fifteen respondents were selected; thus 60 respondents were constituted for the study. The value of the study largely depends upon the different variables taken into consideration for the study. By reviewing relevant literature and discussion with extension scientists, a list of six socio-economic variables viz., Age, Educational Status, Farm size, Farming experience, Risk orientation and Scientific orientation were selected to study the social dimensions exists in the study area and to study the adoption behaviour, different production and protection technologies were selected. To collect the information, a comprehensive semi-structured interview schedule was constructed. Utmost care was taken to ensure that the items were clear and unambiguous. With the semi structured interview schedule; the direct field level personal interviews were undertaken in the study area with sixty cane growers.

RESULTS AND DISCUSSION

Social dimension gives a clear-cut picture about the cane farmers' background, their characteristics and the condition in which they operate the farming. The adoption behavior analysis paves the way to understand the technologies which already reached and adopted by the farmers and the technologies yet to reach the farmers. Hence, these two dimensions gives holistic view about the cane cultivation in the particular area.

Social Dimension

It could be observed from Table 1 that fifty-five per cent of sugarcane farmers were found to be in between 35 -50 age group, whereas thirty per cent of sugarcane farmers were in above 50 years in age category. The results are in line with the findings of Karpagam *et al.*, (2019) and Mooventhan *et al.*, (2015) who reported that very meager percent (15.67) of the dairy farmers in North hill zone of Chhattisgarh were of the age up to 35 years. The educational status analysis revealed that in total seventy per cent of the respondents educated up to High school and lesser percentage (30%) of the respondents educated beyond the high school. The results are in line with the findings of Karpagam (2000 and 2009) and Karpagam *et al.*, (2009). It is quite clear from the findings that majority of the farmers (95.00%) in the study area were belongs to big farmers category who possessed more than five acres of sugarcane area. Very meager percent of the respondents comes under marginal (3.33%) and small (1.67%) categories. Sugarcane is a cash crop and required high cost for cultivation and elsewhere in the study it was observed that farming experience of the respondents were also in higher rate. Therefore, over a period of experience they might have developed more area under sugarcane cultivation. Nearly fifty per cent of the respondents were had more than 10 years of experience in



**Karpagam et al.**

cane cultivation and thirty-five per cent of the respondents had 5-10 years of experience in cane cultivation. It may be due to the reason that sugarcane is the long duration crop and it is being cultivated for several ratoons. It was observed from the study that some farmers were going for more than 7-8 ratoons. This may be resulted in higher farming experiences among the cane farmers. Similar findings were reported by Sunitha (1998), Balasubramaniam (2005) and Dhamodaran (2001) and Karpagam *et al.*, (2019). Study on risk orientation revealed that medium level of risk orientation was observed more among cane farmers (70.00%). It is quite natural that cane cultivation required higher investment; hence the farmers who could be able to take more economic risk will opt for cane cultivation. The results were in agreement with Karpagam (2007) and Karpagam *et al.*, (2019) who observed that the majority of grape growers (75%) had medium level of risk orientation and majority of the cane farmers (83%) had medium to high level of risk orientation. Further, it is inferred from the table 1 that medium level of scientific orientation was found among the majority (81.67%) of the respondents in the study area. It was learnt during the survey that irrespective of categories, majority of the respondents were easily get help and support from sugar factories for majority of the cultivation practices. Hence their dependency on sugar factories for technological backstopping was more which in turn resulted in their scientific orientation towards the sugarcane cultivation is not at the higher level.

Extent of adoption for sugarcane production technologies

In the present study adoption level for production technologies were studied in three-point continuum and respondents were classified into three categories viz., complete adoption, partial adoption and not adoption categories. It can be observed from the Table 2 that technologies viz., earthing-up (95.00%), basal dose of 'P' fertilizer, de-trashing, stubble shaving (91.67%) were fully adopted by more than 90 per cent of the respondents in the study area. Whereas, off-barring (88.83), secondary tillage, FYM application (86.67%), two split application of N and K (85.00%) were adopted by more than 80 per cent of the respondents in the study area. E.I.D Parry sugar mill providing SSP fertilizer in loan basis to all the registered cane farmers and advised them to apply in basal dose, hence the higher adoption rate was observed for the particular practice. Regarding planting season, primary tillage (50.00%), wider row spacing (46.67%), intercrop (38.3%) were adopted by lesser than 50 per cent of the respondents in the study area. Very low adoption pattern (less than 20.00%) was observed for bud chip settling, drip irrigation, removal of water shoots and mechanical harvester. Normally farmers' not removing water shoots because of its added advantage for more weightages for their products. Drip irrigation was also found lower adoption because of the planting method was narrow spacing and the water quality in the study area was also not supporting for drip irrigation. Hence the result was obtained. In study area the narrow space planting method is predominantly followed, hence the use of mechanical harvester is also very low. But the sugar mill taking initiatives to increase the area under wider row spacing in recent years and slowly the adoption rate for wider row spacing is accelerating trend.

Extent of adoption for sugarcane protection technologies

It can be observed from Table 3 that the technologies viz., Trichogramma for INB (93.33%), Integrated Weed Management (85.00%), use of healthy planting material (83.33%) were fully adopted by more than 80 per cent of the respondents in the study area. Tricho cards were supplied by the sugar mill to the farmers at nominal rate; hence the adoption rate was higher for the technology. Whereas, pheromone trap for INB (35.00%), soil trenching of recommended termiticides (31.67%) were adopted by less than 50 per cent of the respondents in the study area. Very low adoption rate (8.333%) was found for white grub management. It is because of the study area is not faced white grub problem for last ten years but recent year, white grub incidence was noticed and collection of beetle was adopted by very few farmers in some pockets.





Karpagam et al.

CONCLUSION

The investigation on this research issue is a maiden attempt to explore the various dimensions of cane cultivation in coastal district of Cuddalore in Tamil Nadu State. The results on social dimensions revealed the clear picture of social dimensions of cane farmers in the study area which will helpful for the extension personnel to develop the “Target Group Approach” extension model for the study area. Further, the results of adoption behavior of production and protection technologies were brought out the technologies which are widely adopted and which are lesser adopted by the cane farmers. These findings will certainly helpful to the extension workers, researchers and sugar factory personnel to re-orient their extension strategies for cane technology transfer and to reduce the yield gap.

REFERENCES

- Balasubramaniam, P. (2005). Developing TOT strategy for water management in canal command area of lower Bhavani project. Unpub. Ph.D., Thesis, TNAU, Coimbatore.
- Dhamodaran, T and Vasantha Kumar, J. (2001). Relationship between selected characteristics of registered cane growers and their extent of adoption of improved sugarcane cultivation practices. *J. Extn. Edu.*, 12(2):3138-3143.
- Karpagam, C. (2000). A study on the Knowledge and Adoption Behavior of Turmeric Growers in Erode district of Tamil Nadu State. Unpub. M.Sc. (Ag.) Thesis, UAS, Dharwad.
- Karpagam, C. (2007). Farmers' Interest Group in grape production - an impact analysis. Unpub. Ph.D. Topical Research Report, TNAU, Coimbatore.
- Karpagam, C. (2009). Socio technological analysis of drip irrigation. Unpub. Ph. D Thesis, TNAU, Coimbatore.
- Karpagam, C., Ravichandran, V., Ravikumar Theodore and Cinthia Fernandez, C. (2009). Existing Social – Dynamics among drip and non-drip users – A sociological enquiry. *Journal of Extension Education*. 21 (4) : 4300-4303.
- Karpagam, C., Ravichandran, V and Ravikumar Thodore. (2011). Social-dynamics among sugarcane, onion and leaf banana drip and non-drip users – a sociological enquiry. *Journal of Sugarcane Research*. 1(1): 75-79.
- Karpagam, C., Puthira Prathap, D and Moovendhan, P. (2016). Farmer let gross root level entrepreneurial initiatives for sustainable sugarcane production system in Tamil Nadu, India. *Journal of Applied and Natural Science*, 8(4).
- Karpagam, C., Selvaraj, T., Mooventhana, P and Venkatasubramanian, V. (2019). Socail and technological dimensions and constraint analysis in sugarcane cultivation of Theni district of Tamil Nadu, India. *Journal of Applied and Natural Science*. 11 (9): 581-586.
- Mooventhana, P., Kadian, K.S., Senthilkumar, R and Karpagam, C. (2015). Socio-econmoc profiling of tribal dairy farmers in Northern hills zone of Chhattisgarh. *Journal of Extension Education*. 27(3): 5517-5523.
- Ramasubramanian, T and Karpagam, C. (2014). FAQs on early shoot borer, *Kissan world*, 41(9):19-21
- Sunitha Varghese. (1998). Knowledge and Adoption of Eco-friendly Farm Technologies in Paddy. Unpub. M.Sc.(Ag.) Thesis, TNAU, Madurai.

Table 1. Social dimensions of cane farmers in the study area (n=60)

S. no	Category	Frequency	Percentage	Rank
A. Age				
1	<20	0	0	IV
2	21 – 35	9	15	III
3	35 – 50	33	55	I
4	>50	18	30	II
B. Educational status				
1	Illiterate	1	1.67	IV





Karpagam et al.

2	Primary School	9	15	III
3	Middle School	11	18.33	II
4	High School	21	35	I
5	Higher Secondary	9	15	III
6	Collegiate	9	15	III
C. Farm size				
1	Small farmers (<2.5 acres)	1	1.67	III
2	Marginal farmers (2.5 – 5 acres)	2	3.33	II
3	Big farmers (>5 acres)	57	95.00	I
D. Farming experience				
1	< 1 years	0	0.00	IV
2	2-5 years	10	16.67	III
3	5-10 years	21	35	II
4	> 10 years	29	48.33	I
E. Risk orientation				
1	Low	10	16.67	II
2	Medium	42	70.00	I
3	High	8	13.33	III
F. Scientific orientation				
1	Low	11	18.33	II
2	Medium	49	81.67	I
3	High	0	0	III

Table 2. Extent of adoption for sugarcane production technologies

Production technologies	Fully adopted		Partial adopted		Not adopted	
	No	%	No	%	No	%
Planting season	30	50.00	25	41.67	5	8.33
Primary tillage with mould board / disc plough	30	50.00	19	31.67	11	18.33
Secondary tillage	52	86.67	7	11.67	1	1.67
Cultivation of Green manure crop - Daincha / Sun hemp	31	51.67	17	28.33	12	20.00
FYM Application	52	86.67	7	11.67	1	1.67
Seed rate	40	66.67	19	31.67	1	1.67
Micro nutrient application	35	58.33	15	25.00	10	16.67
Wider spacing with dual row planting	28	46.67	8	13.33	24	40.00
Bud chip settlings used / acre	9	15.00	5	8.33	46	76.67
Intercrop	23	38.33	16	26.67	21	35.00
Gap filling	57	95.00	2	3.33	1	1.67
Basal dose of P Fertilizer	55	91.67	5	8.33	0	0.00
Two split application of N and K	51	85.00	6	10.00	3	5.00
Bio fertilizer application	24	40.00	17	28.33	19	31.67
Irrigation schedule stage wise	38	63.33	21	35.00	1	1.67
Earthing up	57	95.00	3	5.00	0	0.00
Detrashing	55	91.67	5	8.33	0	0.00





Karpagam et al.

Propping	13	21.67	16	26.67	31	51.67
Trash mulching	46	76.67	9	15.00	5	8.33
Removal of water shoots	5	8.33	14	28.33	41	68.33
Drip irrigation	12	20.00	4	6.67	44	73.33
Mechanical Harvester	9	15.00	7	11.67	44	73.33
Stubble shaving	55	91.67	3	5.00	2	3.33
Off barring	53	88.33	4	6.67	3	5.00

Table 3. Extent of adoption for sugarcane Protection technologies

Protection Technologies	Fully adopted		Partial adopted		Not adopted	
	No	%	No	%	No	%
Sett treatment	11	18.33	18	30.00	31	51.67
Use of healthy planting material	50	83.33	8	13.33	2	3.33
Recommended chemical for ESB	33	55.00	23	38.33	4	6.67
Trichogramma for INB	56	93.33	3	5.00	1	1.67
Pheromone trap for INB	21	35.00	4	6.67	35	58.33
Change of lure for every 45 days in Pheromone trap	10	16.67	8	13.33	42	70.00
Collection of beetle after summer shower for white grub management	5	8.33	10	16.67	45	75.00
Soil trenching of recommended termiticides	19	31.67	19	31.67	22	36.67
Integrated weed management	51	85.00	8	13.33	1	1.67

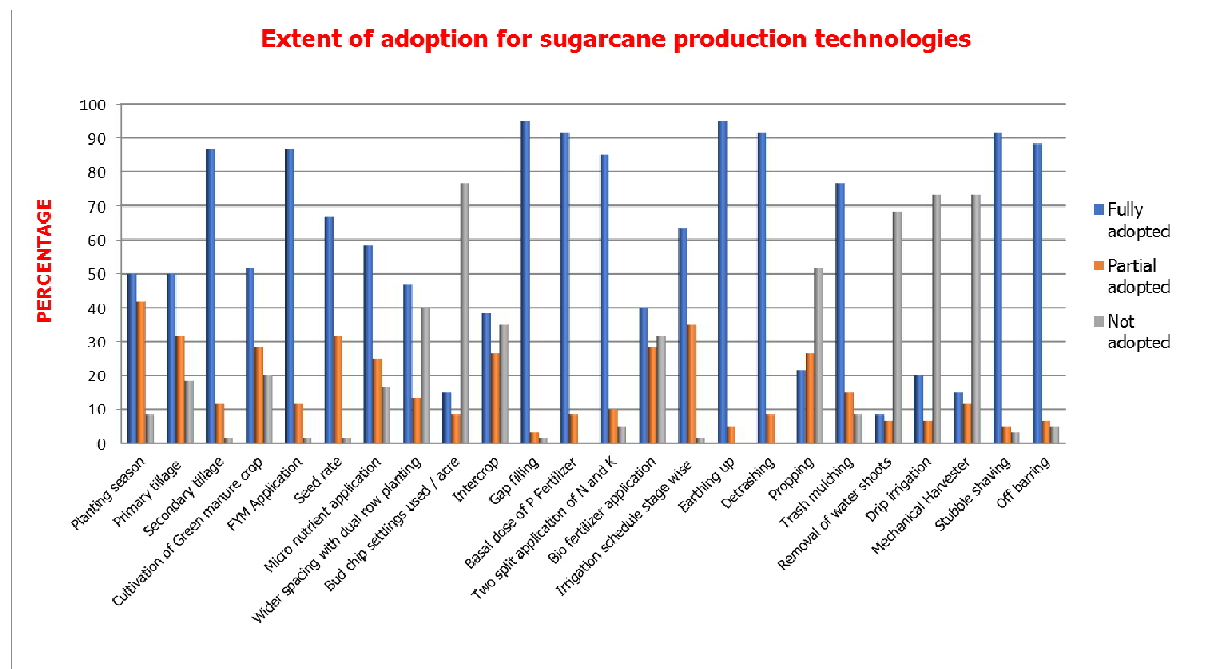


Figure 1. Extent of adoption for sugarcane production technologies



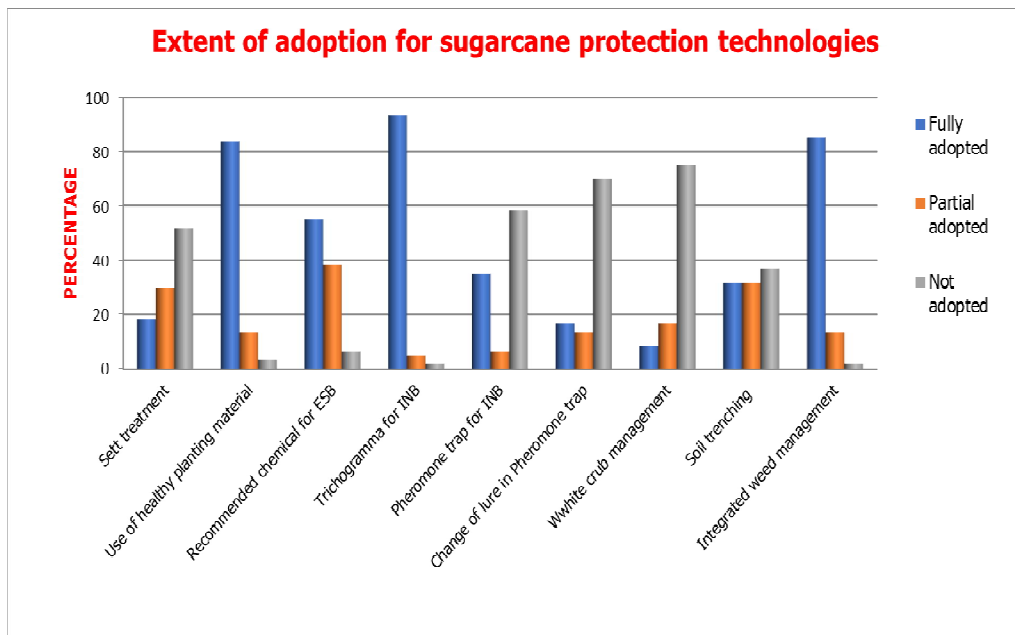


Figure 2. Extent of adoption for sugarcane production technologies





Chemical Composition and Antioxidant Activity of Essential Oil of *Achillea santolina*

Jehad Al-Shuneigat^{1*}, Sameeh Al- Sarayreh¹, Mahmoud Al-Qudah², Yousef Al-Sarairoh³ and Ibrahim Al-Tarawneh⁴

¹Faculty of Medicine, Department of Biochemistry and Molecular Biology Mutah University, Mutah, Jordan.

²Faculty of Science, Department of Chemistry Yarmouk University, Irbid, Jordan.

³Faculty of Medicine, Department of Pharmacology Mutah University, Mutah, Jordan.

⁴Faculty of Science, Department of Chemistry, Albalqa' Applied University, Albalqa, Al- Salt, Jordan

Received: 22 July 2019

Revised: 25 Aug 2019

Accepted: 27 Sep 2019

*Address for Correspondence

Jehad Al-Shuneigat

Faculty of Medicine,

Department of Biochemistry and Molecular Biology,

Mutah University, Mutah, Jordan.

Email: Dr.Jehad@mutah.edu.jo.



This is an Open Access Journal / article distributed under the terms of the **Creative Commons Attribution License** (CC BY-NC-ND 3.0) which permits unrestricted use, distribution, and reproduction in any medium, provided the original work is properly cited. All rights reserved.

ABSTRACT

The aim of the present study was to investigate the chemical composition of the essential oil from the aerial parts of *Achillea santolina* and its *invitro* antioxidant activity. Gas chromatography–mass spectrometry (GC-MS) was used to study essential oil composition while antioxidant effectiveness of the essential oil was examined by three different radical scavenging methods: 2,2-diphenyl-1-picrylhydrazyl (DPPH) free radical scavenging activity, ferrous radical scavenging activity and 2,2'-azino-bis(3-ethylbenzothiazoline-6-sulphonic acid (ABTS) ferrous radical scavenging activity. Sixty components accounting for 100% of the oil were identified. The major identified compounds were: cis-sabinene hydrate 10.64%, 1,8-cineole 4.12%, cis-Rose oxide 3.79%, α -Terpinene 1.57, p-cymene 1.05%, dehydro sabina ketone 1.04%, cis-para-meth-2-en-1-ol 1.25%, trans-chrysanthemol 1.93%, camphor 2.01%, Borneol 3.74%, Terpinen-4-ol 10.6%, α -Terpinol 3.97%, cis-chrysanthenyl acetate 6.05%, Bornyl acetate 1.98%, trans-Muurolo-4(14),5-diene 4.84%, 6-methyl-alpha-Ionone 2.23%, spathulenol 3.7%, viyidiflorol 2.03%, trans-Arteannuic alcohol 3.2%, epi- α -Muurolo-1 1.17%, α -cadinol 4.69%, α -Muurolo-1 1.07%, patchouli alcohol 1.87%, E-Bisabol-11-ol 1.73%, valeranone 2.75%, 10-nor-calamenen-10-one 2.36%, Drimenol 2.33%. The major oil components were: Oxygenated monoterpene 55.47%, Oxygenated Sesquiterpene 31.61%, Sesquiterpene hydrocarbon 6.51%, Monoterpene hydrocarbon 5.05%, Ester 0.82%, and others 0.54%. Antioxidant activity tests show that *Achillea santolina* essential oil exhibited less activity than α -tocopherol and ascorbic acid in all three radical scavenging methods.

Keywords: *Achillea santolina*, antioxidant, GCMS, DPPH, ABTS, IC50.





INTRODUCTION

The genus *Achillea* comprises more than 100 species growing wild in different parts of the world (Rahimmalek *et al.*, 2009). *Achillea santolina* is a perennial herbal plant 10-30 cm long with aromatic smell. In folk medicine *Achillea santolina* has been used as antidiabetic, antimicrobial anti-inflammatory, anti-diuretic as well as in gastrointestinal disorders and in pain relieve (Alwwadi 2013; Cowan 1999). The plant produces two types of oil fixed oil (nonvolatile) and volatile oil known as essential oil. EOs are normally hydrophobic, colorless or pale yellow with lower density than water. It can be obtained from many different parts of plants including leaves, fruits, flowers and seeds (Naeem *et al.*, 2018; Al-Shuneigat *et al.*, 2015). Essential oils are secondary metabolites while the primary metabolites are the essential nutrients for the survival of plant including carbohydrates, lipids, and proteins. Secondary metabolites are nonessential for plants growth (Yang *et al.*, 2018; Al-Shuneigat *et al.*, 2014).

Extraction of essential oil from plants is performed by many methods including steam distillation, high-pressure solvent extraction, hydrodistillation and microwave hydrodiffusion (Rassem *et al.*, 2016). Essential oil constituents fall into two chemical classes: terpenes and phenylpropanoids Essential oil is complex mixture of constituents that possesses a broad-spectrum of antimicrobial, antioxidant and antifungal activities (Khayyat and Roselin 2018). Oxidative stress can occur when there is disturbance in the balance between free radicals and antioxidants in the body. Oxidative stress is harmful to our body it may causes damages to cellular membrane, proteins, and DNA that may lead to different pathological conditions including: diabetes, cancer, hypertension, ischemia and neurodegenerative conditions, such as Alzheimer's and Parkinson's diseases (Burton and Jauniaux 2011). Our body produces reactive oxygen species (ROS). ROS plays a beneficial role in our body as long as their concentrations are low (Esra *et al.*, 2012). At the same time the body has antioxidant defense against ROS including enzymatic and nonenzymatic compounds and pathways that keep ROS at low levels.

Reactive oxygen species can be divided in to two groups: free radicals and nonradicals. Free radicals are molecules with one or more unpaired electron. Examples of free radicals include: superoxide and hydroxyl radical. While the nonradicals are formed when two free radicals share their unpaired electrons (Esra *et al.*, 2012). Antioxidants neutralize free radicals by donating an electron. Our body naturally has antioxidants such as glutathione. Our diet is also an important source of antioxidants for example vitamins A, C, and E. Plants essential oils has potential antioxidant capacities which can be attributed to the presence of terpenes and phenolic compounds (Torres-Martínez *et al.*, 2017). The aim of the present study was to report on the chemical composition of the essential oil from the aerial parts of *Achillea santolina* collected from Mutah, Alkarak, south Jordan and its antioxidant activity.

MATERIALS AND METHODS

Collection and Authentication of Plants

Fresh amount of wild *Achillea santolina* was collected from Mutah, Alkarak Province, south Jordan, during the flowering period and the vegetative phase. The plant materials were taxonomically identified and authenticated by Professor Saleh Al-Quran, Botanical Survey, Department of Biology, Mutah University.

Isolation of Essential Oil

The collected *Achillea santolina* were finely chopped and subjected to hydrodistillation for 4 h using a Clevenger-type apparatus, yielding 0.19% (v/wt), pale yellowish oil. Subsequently, oil was dried over anhydrous sodium sulfate and immediately stored in GC-grade hexane at 4°C until the analysis by gas chromatography/mass spectrometry (GC/MS) was done.





Essential Oil Composition

GC–FID analysis

The oils were analyzed in an Agilent (Palo Alto, USA) 6890N gas chromatograph fitted with a 5% phenyl–95% methylsilicone (HP5, 30 m × 0.25 mm × 0.25 μm) fused silica capillary column. The oven temperature was programmed to run from 60°C to 240°C at 3°C/min with hydrogen being used as the carrier gas (1.4 mL/min). 1.0 μL of a 1% solution of the oils in hexane was injected in split mode (1:50). The injector was kept at 250°C and the flame ionization detector (FID) was kept at 280°C. Concentrations (% contents) of oil ingredient for *Achillea santolina* were determined using their relative area percentages obtained from GC chromatogram, assuming a unity response by all components.

GC–MS analysis

Chemical analysis of the essential oils was carried out using gas chromatography–mass spectrometry (Agilent (Palo Alto, USA) 6890N gas chromatograph). The chromatographic conditions were as follows: column oven program, 60°C (1 min, isothermal) to 246°C (3 min, isothermal) at 3°C/min, the injector and detector temperatures were 250°C and 300°C, respectively. Helium was the carrier gas (flow rate 0.90 ml/min) and the ionization voltage was maintained at 70eV. A HP-5 MS capillary column (30 m × 0.25 mm i.d., 0.25 μm film thicknesses) was used. A hydrocarbon mixture of *n*-alkanes (C₈–C₂₀) was analyzed separately by GC-MS under same chromatographic conditions using the same HP-5 column. Kovats Retention Indexes (KRIs) were calculated by injection of a series of *n*-alkanes (C₈–C₂₀) in the same column and conditions as above for gas chromatography analyses. Identification of the oil components were based on computer search using the library of mass spectral data and comparison of calculated Kovats retention index (KRI) with those of available authentic standards and literature data.

Antioxidant tests

DPPH free radical scavenging activity

The total radical scavenging capacity of the essential oil obtained was determined and compared to those of the positive controls (ascorbic acid and α-tocopherol) according to the procedure described in Al-Qudah *et al* (2017). Briefly, a 1.0 mL sample of various concentrations (0.005 - 0.50 mg/mL) of the tested essential oils (dissolved in methanol) was to 2 mL of 0.1 mM DPPH• methanolic solution. The solutions were allowed to stand at room temperature in the dark for 30 min, then, the absorbance of each solution was measured at 517 nm using a UV- visible spectrophotometer. All determinations were performed in triplicate. The ability to scavenge the DPPH• radical was calculated using the following equation:

$$\text{DPPH}\cdot \text{ scavenging effect (\%)} = (A_c - A_s) / (A_c) * 100 \%$$

Where A_c is the absorbance of the blank and A_s is the absorbance of the tested solution. The IC₅₀ was determined from the sigmoidal curve obtained by plotting the percentages of DPPH scavenging relative to the control versus logarithmic concentration of test compound using nonlinear regression analysis of GraphPad Prism 6 (GraphPad Software, San Diego, California, USA). Each concentration was tested thrice in 3 independent experiments.

ABTS radical scavenging assay

The total antioxidant activity, measured by the radical cation 2,2'-azino-bis(3-ethylbenzothiazoline-6-sulphonic acid (ABTS^{•+}) decolorization assay method, was evaluated according to the procedure described by Al-Qudah *et al* (2017). The ABTS^{•+} cation radical solution was prepared by reacting similar quantities of 7 mM of ABTS and 2.4 mM of potassium persulfate (K₂S₂O₈) solutions for 16 h at room temperature in the dark. Before use, this solution was





Jehad Al-Shuneigat et al.

diluted with methanol until an absorbance of 0.75 ± 0.02 at 734 nm was obtained. The reaction mixture comprised 3 mL of ABTS^{•+} solution and 1 mL of the essential oil solutions at various concentration (0.005 - 0.50 mg/mL). The absorbance's of all prepared solutions, including the blank sample, were measured at 734 nm using a UV- visible spectrophotometer and after at least 5 minutes of incubation. The ABTS scavenging capacity of the essential oils was compared with that observed for ascorbic acid and α -tocopherol as positive controls. The percentage inhibition was calculated according to the equation:

$$\text{ABTS radical scavenging activity (\%)} = (A_{\text{blank}} - A_{\text{sample}} / A_{\text{blank}}) \times 100 \%$$

Where A_{blank} is the absorbance of the blank solution and A_{sample} is the absorbance of the remaining ABTS^{•+} solutions in the presence of the scavenger. The IC_{50} was determined from the sigmoidal curve obtained by plotting the percentages of ABTS^{•+} scavenging relative to the control versus logarithmic concentration of test compound using non-linear regression analysis of GraphPad Prism 6 (GraphPad Software, San Diego, California, USA). Each concentration was tested thrice in 3 independent experiments.

Ferrous radical scavenging assay

The ability of the essential oils and the control antioxidants to chelate ferrous ion from the formation of ferrozine-Fe²⁺ complex was determined as recently described in our publication Al-Qudah *et al* (2017) with some modifications. Briefly, a 3 mL of methanol solution containing the different concentrations of the tested essential oils (0.005 - 0.50 mg/ml) was added to a 0.25 mL of 2 mM iron(II) chloride (FeCl₂) reagent. Subsequently, a 0.2 mL of 5 mM ferrozine solution was added to the mixture and allowed to stand at r.t. for 10 min after vigorous shaking. The reduction in the absorbance of the red color was measured spectrophotometrically at 562 nm. The percentage of inhibition of ferrozine-Fe²⁺ complex formation by each concentration of the oil was calculated relative to the control lacking the test material using the same equation above. The IC_{50} for chelating Fe²⁺ was determined from the sigmoidal curve obtained by plotting the percentages of chelating Fe²⁺ vs. the logarithmic concentration of the test compound (in g/mL) using the non-linear regression analysis of the GraphPad Prism 6 as described above. The chelating activity test was conducted in triplicate for each concentration of the essential oil in each of the three independent experiments.

RESULTS AND DISCUSSION

Chemical Composition of the Essential Oil of *Achillea santolina*

The chemical composition of the aerial parts of *Achillea santolina* essential oil was determined using GC-MS techniques. The identified components of the essential oils, their percentages and retention indices are given in Table 1. Sixty components accounting for 100% of the oil were identified. The major identified compounds were: cis-sabinene hydrate 10.64%, 1,8-cineole 4.12%, cis-Rose oxide 3.79%, α -Terpinene 1.57, p-cymene 1.05%, dehydro sabina ketone 1.04%, cis-para-meth-2-en-1-ol 1.25%, trans-chrysanthemol 1.93%, camphor 2.01%, Borneol 3.74%, Terpinen-4-ol 10.6%, α -Terpinol 3.97%, cis-chrysanthenyl acetate 6.05%, Bornyl acetate 1.98%, trans-Muurola-4(14),5-diene 4.84%, 6-methyl- α -Ionone 2.23%, spathulenol 3.7%, viyidiflorol 2.03%, trans-Arteannuic alcohol 3.2%, epi- α -Muurolol 1.17%, α -cadinol 4.69%, α -Muurolol 1.07%, patchouli alcohol 1.87%, E-Bisabol-11-ol 1.73%, valeranone 2.75%, 10-nor-calamenen-10-one 2.36%, Drimenol 2.33%. The major oil components were: Oxygenated monoterpene 55.47%, Oxygenated Sesquiterpene 31.61%, Sesquiterpene hydrocarbon 6.51%, Monoterpene hydrocarbon 5.05%, Ester 0.82%, and others 0.54%. Bader *et al* (2003) showed that the essential oil of *Acillea santolina* contained mainly 1,8-cineole, camphor, 4-terpineol and trans-carveol. Berramdane *et al* (2018) reported that oxygenated monoterpenes made up (65.91%) of *Achillea santolina* essential oil which agree with our findings and the major constituents in the flowers, leaves and stems were: camphor, 1,8-cineole and α -terpineol. El-Shazly *et al* (2004) were able to detect 54 volatile



**Jehad Al-Shuneigat et al.**

components of *Achillea santolina* essential oil and the major identified compounds were 1,8-cineole, fragranol, fragranol acetate and terpin-4-ol. Wink *et al* (2004) detected 54 volatile components from *Achillea santolina* essential oil and the major components were 1,8-cineole, fragranol, fragranol acetate and terpin-4-ol. The compositions of the EOs are influenced by various parameters including geographical and climatic conditions, genetic diversity and type of the plant organs beside time and season of harvesting of the plants which has a great effect. In addition some studies reports the essential oil composition of the aerial parts of the plants some on the leaves others on stem and leaves, before flowering and during flowering and so on which resulted in variable results on the composition of the plants essential oil. Method of essential oil extraction plays a role in essential oil content. Morongiu *et al* (2005) reported that *Pimenta dioica* leaves contain 77.4% eugenol when supercritical fluid extraction method was used but only 45.4% when using hydrodistillation for the same plant sample. (Table 1).

Antioxidant results

Several studies reported that plants essential oils possess potent antioxidant activity (Bernstein *et al.*, 2009; Al-Qudah *et al* 2017, Morongiu *et al.*, 2005). This property is of great interest for disease prevention like cancer, heart disease and immune system diseases and for their potential in food protection. Essential oils are natural products unlike synthetic antioxidants. The most popular synthetic antioxidants are butylated hydroxyanisole and butylhydroxytoluene, both are suspected to be potentially harmful to human health (Lanigan and Yamarik 2002). In this study antioxidant activity of *Achillea santolina* essential oil was determined by three different radical scavenging methods: DPPH, ABST and Ferrous radical scavenging assay. The results are shown in Figures 1, 2 and 3. At concentration of 0.5 mg/ml, the radical scavenging properties of *Achillea santolina* were able to inhibit, 65% of ABTS radical, 70% of DPPH radical and 72% of Ferrous radical. As shown the higher the concentration of *Achillea santolina* the higher the inhibition. (Figure 1, Figure 2, Figure 3). In addition, half maximal inhibitory concentration (IC₅₀) values were determined. The IC₅₀ antioxidant activity of *Achillea santolina* essential oil results are shown in Table 2.

Although the calculated IC₅₀ for *Achillea santolina* essential oil for DPH, ABTS and ferrous radical scavenging are less than those of α -Tocopherol and ascorbic acid still the results showed a good antioxidant activity of the tested oils. Essential oils antioxidant activity relies on its composition. The main components of essential oils are terpenoids and phenylpropanoids (Amorati *et al.*, 2013). Both terpenoid and phenylpropanoid families involve phenolic compounds. In general, phenolic compounds act as antioxidants. In addition, the antioxidant activity of essential oils is synergistic result of all components (Sonam and Guleria 2017).

REFERENCES

1. Al-Qudah MA, Saleh AM, Alhawsawi NL, Al-Jaber HI, Rizvi SA, Afifie FU. Composition, Antioxidant, and Cytotoxic Activities of the Essential Oils from Fresh and Air-Dried Aerial Parts of *Pennisetum spinosa*. Chem. Biodiversity 2017; 14:8 e1700146.
2. Al-Shuneigat J, Al- Sarayreh S, Al-Qudah M, Al-Tarawneh I, Al-Saraireh Y, Al-Qtaitat A. GC-MS Analysis and Antibacterial Activity of the Essential Oil Isolated from Wild *Artemisia herba-alba* Grown in South Jordan. British Journal of Medicine & Medical Research 2015;5: 297-302.
3. Al-Shuneigat J, Al- Sarayreh S, Al-Saraireh Y, Al-Qudah M, Al-Tarawneh I. Effects of wild *Thymus vulgaris* essential oil on clinical isolates biofilm-forming bacteria. IOSR Journal of Dental and Medical Sciences 2014;13:62-66.
4. Alwwadi N. Anti diabetics effect of *Achillea santolina* aqueous leaves extract. Int J Med Plants Res 2013;4: 151-156.
5. Amorati R, Foti MC, Valgimigli L.. Antioxidant Activity of Essential Oils. J Agric. Food Chem 2013;61:10835-10847.
6. Bader A, Flamini G, Cioni PL, Morelli I. Essential oil composition of *Achillea santolina* L. and *Achillea santolina* *Afan.* collected in Jordan. Flavour Fragr J 2003; 18: 36-38.
7. Bernstein N, Chaimovitch D, Dudai N. Effect of irrigation with secondary treated effluent on essential oil, antioxidant activity, and phenolic compounds in oregano and rosemary. Agron J 2009;101: 1-10.





Jehad Al-Shuneigat et al.

8. Berramdane T, Gourine N, Zitouni A, Bombarda I, Yousfi M. Essential oils composition of different *Achillea santolina* L. plant parts growing in Algeria Oriental Pharmacy and Experimental Medicine 2018;18: 265-269.
9. Burton GJ, Jauniaux E. Oxidative stress. Best Pract Res Clin Obstet Gynaecol. 2011;25:287-299.
10. Cowan MM. Plant products as antimicrobial agents. Clinical Microbiology Reviews 1999;12:564-582.
11. El-Shazly M, Hafez1 SS, Wink M. Comparative study of the essential oils and extracts of *Achillea fragrantissima* (Forssk.) Sch. Bip. and *Achillea santolina* L. (Asteraceae) from Egypt. Pharmazie 2004;59:226-2230.
12. Esra Birben E, Sahiner UM, Sackesen C, Erzurum S, Kalayci O. Oxidative Stress and Antioxidant Defense. WAO 2012; 5:9-19.
13. Khayyat SA, Roselin S. Recent progress in photochemical reaction on main components of some essential oils. Journal of Saudi Chemical Society. 2018;22:855-875
14. Lanigan RS, Yamarik TA. Final report on the safety assessment of BHT(1). Int J Toxicol 2002;21:19-94.
15. Morongiu B, Piras A, Porcedda S, Casu R, Pierucci P.. Comparative analysis of supercritical CO2 extract and oil of *Pimenta dioica* leaves. J. Essent. Oil Res 2005;17:530-532.
16. Naeem A, Abbas T, Mohsin Ali T, Hasnai A.. Essential Oils: Brief Background and Uses. Annals of Short Reports 2018;1:1-6.
17. Rahimmalek M, Sayed Tabatabaei BE, Etemadi N, Goli SAH, Arzani A, Zeinali H. Essential oil variation among and within six *Achillea* species transferred from different ecological regions in Iran to the field conditions. Ind Crop Prod 2009;29: 348-355.
18. Rassem MHA, Nour AH, Yunus RM. Techniques For Extraction of Essential Oils From Plants: A Review. 2016. Australian Journal of Basic and Applied Sciences 2016;10:117-127.
19. Sonam KS, Guleria S. Synergistic Antioxidant Activity of Natural Products. Annals of Pharmacology and Pharmaceutics 2017;2:1-6.
20. Torres-Martínez R, García-Rodríguez YM, Ríos-Chávez P, Alfredo SA, López-Meza JE, Ochoa-Zarzosa A et al. Antioxidant Activity of the Essential Oil and its Major Terpenes of *Satureja macrostema* (Moc. and Sessé ex Benth.) Briq. Pharmacogn Mag 2017;13:S875-S880.
21. Wink M, HAFEZ SS, El-Shazly AM. Comparative study of the essential oils and extracts of *Achillea fragrantissima* (Forssk.) Sch Bip. and *Achillea santolina* L. (Asteraceae) from Egypt. PHARMAZIE GOVI-VERLAG GMBH 2004;59: 226-230.
22. Yang L, Wen K-S, Ruan X, Zhao YX, Wei F, Wang Q. Response of Plant Secondary Metabolites to Environmental Factors. *Molecules* 2018;23:1-26.

Table 1. Constituents (%) of the essential oil of *Achillea santolina* grown in south Jordan

	tr	KI	Compound	%A
1	4.425	942	α -pinene	0.14
2	4.774	980	Sabinene	0.16
3	4.842	988	β -pinene	0.1
4	4.909	995	yomogi alcohol	0.45
5	5.164	1025	α -terpinene	1.57
6	5.233	1033	p-cymene	1.05
7	5.317	1043	1.8-cineole	4.12
8	5.465	1060	Artemisia ketone	0.33
9	5.515	1066	\square -terpinene	0.97
10	5.65	1082	cis-sabinene hydrate	10.64
11	5.76	1094	Terpinolene	0.45
12	5.868	1107	3-methyl butyl-2-methyl butanoate	0.38
13	5.918	1113	cis-Rose oxide	3.79
14	5.962	1118	trans-thujone	0.61





Jehad Al-Shuneigat et al.

15	6.058	1129	dehydro sabina ketone	1.04
16	6.123	1136	cis-para-meth-2-en-1-ol	1.25
17	6.221	1148	iso-3-thujanol	0.33
18	6.275	1154	trans-para-meth-2-en-1-ol	0.45
19	6.323	1159	trans-chrysanthemol	1.93
20	6.362	1164	Camphor	2.01
21	6.425	1171	iso Borneol	0.29
22	6.486	1178	cis-chrysanthenol	0.87
23	6.538	1184	Pinocarrone	0.82
24	6.6	1191	Borneol	3.74
25	6.645	1197	Terpinen-4-ol	10.6
26	6.759	1208	α -Terpinol	3.97
27	6.917	1224	β -Terpineol	0.35
28	7.359	1268	cis-chrysanthenyl acetate	6.05
29	7.425	1274	trans- Myrtanol	0.15
30	7.564	1288	Bornyl acetate	1.98
31	7.648	1296	Perilla alcohol	0.18
32	7.832	1315	6-hydroxy-carvotan acetone	0.13
33	8.568	1391	E-Jasmone	0.54
34	8.624	1397	B-Longipinene	0.52
35	9.527	1488	Germacrene D	0.2
36	9.641	1499	trans-Muurolo-4(14),5-diene	4.84
37	9.742	1509	β -Amcrphene	0.33
38	9.794	1514	6-methyl-alpha-Ionone	2.23
39	9.974	1532	Zon arene	0.38
40	10.302	1565	Elemol	0.3
41	10.476	1582	caryophyllenyl alcohol	0.31
42	10.681	1606	Spathulenol	3.7
43	10.8	1614	Viyidiflorol	2.03
44	10.851	1619	salvial-4-(14)-en_1_one	0.33
45	10.883	1622	Guaiol	0.35
46	11.019	1636	trans-Arteannuic alcohol	3.2
47	11.158	1650	epi- α -Muurolol	1.17
48	11.247	1659	α -cadinol	4.69
49	11.326	1667	α -Muurolol	1.07
50	11.434	1677	patchouli alcohol	1.87
51	11.477	1682	7-epi- α -Eudesmol	0.69
52	11.519	1686	E-Bisabol-11-ol	1.73
53	11.736	1707	Valeranone	2.75
54	11.815	1714	10-nor-calamenen-10-one	2.36
55	11.958	1727	2Z,6Z-farnesol	0.18
56	12.336	1762	Chamazulene	0.24
57	12.392	1773	Ambroxide	0.15
58	12.475	1782	Z-lanceol	0.17
59	12.92	1817	Drimenol	2.33
60	13.459	1870	cis-9-Hexa decenoic acid heptyl ester	0.44
Monoterpene hydrocarbon				5.05





Jehad Al-Shuneigat et al.

Oxygenated monoterpene	55.47
Sesquiterpene hydrocarbon	6.51
Oxygenated Sesquiterpene	31.61
Ester	0.82
Other	0.54

Table 2. The IC₅₀ antioxidant activity of *Acillea santolina* essential oil and positive controls (ascorbic acid and α-tocopherol) determined by DPPH, ABST and metal ion chelating assays.

Name of plant	IC 50		
	(DPPH)	(APTS)	(Ferrous)
<i>Achillea santolina</i> فيلقولة	0.05641 ± 0.01056	0.07612 ± 0.00776	0.12758 ± 0.01317
α-Tocopherol	0.0023 ± 1.70 * 10 ⁻⁵	0.00177 ± 4.71*10 ⁻⁵	0.00293 ± 2.02 * 10 ⁻⁵
Ascorbic acid	0.00178 ± 2.30 * 10 ⁻⁶	0.00155 ± 4.71 *10 ⁻⁵	0.00189 ± 4.72 * 10 ⁻⁵

The IC₅₀ values were obtained from the generated sigmoidal curves of plotting the mean percentages of scavenging activity vs. logarithmic concentrations of *Acillea santolina* essential oil (in g/ml) using non-linear regression analysis of GraphPad Prism 6 software. The results are expressed as the IC₅₀ values (mg/mL) from three independent experiments performed in triplicates.

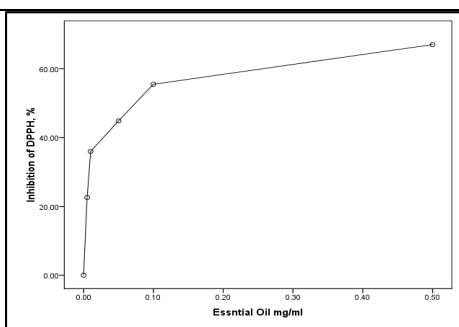


Figure 1. Antioxidant activity DPPH radical scavenging ability of *Acillea santolina* essential oil

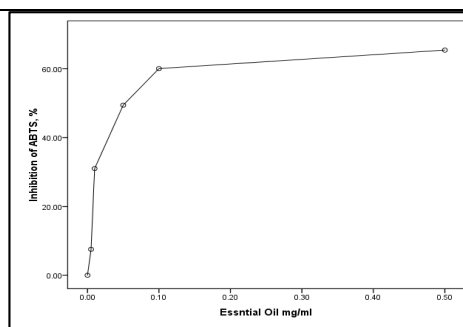


Figure 2. Antioxidant activity ABTS radical scavenging ability of *Acillea santolina* essential oil

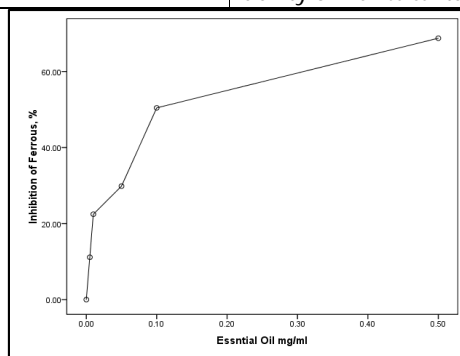


Figure 3. Antioxidant activity ferrous radical scavenging ability of *Acillea santolina* essential oil





Fractures Systems Analysis and Classification in NW Plunge of Surdash Anticline, Sulaimaniya, NE of Iraq.

Summood A.Hussien^{1*}, Manal Sh.Al-Kubaisi¹ and Ghafor A.Hamasur².

Department of Geology, College of Science, Baghdad University, Iraq.

Received: 17 July 2019

Revised: 20 Aug 2019

Accepted: 23 Sep 2019

*Address for Correspondence

Summood A.Hussien

Department of Geology,

College of Science,

Baghdad University, Iraq.

Email: ghna983@gmail.com



This is an Open Access Journal / article distributed under the terms of the **Creative Commons Attribution License** (CC BY-NC-ND 3.0) which permits unrestricted use, distribution, and reproduction in any medium, provided the original work is properly cited. All rights reserved.

ABSTRACT

Sara anticline is part of Surdash anticline which is located in High Folded Zone in Sulaimaniya Governorate, NE Iraq. The fractures systems including (Joint sets, faults and Stylolites) in the study area were studied and their attitudes were reordered. Geometrical classification of the predominant joint sets according to the diagram of Hancock and Atiya, (1979) was performed by using Rocscience Dips v6.008 Software by taking four traverses and 23 stations distributed along these traverses where Kometan and Qamchuqa Formations were exposed to evaluate the predominant types of fractures systems and to calculate their ratings. The dominant shear joint sets are (hko>a, hko>b, hol>c, hkl), okl>c and hol>cless dominant while hol>b joint set type present only in one station (Y6). The wide spread joint type is (hko>a) among the shear joint subsystems with rating about 40.7% while the less dominant is (hol>b) with rating 1.31%. The orthogonal joint are (ac, ab and bc) joint sets (20.02%) with dominant to (ac) type with rating about (14.22%). Different faults types were found. Also, Styloites are present and classified where the non-tectonic type is the predominate type in the study area.

Keywords: Rocscience Dips v6.008, Joint sets, Geometrical analysis.

INTRODUCTION

Fracture is defined as a structure defined by two surfaces or a zone across which a displacement discontinuity occurs (1). Fractures used as a general and scale invariant term for a surface in a material across which there has been loss of continuity (i.e., a discontinuity in displacement) and strength (2). Complex processes are thought to be related to the origin of fractures that are related to geological history of the area. Stresses with diverse origin are responsible for fractures creation, such as: (a) tectonic stresses related to the deformation of rocks; (b) residual stresses due to events that happened long before the fracturing; (c) contraction due to shrinkage because of cooling of magma or





Summoed A.Hussien et al.

desiccation of sediments; (d) Surficial movements such as landslides or movement of glaciers; (e) erosional unloading of deep-seated rocks; and (f) weathering, in which dilation may lead to irregular extension cracks and dissolution may cause widening of cavities, cracks (3). Different types of fractures are present such as (joints ,faults ,stylolite ,foliation ,striation and others (2). In order to classify different fracture types ,the orthogonal tectonic axes (a), (b), and (c) are used in the classification. These axes are geometrically related to the hinge line of the anticline and bedding planes, where axis (a) is perpendicular to the fold hinge line (in the case that the hinge line is horizontal), (b) is parallel to the hinge line and (a) + (b) lies within the plane parallel to the bedding plane, (c) axis is perpendicular to (a-b) plane so it's perpendicular to the bedding plane (4).

Geometrical classification of Joint sets

Joints are surfaces or simple fractures with no displacement or partings in a rock across that do not display any proof of shear movement and they identically occur perpendicular to bedding planes of sedimentary rocks .They have a role in controlling the shape of many spectacular landforms and sub-surface transport of fluids (water and hydrocarbons) (5). 23 stations were selected ,they distributed along 4 traverses named (X,J,Y and Z) extended perpendicular to sub-perpendicular to the fold axis where Z traverse extends in NE limb ,Y and J traverses extend in SW limb , while X traverse extends on both limbs of Surdash anticline as shown in Figure (1). More than 75 readings of attitude of bedding planes and 458 readings of Joint sets were measured and recorded. These measurements were the input data in Rocscience Dips v6.008 software to analyze and classify these joint sets according to the diagram of (6) as in Figure 2. Figures 3,4,5,6,,7,8,9,10,11,12 and shows the results of geometrical analysis and classification of joint sets .

Faults types in the studied area

Fault is a surface or a narrow zone within the earth's crust along that one side has moved relative to the other side in a direction parallel to the surface or the zone, they considered as brittle fracture or a closely spaced shear fracture zones (7). The displacement term means fault two sides relative movement of which is measured in any selected direction. A shear zone is a relatively narrow zone with sub-parallel boundaries in where shear strain is concentrated (8). Minor vertical fault with attitude $252^{\circ}/84^{\circ}$ and vertical displacement about (25) cm was observed in Kometan Formation as shown in figure (14a). Minor reverse fault with attitude $038^{\circ}/80^{\circ}$ that exist in traverse (Z) within Qamchuqa Fn. extends along Wurchach Valley as shown in figure (14) b. Large sinistral strike - slip fault with attitude $130/68^{\circ}$ and rake angle of striation about 8° from SW ,that is transverse (sub-perpendicular) to Sara(Surdash anticline) fold axis and extends a long entire Qamchuqa gorge cutting both Kometan and Qamchuqa Formations of the SW limb with horizontal displacement of about (70)m ,as shown in (15). Another dextral strike-slip fault with dip $075/70^{\circ}$, that is also transverse to Surdash fold axis, cutting Kometan and Qamchuqa of the SW-limb at Jasana-gorge as shown in Figure (16). Sinistral Strike-Slip fault cut the rock mass of limestone of Kometan Formation as shown in Figure (17) .Normal fault that is cut the layers of limestone of Kometan Formation, its attitude $303/52^{\circ}$, as shown in figure (18).

Stylolites

Sylolite in Dukan area within Kometan Formation including the studied area were classified by (9) and divided them into two types according to their origin: Sedimentary (Non tectonic) and tectonic origin. According to (10), Sedimentary Stylolites are usually parallel or sub-parallel to the bedding planes of the sediments.This type of Stylolites are most commonly in the studied area as shown in Figure (19) and extends with the bedding planes of Kometan Formation for several kilometers and sometimes cut by minor faults or joint sets as shown in Figure (20).It





Summoed A.Hussien et al.

is thought to be formed during the diagenetic (compaction) processes as a result to the gravitational loading .They are divided into :Bedding Stylolites formed parallel to the bedding planes and bedding parallel Stylolites formed within the body the sedimentary units not along their bedding planes .

RESULTS AND DISCUSSION

The rating percentage of each type of joint sets in the studied area is determined and the results are as shown in Figure 26. The dominant shear joint sets (hko>a, hko>b, hol>c ,hkl), okl>c and hol>cless dominant while hol>b joint set type present only in one station (Y6) .The wide spread joint type is (hko>a) among the shear joint subsystems with rating about 40.7% while the less dominant is (hol>b) with rating 1.31% . The orthogonal joint (ac,ab and bc) joint sets (20.02%) with dominant to (ac) type with rating about (14.22%),figure (21). Different types of faults are present in the study area like: Normal, reverse and strike-slip faults .Also, Stylolites are present in the study area in both types Tectonic and non-tectonic Stylolites.

CONCLUSIONS

The dominant shear joint sets (hko>a, hko>b, hol>c ,hkl), okl>c and hol>cless dominant while hol>b joint set type present only in one station (Y6) .The wide spread joint type is (hko>a) among the shear joint subsystems with rating about 40.7% while the less dominant is (hol>b) with rating 1.31% . The orthogonal joint (ac,ab and bc) joint sets (20.02%) with dominant to (ac) type with rating about (14.22%). Different types of faults are present such as :normal, reverse and strike slip faults. For the first time a large sinistral strike - slip fault was reordered with attitude 130/68° and rake angle of striation about 8° from SW ,that is transverse (sub-perpendicular) to Surdash anticline fold axis and extends a long entire Qamchuqa gorge cutting both Kometan and Qamchuqa Formations of the SW limb with horizontal displacement of about (70)m. Non-tectonic Stylolites represented by bedding and bedding parallel Stylolites. Tthe tectonic Stylolites are present, too.

REFERENCES

1. Schultz, A.R.and Fossen,H.,2008.Terminology for structural discontinuities .AAPG Bulletin, V. 92, No. 7 , p. 853–867.
2. Van der Pluijm, B. A., and Marshak, S., 2004. Earth Structure: An Introduction to Structural Geology and Tectonics, Second edition, WCB/ McGraw-Hill, USA, 656 P .
3. Singhal, B. B. S. and Gupta, R. P. *Applied Hydrogeology of Fractured Rocks*. Springer Science+Business Media B.V. 2010.p.13-33. DOI 10.1007/978-90-481-8799-7_2.
4. Turner, F.J. and Weiss, L.E. 1963. Structural Analysis of Metamorphic Tectonites. McGraw-Hill book Co. Inc., New York, 545 P.
5. Barno,S.M.J,2014. Structural analysis of Kosrat anticline and its tectonic implications ,Northeastern Iraq .University of Baghdad ,College of Science Unpub. thesis , 199 p.
6. Hancock, P. L., and Atiya, M. S., 1979. Tectonic significance of mesofracture systems associated with the Lebanese segment of the Dead Sea transform fault. *Journal of Structural Geology*, Vol. 1, p. 143 – 153.
7. Twiss ,R.J., & Moores , M. ,2006.*Structural Geology* ,2nd edition,W.H Freeman.763 p .
8. Groshong,H.R,Jr.,2006. 3 D structural geology : A practical guide to quantitative surface and subsurface map interpretation 2 nd edition .Dee Hamner Rd.Northport, USA.400 p .
9. Al-Bassam,S.KH.,&Fouad ,A.F.S,2012.Tectonic classification and geochemical significance of Stylolites in the Kometan formation (Touronian) in Dokan area ,Sulaimaniyah,NE Iraq .IraqiBull.of geology and mining ,Vol.8,No.3.p53-73
10. Ramsey,J.G. and Huber,M.I.,1983.The Techniques of Modren Structural geology .vol.Strain Analysis .Academic Press ,London ,307p.





Summood A.Hussien et al.

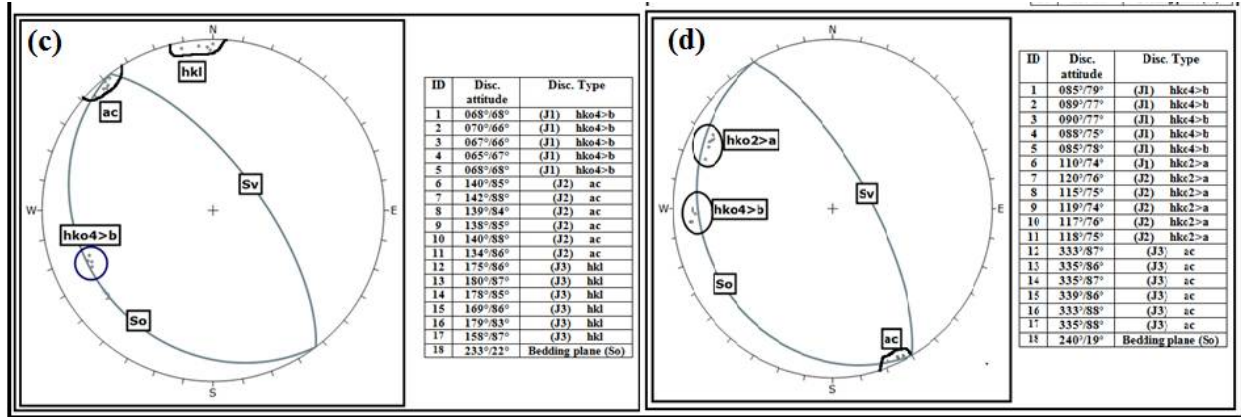


Figure 3. Synoptic joints plane, (a) StationX1,(b) station X2,(c)station X3and (d) station X4 .

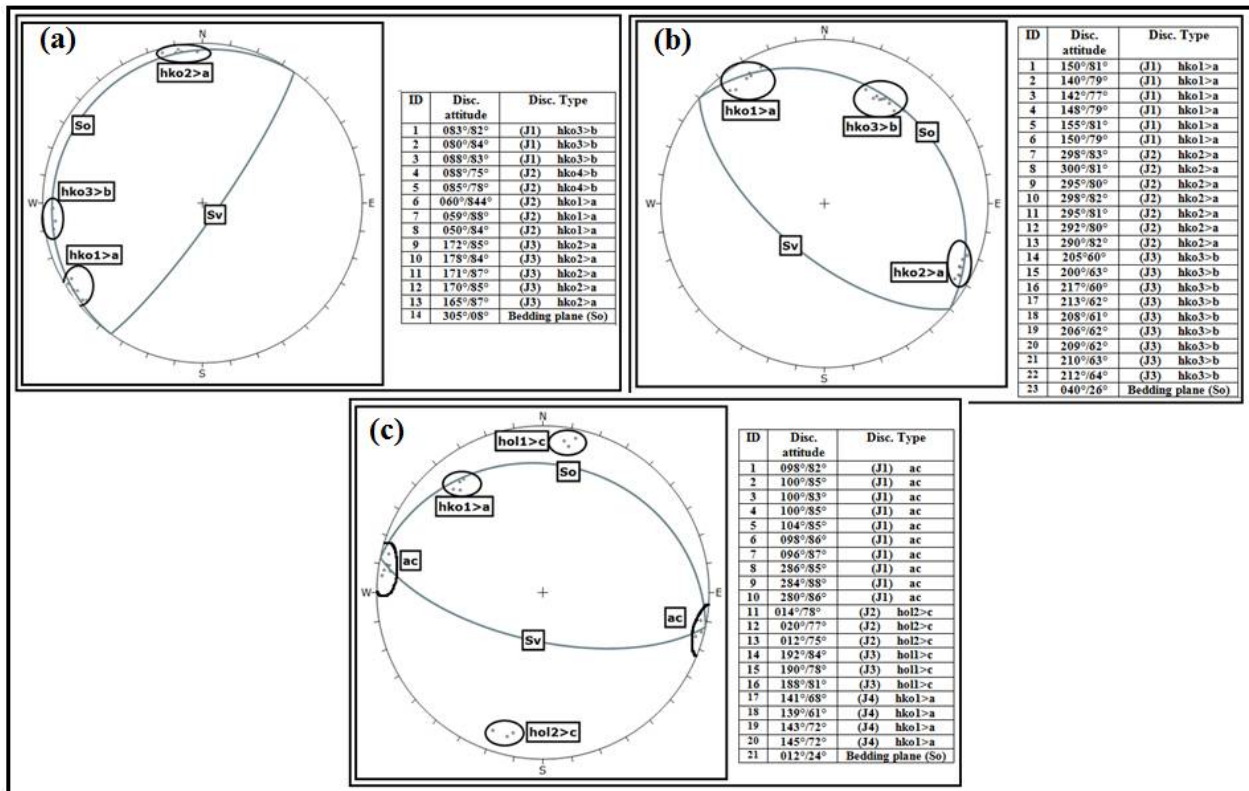


Figure 4. Synoptic joints plane, (a) stationX5, (b) station X6 and (c) station X7



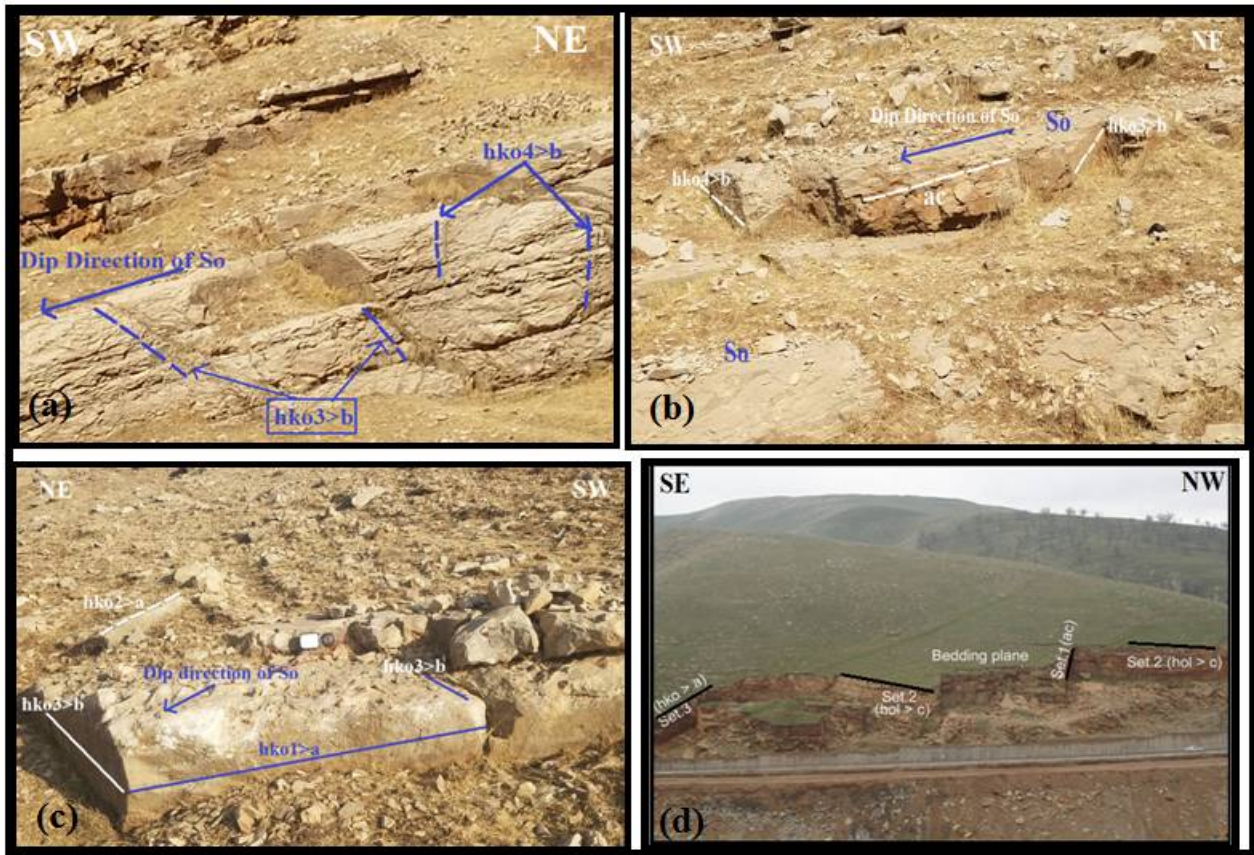
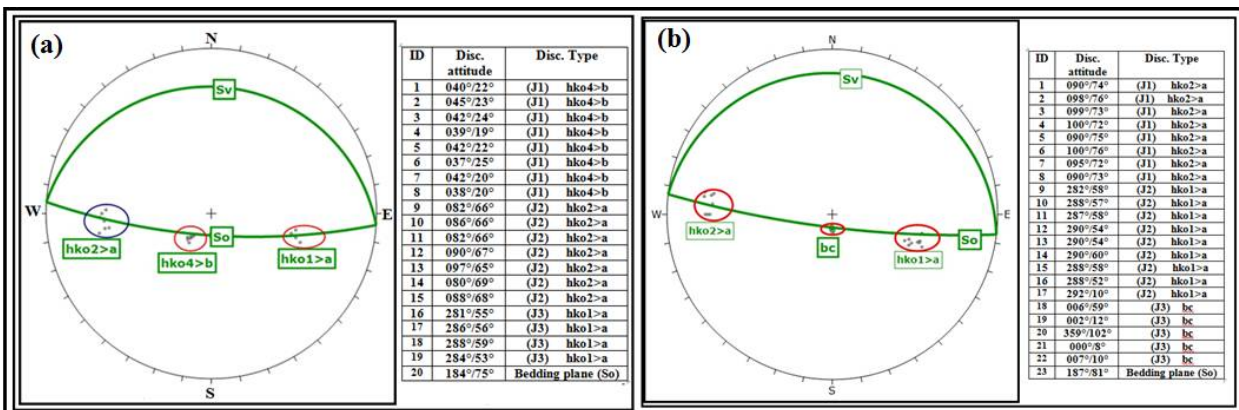


Figure 5. Joint sets types in (a) StationX2, (b) X3,(c)X6 and (d) X7





Summood A.Hussien et al.

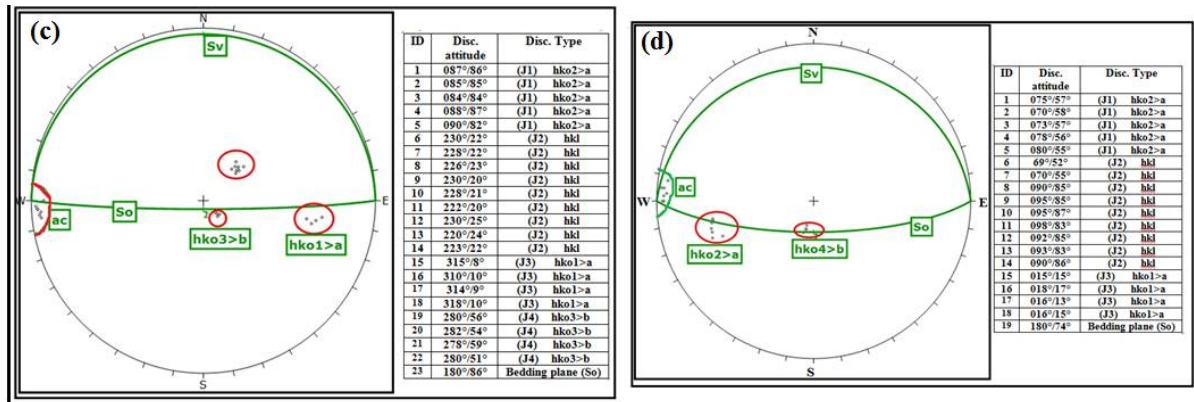


Figure 6. Synoptic joints plane, (a) StationJ1, (b) station J2, (c) station J3 and (d) station J4

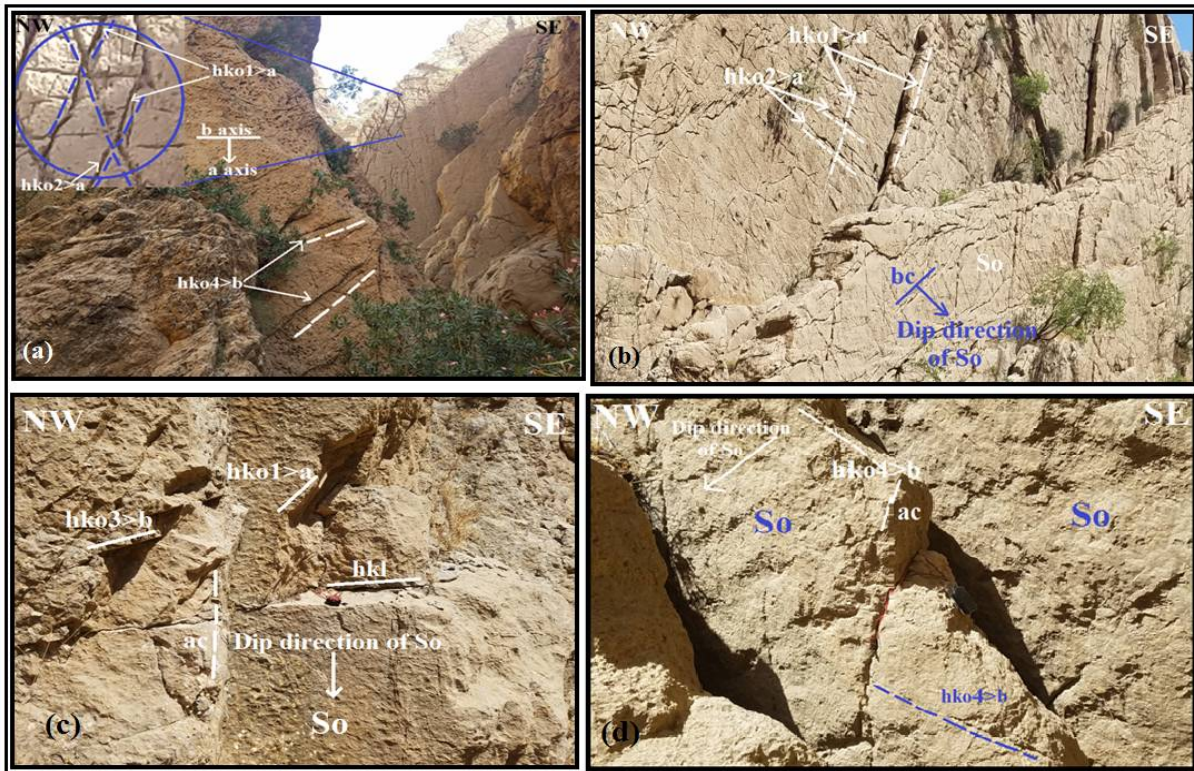


Figure 7. Joint sets types in (a) StationJ1,(b) station J2,(c)station J3and (d) station J4





Summood A.Hussien et al.

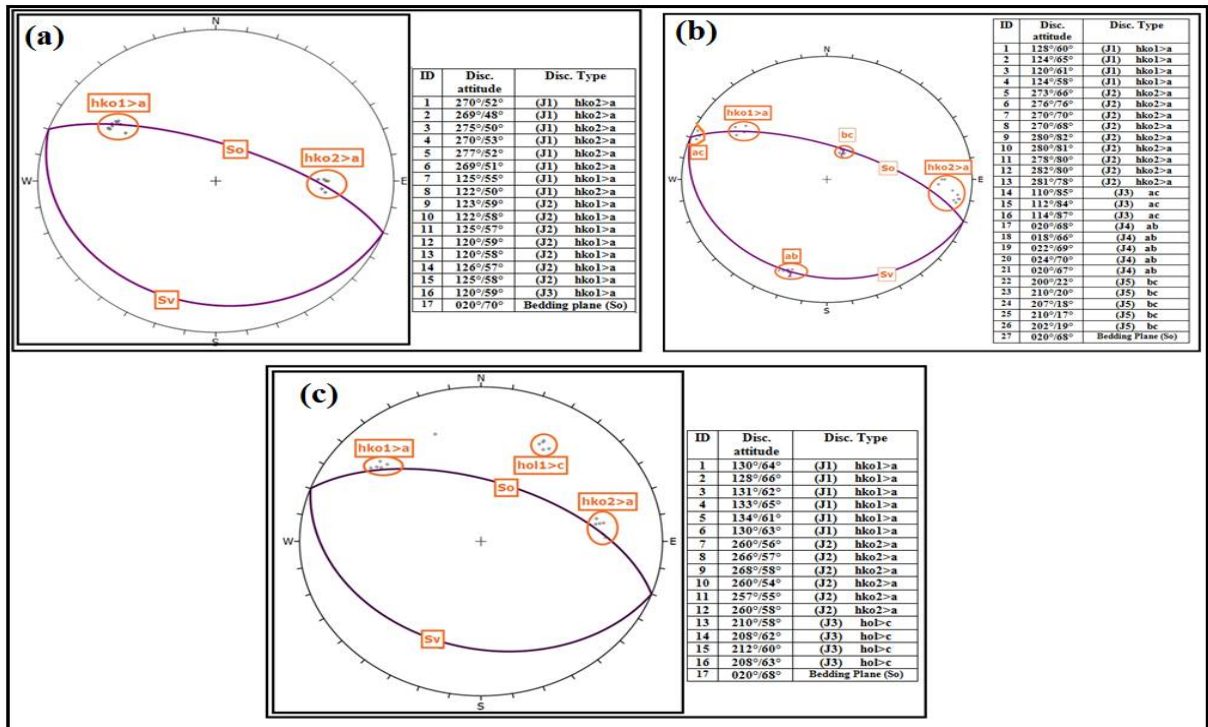


Figure 8. Synoptic joints plane, (a) Station Z1, (b) station Z2, and (c) station Z3

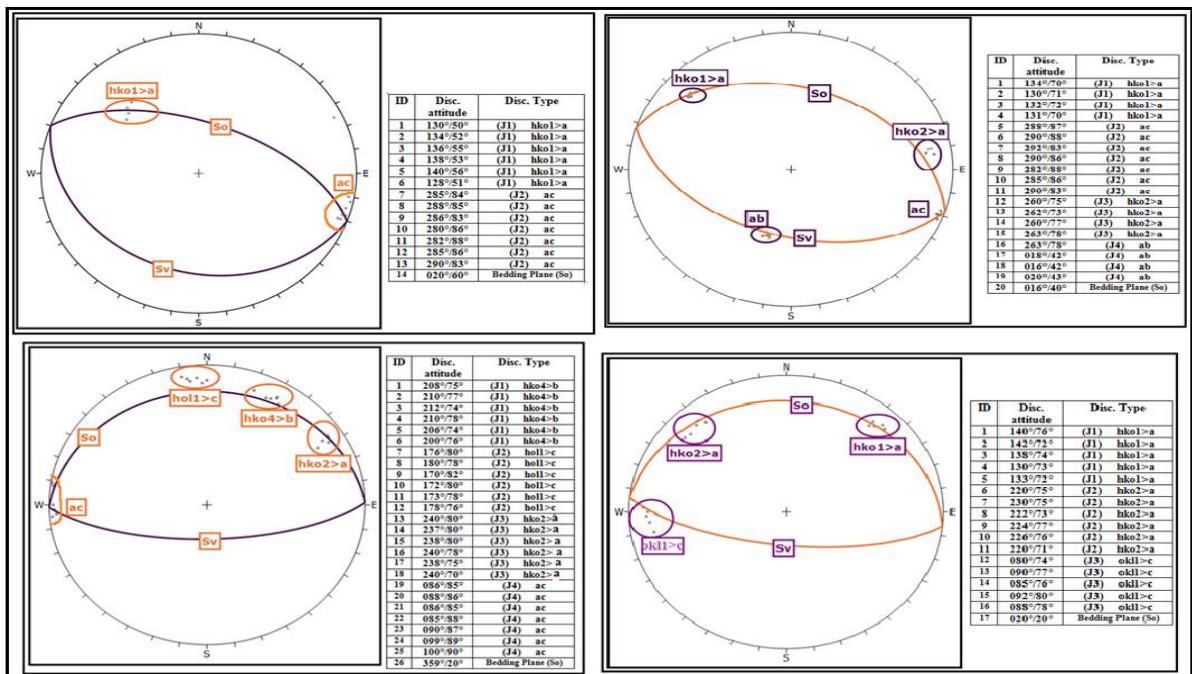


Figure 9. Synoptic joints plane, (a) Station Z4, (b) station Z5, (c) station Z6 and station Z7



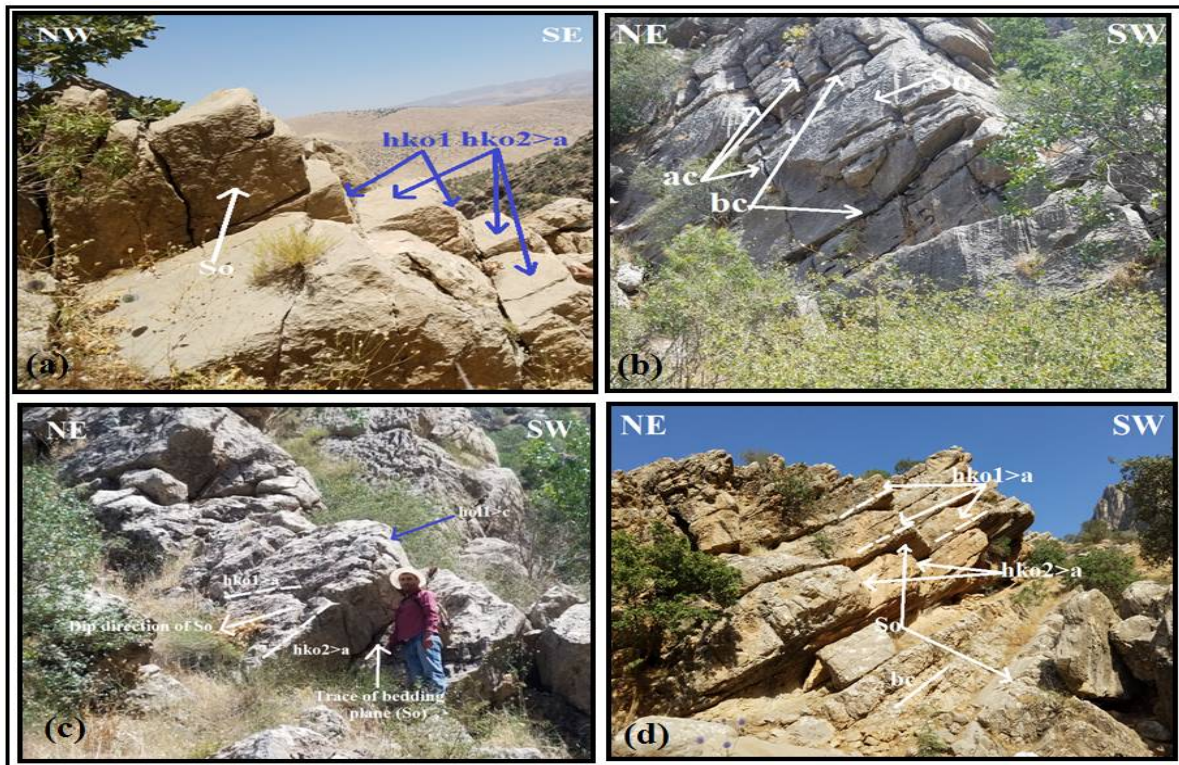


Figure 10. Joint sets types in (a) and (b) Station Z2, (c) station Z3 and (d) station Z5

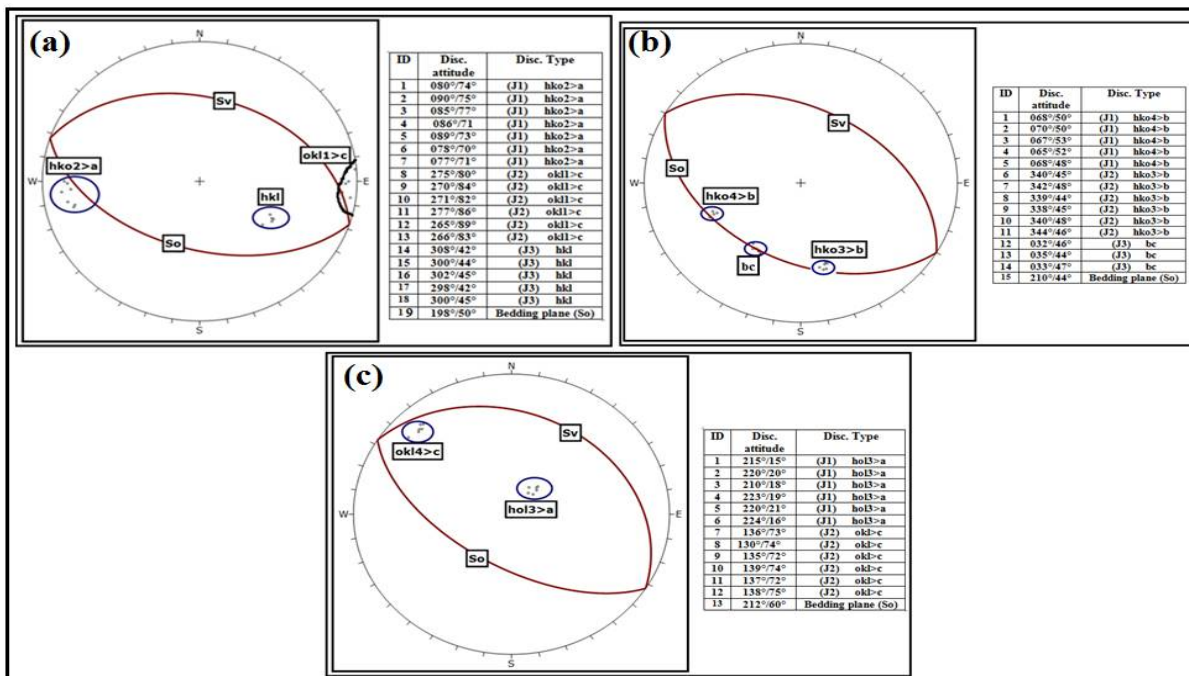


Figure 11. Synoptic joints plane, (a) Station Y1, (b) station Y2 and (c) station Y3





Summoed A.Hussien et al.

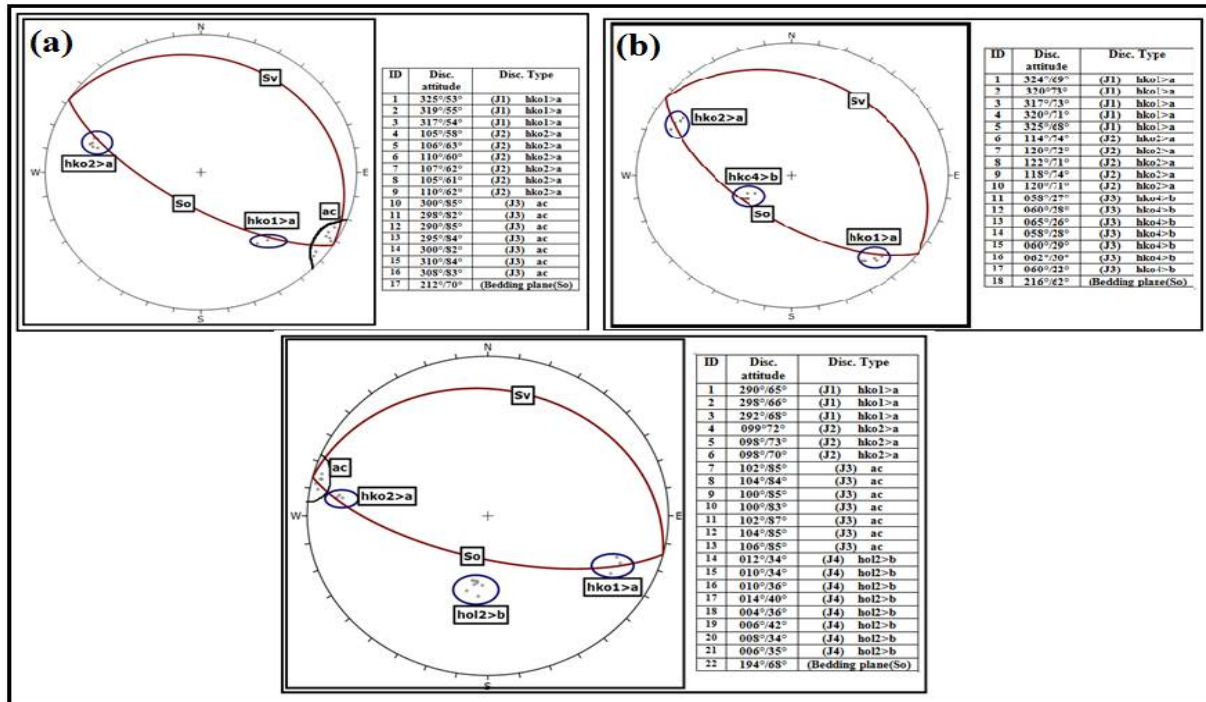


Figure 12. Synoptic joints plane, (a) Station Y4, (b) station Y5 and (c) station Y6.

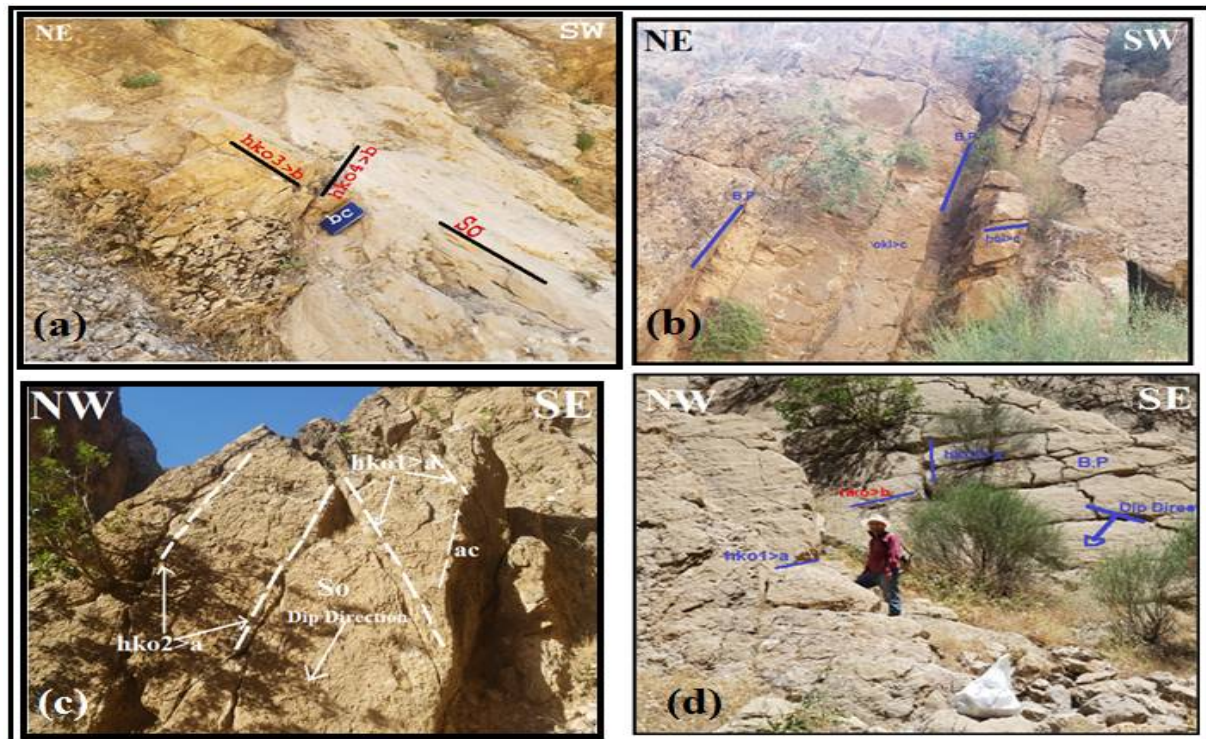


Figure 13. Joint sets types in (a) Y2 (b) Station Y3, (c) station Y4 and (d) station Y5





Figure 14. Shows in (a) the vertical fault in Kometan Formation and (b) reverse fault at at the contact between Kometan and Shiranish formations.



Figure 15. Sinsitral strike-slip fault in Qamachuqa gorge



Figure 16. Satallite image shows the dextral strike-slip fault in Jasana gorge

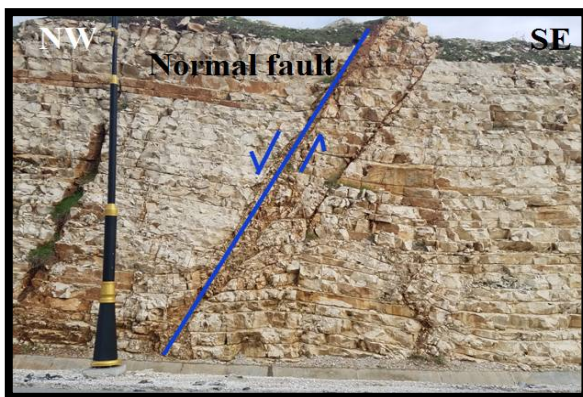


Figure 17. Dextral strike-slip fault within Kometan Formation at the NE limb



Figure 18.e Normal fault within Kometan Formation at the NE limb.





Summood A.Hussien et al.



Figure 19. Non tectonic or Sedimentary type within Kometan at the NE limb.



Figure 20. Tectonic Stylonites within Kometan Fn. at SW limb of Surdash anticline

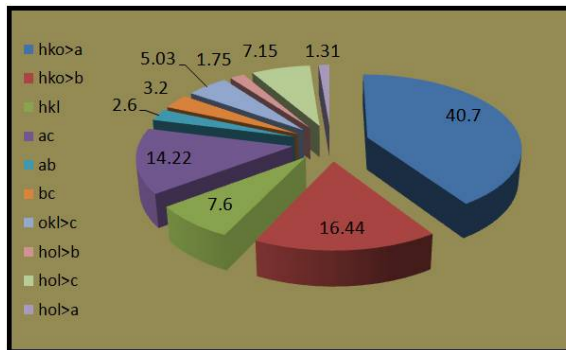


Figure 21. Joints sets rating in the studied area in Surdash anticline





RESEARCH ARTICLE

Analysis of Single Nucleotide Polymorphism in a Quantitative Trait Locus Associated With Host Resistance against Ticks in Vechur and Crossbred Cattle of Kerala.

Bhagyashree M. Kamble^{1*}, C.N.Dinesh¹, P.M.Rojan¹, Reghu Ravindran², K.A.Bindu³, V.N.Muhasin Asaf¹, T.R.Sreeshma¹, T.Deepna¹, K.V.Megnath¹ and Arifa Abdulkhader¹

¹Department of Animal Genetics and Breeding, College of Veterinary and Animal Sciences, Pookode, Wayanad-673 576, Kerala, India.

²Department of Veterinary Parasitology, College of Veterinary and Animal Sciences, Pookode, Wayanad - 673 576, Kerala, India.

³Department of Animal Breeding, Genetics and Biostatistics, College of Veterinary and Animal Sciences, Mannuthy, Thrissur-680 651, Kerala, India.

Received: 18 July 2019

Revised: 21 Aug 2019

Accepted: 23 Sep 2019

*Address for Correspondence

Bhagyashree M.Kamble

Department of Animal Genetics and Breeding,
College of Veterinary and Animal Sciences,
Pookode, Wayanad-673 576, Kerala, India.

Email: kamblebm23@gmail.com



This is an Open Access Journal / article distributed under the terms of the **Creative Commons Attribution License** (CC BY-NC-ND 3.0) which permits unrestricted use, distribution, and reproduction in any medium, provided the original work is properly cited. All rights reserved.

ABSTRACT

The present study aimed to study the singlenucleotide polymorphism in a quantitative trait locus and to find out the allelic and genotypic frequencies in a population of Vechur and crossbred cattle of Kerala state. The quantitative trait locus #101169 was reported to be associated with resistance/susceptibility to tick infestation in cattle. Polymerase Chain Reaction-Restriction Fragment Length Polymorphism technique was used to analyze the single nucleotide polymorphisms 109162468 located in the selected quantitative trait locus. It was found that all the animals under study were monomorphic with CC genotype.

Keywords: cattle, ticks, host resistance, QTL, SNP, PCR-RFLP, Vechur.

INTRODUCTION

Ticks and tick-borne diseases (TTBD) are important risk factors for cattle production which causes enormous economic loss. It mainly affects the bovine production in tropical and subtropical countries such as India, Pakistan and Bangladesh (Ghosh *et al.*, 2007). Tick infestation also results in anemia, stress and irritation, depression of



**Bhagyashree M.Kamble et al.**

immune function and damages to hides and skins. The worldwide economic loss due to TTBDs has been estimated to be approximately US\$20 to US\$30 billion per annum (Lew-Tabor and Valle 2016) and for India the loss was US\$ 498.7 million per annum (Minjauw and Mc Leod, 2003). The conventional measures to control ticks are mainly based on chemical acaricides. However, it is becoming less effective due to the development of acaricide-resistant ticks (Li et al., 2005). Hence, the breeders are increasingly attracted to the idea of selection and breeding of naturally resistant breeds as a solution against tick infestation (Hayward, 1981). It is expected that improvement of host's resistance against ticks provide a cheap, effective, sustainable and environmentally friendly solution to control ticks (Ghosh et al. 2006). Cattle show variation in resistance and susceptibility to tick infestation. Several morphological, physiological and behavioral traits influence the resistance of cattle to ticks. Factors such as sex (Utech and Wharton, 1982, Hughes and Randolph, 2001 and Silva et al., 2010), age (Utech et al. 1978), lactation (Da Silva et al. 2014) and pregnancy (Utech et al. 1978 and Silva et al. 2010) influence the expression of tick resistance. In addition environmental factors like season, temperature, humidity and sunlight play a great role in variation in tick infestation (Kitaoka, 1962, Wharton and Roulston, 1970, Khan et al. 1993 and Urquhart, 1996). Skin thickness and coat characteristics like coat colour, coat type, hair length and hair density influence tick load in cattle (Verissimo et al. 2002, Foster et al. 2007 and Gasparin et al. 2007).

There are also breed differences in host resistance against tick infestation. Generally, *Bos indicus* (*B.indicus*) breeds were found to be significantly more resistant to tick infestation than *Bos taurus* (*B.taurus*) cattle (Kelly, 1932 and Minjauw and Mc Lead, 2003). Hence, a tick control strategy can be devised through crossbreeding Taurus cattle with *B.indicus* breeds and increasing *B.indicus* inheritance in the progeny (Hue et al. 2014). But selection of resistant animals based on tick resistance phenotype using repeated tick counts is difficult, time-consuming and expensive (Henshall et al., 2003) objective measures based on genomics are more desirable than conventional selection procedures. Several studies have identified many quantitative trait loci (QTLs) and single nucleotide polymorphisms (SNPs) that are associated with host resistance to ticks (Gasparin et al. 2007, Machado et al. 2010 and Mapholi et al. 2016). Hence the present study was aimed to identify polymorphisms in the QTL#101169 that was reported to be associated with resistance/susceptibility to tick infestation in cattle.

MATERIALS AND METHODS

The design of this experiment was approved by the Institutional Animal Ethics Committee. Blood samples were collected from 45 Vechur and 74 crossbred cattle from the Kerala Veterinary and Animal Sciences University farms. Genomic DNA was extracted from whole blood using the Wizard® Genomic DNA Purification Kit (Promega Cat. No. A1125) as per the manufacturer's protocol. The quality, concentration and purity of DNA were assessed and DNA working solution was prepared to a final concentration of 25 ng/μL. The QTL #101169 was downloaded from the Animal QTLdb (<https://www.animalgenome.org/cgi-bin/QTLdb/index>) and SNP rs109162468 located in the QTL was used for the polymorphism study by Polymerase Chain Reaction-Restriction Fragment Length Polymorphism (PCR-RFLP) assay. First, the PCR reaction was carried out using custom designed primers in a final volume of 25 μL reaction mixture in 0.2 μL thin PCR tubes. The PCR reaction mix contained: 2 μL genomic DNA working solution, 12.5 μL Emerald Amp GT PCR master mix (Takara Cat. No. RR310A), 10 pM each primer (Forward: 5'-CCCAGTCCTCCTCAACTCAC-3' and Reverse: 5'-GTGTCCGTGAGCTTCTCCTC-3') and nuclease free water to make the volume 25 μL.

The amplification was carried out using the following conditions: initial denaturation at 94°C for 5 min, followed by 30 cycles of denaturation at 94°C for 30 seconds; annealing at 61°C for 30 sec and extension at 72°C for 30 sec and final extension at 72°C for 5 min. The PCR products were resolved in 2 per cent (w/v) submarine horizontal low EEO agarose gel electrophoresis with a 100bp DNA ladder (HiMedia, MBT049-50LN) as marker for verification of specific amplification. The restriction enzyme (RE) digestion of the PCR products was done by using HphI enzyme (New England Bio labs, #R0158S) as per the manufacturer's instruction. The digestion reaction mix contained 2.5 μL of 10X



**Bhagyashree M.Kamble et al.**

RE buffer, one unit of restriction enzyme and approximately 22.3 µL of PCR product. The RE digestion reaction was carried out in 200µL thin PCR tubes by incubating overnight (14 to 16 hrs) at the optimum temperature and then the enzyme was deactivated at the required temperature in a water bath. Next, the digestion products were subjected to 2.5 per cent (w/v) submarine horizontal low EEO agarose gel electrophoresis with 50bp marker (HiMedia Cat. No: MBT084-50LN) and the fragmentation pattern was photographed by a gel documentation system (Fig.1A). The genotype was confirmed by sequencing of the PCR products by M/S AgriGenom Lab Private Limited, Cochin, India by Sanger dideoxy chain termination method. The sequence data were analyzed by FinchTV 1.4 (<https://finchtv.software.informer.com/1.4/>)(Fig.1B). The number of individuals belonging to different genotypes were recorded by direct counting (Falconer and Mackay, 1996). The allelic and genotype frequencies were estimated by POPGENE 1.32 (<https://www.mybiosoftware.com/popgene-1-32-population-genetic-analysis.html>) for the analysis of genetic variation among and within populations.

RESULTS AND DISCUSSION

The PCR-RFLP revealed a single banding pattern of size 303 bp indicating a monomorphic nature for the rs109162468 locus for both Vechur and crossbred cattle. The genotype was confirmed by sequencing (Fig.1A and 1B). All the individuals were CC genotype with frequency equal to one indicating the absence of mutation. This showed the conserved nature of the locus in both Vechur and the crossbred population under study.

ACKNOWLEDGEMENTS

We sincerely thank the Kerala Veterinary and Animal Sciences University and the Kerala State Council for Science, Technology and Environment for funding and facilities provided for conducting this research work.

REFERENCES

1. Ghosh S, Bansal, GC, Gupta SC, Ray D, Khan MQ, Irshad H, *et al.* Status of tick distribution in Bangladesh, India and Pakistan. *Parasitol Res* 2007; 101:207-216.
2. Lew-Tabor AE, Valle MR. A review of reverse vaccinology approaches for the development of vaccines against ticks and tick borne diseases. *TICKS TICK-BORNE DIS* 2016; 7:573-585
3. Minjauw B, McLeod A. Tick-borne diseases and poverty: the impact of ticks and tick-borne diseases on the livelihoods of small-scale and marginal livestock owners in India and eastern and southern Africa. Edinburgh (UK): DFID Animal Health Programme, Centre for Tropical Veterinary Medicine; 2003.
4. Li AY, Davey RB, Miller RJ, George JE. Mode of inheritance of amitraz resistance in a Brazilian strain of the southern cattle tick, *Boophilus microplus* (Acari: Ixodidae). *EXP APPL ACAROL*. 2005; 37:183.
5. Hayward S. Opening address. In: Whitehead GB, Gibson JD, editors. *Tick biology and control*. Grahamstown: Rhodes University; 1981. p xiii–xiv.
6. Ghosh S, Azhahianambi P, de la Fuente J. Control of ticks of ruminants, with special emphasis on livestock farming systems in India: present and future possibilities for integrated control—a review. *EXP APPL ACAROL* 2006; 40:49-66.
7. Utech KBW, Wharton RH. Breeding for resistance to *Boophilus microplus* in Australian Illawarra Shorthorn and Brahman x Australian Illawarra Shorthorn cattle. *Aust Vet J* 1982; 58:41-46.
8. Hughes VL, Randolph SE. Testosterone depresses innate and acquired resistance to ticks in natural rodent hosts: a force for aggregated distributions of parasites. *J Parasitol* 2001; 87:49-54.
9. Silva AM, Alencar MM, Regitano LCA, Oliveira MCS. Infestação natural de fêmeas bovinas de corte por ectoparasitas na região sudeste do Brasil. *Rev Soc Bras Zoot* 2010; 39:1477-1482.





Bhagyashree M.Kamble et al.

10. UtechKBW, SeifertGW, Wharton RH. Breeding Australian Illawarra Shorthorn cattle for resistance to *Boophilus microplus*. I. Factors affecting resistance. Aust J Agric Res 1978; 29:411-422.
11. Da Silva JB, Rangel CP, de Azevedo Baeta B, Da Fonseca, AH. Analysis of the risk factors relating to cows' resistance to *Rhipicephalus microplus* ticks during the peripartum. EXP APPL ACAROL2014; 63:551-557.
12. Kitaoka S. Physiological and ecological studies on some ticks. VIII. Diurnal and nocturnal changes in feeding activity during the blood-sucking process of *Haemaphysalis bispinosa*. Natl InstAnim Health Q (Yatabe) 1962; 2:106-111.
13. Wharton RH, Roulston WJ. Resistance of ticks to chemicals. Annu Rev Entomol 1970; 15:381-404.
14. Khan MN, Hayar CS, Iqbal Z, Hayat B. Prevalence of ticks on livestock in Faisalabad (Pakistan). Pak Vet J 1993; 13:182-182.
15. Urquhart GM, Armour J, Duncan JL, Dunn AM, Jennings FW. Veterinary Parasitology. 2nd ed. Oxford (UK): Blackwell Science; 1996.
16. Verissimo CJ, Nicolau CVJ, Cardoso VL, Pinheiro MG. Haircoat characteristics and tick infestation on Gyr (Zebu) and crossbred (Holstein x Gyr) cattle. Arch Zootec 2002; 51:389-392.
17. Foster A, Jackson A, D'Alterio GL. Skin diseases of South American camelids. In Pract 2007; 29:216.
18. Gasparin G, Miyata MLL, Coutinho LL, Martinez ML, Teodoro RL, Furlong J, et al. Mapping of quantitative trait loci controlling tick [*Rhipicephalus (Boophilus) microplus*] resistance on bovine chromosomes 5, 7 and 14. Anim Genet 2007; 38: 453- 459.
19. Kelley, RB. Zebu (Brahman) cross cattle and their possibilities in north Australia. Pamphlet no. 27. Rockhampton (Qld): Council Scient and Indust Research; 1932.
20. Dicker RW, Barlow R. Measurement of bush tick infestation in Hereford and first cross heifers. In Proceedings of the Australian Association of Animal Breeding and Genetics 1979; 1:169-171.
21. Hùe T, Hurlin JC, Teurlai M, Naves M. Comparison of tick resistance of crossbred Senepol x Limousin to purebred Limousin cattle. TROP ANIM HEALTH PRO 2014; 46:447-453.
22. Henshall J, Prayaga KC, Burrow HM. Covariance structures for modeling repeated tick counts in beef cattle. In 'Proceeding of 5th conference of Association for the Advancement of Animal Breeding and Genetics 2003:119-122.
23. Machado MA, Azevedo ALS, Teodoro RL, Pires MA, Peixoto MGCD., de Freitas C, et al. Genome wide scan for quantitative trait loci affecting tick resistance in cattle (*Bos taurus* x *Bos indicus*). BMC Genomics 2010; 11: 280-291.
24. Mapholi NO, Maiwashe A, Matika O, Riggio V, Bishop SC, MacNeil MD, et al. Genome-wide association study of tick resistance in South African Nguni cattle. TICKS TICK-BORNE DIS 2016; 7:487-497.
25. Falconer DS, Mackay TFC. Introduction to Quantitative Genetics. 4th ed. Essex: Prentice Hall; 1996.

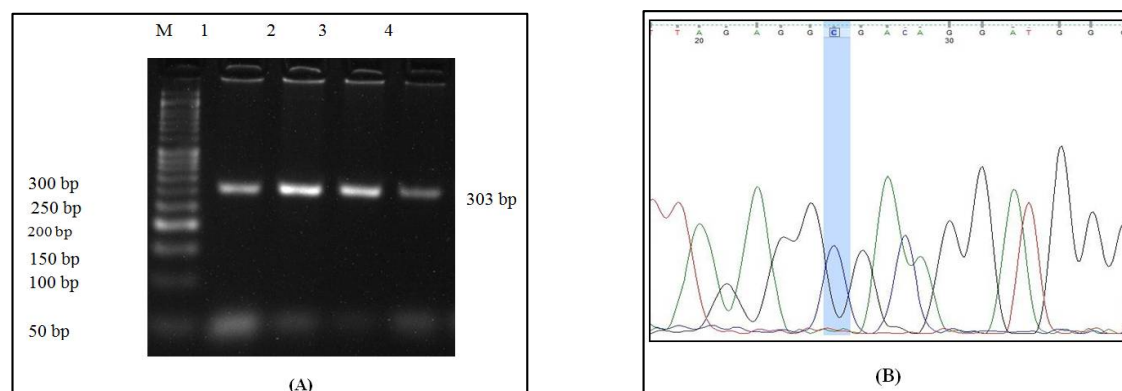


Fig 1. Study of genetic polymorphism at SNP rs109162468 of QTL# 101169. Representative photograph of PCR-RFLP results is shown here. The SNP locus was not polymorphic in the population under study. Sample numbers are given on the top of the gel and fragment sizes are shown on the right side. M- Himedia 50 bp DNA ladder marker, 2.5 % agarose gel at 125 V for 3 hrs (A). Chromatogram confirming the CC genotype (B)





Biological Activities of Hydroxyapatite / Titania Porous Ceramic Prepared by Polymeric Sponge Method

Sara H. Shahatha*, Ali A. Taha and Mudthafer A. Mohammad

Applied Sciences Department, University of Technology, Baghdad, Iraq.

Received: 14 July 2019

Revised: 16 Aug 2019

Accepted: 19 Sep 2019

*Address for Correspondence

Sara H. Shahatha

Applied Sciences Department,

University of Technology,

Baghdad, Iraq.

Email: sarahamid_91@yahoo.com



This is an Open Access Journal / article distributed under the terms of the **Creative Commons Attribution License** (CC BY-NC-ND 3.0) which permits unrestricted use, distribution, and reproduction in any medium, provided the original work is properly cited. All rights reserved.

ABSTRACT

Hydroxyapatite is widely used in medical applications as bone replacement due to its biocompatibility and similarity to natural bone component. In this study, HAp powder was synthesis by solid state methods. Porous HAp and Titanium dioxide scaffolds were prepared by polymeric sponge methods with solid loading of 55% of HAp and 5 to 25% of Titania. The loaded sponges were evacuated under vacuum of 10^{-1} Torr and fired to 1250°C. The biological properties of HAp/ TiO₂ samples are highly hemocompatible material, anti- bacteria, anti-biofilm formation and have the potential to regenerate the cells. The hemolysis activity of HAp/TiO₂ the highest value was 4.96%, while the composite revealed low bacterial adhesion was 0.123 against *E. Coli* at 25°C. Furthermore, anti-biofilm activity of HAp/TiO₂ against *P. auroginosa* was 0.838. On the other hand, 25µg/ml of composite showed high ability to enhance the lymphocytes viability (945%), as normal cells, when compared to the viability of L20B cell line (894%), as cancer cells.

Keywords: Hydroxyapatite, Titanium dioxide, Polymeric sponge method, biofilm, Hemolysis, cells viability, bacteria adhesion.

INTRODUCTION

Hydroxyapatite HAp, Ca₁₀(PO₄)₆(OH)₂ is one of the inorganic minerals that existed in human bone. It has many applications in orthopedics and dental implants due to its great bioactivity" (1). Moreover, commercial hydroxyapatite shows very low porosity and it cannot be utilized effectively for "adsorption based biomedical applications, especially drug delivery, protein and nucleic acid fractionation" (2). Lately, replication technique has been showed to be a promising and efficient technique due to its potential in manufacturing HAp/ TiO₂ porous scaffolds with "high porosity, excellent interconnections between the macropores and similar pore shape with that of spongy bone" (3). It





Sara H. Shahatha et al.

has been notified that HAp/ TiO₂ can be a good mixer of mechanical properties for bioactivity (4). Because of their "high specific strength and excellent corrosion resistance" (5). Titania are amongst the most successful ceramic oxides "biomaterials for orthopedic and dental applications". TiO₂ also shows good permeability and high biocompatibility, serving to improve the cell vitality (6). Executing of the (HAp/ TiO₂) composites material in a living body rely on a number of factors: "stability of the HA structure, which is influenced by the fabrication method of the implant materials, sintering process these are the most important manufacturing steps which determines mostly of the final properties of the ceramic and their behavior in service" (7). Hemolysis, describe as the "release of hemoglobin into plasma due to damage of erythrocytes membranes", was determined by the method given by Singh and Ray (8).

Hemocompatibility is a necessary study to be done prior to the employment of hydroxyapatite in blood. When blood is in touch "with non-hemocompatible material, it causes the activation of coagulation and immune system in human body which may threaten a patient's life". Yet, it is necessary to study the behavior hemocompatibility study particularly hemolysis test on the HAp/ TiO₂ to include the safety of patients (9). The goals of this work was to develop new method to create HAp based biocomposites starting from tri calcium phosphate and calcium hydroxide by solid state reaction and reinforce it with Titania powder to create a bioceramic composite and study its biological properties.

MATERIALS AND METHODS

Synthesis of Hydroxyapatite/ Titania Porous Composite

In this study, the fabrication of high porous HAp/ TiO₂ biocompatibility ceramic foam was done. Initially HAp powder was produced by solid state synthesis the starting material that have been used were commercial tricalcium phosphate (Himedia, India) and calcium hydroxide, Ca(OH)₂ (Himedia, India), the powders mixed in 3:2 molar ratio and were mechanically dispersed in de-ionized water to solid loading 55%, after that adding TiO₂ 5, 10, 15, 20, 25 wt% from the total solid loading, 4% PVA (poly vinyl alcohol) as a binder and magnetic stirring for 2 hours until the PVA dissolve and the slurry is ready for the dipping process, these slips having pH=12. Polymeric sponges that used each cut into a dimension of 1 cm³. The sponges were squeezed by hands then put in a bell jar and evacuated to 10⁻¹ Torr to remove the trapped air and make sure that the sponge is fully saturated with the slurry. Any excess slurry was extracted by squeezing the template through a roller. The loaded samples were dried in microwave oven for 10 to 25 minute according to thickness of solid loading. The Samples were sintered at "1250 °C with heating rate of 5 °C/min", three hours of soaking time.

Hemolysis Assay

Hemolysis assay was done established on the experiment study (10) with some modification. In brief, 200 µl of the detached blood was diluted with 1600 µl normal saline. 200 µl of different concentration of HAp/TiO₂ (2, 4, 6, 8, 10 mg/ml) were added to this diluted blood among with controls. Furthermore, Distilled water was utilized as positive control (100% lysis) and normal saline as negative control (0% lysis). The sample were incubated in 37 °C for 1 h and then "centrifuged at (2000 rpm) for 5 min. The absorbance was measured at 541 nm by UV- Vis spectrophotometer and the percentage of hemolysis was computes using the following relationship":-

$$\text{Percentage of hemolysis (\%)} = \frac{(B_h - B_n)}{(B_p - B_n)} \dots \dots \dots (1)$$

Where B_h, B_n and B_p are "the absorbance of the hydroxyapatite, negative and positive controls, respectively. The experiments were performed using fresh blood from healthy donors".





Sara H. Shahatha et al.

Cytotoxicity Assay Cells Culturing

Cancer cell line L20B (mouse Fibroblast L cells) and Lymphocytes line (Human cells) were obtained from Central General Health Laboratory and Biotechnology research center / University of Al Nahrain, Baghdad/ Iraq. The cells suspended in Minimum Essential Media (MEM) after incubation in CO₂ incubator overnight at 37 °C. The MEM media discharged and phosphate buffer saline was added for washing. For cells detachment, Trypsin-EDTA was added for (1-2) min then discharged. Then, the cells re-suspended MEM medium includes 10% Fetal Bovine Serum (FBS). The results was determined by Eliza at (620 nm).

MTT Assay

Cell viability determined MTT assay , by adding 100µl of each cell lines suspensions in microtiter plate wells and incubated at 37 °C in CO₂ incubator overnight. Then, HAP+ Titania with different "concentration (6.25, 12.5, 25, 50 and 100 mg/ml)" was added to the wells and incubated in CO₂ incubator. After incubation overnight, media and composites particles were discharged from microtiter plate and one hundred microliters of "MTT [3-(4, 5dimethylthiazol-2)-2,5diphenyltetrazolium bromide] was added to each well". After 1h incubation, 100 µl of dimethyl sulfoxide were added to each well. The results were read by automated plate reader at 620nm.

Bacterial Adhesion Assay

The adhesion tests were done by dispensing 200 µL of bacterial suspensions (from microbiology labs. in the University of Technology) in 96 well microtiter plate. "The time of attach for the adhesion test was 4 h, and each test was done under different temperatures: 35 °C (no temperature shift relating to growth temperature in brain heart medium), 25 °C and 4 °C during the 4 h of adhesion assay". The quantification of bacterial adhesion was done by the crystal violet staining method according to Rodrigues et al (11). The unattached cells were "removed by washing the wells three times with water. The adherent microorganisms were fixed with 200 µL of methanol for 15 min. The wells were then stained for 15 min with 200 µL crystal violet (1% w/v aqueous solution), rinsed under the running tap water". The bound dye was resolubilized with 200 µL of glacial acetic acid (33%, v/v) and the "optical density of each well was measured by an automated plate reader at 630 nm". The same procedure was done for biofilm Assay except the time of incubation was 24 hrs instead of 4 hrs and the bacteria was *P. aeruginosa* only.

Anti -Bio Film Test

Concentrations of (6.25, 12.5, 25, 50 and 100 mg /ml) of HAP+ Titania has been prepared in DW. Add immediately 10 µl from each concentration to single well in the microplate that includes 180 µl of BHI broth and inoculated with 10 µl of overnight *P. aeruginosa* culture. After incubation for 24 h at 37 °C , the contents of plate was removed and washed 4 times with DW (pH = 7) to remove free bacteria . Bacterial biofilms were fixed by "95% ethanol and stained with 0.1% (w/v) crystal violet. Rinsed off 5 times with DW to remove excess stain and kept to dry. Then, add 200 µl of 33% glacial acetic acid to each well and read after 15 minutes by microplate reader at 630 nm". The absorbance considered the value of bacterial adhesion on the surface of nanoparticles and biofilm formation. Average of doubled reads of each concentration were calculated. This technique was done according to the references (12) with some modifications.



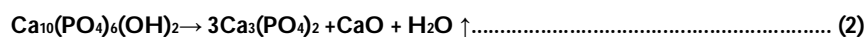


Sara H. Shahatha et al.

RESULTS AND DISCUSSION

Analysis of XRD Patterns for HAp/ TiO₂

Fig.1 show the XRD analysis, the “phase composition” of the composites with 25 wt. % titanium oxide showed the existence of “HAp, α -TCP, β -TCP, rutile (TiO₂) and perovskite (CaTiO₃)” as determined by XRD at sintering temperature 1250 °C. The next equation has been suggested to calculate the decomposition of HAp when it is sintered at high temperatures (13):-



Furthermore, Titanium oxide is a “chemically stable” material with transformation from “anatase to rutile” at temperatures ranging between (450 and 950 °C) [14]. Yet, the formation of “CaTiO₃” suggest that the reaction between (HAp and Titania) has done through thermal treatment. The next chemical reaction is proposed:-



In accord with stage compositions it is clear that “CaTiO₃” is a result of the reaction “sintering process” that done between “TiO₂ and CaO”, which is one of the decomposition materials of HAp (Eq. (2)). Increasing the amount of Titania leads to a higher concentration of “CaTiO₃” in the composite and the existence of β -TCP is obvious, which leads to that part of α -TCP has transformed to β -TCP. According to the results, the reactivity of Titania with HAp is very high, leading to the disassociation of the majority of the HAp phase, forming Ca₃(PO₄)₂ during the reaction.

Morphological Characterization

Representative optical and SEM pictures of HAp/TiO₂ samples sintered at 1250°C are respectively showed in Figs. 2&3. A high densification regime is suggested after sintering at 1250°C which showed that the sintering process almost complete and subsequently grain growth occurred at temperature 1250°C with no decomposing of HAp to Tri calcium phosphate. Furthermore TiO₂ particles were well merged with the hydroxyapatite matrix and causes formation of glassy phase. We can point out that the evolution of microstructure and crystalline phases observed at sintering temperature of 1250°C and for hydroxyapatite glass ceramic doped with 25 wt% TiO₂ particles.

Hemolysis Test

The percentage of hemolysis of the (HAp and the composites) specimens is shown in Fig 4. The increase in “concentration from (2 to 10 mg/ml) cause significant change in the percentage of hemolysis of the samples. The percentage of hemolysis of the samples at all concentrations is less than (4.96%). By indicate to the (ASTM F 756 00 standard), the specimens with percentage of hemolysis less than 5 % is a highly hemocompatible and safe biomaterial” (15). There is difference in the percentage of hemolysis for concentration (8 and 10 mg/ml) but still consider as highly hemocompatible according to the standard. Also this highly hemocompatible attributed to the addition of Ca(OH)₂ and TCP both of these materials are highly biocompatible beside that the reinforcing materials are biocompatible as well suggesting that solid state reaction does not impact the hemocompatibility of the specimens.

Cytotoxicity Test

Lyomyosarcoma (L20B-mouse Fibroblast L cells) and (lymphocyte-Human cells) have been used and handle with different concentrations of (HAp/ titania) particles ranging from (6.25 to 100mg/ml), and the viability was analyzed





Sara H. Shahatha et al.

by the MTT assay (MTT assay defined as colorimetric method depends on metabolism of living cells The tetrazolium dye reduced by cytoplasmic enzymes, NAD(P)H (oxidoreductase enzymes), which has the ability to reduce tetrazolium dye to a purple colored insoluble formazan) (16). The viability of (HAp/ composites) against (L20B-mouse Fibroblast L cells) and (Lymphocyte-Human cells) growth were determined by growth inhibition values determined by Equation (4) through tetrazolium dye absorption values:-

$$\text{Cell viability (\%)} = \frac{\text{total viable cells (unstained)}}{\text{total cells counted (stained \& unstained)}} \times 100 \dots \dots \dots (4)$$

From Fig (5) it has been found out the highest value (HAp/TiO₂) the highest value for Lymphocytes is (945%) and the lowest value is (290%) while in L20B the highest value is (894%), and the lowest is (270%). Cell proliferation in response to various concentrations of particles showed in the culture media was analyzed by the MTT assay. There were changes in the cell viability at lower concentrations and as the concentration increased, cell viability increased. In comparison with the control group (Lymphocytes) cells cultured in medium containing (HAp and the composites) for 24 h showed an increased in viability. The differences in cell viability with various concentration materials is given in Fig (7) upon increasing the amount of doped, the value of doping materials in the HAp particles increases. This guides to the decrease in the particle size. Take in consideration the results of MTT assay, "it is evident that cell survival was highly rely on the extract concentration, while it was just slightly rely on the particle size showing the cytotoxicity increase with the extract concentration, caused mainly by the decrease in pH after HAp degradation to TCP and CaO" (17).

Bacterial Adhesion Test

The bacterial adhesion assay of *E. coli*, *P. aeruginosa* and *S. aureus* under various incubation temperatures (4, 25, 37 °C) were determined by crystal violet test. High adhesion of *E. coli*, on HAp/ TiO₂ particles, was observed among examined bacteria at 4, 25 and 37 °C within 4 hrs of incubation. From Fig 6, it has been found out that in HAp the highest value of bacteria adhesion is (0.084) for *E. coli* when the temperature was (4 °C) this value increases when the temperature is (25 °C) to (0.123) for *S. aureus* and then decreases to (0.097) for *S. aureus* when the temperature is (37°C), while in HAp/TiO₂ composite the adhesion value was (0.148) for *S. aureus* when the temperature is (4 °C) then decreases to (0.139) is also for *S. aureus* when the temperature is (25 °C) then increases to (0.168) for *S. aureus* when the temperature is (37 °C).

The differences of the results attributed to surface topography which is porous nature of the mineral deposit can impact by the term of bacterial adhesions (18). "Surface topography of a scale comparable with microbial cell with dimensions (about 1–2 μm) was seen as a crucial and positive contributing factor to bacteria-surface interaction and bacterial attachment. A clear pattern of bacterial attachment was seen when the spatial distance of an array of surface posts approached the size of some Gram-negative and Gram-positive microorganisms: *P. aeruginosa*, *E. coli* and *S. aureus*". Also some materials are naturally prostrate to bacterial adherence due to their chemical or physical characteristics. "Basically this seems to be the case with some porous bioceramics utilized in bone tissue engineering that act as three-dimensional porous scaffolds for natural bone ingrowth. The rough and porous surface configuration needed for the ingrowth offers such surface irregularities also to allow bacterial colonization".

In biological view Lectins are involved in the bacterial adhesion process (19), and 4 hrs of incubation was enough to promot alternations in the bacterial surface properties (20), carbohydrate-binding proteins represented by (Lectins) represent as a specific class which is differ from enzymes and antibodies, which are contained in various organisms and are responsible for cell-cell interactions (21). By attaching the *E. coli* to abiotic surfaces the compositions of proteins in the outer membrane are altered, while fimbriae play a function in nonspecific adhesion. By attaching the *E. coli* to abiotic surfaces the compositions of proteins in the outer membrane are altered, while fimbriae play a role in nonspecific adhesion (22). On the other hand the main reason to reduce the bacteria adhesion is calcium hydroxide





Sara H. Shahatha et al.

act as an antibacterial effect as long as a high pH is preserved (23) as we mention earlier in chapter two. Bystrom et al. (24) reported that “in vivo study that root canals treated with $\text{Ca}(\text{OH})_2$ had fewer bacteria than other biomaterials. They attributed this to the fact that Ca (OH) could be packed into the root canal system allowing hydroxyl ions to be released over time”.

Biofilm Assay

The biofilm assay of *P. aeruginosa* under incubation temperatures of 4, 25, 37 °C were determined. From Fig 7, it found out that (HAp/titania) the higher value is (0.838) and the lowest value is (0.660) but all the values was under control so it was a successful test and that because antimicrobial potential of $\text{Ca}(\text{OH})_2$ on biofilms, at first the expression biofilm was came in to “designate the thin layered condensations of microbes that may occur on various surface structures in nature (25). Free-floating bacteria existing in an aqueous environment, the so-called planktonic form of microorganisms, are a prerequisite for biofilm formation (26). Biofilms may thus become founded on any organic or inorganic surface substrate where planktonic microorganisms prevail in a water-based solution” (27). This results agree with Sathiskumar et al. (28). The generated composites by biowaste to create HAp validated biophysical techniques showed effective biofilm inhibitory.

CONCLUSION

Porous ceramic of HAp/ TiO_2 had been successfully prepared by polymeric sponge method. The porosity ratio and microstructure could be enhanced by controlling titania ratio and rheological properties, while the characterizations referred to the novel biomaterial composite. On the other hand, the hemolysis test explained that the HAp/ TiO_2 specimens are highly hemocompatible material and have a potential to regenerate the cells. Furthermore, the generated composites by solid state reactions showed effective to reduce bacterial adhesion and biofilm inhibitory. Overall, this study introduces HAp/ TiO_2 porous ceramic composites as promised candidate for bone replacement and regeneration.

REFERENCES

1. E. Mohseni, E. Zalnezhad, A.R. Bushroa, 2014. International Journal of Adhesion & Adhesives 48 , 238–257.
2. W K Cheah, K Ishikawa, R Othman, F Y Yeoh , 2017. Nanoporous biomaterials for uremic toxin adsorption in artificial kidney systems: A review. J Biomed Mater Res B 105(5): 1232-1240.
3. A.Manonukul, M. Tange, P. Srikudvien, N. Denmud, P. Wattanapornphan, 2014. Rheological properties of commercially pure titanium slurry for metallic foam production using replica impregnation method, Powder Technol. 266 , 129–134.
4. Ravarian R, Moztarzadeh F, Solati Hashjin M, Rabiee SM, Khoshakhlagh P, Tahriri M. 2010. Synthesis, characterization and bioactivity investigation of bioglass/hydroxyapatite composite. Ceram Int; 36:291-7.
5. Ye, H., Liu, X.Y., Hong, H., Characterization of sintered titanium/hydroxyapatite biocomposite using FTIR spectroscopy. J. Mater. Sci.: Mater. Med. 20, 843–850, (2009).
6. Fidancevska, E., Ruseska, G., Bossert, J., Lin, Y.M., Boccaccini, A.R., 2017. Fabrication and characterization of porous bioceramic composites based on hydroxyapatite and titania, Mater. Chem. Phys. 103, 95–100.
7. Cornelia Marinescu, Ancuta Sofronia, Elena M. Anghel, Radu Baies, Daniel Constantin, Ana-Maria Seciu, Oana Gingu, Speranta Tanasescu, 2017. “Microstructure, stability and biocompatibility of hydroxyapatite - titania nanocomposites formed by two step sintering process”, Arabian Journal of Chemistry.
8. Singh DK, Graft AK. 1994. Graft copolymerization of 2-hydroxymethacrylate onto chitosan film and their blood compatibility. J. Appl. Polym. Sci.: 53:1115–1121.
9. UTSeifert, VBiehl, J Schenk, 2002. In vitro hemocompatibility testing of biomaterials according to the ISO 10993-4. Biomol Eng 19(2-6): 91-96.



**Sara H. Shahatha et al.**

10. S Jadalannagari, KDeshmukh, SRRamanan, MKowshik. 2014. Antimicrobial activity of hemocompatible silver doped hydroxyapatite nanoparticles synthesized by modified sol–gel technique. *Appl Nanoscience* 4(2): 133-141.
11. Rodrigues LR, Banat MI, van Der Mei HC, Teixeira JA, Oliveira R. 2006. Interference in adhesion of bacteria and yeasts isolated from explanted voice prostheses to silicone rubber by rhamnolipid biosurfactants. *J Appl Microbiol*; 100: 470-480.
12. Mohammad Hassani Sangani, Mahboobeh Nakhaei Moghaddam and Mohammad Mahdi Forghanifard, 2014. Inhibitory effect of zinc oxide nanoparticles on pseudomonas aeruginosa biofilm formation. *Nanomed J*, Vol. 2, No. 2.
13. M.Ogiso,Y.Yamashita,T. Matsumoto, 1998. Differences in microstructural characteristics of dense HA and HA coating. *J. Biomed. Mater. Res.* 41, 296.
14. S.J. Scheider, *Engineering Materials Handbook*, 1991. vol. 4, Ceramics and Glasses, ASM International, The Materials Information Society, Materials Park, OH, USA.
15. G Radha, S Balakumar, B Venkatesan, E Vellaichamy, 2015. Evaluation of hemocompatibility and in vitro immersion on microwave-assisted hydroxyapatite–alumina nanocomposites. *Mater Sci Eng C-Mater* 50: 143-150.
16. Takuya Junior Matsumotoa, Sang-Hyun Ana, Takuya Ishimoto, Takayoshi Nakanob, Takuya Matsumotoa, Satoshi Imazato, 2011. *Dental materials* 27, e205–e212.
17. Karadzic I, Vucic V, Jokanovic V, Debeljak-Martacic J, Markovic D, Petrovic S, et al. 2014. Effects of novel hydroxyapatite-based 3D biomaterials on proliferation and osteoblastic differentiation of mesenchymal stem cells. *J Biomed Mater Res A.*; 103:350–357.
18. Rizzello, L., Galeone, A., Vecchio, G., Brunetti, V., Sabella, S., and Pompa, P. P. , 2012. Molecular response of *Escherichia coli* adhering onto nanoscale topography. *Nanoscale Res. Lett.* 7:575.
19. Piconi, C and Maccauro, G , 1991. Zirconia as a ceramic biomaterial" *Biomaterials*, Vol 20 (1): p 1-25.
20. 146. Zeraik, A.E., and Nitschke, M., 2012. Influence of growth media and temperature on bacterial adhesion to polystyrene surfaces. *Brazilian Archives of Biology and Technology*, 55 (4).
21. Tielker, D., Hacker, S., Loris, R., Strathmann, M., Wingender, J., Wilhelm, S., Rosenau, F. and Jaeger, K., 2005. *Pseudomonas aeruginosa* lectin LecB is located in the outer membrane and is involved in biofilm formation. *Microbiology*, 151 (5).
22. Otto, K., Norbeck, J., Larsson, T., Karlsson, K. and Hermansson, M., 2001. Adhesion of type 1-fimbriated *Escherichia coli* to abiotic surfaces leads to altered composition of outer membrane proteins. *Journal of bacteriology*, 183 (8).
23. Siqueira JF, Lopes HP, 1999. Mechanisms of antimicrobial activity of calcium hydroxide: a critical review. *International Endodontic Journal* 32, 361–9.
24. Byström A, Claesson R, Sundqvist G, 1985. The antibacterial effect of camphorated paramonochlorophenol, camphorated phenol, and calcium hydroxide in the treatment of infected root canals. *Endodontics & Dental Traumatology* 1, 170–5.
25. Svensater G, Bergenholtz G, 2004. Biofilms in endodontic infections. *Endodontic Topics* 9, 27–36.
26. Pameijer CH, Stanley HR, 1998. The disastrous effects of the "total etch" technique in vital pulp capping in primates. *American Journal of Dentistry* 11, S45–54.
27. Stoodley LH, Costerton JW, Stoodley P, 2004. Bacterial biofilms: from the natural environment to infectious diseases. *Nature Reviews Microbiology* 2, 95–108.
28. Swamiappan Sathiskumar, Sekar Vanaraj, Devaraj Sabarinathan, Kathirvel Preethi, 2018. "Materials Research Express".





Sara H. Shahatha et al.

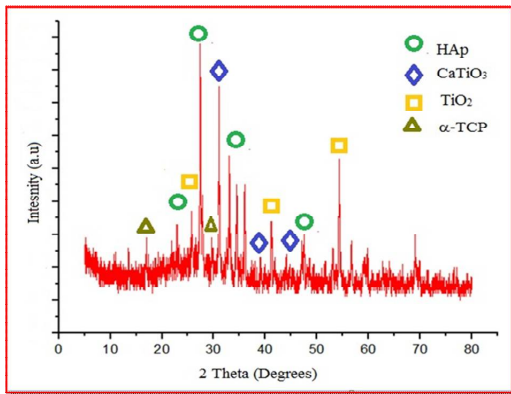


Fig. 1. XRD patterns of HAp/ TiO₂ powder sintered at 1250°C.



Fig. 2. Optical micrograph of polymeric foam.

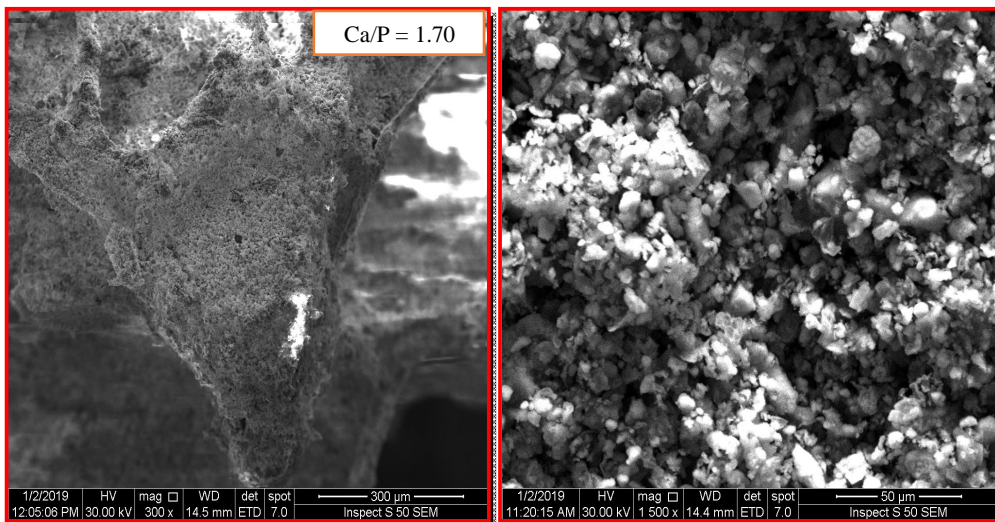


Fig. 3. SEM image of hydroxyapatite/TiO₂ porous ceramic sintered at 1250 °C

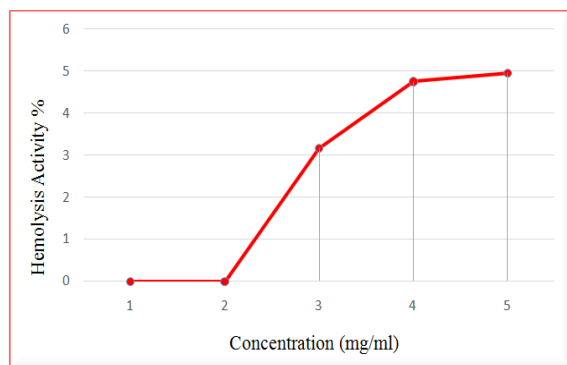


Fig. 4. Hemolysis activity of HAp/TiO₂.

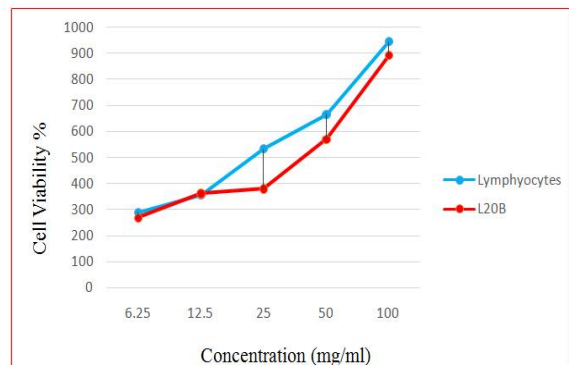
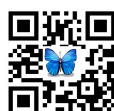


Fig. 5. Cells viability at different concentrations of HAp/TiO₂.





Sara H. Shahatha et al.

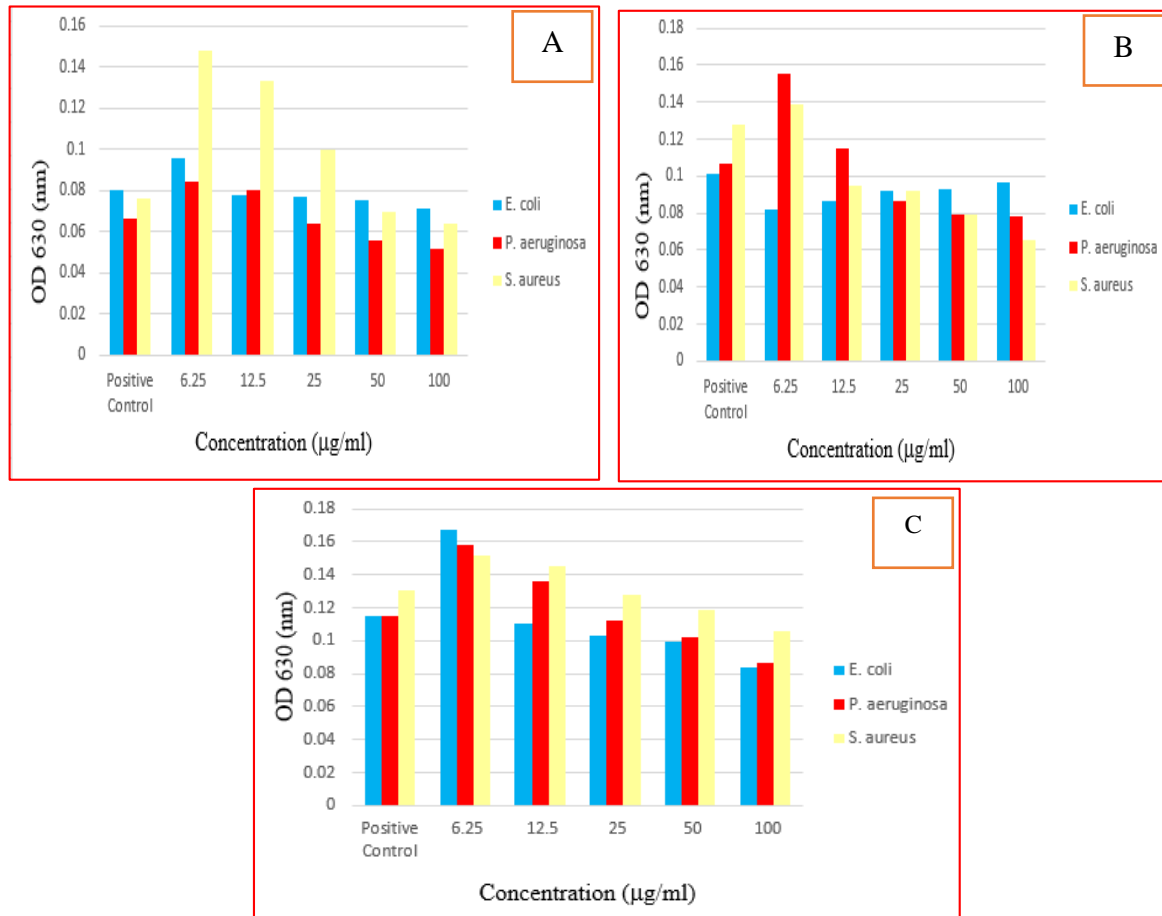


Fig. 6. Determination of bacterial adhesion on different concentrations of Hap/ TiO₂ particles under different incubation temperatures for 4 hrs, A: at 4°C, B: at 25°C, C: at 37°C

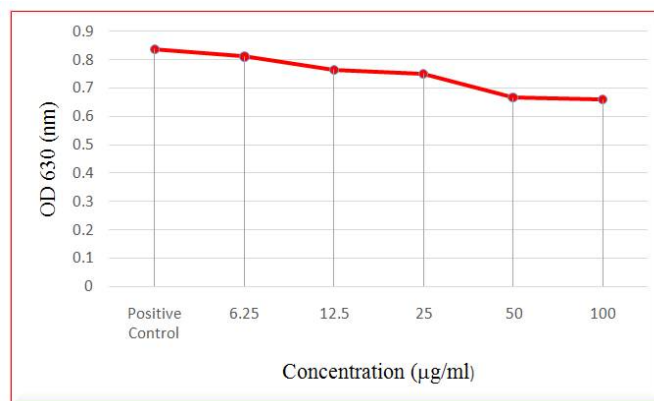
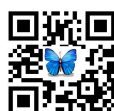


Fig. 7. Anti- Biofilm effect of Hap/ TiO₂ particles against *P. aeruginosa* at 37°C.





Studies on Assessing the Extent of Pond Water Pollution in Muthupettai Block, Thiruvarur District, Tamil Nadu

M.P.Sugumaran* and S.Sangeetha

Department of Environmental Sciences, AC & RI, Coimbatore, 641 003, TamilNadu, India.

Received: 17 July 2019

Revised: 22 Aug 2019

Accepted: 26 Sep 2019

*Address for Correspondence

M.P.Sugumaran

Department of Environmental Sciences,
AC&RI, Coimbatore, 641 003,
TamilNadu, India.

Email: Sugumar.ens@gmail.com



This is an Open Access Journal / article distributed under the terms of the **Creative Commons Attribution License** (CC BY-NC-ND 3.0) which permits unrestricted use, distribution, and reproduction in any medium, provided the original work is properly cited. All rights reserved.

ABSTRACT

The study was aimed to make an assessment of health risk due to pollution and assessing the impact of discharges from the sewage contamination on the Pattukkottai town. Samples were collected from ponds of Pattukkottai block, in Thanjavur District during Feb'12, Mar'12, Apr' 12 & May' 12. The physico chemical characteristics like pH, EC, Colour, Odour, Total Dissolved salts (TDS), Dissolved Oxygen (DO), Biological Oxygen Demand (BOD), Chemical Oxygen Demand (COD), Hardness, Acidity, Alkalinity and Chloride were analysed. The water samples were collected during hours from 8 to 11 a.m.during winter and Summer Seasons. Then the important water quality parameter *E.coli* and the availability and diversity of Phytoplankton and Zoo plankton were analysed. The results revealed that in all the samples of pond water, microbial contamination of *E.coli* showed positive so, the results revealed that the pond waters were not fit for drinking purpose. Through biological studies revealed that the water available in the area is under recommended limits for human use, it is unsafe on account of poor microbiological quality of pond water in this area. The Most Prable Number (MPN) test results revealed that the P5 pond water *E.coli* was present high (127 MPN/100ml) in the month of April compared to other pond water samples. In general the untreated sewage water and domestic wastes contaminates all the ponds in Pattukkottai block and they were unfit for use.

Keywords: *E.coli*, contamination, Phytoplankton, Pattukkottai, pond water.

INTRODUCTION

Pattukkottai is a town and a municipality in Thanjavur district in the Indian state of Tamil Nadu. Pattukkottai is located at 10.43° N 79.32°E. It is a peaceful town situated in the Cauvery delta and comes under the Tropical Dry Evergreen Forest region. It receives maximum rainfall during winter months as it lies along the Coromandel Coast of





Sugumaran and Sangeetha

South India. It has an average elevation of 5 metres (16 feet) and city lies in Thanjavur District in the State of Tamil Nadu, It is one of the Divisional Head Quarters of all Departments, 48 Km from Thanjavur. In Pattukkottai, as like any other sub urban town, five ponds are mostly affected by sewage water and agricultural runoff. All ponds are surrounded by temples, agricultural fields, and human settlements. There is a solid waste dumping site on fringe of the ponds. Now this study area is merged in the Pattukkottai Municipal Corporation limits. The upper catchment area of the ponds includes rural and agricultural areas. The inlet and outlet of the ponds are open. The runoff in the monsoon and sewage from the area are disposed into the ponds, as there is no proper sewage collection and disposal system. The overflow from the pond flows into nearby open channel and is ultimately disposed into river without any treatment. Locals are not using the pond water for drinking, washing or bathing and cattle washing. Pond is totally infested with *Eichhornia* sp. The main body of the pond remains full of water and is perennial. Apart from *Eichhornia* sp, there is tremendous load of phytoplankton in the pond due to the addition of organic matter. Though there are programmes on algal blooms throughout the country, research is not ample in these areas.

MATERIALS AND METHODS

Study area and collection of water samples

The ponds were monitored seasonally in the year of Feb'2012 – June'2012. The samples were collected in the month of February'12, March'12, April'12 & June'12 representing winter and summer season respectively. The samples were collected in the morning between 8 am- 10 am. The pond water is used for bathing the cattle's and construction purpose. During rainy season the pond overflows and emits noxious smell. All ponds are located at the temples about 1-2 km. from Pattukkottai Bus stand. Water samples were collected from 5 sampling points of pond in Pattukkottai block (Fig.1). The samples were collected in clean polythene bottles without any air bubbles. The bottles were rinsed before sampling and tightly sealed after collection and labeled in the field. A total of 5 water samples from pond used by people of Pattukkottai city were collected in clean polythene bottles and brought to the laboratory. The samples were chemically preserved by the addition of 3 - 5 ml concentrated HNO_3 per litre of the sample.

Collection, preservation and analysis of water samples were carried out following the Standard reference (APHA, 1998). The water samples were analysed for various physico-chemical parameters, biological parameters and bacterial density as well as diversity. Analysis was carried out for various water physico-chemical parameters such as pH, total solids, Total Dissolved solids (TDS), total hardness (TH), total alkalinity, calcium, chloride and chemical oxygen demand (COD) by using standard methods. pH was measured using standard pH meter, total solids (TS), total dissolved solids (TDS) by standard methods, calcium content by EDTA titrimetric method, chloride content by argentometric method, Total hardness was calculated by complexometric titration using EDTA, methyl orange alkalinity and chemical oxygen demand (COD) by open reflux method.

RESULTS AND DISCUSSION

The water samples collected from the five ponds located in Pattukkottai were Kasankulam, MattuchandaiKulam, Kottaikulam, NadiyamankovilKulam, AyyanarkovilKulam (Table.2). EC Values indicate the presence of high contents of dissolved salts in water (Abdullah & Mustafa, 1999). EC Values ranges from (P1) 0.6 dSm^{-1} in winter & 0.65 in summer, (P2) 0.5 dSm^{-1} in winter & 0.72 dSm^{-1} in summer, (P3) 0.8 dSm^{-1} in winter & 0.65 in summer, (P4) 0.75 dSm^{-1} in winter & 1.15 in summer, (P5) 0.6 dSm^{-1} in winter & 0.8 dSm^{-1} in summer (Table. 1). The total alkalinity values ranged from (P1) 1740 mg/1 (Winter) to 1752 mg/1 (Summer), (P2) 1920 mg/1 (Winter) to 1920 mg/1 (Summer), (P3) 3860 mg/1 (Winter) to 3920 mg/1 (Summer), (P4) 3440 mg/1 (Winter) to 3653 mg/1 (Summer) & (P5) 3900 mg/1 (Winter) to 3960 mg/1 (Summer). The values in monsoon or winter may be due to the dilution of the pond water with rain water.



**Sugumaran and Sangeetha**

The acidity values ranged from (P1) 1380 mg/l (winter) to 1386 mg/l (Summer), (P2) 1200 mg/l (Winter) to 1310 mg/l, (P3) 1210 mg/l (Winter) to 1236 mg/l (Summer), (P4) 1016 mg/l (Winter) to 1152 mg/l (Summer) & (P5) 1322 mg/l (Winter) to 145 mg/l (Summer). According to WHO 1991 Standard (100 – 500 mg/l) and basic permissible limits (Table. 1), the values found in summer are very high. Water hardness up to 60 mg/l are considered as soft water, from 61 – 120 mg/l considered as moderately hard water, from 121 – 180 mg/l as hard water and above 180 mg/l very hard water (Kannan, 1991). The values found in the present study are in the ranges of 90 mg/l to 240 mg/l which fall in the category of moderately hard water and very hard water, which is not useful for drinking purpose.

The TDS results were gradually increased from winter to summer and it ranges from (P1) 430 mg/l to 466 mg/l, (P2) 300 mg/l to 475 mg/l, (P3) 380 mg/l to 480 mg/l, (P4) 560 mg/l to 740 mg/l & (P5) 360 mg/l to 480 mg/l respectively. The lower values in the winter / monsoon may be due to dilution of pond water by rain water. The higher values in the following seasons may be due to continuous inflow of sewage without any dilution by rain water. The same fashion followed in the results of Suspended Solids (SS). The values show lower concentration in monsoon and higher concentration in summer. This high level of TDS values may be due to high salt content and also renders it unsuitable for irrigation. DO indicates the water quality in terms of various macro as well as microphytes. In the present study the maximum DO value of (P1) 2.6 mg/l was observed in the month of March, (P2) 2.9 mg/l in the month of April, (P3) 5.9 mg/l in the month of May, (P4) 9.6 mg/l in the month of Feb. & March, and (P5) 5.9 mg/l in the month of May '12 were observed. In present study the BOD levels in the sampling points of (P4) & (P5) are higher than the permissible limit. (Shobana, 2008). In current study the COD values in the sampling points of (P4) & (P5) are higher than the permissible limit of CPCB (250 mg/l) viz., 309 mg/l (P4), 258 mg/l (P5) during the month of February. Sewage disposal in natural waters is a common practice among many nations. Large inputs of organic matter and nutrients from raw sewage to a weak hydrodynamic environment poses environmental and health problems by deterioration of water quality (Rajagopalan, 2005). Inadequate or faulty sewerage and/ of sewage treatment system are major causes of pollution in natural waters.

CONCLUSION

Because of presence of various pathogenic bacteria and toxic Cyanobacteria like *Anacystis* sp., the pond is not useful for any purpose like drinking, washing and bathing. By proper treatment and management of the pond this area can be converted into recreation centre. The adjacent pond with controlled growth of *Eicchornia* sp. has a potential for development as habitation for many birds, as it has already dense canopies of trees in the centre of the pond. The area needs appropriate drainage system so that the sewage can be disposed at a place other than the pond. This will help in restoring the natural aquatic ecosystem of the pond. The good pond ecosystem will reduce the health hazards like epidemic of cholera and dysentery. Dredging has to be carried out to remove the organic wastes settling at the bottom of the pond.

REFERENCES

1. American Public Health Association (1995) Standard methods for examination of water and wastewater. 19th edition. American Public Health Association, Washington, D.C.USA.
2. Kannan K (1991). Fundamentals of environmental pollution. S Chand and Company Ltd New Delhi.
3. Rajagopalan. V., 2005. Status of Sewage treatment in India. Central Pollution Control Board.
- a. Shobana, J. 2008. Degradation of sewage waste water, biabsorption of heavy metals – copper and zinc and anatomical study of affected parts of aquatic plants, water hyacinth- *Eicchornia* sp. B.Sc., Dissertation, University of Madras.
4. WHO 1991 – Guidelines for drinking water quality 2nd edition; Geneva vol.I, p.56





Sugumaran and Sangeetha

Table 1. Physico-Chemical and Biological analysis of Pond water

Physico chemical parameters	Kasankulam		Mattuchandai Kulam		Kottaikulam		Nadiyamman kovilKulam		AyyanarkovilKulam	
	Feb.12	May.12	Feb.12	May.12	Feb.12	May.12	Feb.12	May.12	Feb.12	May.12
pH	7.16	7.05	7.82	7.32	7.35	7.16	8.47	8.03	7.87	7.42
EC dSm ⁻¹	0.60	0.65	0.50	0.72	0.80	0.65	0.75	1.15	0.60	0.80
TDS mg L ⁻¹	430.00	466.00	300.00	475.00	380.00	482.00	560.00	740.00	360.00	486.00
Acidity mg L ⁻¹	1380.00	1386.00	1200.00	1340.00	1210.00	1236.00	1016.00	1152.00	1322.00	1450.00
Alkalinity mg L ⁻¹	1740.00	1752.00	1920.00	1920.00	3860.00	3920.00	3440.00	3653.00	3900.00	3960.00
Calcium mg L ⁻¹	90.00	145.00	126.00	172.00	140.00	170.00	220.00	240.00	142.00	176.00
Magnesium mg L ⁻¹	410.00	416.00	140.00	172.00	170.00	175.00	240.00	240.00	170.00	236.00
DO mg L ⁻¹	2.00	2.40	2.20	2.60	5.60	5.90	9.60	6.10	5.00	5.90
BOD mg L ⁻¹	8.13	8.06	12.00	12.10	27.80	27.85	35.10	35.50	30.80	30.00
COD mg L ⁻¹	140.00	138.00	185.00	180.60	140.00	144.10	309.00	290.25	258.00	285.50
Chlorides mg L ⁻¹	142.00	148.00	99.26	126.00	113.40	134.00	184.30	199.20	148.80	184.60
Coliforms	17.00	33.00	11.00	31.00	31.00	63.00	45.00	98.00	112.00	117.00

Table 2. Descriptions of Sampling Locations

SAMPLE NO	LOCATION	BRIEF DESCRIPTION
P1	Kasankulam	Pond is located at om sakhthikovil. Pond water is used for bathing and construction purposes. (surface area 3 Ha)
P2	Mattuchandaikulam	Pond receives sewage contaminations. During rainy season the pond over flows and emits noxious smell.
P3	Kottaikulam	Pond situated in the bypass of Thanjavur road.
P4	Nadiyamankovilkulam	Pond is located at Nadiyamman kovil.150 families were living around the pond.
P5	Ayyanarkovilkulam	Pond is located at Ayyanarkovil on the way of Rameswaram road. Pond fully infested with Eicchornia sp.

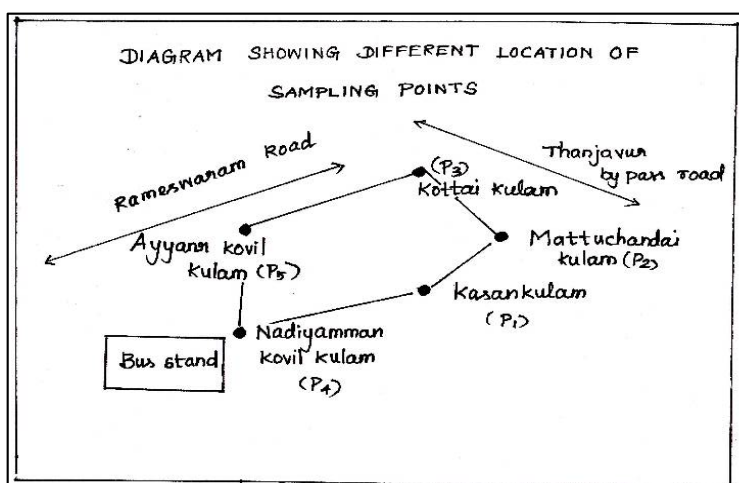


Fig. 1. Location map of Sampling points





RESEARCH ARTICLE

Molecular Detection of Adenovirus in Patients with Acute Exacerbation of Asthma in Wasit Province

Mohammad Kadhim Jinam^{1*}, Rana Hussein Raheema¹ and Jalal AbdulRazzaq Tofah²

¹Department of Medical Microbiology, Faculty of Medicine, University of Wasit, Iraq.

²Ph.D. Microbiology, Ministry of Health, Wasit Health Directorate, Wasit Governorate, Iraq.

Received: 20 July 2019

Revised: 24 Aug 2019

Accepted: 26 Sep 2019

*Address for Correspondence

Mohammad Kadhim Jinam

Department of Medical Microbiology,

Faculty of Medicine,

University of Wasit, Iraq.

Email: Mohamad200472@yahoo.com



This is an Open Access Journal / article distributed under the terms of the **Creative Commons Attribution License** (CC BY-NC-ND 3.0) which permits unrestricted use, distribution, and reproduction in any medium, provided the original work is properly cited. All rights reserved.

ABSTRACT

This study aimed to determine the incidence of human Adenovirus (HAdV) in patients with asthma exacerbation in Wasit province, Iraq. Blood samples were collected from patients for total and differential white blood cells (WBCs). Results showed that the total and differential WBCs have a significant correlation ($P < 0.05$) for neutrophils, lymphocytes, eosinophils and basophils counts among different groups studied. Enzyme-linked immunosorbent assay (ELISA) technique has been applied for the detection of total-IgE antibodies. Results revealed that the highest total-IgE antibodies titer in sera were significantly different ($p < 0.05$) among groups. Also, serum samples were used to evaluate the IgM and IgG antibodies, with IgM 18.33 % compared to 3.33 % in the control group, whereas IgG was 71.67% compared to 23.33% in the control group. A total of 90 nasopharyngeal swabs were used for the detection of suspected Adenovirus. The DNA was extracted and runs into the polymerase chain reaction. Results showed 10% ($n=6$) were positive samples for the type III gene and 21.66 % ($n=13$) for the type VII gene of Adenovirus.

Keywords: human Adenovirus, asthma, total-IgE, Adenovirus IgM & IgG, PCR.

INTRODUCTION

Asthma is a heterogeneous disease, characterized by chronic airway inflammation. History of respiratory symptoms including wheeze, shortness of breath, chest tightness and cough is the cornerstone to identifying this disease. However, these symptoms are varied in terms of time, intensity, frequency and variable expiratory airflow limitation among patients (1)(2). It also characterized by acute episodes of airway obstruction precipitated by respiratory infection and the release of IgE dependent mediators. Airway inflammation resulting from an inappropriate response





Mohammad Kadhim Jinam et al.

to either infectious or allergic antigens which is found common in the different manifestations of asthma (3). These synergism effects might be due to the reaction between allergens and viruses. When the virus attacks the bronchial cells, they produce various cytokines and chemokines and the cells been hyper responsiveness. In other words, the virtual infection might create a preparatory step as the first stage in the development of asthma (4). Evidence for the importance of viral respiratory infections in the development of asthma comes from studies indicating that severe paramyxoviral infections early in life impart a markedly increased risk for asthma later in childhood. In addition, the interaction between genetic and environmental factors considered a causative agent of asthma (5). However, the precise etiology of asthma has not been established yet.

For many years, it has been considered that viral respiratory tract infection is one of the important triggers of acute asthma, especially severe attacks leading to hospital admission in both children and adults (6). McCoy et al suggested that influenza, as a viral infection, leads to increase mortality rate in patients with asthma during winter since the influenza virus infection increase in this season (7). Adenovirus is the most common causative agent of respiratory system diseases. However, many serotypes of this virus may cause other illnesses, for example, conjunctivitis, gastroenteritis, rash illness, and cystitis. The respiratory illness by adenovirus infection itself ranges from cold, pneumonia, croup, or bronchitis. The fate of adenovirus infection could be complicated in patients with compromised immune systems (8). Adenoviruses are chemical and physical agents resistant and stable in adverse pH conditions. These features allowing survival of the virus for prolonged time outside of the host and liquid. In addition, the spread of adenoviruses is basically by respiratory droplets; however, it can spread via feces (9). The aim of the present study is to determine the role and incidence of *Adenovirus* in asthmatic exacerbation in the Wasit province in Iraq.

MATERIALS AND METHODS

Samples were collected from 90 persons in total, 60 specimens from subjects suffering from exacerbation asthma and 30 specimens were collected from an apparently stable control group, who had no history of asthma. The sample was collected from the patients who were admitted to Al-Karrama'a Teaching Hospital and Al-Zahra'a General Teaching Hospital in Wasit province/Iraq during the period from December 2018 to April 2019. The patient's age was ranged from 5≥60 years. Two specimens of nasopharyngeal swab were taken from each patient and 3-5 ml of venous blood analyzed freshly. Ethical verbal and written consent were taken from patients. Nasopharyngeal swabs were taken by inserting dry calcium alginate, aluminum-shafted swab into the nasopharyngeal area.

The swab was allowed to remain in nasal for 10-30 seconds and then rotated and withdrawn. One swab from each patient was placed in 3 ml transport medium, vircell, then store at -80°C until used for PCR. A total of 3 ml of venous blood was drawn from each patient, 1 ml in EDTA as anticoagulant for total and differential white blood cell count. Two ml of blood which was left to clot and separation of serum by centrifugation at 3000 r.p.m. for 10 minutes, then sera samples were carefully transferred to Eppendorf tubes and store at -20°C until use (as described by preanalytics)(10). Thirty specimens were collected from apparently stable control group, who had no history of asthma. Total and differential of White blood cells, lymphocytes, neutrophils, eosinophils, basophils and monocytes count by using the automatic hematology system, Human Count. (11)(12), also Total IgE-HRP EIA was estimated by ELISA and finally estimation of (IgM & IgG).

DNA Extraction

All nasopharyngeal were selected for DNA extraction using (innuPREP Virus kit analytikjena) as described by the manufacturer's instructions.



**Mohammad Kadhim Jinam et al.****Polymerase Chain Reaction (PCR)**

Two pair of specific primer was tested to amplify adenoviral capsid penton genes, the primer was specific for detection of Human adenovirus type III penton gene, as a forward primer '5' AAT CAACACAGCCTACCGCA3' and reverse 5' GACTT GTCTTG TGG AGCGGA3' with product size 178 bp and the primer was specific for detection of adenovirus type VII penton genes a forward primer '5' ATGCACCAATCCCTGCATGA 3' and reverse 5' CGGTG CGCATCA TTG AGAAG 3' with product size 344 bp. A master mix tube contains all the components required for conventional –PCR except template DNA. After optimization, the amplification program for human adenovirus type III penton gene used 95°C for 2 min as initial denaturation, then followed by 30 cycle as 95°C for 30 sec, 58°C for 30 sec and 72°C for 40 sec; final extension done at 72 °C for 5 min and for human adenovirus type VII penton gene the amplification program used 95°C for 2 min as initial denaturation, then followed by 30 cycle as 95°C for 30 sec, 58.5°C for 30 sec and 72°C for 20 sec; final extension done at 72 °C for 5 min.

Gel electrophoresis

Amplified PCR products were electrophoresis through 1.5 % agarose gel in TBE buffer. Target bands of primer were visualized by staining with ethidium bromide. DNA marker and negative control were included in each run and visualized under UV light at 350 nm.

Statistical analysis

All results were performed by statistical tests. Normally distributed data were expressed as mean \pm SD. Difference between the groups examined using the t – test and a p-value of ≤ 0.05 was taken as statistically significant, using SPSS. V.25.

RESULTS**Asthma Distribution by Age and gender**

The demographical distribution of the study groups according to different age was shown in table 1. The results show that the age was ranged between 5 \geq 60 years and the highest incidence was in the age interval of 5-15 years with 30% of total patients. The incidence of disease decreased gradually with age to finally reach 5% of age 56- \geq 60. Results showed that the number of male patients was higher, 32 (53.33%), compared to females 28 (46.47%) as shown in table 1.

The monthly distribution of cases during the period of study showed that the highest frequency was during January and February with 31 (21.67%) and 18 (30%) out of 60 patients respectively, as shown in table 2. The number of patients was varying among the months of the year. January and February had a higher rate of patients consulted, while April had fewer numbers.

Total and differential White Blood Cells (WBCs) count

In this study, WBCs count was 11.578 ± 3.149 and 5.957 ± 1.041 in asthmatic patients and control groups, respectively as shown in Table 3. For white blood cell count, there was a significant difference ($P < 0.05$) between different study groups using the t-test. This agreed with Darwish, 2011(13) and Bicer *et al.*, 2013(14) who found the mean level of white blood cell count higher in asthmatic patients compared to controls. We show a significant correlation by using t-test ($P < 0.05$) in neutrophils, lymphocytes, eosinophils and basophils counts among different groups' studied as shown in Table 3. For monocytes included in this study, there were no significant differences between asthmatic



**Mohammad Kadhim Jinam et al.**

patients and control groups. Similar results were reported by Alaa and Thanaa, (2013)(15) who found the monocyte 0.511 ± 0.432 compared control group 0.46 ± 0.169 .

Estimation of Total IgE

In this study, IgE levels in serum were significantly higher in asthma patients 87.649 ± 8.247 IU/ml compared to 33.562 ± 6.877 IU/ml in the control group ($p < 0.05$)(Table 4). This result concurs to a study by Iama et al., 2013(16) and Afshari et al., 2007(17). Particularly, the higher level of total serum IgE in asthmatic patients was in the age group of 8–14 years (18).

Detection of Adenovirus IgM and IgG by ELISA test

IgM and IgG antibodies for adenovirus were detected in 90 cases for asthmatic patients and control group. In terms of IgM, there was a significant difference between asthmatic patients with positive sera 18.33% compared to 3.33% of the control group. The same trend has been seen in the IgG antibody level with 71.67% for asthma patients and it is significantly higher than the control group with 23.33% as shown in Table 5.

Detection of HAdVs DNA by using PCR

A total of 90 nasopharyngeal swabs were enrolled in this study for the detection of HAdV DNA using a (bioneer kit). Two primers pairs were used by the polymerase chain reaction to amplify the adenoviral capsid penton genes (III&VII). Results showed that the Human adenovirus type III gene was detected in 10 % of the asthmatic patients as shown in table 6 and Figure 1. The human adenovirus type VII gene among asthmatic patients was reported as 21.66 % in asthmatic patients as shown in table 7 and Figure 2. In agreement with Khalaf and Al-Sadi., 2017(19) showed a low HAdV infection of the upper respiratory tract in Iraqi children, we also show similar results.

DISCUSSION

The precise detection of causes and inducer of diseases is the corner stone to design an effective treatment strategies. Asthma is one of the diseases that still lack of clear etiology. This study was aimed to determine one the suggested cause of asthma exacerbation, the adenovirus infection as one of respiratory tract infection causes. The increase in incidence of asthma shown to be higher in the coldest months. This might be due to increasing the prevalence of respiratory disorder that known as inducer of asthma exacerbation in winter months than in other months, for example, July (20)(21). Wu and his group suggest a link between viral bronchiolitis peak during winter in infancy and develop asthma later in childhood (22).

In this study increase in WBCs count in asthmatic patients was agreed with Darwish, 2011 and Bicer et al., 2013 who found the mean level of white blood cell count was higher in asthmatic patients compared to controls. Asthma biomarkers in peripheral blood are easy to obtain because inflamed tissue release chemoattractants and cytokines that recruit activated immune cells from the peripheral blood. The dynamic process of immune cells entering and leaving the bloodstream can be used as an indirect readout of disease state (23), while there was significant correlation in neutrophils, lymphocytes, eosinophils and basophils counts among different groups studied. The neutrophil has found to increase in patients with asthma compared with the control group in present study. Earlier studies were show increase in their level in the airways of persons who have severe asthma, during acute exacerbations and smoking (24). The increase in the percentage of these cells in the peripheral blood of patients in the present study may refer to the role of these cells in allergic inflammation, especially in the recognition phase. It is a well-documented that lymphocytes are an important part of the defense against viral infection (25)(26)(27). The



**Mohammad Kadhim Jinam et al.**

lymphocytosis is thought to be due to infectious causes like *cytomegalovirus*, *Epstein-Barr virus* and *adenovirus* or due to lymph proliferative disorders which may occur in the course of autoimmune disorders (28). Eosinophils and basophils play a major role in allergic reactions because of containing a high-affinity IgE receptor (Fc ϵ R1), soitis response to allergen immediately(29). Increased numbers of eosinophils in peripheral blood and in airway secretion are a characteristic feature of asthma. Bousquet *et al.*, 1990(30), have shown that the number of eosinophils in peripheral blood and in bronchial lavage from patients with asthma is associated with more severe disease. Similar results have been reported in many other studies by Tonnel *et al.*, 2000(31); Al – Mashhadani *et al.*, 2010(32); Al-Jebouri and Taha, 2015(33), Caughey *et al.*, 2007(34). The IgE is an antibody responsible for the activation of allergic and it is important to the pathogenesis of allergic diseases and the development and persistence of inflammation (35). Systemic IgE has been found to increase in infection by *Epstein Barr virus*, *Cytomegalovirus*, *Measles virus*, vaccination with whole virion influenza vaccine and *Rhinovirus*(36)(37)(38)(39). In this study serum, IgE levels were increased in asthma patients with agree to study by lama *et al.*, 2013(16) and Afshari *et al.*, 2007(17).

Particularly, the higher level of total serum IgE in asthmatic patients was in the age group of 8-14 years (18) with agree to our findings. Strachan and Cook (Strachan and Cook, 1998)(40) showed the potential role of IgE due to passive smoking on asthma in the study conducted in children. Therefore, the IgE consider a marker to use in monitoring the clinical course and to choose a suitable therapy (41). The elevated level of total serum IgE may demonstrate the allergic etiology of asthma, also reveals the significant association with exposure to cigarette smoke and raised eosinophil count with the elevated level of total serum IgE in asthmatics (16). Adenovirus IgM was showed to be higher in asthmatic patients together with the IgG antibody level. IgM is phylogenetically the earliest antibody class identified and the first immunoglobulin isotype to appear in the circulation after exposure to a new antigen. IgM plays an important role in the ontogeny of B cells and in early cognate immune responses (42). The demonstration of IgM antibodies to a specific infectious agent can be used as an indicator of recent infection (43). The presence of specific antibodies or viral strains can confirm the presence of adenoviruses. Identification of infection is confirmed by specific IgM and IgG antibodies (44).

Polymerase Chain Reaction can detect a low viral load of suspect clinical samples and proved to be a rapid and sensitive assay for HAdVs detection. This method could be used as a direct method during outbreaks of a specific type when decision making is depended on these results (19). In the present study, we used the PCR to show that the Human adenovirus type III gene was detected in 10 % of the asthmatic patients and 21.66 % for the type VII gene. In agreement, Khalaf and Al-Sadi, 2017(19) showed a low HAdV infection of the upper respiratory tract in Iraqi children. The other parts of the world reported about the same values with 10.3% in Korea (45), Australia was 7.3% (46), Peru was 6.2% (47) and Kenya was 14% (48). However, the percentage in Taiwanese was in a high incidence rate of HAdVs (83.5%) in children with respiratory tract infections (49). Moreover, the negative cases for HAdVs in asthmatic patients may be affected by other causes of respiratory tract viral infection rather than Adenovirus. Major pathogens that cause upper respiratory tract infection are *Influenza virus*, *Parainfluenzavirus*, *Human rhinovirus /enterovirus*, *Human metapneumovirus*, *Human coronavirus* and *human rhinoviruses* (50).

Furthermore, the most common bacterial agents that cause respiratory tract infection are *Haemophilus influenza*, *Streptococcus pneumonia*, *Escherichia coli*, *Klebsiella pneumoniae*, *Mycoplasma pneumonia*, and *Chlamydia trachomatis* (51). In addition, Atia *et al.*, 2018 (52) isolate *S. pneumonia*, *P. aeruginosa*, *S. aureus*, *Enterobacter* spp, and *Citrobacter* upper respiratory tract and consider them clinically important pathogens for this system. In conclusion, the exacerbation of asthma is most common in cold months, January and February, with a high level of allergy and virus infection markers. However, there was no relationship between infection with human adenovirus and asthma exacerbation as approved by PCR. The increase in nonspecific markers during asthma exacerbation needs to be specified and further investigation.





Mohammad Kadhim Jinam et al.

REFERENCES

1. Qiu, W.; Rogres, A.J.; Damask A.; Raby, B. A.; Klanderma, B. J.; Duan Q. L.; Tyagi, S.; Niu, S.; Anderson C.; Cahir Mcfarland, E.; Mariani, T. J.; Careg, V. and Tantisira, K. G. (2014). Pharmacogenomics: novel loci identification via integrating gene differential analysis and eQTL analysis. *Hum. Mol. Genet.*; 23 (18): 5017 – 5024.
2. Global Initiative for Asthma (GINA) (2015). Global strategy for asthma management and prevention: updated 2015. http://www.ginasthma.org/local/uploads/files/GINA_Report_2015_May19.pdf.
3. Murphy, D. M. and O'Byrne, P. M. (2010). Recent advances in the pathophysiology of asthma. *CHEST.*; 137: 1417 – 1426.
4. Tsukagoshi, H.; Ishioka, T.; Noda, M.; Kozawa, K. and Kimura, H. (2013). Molecular epidemiology of respiratory viruses in virus – induced asthma. *Front. Microbiol.*; 4: 278.
5. Dorothy S. Cheung & Mitchell H. Grayson (2012). Role of Viruses in the Development of Atopic Disease in Pediatric Patients. *Curr Allergy Asthma Rep* (2012) 12:613–620.
6. Johnston, S. L.; Pattermore, P. K.; Sanderson, A. G.; Smith, S.; Lampe, F.; Josephs L.; Symington P.; O'Toole, S.; Mgint S. H.; Tyrrell, D. A. and Holgate, S. T. (1995). Community study of role of viral infection in exacerbations of asthma in 9 – 11 year old children. *Br. Med. J.*; 310: 1225 – 1229.
7. McCoy, L.; Redelings M.; Sorvillo, F. and Simon, P. (2005). A multiple cause – of – death analysis of asthma mortality in the United States, 1990 – 2001. *J. asthma.*; 42 (9): 757 – 763.
8. Gray, G. C., (2006). Adenovirus transmission—worthy of our attention. *J Infect Dis* 194 (7): 871–3.
9. O'Leary, S.; Vorrat, J., (2005). Postoperative bleeding after diathermy and dissection tonsillectomy. *Laryngoscope.* 115(4):591-4.
10. Preanalytics. (2016). VACUETTE® Preanalytics Manual. www.gbo.com/preanalytics.
11. Naushad, H. (2015). Leukocyte count (WBCs). www.medscape.com.
12. Curry, C. V. (2015). Differential blood count. www.medscape.com.
13. Darwesh, M. F. (2011). Immunological aspects on asthmatic patients. Collage of Science, Kufa university, Iraq: 1 – 6.
14. Bicer, S. ; Giray, T. ; Çöl, D. ; Çiler Erdağ, G. ; Vitrinel, A. ; Gürol, Y. ; Çelik, G. ; Kaspar, Ç. and Küçük, Ö. (2013). Virological and clinical characterizations of respiratory infections in hospitalized children. *Ital. J. Pediatr.* ; 39: 22.
15. Alaa, J. H. and Thanaa A. M. (2013). Immunological study of patients with asthma. *Babylon J. Uni. Pure Appl. Sci.*; 7 (21): 2400 – 2407.
16. Lama, M.; Chatterjee, M. and Chaudhuri, T. K. (2013). Total serum immunoglobulin e in children with asthma. *Indian J. clin. Biochem.*; 28 (2): 197 – 200.
17. Afshari JT, Hosseini RF, Farahabadi SH, Heydarian F, Boskabady MH, Khoshnavaz R, (2007). Association of the expression of IL-4 and IL-13 genes, IL-4 and IgE serum levels with allergic asthma. *Iran J Allergy Asthma Immunol.* ;6:67–72.
18. Cline MG, Burrows B. (1989) Distribution of allergy in a population sample residing in Tucson, Arizona. *Thorax.* ;44:425–431.
19. Rasha J. Khalaf, Hula Y. Fadhil, Iman M. Afi, Salah Ali Namdar (2017). Molecular Diagnosis of Human Adenovirus in Children with Upper Respiratory Tract Infections. *IOSR Journal of Pharmacy and Biological Sciences (IOSR-JPBS).* Volume 12, Issue 3 Ver. I (May. - June. 2017), PP 09-13.
20. Malmstrom, k.; Pitkaranta, A.; Carpen, O.; Pelkonen, A.; Malmberg, L. P.; Turpeinen, M.; Kajsaari, M.; Sarna, S.; Lindahl, H.; Heahela, T. and Makela, M. J. (2006). Human rhinovirus in bronchial epithelium of infants with recurrent respiratory symptoms. *J. Allergy Clin. Immunol.*; 118: 591 – 596.
21. Al – Shami J. A. J. and Al – obaidi, N. (2009). Review of wheezing in children in maternity and children teaching hospital in Al – Diwanayah / Iraq. *Babylon Med. J.*; 6 (3 – 4): 477 – 483.
22. Wu, P.; Dupont, W. D.; Griffin, M. R.; Carroll, K. N.; Mitchel, E. F.; Gebretsadik. T. and Hartert, T. V. (2008). Evidence of a causal role of winter virus infection during infancy in early children asthma. *Am. J. Respir. Crit. Care Med.*; 178: 1123 – 1129.





Mohammad Kadhim Jinam et al.

23. Vijverberg, S. J.; Hilvering, B.; Raaijmakers, J. A.; Lammers, J. W.; Derzee, A. H. M-v. and Koenderman, L. (2013). Clinical utility of asthma biomarkers; from bench to bedside. *Biologics*; 7: 199 – 210.
24. Anuradha Ray ; Jay K. Kolls (2017). Neutrophilic Inflammation in Asthma and Association with Disease Severity . *Trends Immunol.* 2017 Dec ; 38(12): 942–954.
25. Berhrman, R. and Kliegman, R. (2000). *Nelson textbook of pediatrics*. W. B. Saunders company, 16th edition: 664 – 679.
26. Buckley, R. H. (2000). Primary Immunodeficiency disease due to defects in lymphocytes. *New England J. Med.*; 343 (18): 1313 – 1324.
27. Itazawa, T.; Adachi, Y.; Imamura, H.; Okabe, Y.; Yamamoto, J.; Onoue, Y.; Adachi, Y. S.; Miyawaki, T. and Murakami, G. (2001). Increased lymphoid MxA expression in acute asthma exacerbation in children. *Allergy*; 56: 895 – 898.
28. Bailey, NG, Kojo, S, Elenitoba-Johnson, G.(2015).Mature T cell leukemias: Molecular and clinical aspects. *Current Hematologic Malignancy Reports*. vol. 19. 2015. pp. 421-448.
29. Wong, C. K.; Lp, W. and Lom, C. W. K. (2004). Biochemical assessment of intracellular signal transduction pathways in eosinophils: implication for pharmacotherapy. *Clin. Labo. Scie.*; 41 (1): 79 – 113.
30. Bousquent, J.; Chanez, P.; Lacoste, J. Y.; Barneon, G.; Ghavanian, N.; Enander, I.; Verge, P.; Ahlstedt, S.; Simony-Lafontain, J.; Godard, P. and Michel, F. (1990). Eosinophilic inflammation in asthma. *N. Engl. J. Med.*; 323: 1033 – 1039.
31. Tonnel, D. C.; Gosset, P. L. and Tillie, G. I. (2000). Characteristics of inflammatory response in asthma. *J. Immunol.*; 165 (9): 184 – 185.
32. Al – Mashhadani, M. S.; Najam, W. S. and Kasem, S. E. (2010). Atopic dermatitis and asthma in correlation with cytokines level. *Tikrit Med. J.*; 16 (2): 7 – 12.
33. Al – Jebouri, M. M. and Taha, J. N. (2015). Differential count patterns of leucocytes among asthmatic patients working in gas and oil refineries in Kirkuk, Iraq. *World J. Pharma. Pharmaceut. Sci.*; 4 (5): 29 – 39.
34. Caughey, G.; Xiang, J.; Walter, N. and Paul, J. (2007). White blood cells in lung produce histamine see in allergies. *Exper. Med. J.*; 89: 222 – 227.
35. Boyce, J. A. (2003). Mast cells: beyond IgE. *J. Allergy Immuno.*; 111 (1): 24 – 32.
36. Bahana, S. L.; Horwitz, C. A.; Fiala, M. and Heiner, D. L. (1978). IgE response in heterophil – positive infectious mononucleosis. *J. Allergy CLin. Immunol.*; 62: 167 – 173.
37. Michaels, A. A.; Stevens, M. B. and Adkinson Jr., N. F. (1979). Detection of influenza vaccine specific IgE. *J. Allergy Clin. Immunol.*; 63: 169.
38. Griffin, D. E.; Cooper, S. J.; Hirsch, R. C. and Johson, R. J.; Lindo de Soriano, I.; Roedenbeck, S. and Vaisberg, A. (1985). Changes in plasma IgE levels during complicated and uncomplicated measles virus infections. *J. Allergy Clin. Immunol.*; 76: 206 – 213.
39. Skoner, D. P. Doyle, W. J.; Tanner, E. P.; Kiss, J. and Fireman, P. (1995). Effect of rhinovirus 39 (RV-39) infection on immune and inflammatory parameters in allergic and non-allergic subjects. *Clin. Exp. Allergy*; 25: 561 – 567.
40. Strachan DP, Cook DG.(1998) Parental smoking and allergic sensitisation in children. *Thorax* .;53:117–123.
41. Mesinga TT, Schouten JP, Rijcken B, Weiss ST, van des Lende R(1994). Host factors and environmental determinants associated with skin test reactivity and eosinophilia in a community-based population study. *Ann Epidemiol.* ;4:382–392.
42. Dinakar C. Practical aspects of ambulatory diagnoses and management of immunodeficiency disorders. *Ann Allergy Asthma Immunol.* 2007;99: 201–202.
43. Rolink AG, Andersson J, Grawunder U, Melchers F. Molecular mechanisms guiding B cell development. In: Ochs HD, Smith CIE, Puck JM, eds. *Primary Immunodeficiency Diseases: A Molecular and Genetic Approach*. 2nd ed. New York, NY: Oxford University Press; 2007: 61–70.
44. Kagami H, Atkinson JC, Michalek SM, et al. (1998): Repetitive adenovirus administration to the parotid gland: role of immunological barriers and induction of oral tolerance. *Hum Gene Ther* 9: 305-313.
45. Callaway, Z. ; Kim, S. H. ; Kim, J. Y. ; Kim, D.W. and Kim, C. K. (2011). Adenovirus infection with serious pulmonary squeals in Korean children. *Clin. Respir. J.* ; 5(2): 92-98.





Mohammad Kadhim Jinam et al.

46. Sloots, T. P.; McErlean, P.; Speicher, D.J.; Arden, K. E.; Nissen, M. D. and Mackay, I. M. (2006). Evidence of human coronavirus HKU1 and human bocavirus in Australian children. *J. Clin. Virol.* ; 35(1):99–102.
47. Ampuero, J. S. ; Ocaña, V. ; Gómez, J. ; Gamero, M. E. ; Garcia, J. ; Halsey, E. S. and Laguna-Torres, V. A. (2012). Adenovirus Respiratory Tract Infection in Peru. *PLoS One.* ; 7:e46898.
48. Ahmed, J. A. ; Katz, M. A. ; Auko, E. ; Njenga, M. K. ; Weinberg, M. and Kapella, B. K. (2012). Epidemiology of respiratory viral infections in two long-term refugee camps in Kenya, 2007-2010. *BMC Infect Dis.*; 12:7.
49. Ferone, E. A. ; Berezin, E. N. ; Durigon, G. S. ; Finelli, C. ; Felício, M. C. ; Storni, J.G. ; Durigon, E.L. and Oliveira, D. B. (2014). Clinical and Epidemiological aspects related to the detection of adenovirus or Respiratory syncytial virus in infants hospitalized for acute lower respiratory tract infection. *J. Pediatr*; 90(1):42-49.
50. Chiu Shu-Chun, Lin Yung-Cheng, Wang Hsiao-Chi, Hsu Jen-Jen, Yeh Ting-Kai, Liu Hsin-Fu, Lin Jih-Hui. (2017). Surveillance of upper respiratory infections by using newly multiplex PCR assay compared to conventional methods during influenza season in Taiwan. *International Journal of Infectious Diseases* 2017.06.011
51. Juraina Abd-Jamil , Boon-Teong Teoh , Eddy H Hassan , Nuruliza Roslan and Szaly AbuBakar (2010). Molecular identification of adenovirus causing respiratory tract infection in pediatric patients at the University of Malaya Medical Center. *BMC Pediatrics*, 10:46.
52. Ahmed Atia, Najla Elyounsi , Ahmed Abired , Amal Wanis , Abdulsalam Ashour .(2018). Antibiotic Resistance Pattern of Bacteria Isolated from patients with upper respiratory tract infections; a four year study in Tripoli city. Online: 24 August 2018 (11:46:41 CEST).

Table 1. Distribution of patients according to age.

Age (year)	Patients group No. (%)			Control group No. (%)		
	Male	Female	Total	Male	Female	Total
5 – 15	9	9	18 (30.00 %)	3	3	6 (20.00 %)
16 – 25	7	6	13 (21.67 %)	3	3	6 (20.00 %)
26 – 35	5	5	10 (16.67 %)	3	2	5 (16.67 %)
36 – 45	6	5	11 (18.33 %)	3	2	5 (16.67 %)
46 – 55	3	2	5 (8.33 %)	2	2	4 (13.33 %)
56 ≥ 60	2	1	3 (5.00 %)	2	2	4 (13.33 %)
Total	32	28	60	16	14	30

Table 2. Monthly distribution of asthma cases.

Month	Patients group No. (%)	Control group No. (%)
December	10 (16.67 %)	6 (20%)
January	13 (21.67 %)	6 (20%)
February	18 (30.00 %)	6 (20%)
March	11 (18.33 %)	6 (20%)
April	8 (13.33 %)	6 (20%)
Total	60	30

Table 3. The total and differential white blood cells count of asthmatic patients and control groups

Parameter mean ± SD	Asthmatic patients' group	Control group	P value
WBCs x 10 ³ cell/mm ³	11.578 ± 3.149	5.957 ± 1.041	p < 0.05
NEU x 10 ³ cell/mm ³	6.875 ± 1.727	4.825 ± 0.953	p < 0.05
LYM x 10 ³ cell/mm ³	3.993 ± 0.895	1.782 ± 0.342	p < 0.05





Mohammad Kadhim Jinam et al.

MONO x 10 ³ cell/mm ³	0.683 ± 0.231	0.587 ± 0.201	NS
EOS x 10 ³ cell/mm ³	1.397 ± 0.492	0.210 ± 0.096	p < 0.05
BAS x 10 ³ cell/mm ³	0.311 ± 0.214	0.061 ± 0.019	p < 0.05

Table 4. IgE level IU/ml for asthmatic patients and control groups.

Group	IgE level IU/ml
Asthmatic patients	87.649 ± 8.247
Control	33.562 ± 6.877
P value	p < 0.05

Table 5. Prevalence of ADV-IgM and ADV-IgG

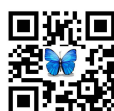
Group	Number of cases	ADV IgM		ADV IgG		ADV IgM & IgG from positive cases
		positive cases	Negative cases	positive cases	Negative cases	
Asthmatic patients	60	11 (18.33%)	49 (81.67%)	43 (71.67%)	17 (28.33%)	6
Control	30	1 (3.33%)	29 (96.67%)	7 (23.33%)	23 (76.67%)	0
P value		p < 0.05	NS	p < 0.05	p < 0.05	p < 0.05

Table 6. Prevalence of Human adenovirus type III gene

Groups	No. of cases	HAdV type III Gene	
		positive cases	Negative cases
Asthmatic patients	60	6 (10.00 %)	54 (90.00%)
Control	30	0 (0%)	30 (100%)
P value		< 0.05	NS

Table 7. Prevalence of Human adenovirus type VII gene

Groups	No. of cases	HAdV type VII Gene	
		positive cases	Negative cases
Asthmatic patients	60	13 (21.66 %)	47 (78.33%)
Control	30	0 (0%)	30 (100%)
P value		< 0.05	< 0.05





Mohammad Kadhim Jinam *et al.*

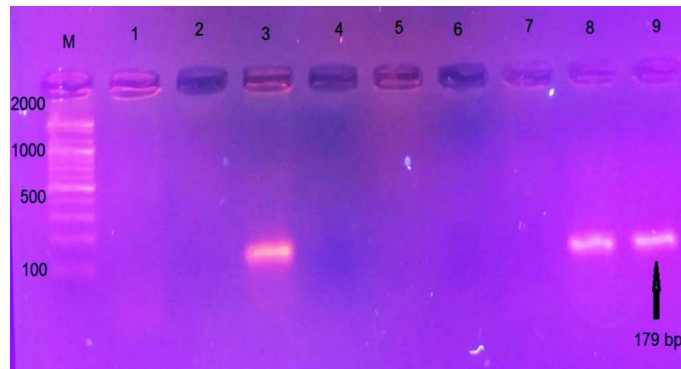


Figure 1. Gel electrophoresis of amplified (Human adenovirus type III) gene, the Amplicon size was 179 bp, Lane M represented marker DNA (2000-100 bp), run on a 1.5 % agarose gel and visualized under UV illuminator.

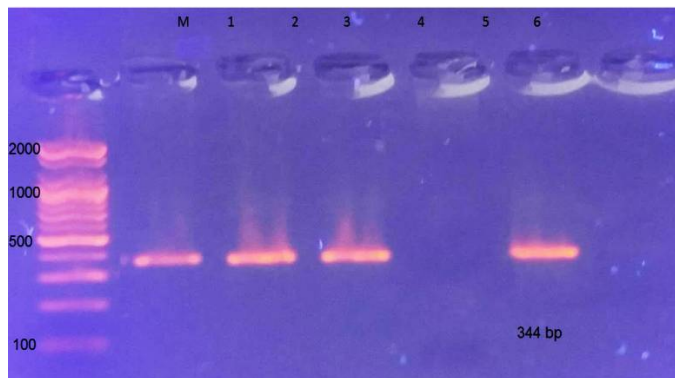


Figure 2. Gel electrophoresis of amplified (Human adenovirus type VII) gene, the Amplicon size was 344 bp, Lane M represented marker DNA (2000-100 bp), run on a 1.5 % agarose gel and visualized under UV illuminator.





Radiographic Evaluation and Management of Abscess at Coronary Band Region in A Holstein Friesian Dairy Cow

R.Anees^{1*}, P.T.Dinesh², C.J.Nithin³, S.Sooryadas⁴, George Chandy⁴, Vinu David.P⁵ and C.P.Abdul Azees⁵

¹M.V.Sc.Scholar, Department of Veterinary Surgery & Radiology, College of Veterinary & Animal Sciences, KVASU, Pookode, Kerala, India.

²Assistant Professor & Head, Department of Veterinary Surgery & Radiology, College of Veterinary & Animal Sciences, KVASU, Pookode, Kerala, India.

³Veterinary Surgeon, Animal Husbandry Department, College of Veterinary & Animal Sciences, KVASU, Pookode, Kerala, India, Kerala.

⁴Assistant Professor, Department of Veterinary Surgery & Radiology, College of Veterinary & Animal Sciences, KVASU, Pookode, Kerala, India.

⁵Assistant Professor, Department of Animal Reproduction, Obstetrics and Gynaecology, College of Veterinary & Animal Sciences, KVASU, Pookode, Kerala, India.

Received: 19 July 2019

Revised: 22 Aug 2019

Accepted: 26 Sep 2019

*Address for Correspondence

R.Anees

M.V.Sc.Scholar,

Department of Veterinary Surgery & Radiology,

College of Veterinary & Animal Sciences, KVASU,

Pookode, Kerala, India.



This is an Open Access Journal / article distributed under the terms of the **Creative Commons Attribution License** (CC BY-NC-ND 3.0) which permits unrestricted use, distribution, and reproduction in any medium, provided the original work is properly cited. All rights reserved.

ABSTRACT

The present case was presented to Teaching Veterinary Clinical Complex, College of Veterinary and Animal Sciences, Pookode, Wayanad, Kerala. A 5 year old Holstein Friesian dairy cow with Symptoms of non-weight bearing right hindlimb and swelling at the coronary band region was presented. Lateral and dorso-plantar radiograph of the affected foot was taken. Deviation of third phalanx, interdigital soft tissue mass and soft tissue swelling at coronary region were identified on radiography. Abscess cavity was incised and drained the pus. A wooden hoof block was applied on the healthy non-painful contralateral claw. Along with daily flushing abscess cavity, parenteral antibiotics and NSAIDs were followed. Animal was shown uneventful recovery on the seventh day of treatment and increase in milk yield was also noticed after the treatment.

Keywords: Coronary band abscess, radiography, dairy cow.



**Anees et al.**

INTRODUCTION

Lameness due to hoof affections are an important issue which deduces the production performance of dairy cattle. Hoof affections are next to mastitis and reproductive disorders affecting production performance in dairy cattle (Kossaibati and Esslemond, 1997). Lameness is a disease of high producing dairy cattle which can cause a significant reduction in milk yield (Mohammadnia and Khagani, 2013). Anderson *et al.* (2017) observed that extension of infection of sole ulcers or abscesses and white line diseases or foreign penetration of inter-digital space and foot rot caused sepsis of distal inter-phalangeal joint. The affected animals were presented with a swollen and painful coronary band with a draining tract at coronary band or under the sole.

MATERIALS AND METHODS

A 5 year Holstein Friesian dairy cow was presented to Teaching Veterinary Clinical Complex, College of Veterinary and Animal Sciences, Pookode with Symptoms of non-weight bearing right hindlimb and swelling at the coronary band region. Animal started showing symptoms 2 weeks before the presentation of animal and milk yield on the day of presentation was 4 litres. There was no previous history of injury at coronary region.

Lameness score

Cow evaluated for lameness using a five point locomotion score as per Sprecher *et al.* (1997). Animal was assessed from the side and behind while standing and during walking. Animal was made to walk on a non-slippery surface for 6 to 10 continuous steps. Lameness were classified as: 1 – non-lame (normal gait), 2 – mildly lame, 3 – moderately lame, 4 – lame and 5 – severely lame

Radiography

Radiographs were taken using a portable X- ray machine EP CORSA 2.4 with 8 MAS and 50 KVP settings. Lateral and dorso-plantar views were taken. Radiographs were examined and radiographic changes were recorded.

Physiological parameters

Rectal temperature, pulse rate, respiratory rate and colour of visible mucous membrane of the animal was monitored and recorded on the day of presentation.

Restraint of the animal

Animal was restrained manually using ropes. Hind limb was restrained and lifted up by beam hook method in which one end of the rope was used to form a loop above the hock joint and the other end of rope was passed upward through the ring of beam hook or through a pole fixed at a height above the back side of animal and the rope was pulled downward by assistant. Head was controlled by an assistant.

Foot examination

Preliminary examination was done by visual assessment and pain in hoof was checked by a hoof tester after proper restraint and washing of the claws.



**Anees et al.**

Therapeutic hoof trimming

Claws of the cow was trimmed after taking claw measurements by a modification of Dutch method of hoof trimming suggested by Amstel and Shearer (2006). Dorsal hoof wall length of claw was measured with the help of a measuring scale and reduced the dorsal wall length of the inner claw to 7.5cm with hoof nipper. The weight-bearing surface of the claws (wall and sole, but not the heel) was trimmed to remove the overgrowth until a sole thickness of approximately 7mm (not less than 5mm) is retained at the toe. Trimming of the wall and sole resulted in a flat bearing surface, so that it makes right angles to the long axis of the metacarpus (tarsus) in the standing position. The sole was shaped and sloped to interdigital space so that the innermost back portion of the sole slopes toward the centre of the claws. An orthopaedic block or claw block made from wood was applied to healthy contralateral medial claw with the help of acrylic in order to remove all weight bearing from the painful lateral claw.

Treatment of the coronary abscess

The abscess cavity was incised at the dorsal side of the coronary band and the pus inside the abscess cavity was drained out by manual pressure. Flushed the abscess cavity after inserting a Rayel's tube in to cavity with povidone iodine solution and applied seaton with tincture iodine on the day of presentation.

Postoperative treatment

Routine flushing of abscess cavity with normal saline and povidone iodine. Parenteral antibiotic (Dicrysticine, 5g) and NSAID (Megludyne at a dose rate of 0.2mg per Kg) were given postoperatively for seven days.

RESULTS AND DISCUSSION

On clinical examination of the animal, rectal temperature, respiratory rate, pulse shown severe pain on palpation of the Assessment of lameness score in dairy cows facilitates early identification of lameness cases for the treatment (Archer *et al.*, 2010). In present study, five point lameness scoring system by Sprecher *et al.* (1997) which categorized cows in to normal to severely lame groups was used. It was found to be easy in identifying and giving scores for cows based on the presence or absence of arched back during progression and in standing position. A lameness score of five (severely lame) was exhibited by the animal on the day of presentation and it has found to be reduced to one (normal) on the fifteenth day of treatment. Painful lesions on this weight bearing sites leads to severe non-weight bearing lameness.

Lateral and dorso-palmar or dorso-plantar radiographic views were taken in the present study similar to that used by Farrow (1999). Radiographic lesions detected were deviation of third phalanx, soft tissue mass at inter digital space and soft tissue swelling at coronary region. Lateral deviation of the third phalanx was observed in the dorso-plantar view and cranial deviation was observed in lateral view. Radiography is the best way to differentially diagnose the foot affections (Nouri *et al.*, 2011). Hoof block application at the healthy contralateral claw of the affected hoof was found be effective in this case. Because it leads to the early recovery of the case by relieving pain on the affected claw. Block should be retained in position for 15 to 20 days for proper healing (Philip, 2018). Primary objective of treating hoof lesions was to relive weight from the affected claw for the quick recovery (Pyman, 1997). Pain and discomfort caused by hoof lesions could be reduced by corrective hoof trimming and by application of hoof block to the healthy claw (Coetzee *et al.*, 2017).

Animal was shown uneventful recovery on the seventh day of treatment. A random change in milk yield was also observed in the present study. Milk yield was also found to be increased to 10 litres on the fifteenth day of treatment.





Anees et al.

CONCLUSION

From the present study it could be concluded that radiographic evaluation foot was found be very effective in exact confirmatory diagnosis of deviation of pedal bone and extend of soft tissue swelling. Hoof block or orthopaedic block fixation was found to be helpful in early recovery of painful conditions on claw by relieving weight on the affected claw. Use of poly methyl methacrylate as an adhesive for fixation of hoof block was found to be effective. Most appropriate treatment at the right time is the bedrock in treatment of hoof affections dairy cattle.

REFERENCES

1. Amstel, S.R. and Shearer, J.K. 2006. *Manual for Treatment and Control of Lameness in Cattle*. Blackwell publishing, Iowa, USA, 16-29p.
2. Anderson, D.E., Desrochers, A. and Amstel, V.S.R., 2017. Surgical procedures of the distal limb for treatment of sepsis in cattle. *Veterinary Clinics: Food Animal Practice*, 33(2), pp.329-350.
3. Archer, S.C., Green, M.J. and Huxley, J.N., 2010. Association between milk yield and serial locomotion score assessments in UK dairy cows. *Journal of dairy science*, 93(9), pp.4045-4053.
4. Coetzee, J.F., Shearer, J.K., Stock, M.L., Kleinhenz, M.D. and van Amstel, S.R., 2017. An update on the assessment and management of pain associated with lameness in cattle. *Veterinary Clinics: Food Animal Practice*, 33(2), pp.389-411.
5. Farrow, C.S., 1999. Digital Infections in Cattle: Their Radiologic Spectrum. *Veterinary Clinics: Food Animal Practice*, 15(2), pp.411-423.
6. Kossaibati, M.A. and Esslemont, R.J.1997. The costs of production diseases in dairy herds in England. *The veterinary journal*, 154(1), pp.41-51.
7. Sprecher, D.J., Holstelner, D.E. and Kaneene, J.B. 1997. A lameness scoring system that uses posture and gait to predict dairy cattle reproductive performance. *Theriogenology*.47, pp.1179- 1187.
8. Mohamdnia, A. and Khaghani, A. 2013. Evaluation of hooves morphometric parameters in different hoof trimming times in dairy cows. *Vet. Res. Forum*. 4, pp. 245-249.
9. Nouri, M., Nowrouzian, I., Vajhi, A., Marjanmehr, S.H. and Faskhoudi, D. 2011. Morphometric radiographic findings of digital region in culling lame cows. *Asian J. Anim. Sci*, 5(4), pp. 256-267.
10. Philip, L.M. 2018. Colour atlas of hoof care in dairy cattle. (1st Ed.). Kerala veterinary and animal sciences university, Pookode, Wayanad, 124p.
11. Pyman, M.F. 1997. Comparison of bandaging and elevation of the claw for the treatment of foot lameness in dairy cows. *Aust. Vet. J.*75, pp.132-135.



<p>Fig.1.Swelling at the coronary region and inter-digital hyperplasia</p>	<p>Fig.2.Draining of the pus from the abscess cavity</p>	<p>Fig.3.Hoof block to relieve weight bearing from the painful claw</p>
---	---	--





Fig.4.Flushing of abscess cavity with normal saline



Fig.5.Hoof block applied on the healthy side of foot



Fig.6.Adhesive for hoof block application: Poly methyl methacrylate



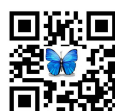
Fig.7.Lateral radiograph: cranial deviation of pedal bone and soft tissue swelling at dorsal and plantar aspect of coronary region



Fig.8.Recovery photo of the foot at the seventh day of treatment



Fig.9.Dorso-plantar radiograph: lateral deviation of pedal bone, soft tissue swelling at coronary region and interdigital soft tissue mass





Cytotoxic Evaluation of *Uncaria gambir* Extract toward Fibroblast Cell

Fayyadhah M Azmi¹, Ahmad Shuhud Irfani Zakaria^{1*}, SNMP Sockalingam¹, Alida Mahyuddin¹, Mazlina M Said² and Rohaya Ahmad³

¹Pediatric Dentistry Unit, Centre for Family Oral Health, Faculty of Dentistry, The National University of Malaysia (UKM), Jalan Raja Muda Abdul Aziz, 50300 Kuala Lumpur, Malaysia.

²Faculty of Pharmacy, The National University of Malaysia (UKM), Jalan Raja Muda Abdul Aziz, 50300 Kuala Lumpur, Malaysia.

³Faculty of Applied Sciences, Universiti Teknologi MARA, 40450 Shah Alam, Selangor, Malaysia.

Received: 09 July 2019

Revised: 14 Aug 2019

Accepted: 26 Sep 2019

*Address for Correspondence

Ahmad Shuhud Irfani Zakaria

Pediatric Dentistry Unit,
Centre for Family Oral Health, Faculty of Dentistry,
The National University of Malaysia (UKM),
Jalan Raja Muda Abdul Aziz,
50300 Kuala Lumpur, Malaysia.
E.Mail : shuhud_zakaria@ukm.edu.my



This is an Open Access Journal / article distributed under the terms of the **Creative Commons Attribution License** (CC BY-NC-ND 3.0) which permits unrestricted use, distribution, and reproduction in any medium, provided the original work is properly cited. All rights reserved.

ABSTRACT

Uncaria gambir extracts consist of catechins that have been shown to possess anti-inflammatory and antibacterial properties. This property shows some clinical potential but the cytotoxicity of the extracts found in Malaysia has not been reported. Hence, the study aimed to determine the cytotoxicity of Malaysian *Uncaria gambir* extracts toward fibroblast cells *in vitro*. *Uncaria gambir* extracts were dissolved in 1% DMSO and diluted with culture media into eight different concentrations, ranging from 1000 µg/ml to 7.8 µg/ml. MC3T3 fibroblast cells were seeded in the 96-well plates and incubated for 24 hours. Then, the cells were exposed to various concentrations of the extracts in triplicates and incubated for another 24 hours. 10% DMSO and culture media were used as positive and negative control respectively. Cell viability was measured using Alamar Blue, DNA Fluorescence and Neutral Red Uptake (NRU) assay. Morphological changes of the cells were determined using Live/Dead cell analysis. Both DNA Fluorescence and Alamar Blue assays showed no cytotoxic effects of the extract towards the fibroblast cells at all concentrations. However, NRU assay showed that the extract was not cytotoxic at a concentration lower than 500 µg/ml and cytotoxic at 1000 µg/ml concentration. The extracts at all concentrations showed a statistically significant difference when compared to positive control with $p < 0.05$ for all assays tested. The half-maximal inhibitory concentration (IC₅₀) of the extract measured using Alamar Blue, DNA Fluorescence and NRU assay were 1751 µg/ml, 3109 µg/ml and 1031 µg/ml





Fayyadhah M Azmi et al.

respectively. Live/Dead cell analysis showed a mixture of red and green fluorescence in a low-density cell population at 1000 µg/ml concentration as compared to the negative control. Cell density increased and more cells with green fluorescence were seen as the concentration of the extract reduced. Conclusively, the Malaysian *Uncaria gambir* extracts were not cytotoxic toward MC3T3 fibroblast cells at a concentration below 500 µg/ml when tested *in vitro*.

Keywords: *Uncaria gambir*, cytotoxicity, MC3T3, Live/Dead cell analysis, Alamar Blue assay, DNA Fluorescence assay, Neutral Red Uptake assay.

INTRODUCTION

The *Uncaria* genus has been used for ages as a medicinal product. *Uncaria* composed of 34 species, found mainly in tropical regions and specifically in Malaysia, 14 species of *Uncaria* have been reported (1). One of the species is *Uncaria gambir* (Hunt) Roxb or *Uncaria gambir*, which can be found mainly in Malaysia and Indonesia. Depending on the region, the plant also known as Gambir, Gou Teng, Asen'yaku, Cat's claw, Una de Gato, and Pale Catechu by the local people (2,3). *Uncaria gambir* plant is a woody climber where it can grow about eight feet high and has an oval shape leaves (4). It could be grown only at a specific condition in an area of 200 to 800 meters above the sea level which constantly receives rainfall around ±3.3mm per year and humidity around 70% to 85% with pH range from 4.8 to 5.5 (5). The phytochemical study on *Uncaria gambir* showed that it mainly composed of flavonoids. Catechin is the most abundant, making up to 80% of the total flavonoid constituents of the plant (6,7). Besides that, Taniguchi and his colleagues had isolates other constituents which is four chalcane-flavan dimers, gambiriin A1, A2, B1, and B2 along with catechin, epicatechin, and dimeric proanthocyanidins, procyanidin B1, procyanidin B3, and gambiriin C (8).

Traditionally, it is widely used medicinally as an astringent and for treatment of spongy gum and toothache. Its leaves and young shoots are infused and drunk to treat dysentery and diarrhea or used as a mouth gargle for sore throat. Furthermore, dried *Uncaria gambir* leaves and twigs are being applied on wound, burns and external callous ulcers (9). Besides, in the west, it usually used for tanning, calico printing, and dyeing purpose (10). Catechin and its derivatives had been vastly studied for its antibacterial, anti-oxidant and anti-inflammatory properties (11,12). For example, epigallocatechin gallate (EGCG), a derivative of catechin, can inhibits the adherence ability of *Streptococcus mutans* and reduced its biofilm production (13), which is the critical step in dental caries formation. Furthermore, EGCG also has the ability in reducing the expression of pro-inflammatory mediators such as interleukin 1(IL-1) and interleukin 8 (IL-8) found in inflamed pulp tissue (14). Owing to these properties, *Uncaria gambir* shows the clinical potential that can be explored in dentistry, mainly for the treatment of dental caries, periodontal disease, and pulp therapy. However, the cytotoxicity of this plant has not been widely investigated with only one study done on *Uncaria gambir* that originates from Indonesia in 2011 (7). Furthermore, there are no known studies on the cytotoxicity and safety of Malaysian *Uncaria gambir* that has been reported. Thus, this study aims to investigate the cytotoxicity of Malaysian *Uncaria gambir* toward the fibroblast cells *in vitro*.

MATERIALS AND METHODS

Ethical approval

The ethical approval for this research was obtained from the Research Ethics Committee of National University of Malaysia with the reference number of UKM PPI/111/8/JEP-2017-797.



**Fayyadhah M Azmi et al.**

Preparation of *Uncaria gambir* extracts

Uncaria gambir leaves were acquired and collected from Bukit Diman, Ajil, Terengganu, Malaysia. The voucher specimen (HTBP 4320) was deposited at the Herbarium Botanical Garden, Putrajaya, Malaysia. The leaves were dried and grounded into a fine powder. The finely ground material was weighed and macerated with methanol for 72 hours at room temperature, and the solvent evaporated under reduced pressure. The extraction process was done at the Faculty of Applied Sciences, Universiti Teknologi MARA, Shah Alam. 2000 µg/ml of *Uncaria gambir* methanolic extract was dissolved in 2% Dimethyl sulfoxide (DMSO) (Merck Millipore, Sweden) with ultrasonicator and subsequently filtered through a 0.2 µm syringe filter. The purified extract was then subjected to 2-fold serial dilution to obtain a maximum concentration of 1000 µg/ml in 1% DMSO.

Cell line preparation and cell cultures

The mouse fibroblast cell lines (MC3T3) were obtained from the bank cell (Cell Culture Laboratory, Faculty of Dentistry, National University of Malaysia). The cells were cultured in Dulbecco's Modified Eagle Media (DMEM) (Thermo Fisher Scientific, USA) and supplemented with 10% fetal calf serum (Sigma-Aldrich Germany), 1% penicillin/streptomycin (Thermo Fisher Scientific, USA) and 1% L-glutamate (Thermo Fisher Scientific, USA) at 37°C, 5% CO₂. The cells were passaged every 3 days based on the standard trypsin/EDTA protocol according to Freshney (15). Cells between the fourth and sixth passages were used in this study. 5 x 10³ cells in 100 µL of DMEM were seeded in wells of 96-well plate. The 96-well plate was incubated at 37°C, 5% CO₂ for 24 hours to obtain a semi-confluent layer of cells in each well. After 24 hours of incubation, the DMEM in each well was discarded. 100 µL of the *Uncaria gambir* extract in eight different concentrations, ranging from 1000 µg/ml to 7.8 µg/ml was added into the wells in triplicates. 10% DMSO and culture media were used as positive and negative control respectively. Since 1% of DMSO was used to dissolve the *Uncaria gambir* extracts during its preparation, the question arose whether the presence of DMSO in the extract will affect the cytotoxicity of the extract towards the fibroblast cells. Therefore, 1% of DMSO has also been included in the cytotoxic test as reference control to eliminate biased results. After the exposure, the plates were incubated for another 24 hours. Three plates were used for the cytotoxicity determination, subjected to the cytotoxic tests using Alamar Blue, Neutral Red Uptake and DNA fluorescence assay.

Cytotoxic assays

Alamar Blue assay

This assay measures the ability of the mitochondria to convert the resazurin dye to resofurin. The amount of resofurin produced reflects the number of viable cells. Upon completing the incubation period, 10 µl of resazurin dye (Sigma-Aldrich Germany) was added into the well plate using a multi-channel pipette. The 96-well plate is then incubated at 37°C with 5% CO₂ for 2-4 hours. After the incubation, the amount of the resorufin produced by the cells is determined via spectrophotometer at 570 nm and using 600 nm as a reference wavelength.

Neutral Red Uptake Assay

This assay measures the lysosomal activity of the cells. Intact cells will retain the red dye thus appears blue while disintegrated lysosomal membrane will cause leakage of the dye and appears red. After 24-hour incubation, all media were removed from each well with a multi-channel pipette under the clean hood. 150 µl of phosphate buffer solution (PBS) was added into each well to remove any residual media and later discarded. 50 µl of Neutral Red solution 0.33% in PBS (Sigma Aldrich, Germany) was added into all wells and incubated for 2 hours at 37°C with 5% CO₂. Following incubation, the medium was removed and rinsed with 100 µl of PBS. The PBS was discarded from the well after rinsing. Then, 100 µl of Neutral Red Assay solubilization solution (1% Acetic acid in 50% Ethanol) was added into each well using a multichannel pipette and trituration was done to enhance mixture of the solubilized dye. The absorbance was measured using a spectrophotometer (96-well plate reader) utilizing absorbance at 540 nm wavelength.





Fayyadhah M Azmi et al.

DNA Fluorescence Assay

DNA fluorescence protocol was adapted from the previous study by Rago et al (16) where Bisbenzimidazole H 33258 dye will bind to A-T sequence in minor grooves of double-stranded DNA. After 24 hours of incubation, each well was 'washed' with 100 μ l PBS twice to remove all the residual media. After gentle tapping, the PBS in the wells was discarded. 100 μ l of deionized water was added into each well using the multi-channel pipette and the plate was frozen at -20°C for at least 24 hours. Meanwhile, the fluorochrome in a high salt TNE buffer solution was prepared. First, a stock solution of bisbenzimidazole Hoechst 33258 was made by diluting it 10-fold with molecular biology grade water to a concentration of 1 mg/ml and stored at 4°C foil-wrapped. The fluorescent assay buffer (TNE buffer) was also diluted 10-folds. The fluorochrome in a high salt TNE buffer solution was prepared by adding 400 μ l of Hoechst 33258 per 20 ml of TNE buffer. After removal of the well plate from the freezer, the well plate was thawed until reaching room temperature. 100 μ l of the fluorochrome in a high salt TNE buffer solution was added into each well using a multi-channel pipette. The degree of fluorescence present in each well measured using fluorometer at 360 nm excitation and 460 nm emission wavelengths.

Cell morphological changes via Live/Dead cell analysis

The stock solution of Live/Dead stain (Abcam, United States) was prepared into 200-fold dilutions as per manufacturer instruction, by diluting 5 μ l of 1000x Live/Dead stain with 2 ml PBS to obtain 5x Live/Dead stain. Following 24 hours of incubation, the culture media in each of the 96-well plates was aspirated and been replaced with 200 μ l of 5x Live/Dead stain. The well plate was incubated for 10 minutes at room temperature. Then, the 96-well plate was analyzed and viewed under the confocal fluorescence microscope.

Statistical analysis

For both DNA Fluorescence and NRU assay, the mean percentage of cell viability was calculated using the following formula (Equation 1);

$$\text{Viable cell (\%)} = (\text{absorbance of sample} / \text{absorbance of control}) \times 100$$

The percentage of reduction of Alamar Blue was calculated using this formula (Equation 2) (17).

$$(117216 \times A1) - (80586 \times A2) / (117216 \times P1) - (80586 \times P2) \times 100$$

where,

117216: Molar extinction coefficient (E) of oxidized Alamar Blue at 570 nm

80586: Molar extinction coefficient (E) of oxidized Alamar Blue at 600 nm

A1: Absorbance of test wells at 570 nm

A2: Absorbance of test wells at 600 nm

P1: Absorbance of positive growth control well (cells plus Alamar Blue but no test agent) at 570 nm

P2: Absorbance of positive growth control well (cells plus Alamar Blue but no test agent) at 600 nm

Subsequently, the mean percentage of cell viability for each concentration of *Uncaria gambir* extracts used were compared with positive control using the ANOVA test (post-hoc Dunnett) with *p*-value set as 0.05. The IC₅₀ concentration for each of the cytotoxic tests was determined using a software GraphPad Prism version 8.0.1.



**Fayyadhah M Azmi et al.**

RESULTS

Cell viability

In Figure 1, at 1000µg/ml concentration, the extract gave two contrasting findings. Both Alamar Blue and DNA fluorescence assay showed that the extract was not cytotoxic with the mean percentage of cell viability of more than 70%. Measurement using NRU assay, on the other hand, showed an average of only 53% of the fibroblast cells were viable, indicating some degree of toxicity towards the cells. Nevertheless, no cytotoxic effects were exerted by the extracts at a concentration below 500µg/ml for all cytotoxic assays. 1% DMSO that was used as the solvent showed no cytotoxic effect towards fibroblast cell lines when measured using the three cytotoxic assays with the mean percentage of cell viability exceeding 70% for all concentration. There was a statistically significant difference with $p < 0.05$ for all concentrations of *Uncaria gambir* extracts when compared to positive control using the ANOVA test (post-hoc Dunnet) for all assays.

IC₅₀ (Half maximal inhibition concentration)

The half-maximal inhibitory concentration (IC₅₀) of *Uncaria gambir* extracts measured using Alamar Blue, DNA Fluorescence, and Neutral Red Uptake assay was 1751 µg/ml, 3126 µg/ml, and 1031 µg/ml respectively as shown in Figure 2.

Cell morphological determination

The Live/Dead cell analysis was done using a confocal fluorescence microscope where it revealed the live cells in green fluorescence while the dead cells in red. In positive control (Figure 3 (a)), more cells in red fluorescence can be seen as compared to green, indicating more cell death in this control solution. The density of the cells was also scarce. Contrastingly, in untreated cells (negative control), there was evidence of increased cell proliferation and density in green fluorescence (Figure 3 (b)). At 1000 µg/ml, the Live/Dead cell analysis showed cells in a mixture of both red and green fluorescence with moderate cell density. The red fluorescence can be seen within the cytoplasm of the cells. (Figure 3 (c)). As the concentration of the extract was diluted up to 7.8 µg/ml, the cell density increased and more cells with green fluorescence can be seen as compared to the former concentration. (Figure 3 (d),(e),(f),(g),(h),(i) and (j)).

DISCUSSION

Cytotoxicity is due to an adverse reaction of chemical and physical agents towards cells, and it can be measured by assessing the cellular function and the cell integrity (Cummings et al. 2004) such as cell membrane permeability, enzyme activity, cell adherence, ATP production, and nucleotide uptake activity. The cytotoxicity assay is beneficial because it is fast and cheap, but it is not technically advance to replace the in vivo animal test (18). However, these assays are subjected to numerous variables and are not an optimal method to assess cell proliferation and cell death alone (19). As an example, Alamar Blue could result in false-positive results due to optical interference (18) while in DNA quantification, Hoescht dye can exhibit a sequence-dependent affinity in binding to DNA which can lead to variability in assay results (20).

Therefore, to draw a conclusion of cell toxicity based only on one assay is always premature. Thus, a combination of cytotoxic tests using different types of cytotoxic assays that measure the cell cytotoxicity differently will be more accurate and precise. To compensate for the shortcomings of each cytotoxic assay, we decided to use three different assays, namely Alamar Blue, DNA Fluorescence and Neutral Red Uptake assay. Through this assays combination, we will be able to utilize both colorimetric and fluorometric methods to measure the toxicity of *Uncaria gambir*



**Fayyadhah M Azmi et al.**

extracts toward fibroblast cell lines. Besides, we also performed the Live/Dead cell analysis as a measure to verify the validity of the cytotoxicity tests. In this study, 1% of DMSO was used as a solvent for dilution of *Uncaria gambir* extracts as suggested by Timm et al. (21). However, this leads to the question that if the solution itself can cause cellular damage, would its inclusion as a solvent in the *Uncaria gambir* extracts will affect the outcome as well? Thus, to eliminate the risk of bias, the 1% DMSO also was subjected to cytotoxic tests. The 1% DMSO was serially diluted into different concentrations similar to the method used to dilute the *Uncaria gambir* extracts.

From the results, it is proved that at a concentration of less than 1%, there is more than 70% of the cell viability of the fibroblast cell lines. No significant cytotoxic effects were exerted toward the cell lines by DMSO that was used as the solvent during the preparation of the *Uncaria gambir* extracts. The findings in our study are in agreement with Cheung and his colleagues where they also noted no significant reduction in cell proliferation and viability after been exposed to DMSO at a concentration below 1% (22). The results from our study showed that the Neutral Red Uptake assay was more sensitive compared to other assays, reflected by their low IC⁵⁰ value (23). This sensitivity correlates well with results of the cytotoxicity testing, where it can be hypothesized that the *Uncaria gambir* extract affects the lysosomal activity earlier compared to other organelles, particularly mitochondria and nucleus in the programmed cell death (apoptosis).

The extract at 1000µg/ml concentration might have altered the lysosomal membrane permeability, causing the release of lysosomal protease called cathepsin into the cytosol which in turn initiate the apoptotic pathway (24). The release of cathepsin causes cytosolic acidity (25), and during this condition, the proton leaks out, causing destabilization of the cell membrane and inadvertently cause the loss of pH gradient (26). The imbalance in pH and proton gradient leads to the failure of retention of the neutral red dye within the cell and lysosomes. This explains the findings in our study where less neutral red dye been taken up into the cells at 1000µg/ml concentration. While these processes affect lysosome, the cells still maintain their high ATP level; thus resazurin conversion is still possible in higher concentrations (27). Furthermore, DNA damages do not occur until at the late stage of apoptosis; therefore Hoechst dye is still able to bind to fragmented DNA of 180 to 200 base pairs at 1000µg/ml concentration of the extract (28). Van Tonder et al (32) and Zwolak (33) also reported similar findings on the sensitivity of the NRU assay and the role of lysosomes in programmed cell death.

The results of our cytotoxicity study are in agreement with the findings from the Live/Dead cell analysis. The analysis showed a mixture of red and green fluorescence with minimal cell density at 1000µg/ml concentration, suggesting some degree of cytotoxicity was exerted by the extract towards the cells. Cells with intact cell membranes maintained their cell integrity and the presence of intracellular esterase within the cell cytoplasm generated the green fluorescence. In contrast, the disintegration of the membrane allowed the membrane impermeant dead cell dye to bind to the DNA within the nucleus leading to the formation of red fluorescence. However, as the concentration of the extract reduced, the cell with green fluorescence started to dominate and increased in number, reflecting the non-cytotoxic effects of the extracts towards the cells. Hence, we can suggest that the extract of Malaysian *Uncaria gambir* was not cytotoxic at a concentration below 500µg/ml. The concentration was higher than previously reported studies on *Uncaria gambir* extracts where Ju et al. (29) and Anggraini et al. (7) reported a non-cytotoxic concentration of 60µg/ml and 200µg/ml respectively. However, both studies used different types of cell lines and only used calorimetric measurements for the cytotoxicity assessment. Therefore, a direct comparison of the results would be inappropriate. The cytotoxicity of the *Uncaria gambir* extract can be due to its flavonoids constituents. The previous study was done by Kassim et al. (30) on the determination of flavonoid content within *Uncaria gambir* extracts from Indonesia showed that it consists of (+)-catechin hydrate, (-)-epigallocatechin (EGC), (-)-gallocatechin (GC), (-)-epicatechin (EC) and (-)-epicatechin gallate (ECG). Catechin alone has been proved to improve cell viability (31,32) and exerts an anti-apoptotic effect against oxidative stress (33). However, its derivatives such as (-)-epigallocatechin-3-gallate (EGCg) and (-)-epigallocatechin (EGC) is more toxic toward cells compared to catechin itself due to the presence of gallic moiety within the structures (34–36).





Fayyadhah M Azmi et al.

CONCLUSION

In summary, we can conclude that the Malaysian *Uncaria gambir* extracts were not cytotoxic to the fibroblast cell lines at a concentration below 500 µg/ml. We hypothesized that the cytotoxic effect exerted may be due to the presence of the gallic moiety or other compounds that may be present within the extract of Malaysian *Uncaria gambir*. Therefore, further research investigating the content of the Malaysian *Uncaria gambir* extract is needed.

Conflict of Interest

The authors deny any conflict of interest related to this research.

FUNDING

The research is funded by the Young Researchers Grant, National University of Malaysia (GGPM-2017-106).

ACKNOWLEDGMENTS

The authors would like to thank the National University of Malaysia for providing the Young Researchers Grant and Faculty of Applied Sciences Universiti Teknologi MARA, Tissue Engineering Centre, Hospital Canselor Tuanku Muhriz and Centre of Research and Instrumentation Management, National University of Malaysia for their clinical and technical support throughout this research.

REFERENCES

1. Ibrahim N, Yusof NZ, Ahmad R. Quantification of catechin in leaves and stems of Malaysian *Uncaria gambir* (HUNTER) Roxb. by HPLC-DAD. Malaysian J Anal Sci [Internet]. 2015;20(3):567–72.
2. Hussin M, Kassim MJ. The corrosion inhibition and a adsorption behavior of *Uncaria Gambir* extract on mild steel in 1M HCL. Mater Chem Phys. 2011;125:461–8.
3. Taniguchi S, Kuroda K, Doi K, Tanabe M, Yoshida T, Hatano T. Revised structures of Gambiriins A1, A2, B1 and B2, Chalcane-flavan dimers from Gambir. Chem Farm Bull. 2007;55(2):268–72.
4. Kim Suan. Transformation of rust by *Uncaria Gambir*. Universiti Sains Malaysia; 2009.
5. Roufiq N, Hadad MHE, AM Hasibuan. Status Teknologi Budidaya dan Pengolahan Gambir. Indonesia; 2009.
6. Eni Hayani. Analisis kadar catechin dari gambir dengan berbagai metode. Buletin Teknik Pertanian. 2003;8(1):31–3.
7. Tuty Anggraini, Tai A, Yoshino T, Itani T. Antioxidative activity and catechin content of four kinds of *Uncaria gambir* extracts from West Sumatra, Indonesia. African J Biochem Res. 2011;5(1):33–8.
8. Taniguchi S, Kuroda K, Doi K, Inada K, Yoshikado N, Yoneda Y, et al. Evaluation of gambir quality based on quantitative analysis of polyphenolic constituents. Yakugaku Zasshi [Internet]. 2007;127(8):1291–300.
9. Ahmad R, Salim F. Oxindole Alkaloids of *Uncaria* (Rubiaceae, Subfamily Cinchonoideae): A Review on Its Structure, Properties, and Bioactivities [Internet]. Vol. 45, BS: SNPC. Elsevier; 2015. 485–525 p.
10. Kassim MJ, Hussin MH, Achmad A, Dahob NH, Suan TK, H. Safley Hamdan. Determination of total phenol, condensed tannin, and flavonoid contents and antioxidant activity of *Uncaria gambir* extracts. Maj Farm Indones. 2011;22(1):50–9.
11. Velayutham P, Babu A, Liu D. Green tea catechins and cardiovascular health: an update. Curr Med Chem [Internet]. 2008;15(18):1840–50.
12. Xu X, Zhou XD, Wu CD. The tea catechin epigallocatechin gallate suppresses cariogenic virulence factors of *Streptococcus mutans*. Antimicrob Agents Chemother. 2011;55(3):1229–36.
13. Xu X, Zhou XD, Wu CD. Tea catechin epigallocatechin gallate inhibits *Streptococcus mutans* biofilm formation by suppressing *gtf* genes. Arch Oral Biol [Internet]. 2012;57(6):678–83.



**Fayyadhah M Azmi et al.**

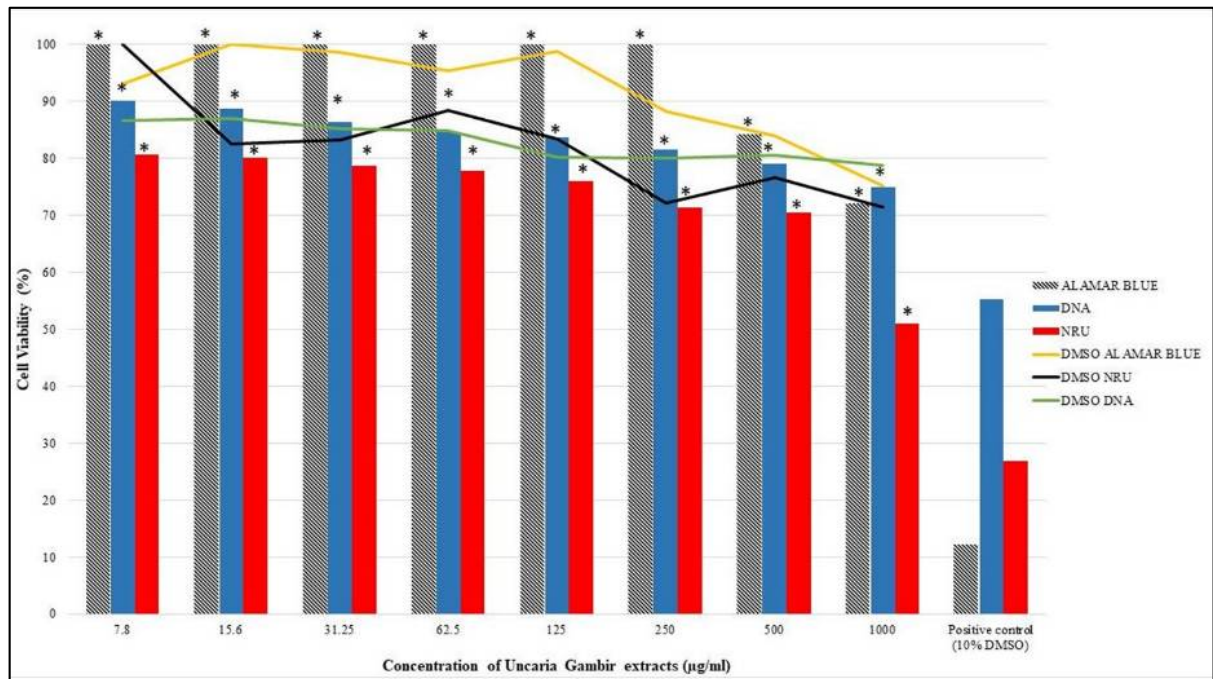
14. Nakanishi T, Mukai K, Yumoto H, Hirao K, Hosokawa Y, Matsuo T. Anti-inflammatory effect of catechin on cultured human dental pulp cells affected by bacteria-derived factors. *Eur J Oral Sci.* 2010;118(2):145–50.
15. Freshney R. *Basic Principles of Cell Culture.* Hoboken, NJ, USA: John Wiley & Sons, Inc.; 2006.
16. Rago R, Mitchen J, Wilding G. DNA fluorometric assay in 96-well tissue culture plates using Hoechst 33258 after cell lysis by freezing in distilled water. *Anal Biochem.* 1990;191(1):31–4.
17. Al-Nasiry S, Hanssens M, Luyten C, Pijnenborg R. The use of Alamar Blue assay for quantitative analysis of viability, migration, and invasion of choriocarcinoma cells. *Hum Reprod.* 2007;22(5):1304–9.
18. Adan A, Kiraz Y, Baran Y. Cell Proliferation and Cytotoxicity Assays. *Curr Biotechnol Pharm.* 2016;17(14):1233–1221.
19. Quent VMC, Loessner D, Friis T, Reichert JC, Hutmacher DW. Discrepancies between metabolic activity and DNA content as a tool to assess cell proliferation in cancer research. *J Cell Mol Med.* 2010;14(4):1003–13.
20. Ramirez CN, Antczak C, Djaballah H. Cell Viability Assessment: Toward Content-Rich Platforms. *Expert Opin Drug Discov.* 2010;5(3):223–33.
21. Timm M, Saaby L, Moesby L, Hansen EW. Considerations regarding use of solvents in in vitro cell based assays. *Cytotechnology.* 2013;65(5):887–94.
22. Cheung WMW, Ng WW, Kung AWC. Dimethyl sulfoxide as an inducer of differentiation in preosteoblast MC3T3-E1 cells. *FEBS Lett.* 2006;121–6.
23. Damiani E, Solorio JA, Doyle AP, Wallace HM. How reliable are in vitro IC 50 values? Values vary with cytotoxicity assays in human glioblastoma cells. *Toxicol Lett.* 2019 Mar 1;302:28–34.
24. Stoka V, Turk V, Turk B. Lysosomal cysteine cathepsins: Signaling pathways in apoptosis. *Biol Chem.* 2007;388(6):555–60.
25. Wang F, Gómez-Sintes R, Boya P. Lysosomal membrane permeabilization and cell death. *Traffic.* 2018;19(12):918–31.
26. Repnik U, Česen MH, Turk B. The use of lysosomotropic dyes to exclude lysosomal membrane permeabilization. *Cold Spring Harb Protoc.* 2016;5:447–52.
27. Helm K, Beyreis M, Mayr C, Ritter M, Jakab M, Kiesslich T, et al. In Vitro Cell Death Discrimination and Screening Method by Simple and Cost-Effective Viability Analysis. *Cell Physiol Biochem.* 2017;41:1011–9.
28. Ioannou YA, Chen FW. Quantitation of DNA fragmentation in apoptosis. *Nucleic Acids Res.* 1996;24(5):992–3.
29. Ju SM, Jun L, Choi HS, Kim SH, Jeon BH. Effect of Several Species of the Family Rubiaceae on cytotoxicity and apoptosis in HL-60. *Korean J Orient Physiol Pathol.* 2006;20(1):187–92.
30. M. Jain Kassim, M. Hazwan Hussin, A.Achmad, N. Hazwani Dahon, Suan TK. Determination of total phenol, condensed tannin and flavanoid contents and antioxidant activity on Uncaria gambir extracts. *Maj Farm Indones.* 2011;22(1):50–9.
31. Cheruku SP, Ramalingayya GV, Chamallamudi MR, Biswas S, Nandakumar K, Nampoothiri M, et al. Catechin ameliorates doxorubicin-induced neuronal cytotoxicity in in vitro and episodic memory deficit in in vivo in Wistar rats. *Cytotechnology.* 2018 Feb 1;70(1):245–59.
32. Sipahi H, Gostner JM, Becker K, Charehsaz M, Kirmizibekmez H, Schennach H, et al. Bioactivities of two common polyphenolic compounds: Verbascoside and catechin. *Pharm Biol.* 2016 Apr 2;54(4):712–9.
33. Tanigawa T, Kanazawa S, Ichibori R, Fujiwara T, Magome T, Shingaki K. (+)-Catechin protects dermal fibroblasts against oxidative stress-induced apoptosis. *BMC Complement Altern Med.* 2014;14(133):1–7.
34. Babich H, Krupka ME, Nissim HA, Zuckerbraun HL. Differential in vitro cytotoxicity of (-)-epicatechin gallate (ECG) to cancer and normal cells from the human oral cavity. *Toxicol Vitro.* 2005;19(2):231–42.
35. Babich H, Zuckerbraun HL, Weinerman SM. In vitro cytotoxicity of (-)-catechin gallate, a minor polyphenol in green tea. *Toxicol Lett.* 2007;171(3):171–80.
36. Ugartondo V, Mitjans M, Lozano C, Torres JL, Vinardell MP. Comparative study of the cytotoxicity induced by antioxidant epicatechin conjugates obtained from grape. *J Agric Food Chem.* 2006;54(18):6945–50.





Fayyadhah M Azmi et al.

ILLUSTRATIONS



*denotes statistically significant difference when compared to positive control with $p \leq 0.05$.

Figure 1. Mean percentage of cell viability of *Uncaria gambir* extracts and the reference control (DMSO) in 3 different assays.

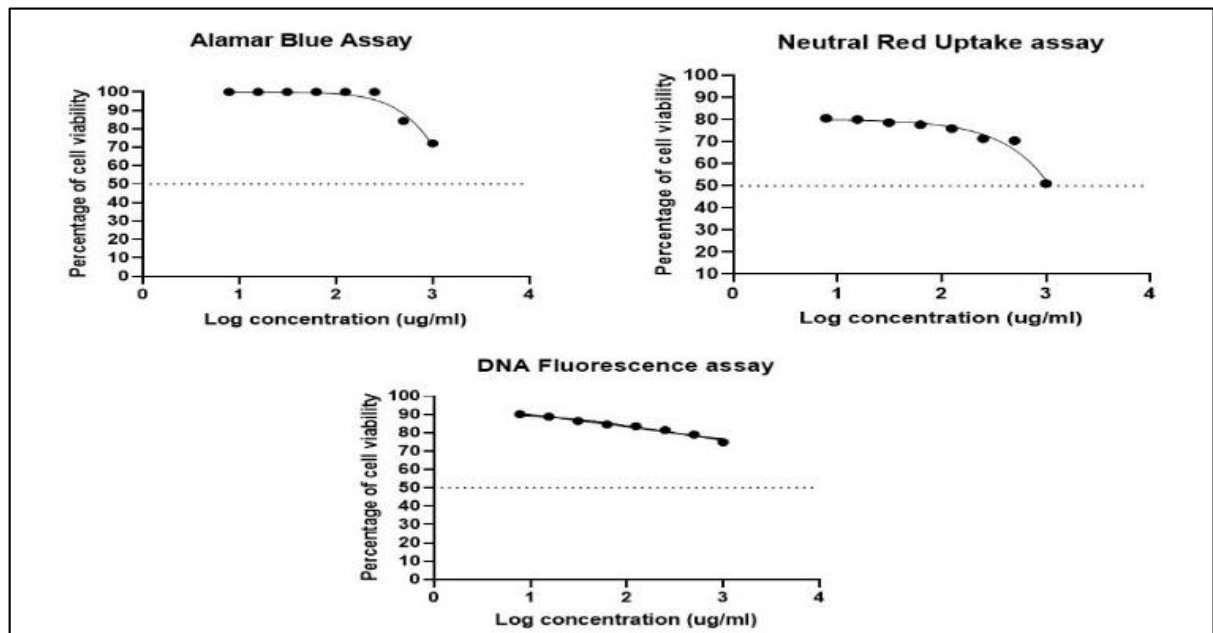
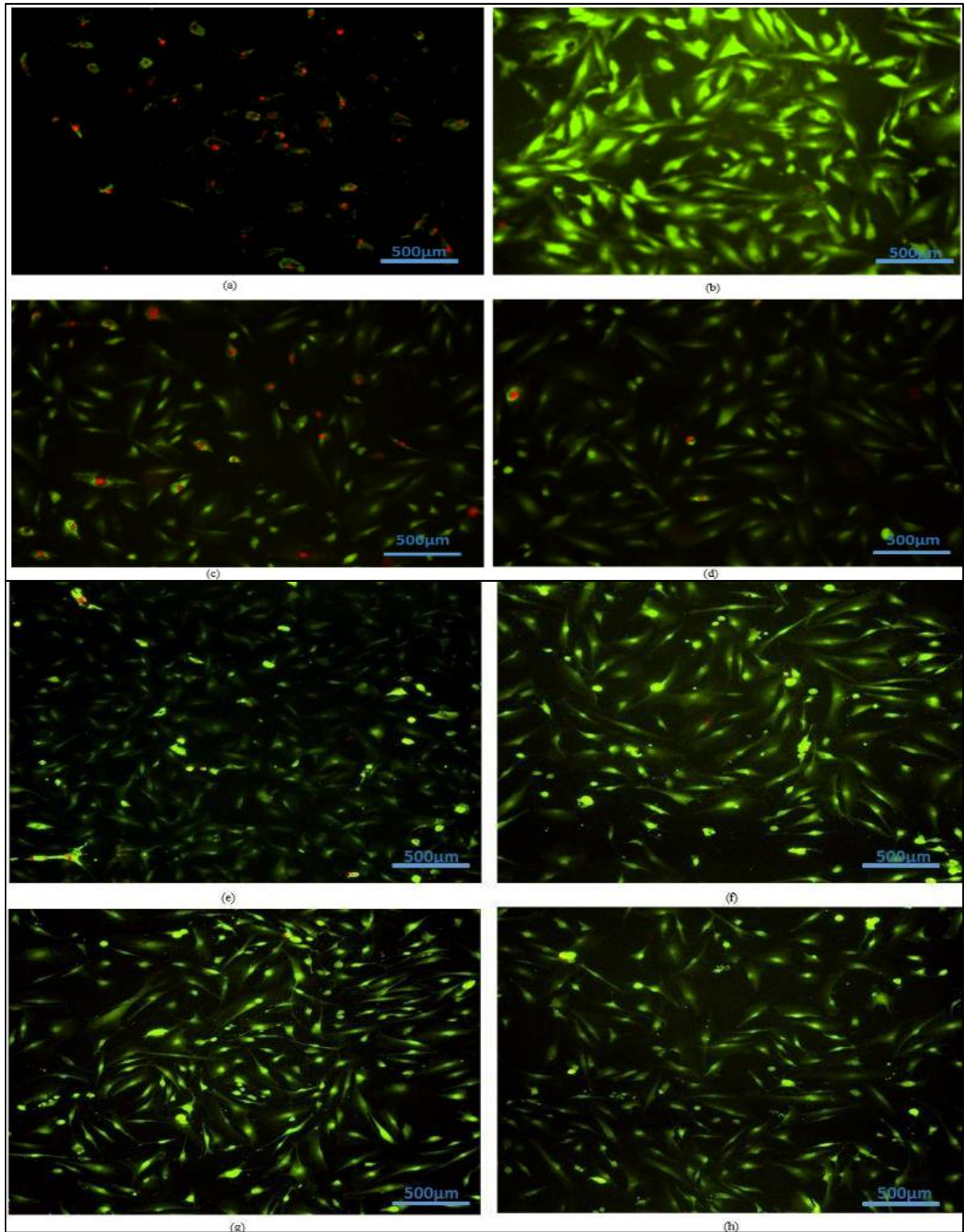


Figure 2. Dose-Response Graph of the assays with IC_{50} .





Fayyadhah M Azmi et al.





Fayyadhah M Azmi et al.

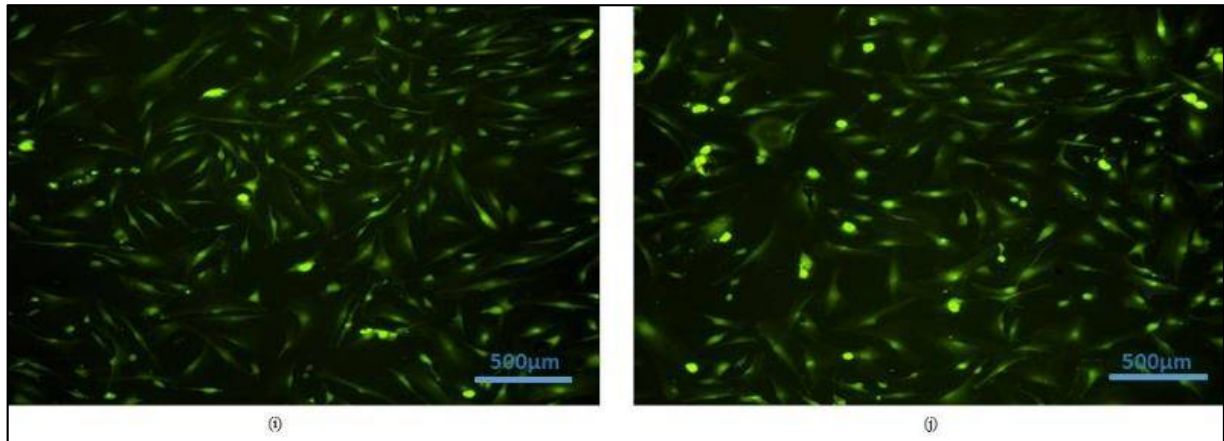


Figure 3. LIVE/DEAD Analysis of fibroblast cell (MC3T3) under confocal fluorescence microscope (x10); (a) Postive control (b) Negative control (c)1000µg/ml of *Uncaria gambir* extract (d) 500µg/ml of *Uncaria gambir* extract (e)250µg/ml of *Uncaria gambir* extract (f) 125µg/ml of *Uncaria gambir* extract (g)62.5µg/ml of *Uncaria gambir* extract (h) 31.25µg/ml of *Uncaria gambir* extract (i)15.62µg/ml of *Uncaria gambir* extract (j) 7.8µg/ml of *Uncaria gambir* extract.





Parasites in the Economically Important Bivalve from the Mediterranean Sea Coast, Egypt

Osama A. Ward¹, Shereen A. Fahmy^{1*}, Rabab M. Alkaradawe² and Samya H. Mohammad³

¹Departments of Zoology, Faculty of Science, Damietta University, Egypt

²Departments of Zoology, Faculty of Science, El- Arish University, Egypt

³Departments of Zoology, Faculty of Science, Port Said University, Egypt

Received: 17 July 2019

Revised: 20 Aug 2019

Accepted: 26 Sep 2019

*Address for Correspondence

Shereen A. Fahmy

Departments of Zoology,

Faculty of Science,

Damietta University, Egypt

Email: shereenfahmy@du.edu.eg

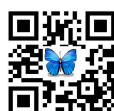


This is an Open Access Journal / article distributed under the terms of the **Creative Commons Attribution License** (CC BY-NC-ND 3.0) which permits unrestricted use, distribution, and reproduction in any medium, provided the original work is properly cited. All rights reserved.

ABSTRACT

This study investigated the parasites of one of the commercial important bivalve species (*Phaphia undulata*) during 2018 from Izbat Alburj Region, Mediterranean Sea, Egypt. The study reported the following parasites in the bivalve: *Entameaba histolytica*, *Tricurus tricura* and *Giardia lambelia*. The most dominant parasites were gill parasites (55.30%), followed by gonad parasite (31.82%) then the intestine parasite (12.86%). The maximum gill infection was detected in winter (93 individuals). While that of the gonad and intestine was recorded in spring (62 and 31 individuals, respectively). This study also indicated that *E.histolytica* existed in the clam throughout the year while the other parasites disappeared in autumn. Seasonal abundance of each parasite species in the infected clam explained that the highest count of *E. histolytica* was recorded in spring and the lowest was in autumn. On the other hand, the highest count of *Giardia lambelia* was recorded in winter, followed by spring while *Tricurus tricura* was more represented in winter, followed by summer. The correlation of parasite number with the environmental factors, clam measurements and clam weights showed a very weak relationship. The current research warns of eating marine bivalves without good cooking for the presence of the harmful phase in the infected clams.

Key words: Parasites, Mediterranean sea, Bivalves, *Phaphia undulata*.





INTRODUCTION

Marine Bivalvia considered as the second largest class of marine mollusca which includes clams, cockles, scallops, oysters, mussels, piddocks and ship worms (Giribet, 2008; Coan and Valentich-Scott, 2012). Bivalve molluscs are key components of the estuarine environments as contributors to the trophic chain, and as filter-feeders, for maintaining ecosystem integrity (Sundaram and Deshmukh, 2011). Oysters, clams and scallops are commercially exploited around the world (Long et al, 2014). Mohammad et al. (2017) stated that the Egyptian Mediterranean coasts are occupied by numerous species of edible clams. During the past decades, populations of some bivalve species declined because of overharvesting, environmental contamination and diseases (Fernández et al, 2014). Generally, bivalves are liable to assault by a wide range of parasites (Leethochavalit et al, 2004). This led to mass mortality of the bivalves and significant losses for associated industries (Hill et al, 2014). Adelle et al. (2014) referred to the presence of *Cryptosporidium* and *Giardia duodenalis* in hemolymph of the bivalves. Another species, *Perkinsus mediterraneus*, a protistan parasite of the European oyster *Ostrea edulis*, farmed along the coast of the Balearic Islands, Mediterranean Sea (Casas et al, 2004). On the other hand, the usual helminth parasites that infect bivalves are trematodes, cestodes and nematodes. Nematodes are uninhabitable parasites of bivalves live in marine water except for *Echinocephalus sinensis* in oysters and *Sulcascaulis sulcata* in scallops and clams (Song et al, 2010). However, larval stage of trematodes is more important than cestodes and nematodes with respect to the bivalves pathogens (Gosling, 2015). Other parasitic infections to marine organisms were studied by many authors (Leethochavalit et al, 2004; Khalil et al, 2014). The clam, *Paphia undulata* is one of the most popular venerid species (BU, 2013) that was previously studied by many authors (EL-Sayed, 2010). It takes its commercial importance according to its cheapness, fleshy and after exporting to Europe (El-Moselhy and Yassien, 2005). This study aimed to identify parasites in one of the important bivalve species, *Paphia undulata*, in the Mediterranean Sea.

MATERIALS AND METHODS

Water samples were seasonally collected on the coast of the Mediterranean sea within the region of Izbet Al burj during 2018. Its location is on the opposite to Ras El Bar (Damietta Governorate) (Figure 1). Its eastern side looks out to the Nile River. So there is a mixing of fresh and marine water in this region. Its geographical coordinates are 31° 30' 30" North, 31° 50' 5" East, about 15 km on the east side of the Nile River at the mouth of the Mediterranean Sea.

Physicochemical parameters (temperature, salinity, pH and conductivity) of water were measured. Bivalve specimens were also collected from the same site using a special trap. Samples were rapidly transported to the laboratory. Each specimen was measured (mm) and weighed (nearest 0.01g). Soft tissue was dissected and weighed. Gills, gonads and intestine were perfectly separated, weighed and preserved in formalin. A small tissue was compressed between two glass slides and examined under the electric microscope (XSZ-107BN).

RESULTS

The highest values were recorded in summer except pH (Tab. 1). A total of 51% of *P. undulata* was infected by three parasitic species, two protozoa (*Entamoeba histolytica* and *Giardia lamblia*) and a nematode (*Tricuru stricura*). Abundance of the three parasite species in *Paphia undulata* was represented in Figure 2. This figure showed that *Entamoeba histolytica* was the dominant species (379 individuals) followed by *Giardia lamblia* (5 individuals), then *Tricuru stricura* that occupied the last position with 3 individuals only. The protozoan parasite *E. histolytica* infested the bivalve throughout the year. Mean while, the other parasites totally disappeared in autumn (Tab.2). Seasonal abundance of these parasitic species infected *P. undulata* during the investigated period was represented in Figure (3). This figure explained the highest count of *Entamoeba histolytica* was recorded in spring and the lowest was in autumn. On the other hand, the highest count of *Giardia lamblia* was recorded in winter, followed by spring and *Tricuru stricura* was represented by 2 individuals in winter, followed by 1 individual in summer.



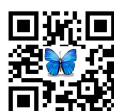


Osama A. Ward et al.

The seasonal parasitic load in different infected organs was shown in Figure (4). The highest infected organ was the gill (55.30%) followed by the gonad (31.82%), then the intestine (12.86%). The peak of infection of gonad parasites was recorded in spring (62 individuals) and declined till it disappeared in Autumn. For intestine parasites, the maximum infection was occurred in spring (31 individuals) followed by winter (15 individuals). The correlation between parasite number in the infected bivalve with either of the environmental factors, clam measurements and clam weights showed a very weak relationship (Tab. 3). However, the matrix showed negative correlation with all parameters (except PH) and shell measurements. When every weak positive correlation was noticed with the bivalve weights. The graph of the variables and observations of each parasite species separately was represented in the factorial map (Figure 5). The existence of *G.lambelia* and *T.tricura* maybe related to climatic characteristics to some extent. On the other hand, there is no significant relation between shell dimensions and the relative abundance of the parasite *E. histolytica*

DISCUSSION

The Mediterranean Sea fishes and sea food especially in coastal waters of Egypt are considered as highly valued fish food. Edible bivalve species, such as *Phaphia undulata*, in addition to other veneroid clams are most common to the consumers in Egypt (Mohammad et al. 2014). In the present study, it was found that 51% of the examined bivalve, *P. undulata* were infected by parasites which include protozoan parasites (*E.histolytica* and *G.lambelia*) and nematode parasite (*T. tricura*). *E. histolytica* attained the highest abundance and intensity (379 individual) followed by *G.lambelia* (5 individual) then *T.tricura* (3 individual). Canestri et al. (2000) studied the occurrence of protozoan parasites on the bivalve *Callista chione* and showed that parasites may play a role in the health of commercial bivalves. *Entamoeba histolytica* is an enteric protozoan parasite which causes amoebic dysentery in humans. Trophozoites which is the amoeboid forms of *E. histolytica* cause the most common infection called a symptomatic stay in the lumen of the colon and turn into cysts which are passed in the feces (Marie and Petri, 2014). The trophozoites of *E. histolytica* may invade the colonic mucosa and cause dysentery or liver abscesses or both leading to morbidity and mortality in developing countries (Haque et al, 2003). In the current study, the two forms of *E. histolytica* (trophozoite and cyst) were observed in the infected bivalves. So, the current study beware of eating bivalves raw without good cooking. The infestation with the examined parasites did not maximized during the same season but there are seasonal variation in the abundance and intensity of these parasites on the bivalve in the present study. The abundance and the intensity of *E. histolytica* increased in spring and declined in autumn. A similar finding was reported by El-Wazzan and Radwan (2013) who found that maximum intensity of infection in the bivalve *Tapes decussates* was in spring. In contrast, a study carried out by Casas et al. (2004) indicated that 70% of oysters were infected with high prevalence in summer and autumn. Concerning *G. lambelia*, it was more represented in winter followed by spring and absent in summer and autumn. So, it may assumed that the rate of parasitism in *G. lambelia* increased in winter, which is characterized by low surface seawater temperature, salinity, pH and conductivity. This may lead to the conclusion that there was an independent behavior of each set of variables with all types of parasites that infected the bivalve. This was assured by Teiet et al. (2016) who proved that two different protozoan parasites species (*Giardia lamblia* and *Cryptosporidium parvum*) gave variation in the prevalence and intensity in the tissue of molluscs. The variation may also result from different hosts for the same species as stated by Schets et al. (2012). They found that *Giardia* sp constituted 10 to 25% in the oyster increase more than double in the mussels. Moreover, the degree of infection maybe related to another factor such as habitat type. Tuntiwaranuruk et al. 2004 found that heavy infections generally occurring in species living at or near the surface in a muddy substrate (Tuntiwaranuruk et al. 2004). However, in the present work, correlation of parasite number with the environmental factors, clam measurements and clam weights showed a very weak relationship. Generally, the most infected part of the bivalves was the gills followed by gonads. The existence of *G.lambelia* and *T.tricura* maybe related to climatic factors to some extent. On the other hand, there is no significant relation between shell dimensions and a relative abundance of the parasite *Entamoeba histolytica*. Additional studies should be done to estimate its epidemiological and biological status in Egypt.





Osama A. Ward et al.

REFERENCES

- Adell, WA, Smith, K, Shapiro, Melli, Conrad, PA, 2014: Molecular Epidemiology of *Cryptosporidium* spp. And *Giardia* spp. In Mussels (*Mytilus californianus*) and California Sea Lions (*Zalophus californianus*) from Central California. Applied and Environmental Microbiology. 80(24): 7732-40.
- BU, 2013: Provision of services for fieldsampling. Species identification and data analysis of benthic faunal communities of Hong Kong marine waters. <http://www.marinespecies.org/index.php>
- Canestri-Trotti, G, Baccarani, EM, Turolla, E, 2000: Monitoring of infections by protozoa of the genera *Nematopsis*. *Perkinsus* and *Porospora* in the smooth Venus clam *Callistachione* from the North-Western Adriatic Sea (Italy). Dis. Aquat. Org. 42:157-61.
- Casas, SM, Grau, A, Reece, KS, Apakupakul, K, Azevedo, C, et al, 2004: *Perkinsus mediterraneus* n. sp., a protistan parasite of the European flat oyster *Ostrea edulis* from the Balearic Islands, Mediterranean Sea. Dis. Aquat. Org. 58:231-44.
- Coan, EV, Valentich-Scott, P, 2012: Bivalve Seashells of Tropical West America. Marine Bivalve Mollusks from Baja California to Northern Peru. Santa Barbara Museum of Natural History Monographs Number 6 (1) 1–596.
- El-Sayed, D, 2010: Genetic Diversity and structural variation of some clams (Family : Veneridae). Doctoral dissertation, Zoology Department, Faculty of Science, Benha University.
- El-Wazzan, E, Hashem, ER, 2013: Histopathological study for evaluation of trematode larval infection in the carpet shell clam *Tapes decussatus* from three Egyptian clam fisheries. Egypt. J. Aqua. Res. 39. 291-301.
- Giribet, G, 2008: *Bivalvia*. Harvard university, <https://www.researchgate.net/publication/281209244>
- Gosling, E, 2015: Diseases and parasites. Marine Bivalve Molluscs 429–477.
- Haque, R, Huston, CD, Hughes, M, Houpt, E, Petri, WA, 2003: Amebiasis. *Jr N Engl J Med*. Apr 17; 348(16):1565-73.
- Hill, KM, Stokes, NA, Webb, SC, Hine, PM, Kroeck, MA, et al, 2014: Phylogenetics of *Bonamia* parasites based on small subunit and internal transcribed spacer region ribosomal DNA sequence data. Dis Aquat Organ 110: 33-54.
- Khalid, M, El-Moselhy, KM, Yassin, MH 2005: Accumulation patterns of heavy metals in Venus clams. *Paphia undulate* (Born. 1780) and *Gafrarium pectinatum* (Linnaeus. 1758) from lake Timsah, Suez Canal, Egypt. Egyptian journal of aquatic research. 31(1):14-28.
- Khalil, MI, El-Shahawy, IS, Abdelkader, HS, 2014: Studies on some fish parasites of public health importance in the southern area of Saudi Arabia. Braz. J. Vet. Parasitol. 23, 4:435-42.
- Leethochavalit, S, Chalermwat, K, Upatham, ES, Choi, KS, Sawangwong, P, Kruatrachue, M, 2004: Occurrence of *Perkinsus* sp. in undulated surf clams *Paphia undulata* from the Gulf of Thailand. Dis. Aqua. Org. 60:165-71.
- Long Shabdin, Mohd, AbgAzizil, Fansuri, Abg Abdullah, Syahidatul, Atiqah, Ab, Rahim, 2014: Marine Gastropod and Bivalves of Sampadi Island. <http://www.researchgate.net/publication/269395974>
- Marie, C, Petri, WA, 2014: Regulation of virulence of *Entamoeba histolytica*. *Annu. Rev. Microbiol.* 68, 493–520.
- Mohammad, SH, Belal, AA, and Hassan, SS, 2014: Growth, age and reproduction of the commercially clams *Venerupis aurea* and *Ruditapes decussatus* in Timsah Lake, Suez Canal, Egypt. Indian journal of geo-marine sciences, 43(4):589-600.
- Mohammad, S, Ibrahim, R, Mohamed, S, 2017: Heavy metals and some nutritional elements in the Mediterranean carpet shell clam *Donax semistriatus*. Indian Journal of Geo-Marine Sciences (IJMS). 46 (6): 1145-1154.
- Schets Harold, HL, Van Den Berg, Ana Maria, De, Roda, Husman, 2012: Determination of the Recovery Efficiency of *Cryptosporidium* Oocysts and *Giardia* Cysts from Seeded Bivalve Mollusks. Journal of Food Protection. 76(1) 93–98.
- Song, L, Wang, L, Qiu, L, Zhang, H, 2010: Bivalve immunity. In Invertebrate Immunity. Landes Bioscience and Springer Science+Business Media. Austin. pp. 44–65.
- Sundaram, Sujit, Deshmukh, VD, 2011: On the commercially exploited edible bivalves off Mumbai. Fishing Chimes. 31,5:23-4.
- Tei, Steven, K, Jhenelle, A, Reid, M, Presta, G, Mayer, 2016: Assessment and Molecular Characterization of Human Intestinal Parasites In Bivalves from Orchard Beach. NY. USA. Environ. Res. Publ. Hlth. 13, 4:381-6.
- Tuntiwaranuruk, C, Chalermwat, K, Upatham, ES, Kruatrachue, M, Azevedo, C, 2004: Investigation of *Nematopsis* spp. Oocysts in 7 species of bivalves from Chonburi Province. Gulf of Thailand. Dis. Aqua. Org. 58:47-53.





Osama A. Ward et al.

Table 1. Physicochemical parameters of sea water samples

Season	Temp. (°C)	Salinity (ppt)	PH	Conductivity (mS/cm)
Winter	19.9	36.82	6.84	52.6
Spring	26.2	38.24	7.19	54.9
Summer	28.8	38.73	6.93	57.2
Autumn	22.6	37.53	6.75	55.3

Table 2. Seasonal variation of parasitic infection in *P.undulata* during the investigated period.

Species / Season	Winter	Spring	Summer	Autumn
<i>Entameaba histolytica</i>	+	+	+	+
<i>Giardia lamblia</i>	+	+	-	-
<i>Tricurur tricura</i>	+	+	+	-

Table 3. Correlations between variables and factors after rotation Varimax

Variables	D1	D2	D3
Temp. (°c)	0.982	0.053	-0.010
Salinity (ppt)	0.980	0.039	-0.027
pH	0.632	0.111	0.331
Conductivity (mS /cm)	0.918	0.009	-0.030
Shell length (cm)	0.183	0.686	-0.129
Shellwidth (cm)	0.006	0.861	-0.101
Shellheight (cm)	0.251	0.650	-0.173
Shellwt. (g)	0.129	0.861	0.119
Tissue wt. (g)	-0.244	0.749	0.128
Total parasite number	-0.013	-0.014	0.958

D1= temperature, salinity, pH& conductivity; D2= shell length, shellwidth, shellheight&weight; D3=parasites number.



Fig. 1. Map showing bivalve in Izbat Alburj (modified from google map).



